Synthesis and Characterisation of Star Polymers

By James Adam Burns

A thesis submitted in partial fulfilment of the requirements for the degree of

Doctor of Philosophy in Chemistry

Department of Chemistry

THE UNIVERSITY OF WARWICK

December 2011

Table of Contents

Table of Contents ii

List of Figures viii

List of Tables xx

List of Schemes xxii

List of Abbreviations xxvi

Acknowledgments xxxii

Abstract xxxiii

Declaration xxxv

1 Introduction 1

1.1 Star polymers 2

1.2 Controlled radical polymerisation (CRP) 4

1.2.1 Free radical polymerisation (FRP) 5

1.2.2 Atom Transfer Radical Polymerisation (ATRP) 6

1.2.3 Reversible Addition Fragmentation chain Transfer (RAFT) polymerisation 7

1.2.4 Nitroxide Mediated Polymerisation (NMP) 10

1.3 Click Chemistry 11

1.4 References 14

2 Synthesis and characterisation of core-first PMMA star polymers 18

2.1 Characterisation of star polymers 20

2.1.1 Conventional GPC 20

2.1.2 Viscometry in GPC (Universal calibration) 22

2.1.3 Multi-angle laser light scattering (MALLS) in GPC 24
2.1.4 Mark-Houwink plots 27
2.1.5 Determining the functionality of star polymers 29
2.1.6 Determining the number of arms using multi-detector GPC 30
2.2 Core-first polymers in literature 31
2.2.1 Core-first stars by ATRP 31
2.2.2 Core-first stars by RAFT polymerisation 32
2.2.3 Core-first stars by NMP 33
2.4 Results and Discussion 38
2.4.1 Synthesis of core-first PMMA stars by ATRP 38
2.4.2 Dilute solution properties of core-first PMMA stars 41
2.5 Conclusions 51
2.6 Experimental 52
2.6.1 Instruments 52
2.6.2 Materials 53
2.6.3 ATR Polymerisation of methyl methacrylate 3 arm star polymer 54
2.6.4 ATR Polymerisation of methyl methacrylate 5 arm star polymer 55
2.6.5 ATR Polymerisation of methyl methacrylate 8 arm star polymer 56
2.6.6 ATR Polymerisation of methyl methacrylate 21 arm star polymer 57
2.7 References 59
3 Synthesis and characterisation of arm-first PMMA star polymers 65
3.1 Introduction 67

3.1.1 Arm-first star synthesis 67
3.2 Results and Discussion 70
3.2.1 Arm-first core cross-linked PMMA stars by RAFT polymerisation 70
3.2.2 Synthesis of RAFT agents 71
3.2.3 The effect of monomer dilution on crosslinking 72
3.2.4 Arm-first star PMMA by RAFT using different crosslinkers 75
3.2.5 Determining the functionality of core cross-linked star polymers 83
3.3 Conclusions 93
3.4 Experimental 94
3.4.1 Instruments 94
3.4.2 General method for calculating the percentage arm incorporation into stars when using an arm-first approach. 95
3.4.3 Materials 95
3.4.4 Synthesis of RAFT agent 1: 2-cyanoprop-2-yl dithiobenzoate 96
3.4.5 Synthesis of RAFT agent 2: 4-cyanopentanoic acid dithiobenzoate 99
3.4.6 Synthesis of PMMA1 macroRAFT agent 100
3.4.7 General procedure for RAFT polymerisation of MMA arm-first star polymer 101
3.5 References 102
4 Synthesis of oil soluble star polymers for use as viscosity modifiers in engine oils 105
4.1 Introduction 107
4.1.1 Viscosity 107
4.2 Results and Discussion 113

4.2.1 Synthesis of oil soluble core cross-linked star polymers 113

4.3 Conclusions 149

4.4 Experimental 151

4.4.1 Instrumentation 151

4.4.2 General method for calculating the percentage arm incorporation into stars when using an arm-first approach. 152

4.4.3 Materials 153

4.4.4 General procedure for arm-first star poly(C12-15MA-co-MMA) synthesis (batch reactions in toluene) 154

4.4.5 General procedure for copolymerisation of C12-15MA and MMA (Bulk reaction in mineral oil) 154

4.4.6 General procedure for copolymerisation of C12-15MA and MMA (Monomer feed reaction in mineral oil) 155

4.4.7 General procedure for arm-first star poly(C12-15MA-co-MMA) synthesis (Using Macro-RAFT agents) 155

4.5 References 157

5 Towards multi-arm star glycopolymers using a combination of RAFT and “click” chemistry 159

5.1 Introduction 161

5.1.1 Copper catalysed azide-alkyne cycloaddition (CuAAC) 164

5.1.2 Thiol-ene click reactions 173

5.1.3 Thiol-yne click reactions 175

5.2 Results and Discussion 178

5.2.1 Synthesis of polymer scaffolds for post polymer modification 178

5.2.2 Post polymerisation modification of poly(propargyl methacrylate) scaffolds 192

5.2.3 CuAAC of sugar azides to linear poly(propargyl methacrylate) scaffold 193

5.2.4 Thiol-yne “click” of thiol sugars to linear alkyne polymers 202

5.2.5 Synthesis of thio mannose 206

5.2.6 Core-crosslinked glycol-star polymers 210

1.4.1 “Exploding” star polymers: mannose glycopolymer core-crosslinked star, with cleavable crosslinker 215

1.4.2 Preliminary study into the synthesis of oil soluble “clickable” star polymers 219

5.3 Conclusions 224

5.4 Experimental 226

5.4.1 Instrumentation 226

5.4.2 Materials 227

5.4.3 General procedure for RAFT polymerisation of propargyl methacrylate, P(PgMA)9 . 227

5.4.4 Synthesis of trimethylsilyl propargyl methacrylate (TMSPgMA) 228

5.4.5 General procedure for RAFT polymerisation of trimethylsilyl propargyl methacrylate 228

5.4.6 Removal of trimethylsilyl protection groups 229

5.4.7 Synthesis of sugar azides 230

5.4.8 Synthesis of thio mannose 231

5.4.9 General procedure for CuAAC of sugar azides to poly (propargyl methacrylate) 235

5.4.10 Thiol-yne click reaction of thio mannose to poly(propargyl methacrylate) 236

5.4.11 Synthesis of N,N'-bis(methacryloyl)cystamine (crosslinker10) 236

5.4.12 General procedure for copolymerisation of "clickable" monomer with C12-15MA .. 237

5.4.13 Removal of TMS groups from P(C12-15MA-co-TMSPgMA) 238

5.5 References 239

6 Conclusions and Further Work 246

6.1 References 253

List of Figures

Figure 1: Different subcategories polymer star architecture 4

Figure 2: Reaction scheme for free radical addition polymerisation, initiation, propagation, chain transfer and termination. 5

Figure 3: General groups of RAFT agents and groups of monomers that they are suitable for the polymerisation thereof. 8

Figure 4: From reference.[15] Guidelines for the selection of RAFT agents for some general polymerisations. For the z group, addition rates decrease and fragmentation rates increase from left to right. The R group fragmentation rates decrease from left to right. Dashed line indicates partial control (i.e. control of molecular weight but poor PDI). MMA = methyl methacrylate, S = styrene, MA = methyl acrylate, AM = acrylamide, AN = acylonitrile, VAc = vinyl acetate. 8

Figure 5: M_p of various linear calibration standards on a plot of logMW against retention time (retention volume) in the GPC. These plots are used as a calibration curve for conventional GPC. ... 20

Figure 6: Representation of the difference in root mean square radius of gyration of linear and star polymers of the same molecular weight. 21

Figure 7: Plot of Log [η].MW against retention volume for polymers of different molecular weights/chemistries and architectures. Copied without editing from reference.[52] 22

Figure 8 : Polymerisation of MMA using 3 arm initiator, by ATRP; (left) Molecular weight evolution with conversion, (right) Plot of $\ln([M]_0/[M]_t)$ against time as a kinetic plot. 39

Figure 9: Star polymers synthesised using a core-first approach ATRP, using initiators with 3, 5, 8 and 21 initiating sites. ~~~ = PMMA 40

Figure 10: CFStar1, 3 arm star PMMA: From multi-detector GPC, green trace is the Mark-Houwink plot, black trace is the molecular weight distribution calculated by universal calibration, dW/dlogMW. 43

Figure 11: CFStar2, 5-arm star PMMA: From multi-detector GPC, green trace is the Mark-Houwink plot, black trace is the molecular weight distribution calculated by universal calibration, dW/dlogMW 43

Figure 12 : CFStar3, 8-arm star PMMA: From multi-detector GPC, green trace is the Mark-Houwink plot, black trace is the molecular weight distribution calculated by universal calibration, dW/dlogMW. 44

Figure 13: CFStar4, 21 arm star PMMA: From multi-detector GPC, green trace is the Mark-Houwink plot, black trace is the molecular weight distribution calculated by universal calibration, dW/dlogM. 45

Figure 14: Mark-Houwink plots of linear PMMA, and 3, 5, 8 and 21 arm star PMMA 45

Figure 15: PMMA 3-arm star polymer: The estimated functionality, f, plotted over the distribution of the polymer, estimated from the radius of gyration contraction factor, g. The Zimm and Stockmayer solution for regular arm star polymers was used to relate g to f. The red box shows the functionality of the initiator ±1. 47

Figure 16: PMMA 5-arm star polymer: The estimated functionality, f, plotted over the distribution of the polymer, estimated from the radius of gyration contraction factor, g. The Zimm and Stockmayer solution for regular arm star polymers was used to relate g to f. The red box shows the functionality of the initiator ±1. 48

Figure 17: PMMA 8-arm star polymer: The estimated functionality, f, plotted over the distribution of the polymer, estimated from the radius of gyration contraction factor, g. The Zimm and Stockmayer solution for regular arm star polymers was used to relate g to f. The red box shows the functionality of the initiator ±1. 49

Figure 18 : PMMA 21-arm star polymer: The estimated functionality, f, plotted over the distribution of the polymer, estimated from the radius of gyration contraction factor, g. The Zimm and Stockmayer solution for regular arm star polymers was used to relate g to f. The red box shows the functionality of the initiator ±1. 49

Figure 19: Cross-linking agents used in arm-first core cross-linked star polymer synthesis. 68

Figure 20: X-ray crystal structure of RAFT agent 1 2-cyanoprop-2-yl dithiobenzoate (RAFT agent 1). 71

Figure 21: GPC chromatograms of polymers formed after reaction of a PMMA macro RAFT agent with 4 equivalents of crosslinker 1 and varying amounts of MMA. 73

Figure 22: Crosslinkers used in this study. Crosslinker 1;ethylene glycol dimethacrylate, crosslinker 2;di (ethylene glycol) dimethacrylate and crosslinker 3; tri(ethylene glycol) dimethacrylate. 75

Figure 23: Molecular weight distributions from of 18 repeat polymerisations of MMA to form precursor arms. The target molecular weight was 10,000 $g.mol^{-1}$ for each. Labelled with the crosslinker (E=EGDMA, D=DEGDMA, and T=TEGDMA) and the number denotes the number of equivalents relative to RAFT agent. 76

Figure 24: (left) M_n vs. conversion for polymerisation of MMA using CPDB in toluene at 65 ^{o}C. (right) first order kinetic plot showing $\ln([M]_0/[M]_t)$ vs. time. 77

Figure 25: MWD of PMMA star polymers made using crosslinker 1 from the analysis by conventional $CHCl_3$ GPC. 78

Figure 26: Conventional GPC analysis of PMMA star polymers made using crosslinker 3 as crosslinker. 80

Figure 27: Conventional GPC analysis of PMMA star polymers made using crosslinker 2 as crosslinker. 82

Figure 28. Mark-Houwink plots from multi-detector GPC. Polymers made using crosslinker 1 as crosslinker. Intrinsic viscosity data is plotted in blue and molecular weight distribution is plotted in black. The experiments are labelled such that the letter denotes the crosslinker (E=crosslinker 1, D=crosslinker 2, and T=crosslinker 3) used and the number is the ratio of crosslinker to PMMA arms. 84

Figure 29: Mark-Houwink plots from multi-detector GPC. Polymers made using crosslinker2 as crosslinker. Intrinsic viscosity data is plotted in blue and molecular weight distribution is plotted in black. The experiments are labelled such that the letter denotes the crosslinker (E=crosslinker 1,

D=crosslinker 2, and T=crosslinker 3) used and the number is the ratio of crosslinker to PMMA arms. 85

Figure 30: Mark-Houwink plots from multi-detector GPC. Polymers made using crosslinker3 as crosslinker. Intrinsic viscosity data is plotted in blue and molecular weight distribution is plotted in black. The experiments are labelled such that the letter denotes the crosslinker (E=crosslinker 1, D=crosslinker 2, and T=crosslinker 3) used and the number is the ratio of [crosslinker] to [PMMA arms]. 86

Figure 31: Calculated functionality for star polymers made using varying amounts of crosslinker 1 as crosslinker. The functionality is calculated based on the equation derived by Zimm and Stockmayer for stars with regular arm lengths: $g=(3/f)-(2/f^2)$, where f is the number of arms and g is the radius of gyration contraction factor. 87

Figure 32: Plot of functionality (number of arms) against molecular weight of the star polymers. Using the equation $f \approx M_{n,star}/M_{n,arm}$ with a constant value of $M_{n,arm}$ calculated to be 9,000 $g.mol^{-1}$ by GPC. 89

Figure 33: Plot of Functionality (number of arms) against molecular weight of star polymer. Star polymers have had their functionalities estimated using a contraction factor from the intrinsic viscosity of the star relative to a linear polymer. The functionality has been determined using a model relating the radius of gyration contraction factor (g) with the functionality of the star polymer: $g= (3f)- (2/f^2)$. Overlaid is the function $f=MW_{star}/M_{n,arm.}$ 90

Figure 34: Calculated functionality for star polymers made using varying amounts of crosslinker1 as crosslinker. The number of arms is calculated based on the equation derived by Zimm and Stockmayer for irregular arm lengths: $g= (3f)/ (f+1)^2$, where f is the number of arms and g is the radius of gyration contraction factor. 91

Figure 35: Plot of functionality (number of arms) against molecular weight of star polymer. Star polymers have had their functionalities estimated using a contraction factor from the intrinsic viscosity of the star relative to a linear polymer. The functionality has been determined using a

model relating the radius of gyration contraction factor (g) with the functionality of the star polymer: $g = (3f)/(f+1)^2$. Overlaid is the function, $f=MW_{star}/M_{n,arm}$. 92

Figure 36: (Black) PMMA core-crosslinked star polymer MWD. (Green) four Gaussian curves calculated by Microcal Origin 8.0. (Red) Sum of the Gaussian curves..... 95

Figure 37: Ball and stick model of the X- crystal structure of RAFT agent 1..... 96

Figure 38: ^{1}H NMR of 2-cyanoprop-2-yl dithiobenzoate (RAFT agent 1)..... 96

Figure 39: A fluid moving under a shear rate, $\dot{\gamma}$ ($\dot{\gamma}=d\gamma/dt$), and a shear stress, τ ($\tau = F/A$)..... 107

Figure 40: Plot of viscosity and temperature for a base oil, and an oil with a VM..... 109

Figure 41: Cartoon describing the increase in volume with temperature of a star VM in solution. The green sphere represents the core of the star, and the blue ribbons represent the polymer arms. .. 110

Figure 42: relationship between shear stability index and viscosity index for VMs of different compositions and architecture. PIB= linear poly(isobutylene), PMA = poly(long chain alkyl methacrylate), Controlled Architecture VM= higher architecture (e.g. Stars, hyper branched) poly(long chain methacrylate). Copied without editing from reference.[170] 112

Figure 43: Plot of log $\ln([M]_0/[M]_t)$ against reaction time. A linear plot shows first order kinetics. .. 115

Figure 44: Molecular weight and PDI evolution with conversion for the bulk polymerisation of $C_{12\text{-}15}$MA / MMA copolymer using RAFT agent 3, targeting 10,600 g.mol^{-1}. 116

Figure 45: MWDs of polymers formed during the bulk co-polymerisation of $C_{12\text{-}15}$MA and MMA at different reaction times. 117

Figure 47: Kinetic plot for reaction E60. Co-polymerisation of $C_{12\text{-}15}$MA and MMA followed by addition of crosslinker 1 after 300 minutes..... 119

Figure 48: Reaction E60: Molecular weight evolution with conversion for the copolymerisation of $C_{12\text{-}15}$MA and MMA followed by the addition of crosslinker 1. 119

Figure 49: Reaction E60: Change in MWD with polymerisation time for the co-polymerisation of $C_{12\text{-}15}$MA and MMA followed by addition of crosslinker 1 after 300 minutes..... 120

Figure 50: Kinetic plot for reaction D62. Co-polymerisation of C_{12-15}MA and MMA followed by addition of crosslinker 2 after 300 minutes 121

Figure 51: Reaction D62. Molecular weight evolution with conversion for the copolymerisation of C_{12-15}MA and MMA followed by the addition of crosslinker 2 121

Figure 52: Reaction D62. Change in MWD with polymerisation time for the co-polymerisation of C_{12-15}MA and MMA followed by addition of crosslinker 2 after 300 minutes 122

Figure 53: Reaction T63. Kinetic plot for reaction. Co-polymerisation of C_{12-15}MA and MMA followed by addition of crosslinker 3 after 300 minutes 123

Figure 54: Reaction T63. Molecular weight evolution with conversion for the copolymerisation of C_{12-15}MA and MMA followed by the addition of crosslinker 3 123

Figure 55: Reaction T63. Change in MWD with polymerisation time for the co-polymerisation of C_{12-15}MA and MMA followed by addition of crosslinker 3 after 300 minutes 124

Figure 56: ^{1}H NMR of p(C_{12-15}MA-MMA) statistical copolymer arms after reaction with crosslinker3. (inset) Possible structure of yielded polymer, with peak assigned. Note the apparent absence of vinyl peaks k. 125

Figure 57: Mayo plot of [RAFT agent 3]/[Monomer] against 1/degree of polymerisation, where DP is calculated by M_n/m_0 where M_n is the number average molecular weight and m_0 is the average RMM of the monomer. 128

Figure 58: Labelled photograph of monomer feed system 131

Figure 59: Molecular weight and PDI evolution with conversion for the bulk polymerisation (i.e. 100% monomer in reactor at the beginning of the reaction) of C_{12-15}MA / MMA copolymer using RAFT agent 3, targeting 10,600g.mol^{-1}. The red line shows the best fit of the data with linear equation shown below. 132

Figure 60: Plot showing the evolution of monomer concentration in the reactor, [M], with time when 50% of monomer is introduced at the beginning of the reaction, and the remaining 50% is fed at

0.3mL/min from 180minutes. Also shown is the concentration of monomer [M] added to the reactor and the overall conversion of the monomer. 133

Figure 61: Molecular weight and PDI evolution with conversion for the polymerisation of C_{12-15}MA / MMA copolymer using RAFT agent 3, targeting 10,600 g.mol^{-1}. 50% of the monomer mixture was present in the reactor at the beginning of the reaction, with the rest fed into the reactor at 0.3 mL/min once the initial monomer present had reached 80% conversion. The red line shows the best fit of the data with linear equation shown below. 134

Figure 62: Plot showing the evolution of monomer concentration in the reactor, [M], with time when 30% of monomer is introduced at the beginning of the reaction, and the remaining 70% is fed at 0.3 mL/min from 150 minutes. Also shown is the concentration of monomer [M] added to the reactor and the overall conversion of the monomer. 135

Figure 63: Molecular weight and PDI evolution with conversion for the polymerisation of long chain alkyl methacrylate / methyl methacrylate copolymer using RAFT agent 3, targeting 10,600 g.mol^{-1}. 30% of the monomer mixture was present in the reactor at the beginning of the reaction, with the rest fed into the reactor at 0.3 mL/min once the initial monomer present had reached 80% conversion. The red line shows the best fit of the data with linear equation shown below. 136

Figure 64: Plot showing the evolution of monomer concentration in the reactor, [M], with time when 10% of monomer is introduced at the beginning of the reaction, and the remaining 90% is fed at 0.3mL/min from 120 minutes. Also shown is the concentration of monomer [M] added to the reactor and the overall conversion of the monomer. 137

Figure 65: Molecular weight and PDI evolution with conversion for the polymerisation of C_{12-15}MA / MMA copolymer using RAFT agent 3, targeting 10,600 g.mol^{-1}. 10% of the monomer mixture was present in the reactor at the beginning of the reaction, with the rest fed into the reactor at 0.3 mL/min once the initial monomer present had reached 80% conversion. The red line shows the best fit of the data with linear equation shown below. 137

Figure 66: Change in molecular weight growth and PDI with conversion of monomer for a series of reactions containing various amounts of monomer at the beginning of the reaction. The remaining monomer was fed into the reactor at 0.03 mL/min after 80% of the initial monomer was consumed. 138

Figure 67: Evolution of the MWD during the polymerisation of $C_{12\text{-}15}$MA / MMA copolymer using RAFT agent 3, targeting 10,600 g.mol^{-1}. 10% of the monomer mixture was present in the reactor at the beginning of the reaction, with the rest fed into the reactor at 0.3 mL/min once the initial monomer present had reached 80% conversion..... 139

Figure 68: GPC spectra of macro-RAFT agent (arm) and after reaction for 3 hours at 90 ^{o}C with 4 equivalents of crosslinker 1 in the presence of Trigonox 21S radical initiator. 141

Figure 69: UV spectra of MMA, $C_{12\text{-}15}$MA and RAFT agent 3 in THF..... 142

Figure 70: UV spectrum from photodiode array connected in series on the GPC detector train. Wavelength against retention time against intensity. (star) marks the star polymer. (triangle) marks the linear arm..... 142

Figure 71: OilStar1, 2 and 3: GPC chromatograms of star polymers formed after reaction of macro-RAFT4 with 4 equivalents of crosslinker 1 for varying reaction times..... 144

Figure 72: Comparison of OilStar3 and 7 - GPC of star polymers formed after reaction of macro-RAFT4 with 4 equivalents of crosslinker 1 and 4.5 equivalents of crosslinker 1. 145

Figure 73: OilStar5, 6 and 7 - GPC of star polymers formed after reaction of macro-RAFT4 with 4.5 equivalents of crosslinker 1 relative to RAFT agent for varying reaction times. 146

Figure 74: OilStar7 and 8 - GPC of star polymers formed after reaction of macro-RAFT4 with 4.5 equivalents of crosslinker 1 relative to RAFT agent for 17 hours. Overlaid with the polymer resulting from 2nd addition of initiator added after 17 hours and reacted for 3 hours..... 146

Figure 75: OilStar7, 9 and 10 - GPC of star polymers formed after reaction of macro-RAFT4 with 4.5 equivalents of crosslinker 1 relative to macro-RAFT4 for 17hours. Overlaid are the star polymers

resulting after reaction with additional crosslinker1 and initiator after 17 hours, and further crosslinker1 and initiator after 20 hours. 147

Figure 76: Oilstar10 - UV spectrum from PDA connected in series on the GPC detector train. Wavelength against retention time against intensity..... 148

Figure 77: (Black) Core-crosslinked star polymer MWD. (Green) 4 Gaussian curves calculated by Microcal Origin 8.0. (Red) Sum of the Gaussian curves..... 152

Figure 78: Example of a core-crosslinked star polymer MW, with the boundaries of the different polymer species marked a, b and c..... 153

Figure 79: Molecular weight distribution of PgMA1. Synthesised using RAFT agent 1 and AIBN in toluene at 65 ^{o}C. 179

Figure 80: P(TMSPgMA)5. Polymerisation of TMSPgMA targeting a DP of 100, first order kinetic plot. 181

Figure 81: P(TMSPgMA)5. Polymerisation of TMSPgMA targeting a DP of 100. Evolution of M_n and PDI with percentage monomer conversion 182

Figure 82: P(TMSPgMA)5. Polymerisation of TMSPgMA targeting a DP of 100. 3D plot of UV wavelength (nm) and retention time in GPC (mins) with the colour intensity representative of UV absorption. 182

Figure 83: P(TMSPgMA)6. Polymerisation of TMSPgMA targeting a degree of polymerisation (DP) of 200, first order kinetic plot. 183

Figure 84: P(TMSPgMA)6. Polymerisation of TMSPgMA targeting a DP of 200. Evolution of M_n and PDI with percentage monomer conversion. 184

Figure 85: P(TMSPgMA)6. Polymerisation of TMSPgMA targeting a DP of 200. 3D plot of UV wavelength (nm) and retention time in GPC (mins) with the colour intensity representative of UV absorption. 185

Figure 86: P(TMSPgMA)7. Polymerisation of TMSPgMA targeting a DP of 300. Plot of $\ln([M]_0/[M]_t)$ against time..... 185

Figure 87: P(TMSPgMA)7. Polymerisation of TMSPgMA targeting a DP of 300. Evolution of M_n and PDI with monomer conversion. 186

Figure 88: P(TMSPgMA)7. Polymerisation of TMSPgMA targeting a DP of 300. 3D plot of UV wavelength (nm) and retention time in GPC (mins) with the colour intensity representative of UV absorption. 187

Figure 89: (Left) ^{1}H NMR of P(TMSPgMA)5 and after deprotection, P(PgMA)5. (Right) ^{1}H NMR of P(TMSPgMA)6 and after deprotection, P(PgMA)6. Green boxes highlght the chemical shift of where the alkyne and TMS protons appear in ^{1}H NMR. 189

Figure 90: MWD from GPC of different P(TMSPgMA) before and after deprotection of the propargyl groups with TBAF to yield P(PgMA). 190

Figure 91: MALDI TOF spectrum of P(PgMA)1 (Matrix: trans-2-[3-(4-tert-Butylphenyl)-2-methyl-2-propenylidene]malononitrile (DCTB), salt: NaI, laser power: 30%) 191

Figure 92: IR spectra for the reagents and product of the CuAAC of P(PgMA)6 and mannose azide. 194

Figure 93: DMF GPC of P(PgMA)6 before and after CuAAC reaction with mannose azide. 194

Figure 94: ^{1}H NMR spectrum of P(PgMA)6 after CuAAC reaction with mannose azide in DMSO at ambient temperature using TBTA copper complex as copper catalyst. Assigned peaks are from the resultant glycopolymer. Peaks for TBTA, DMSO and H_2O are also present 195

Figure 95: FT-IR of mannose azide and mannose polymers synthesised by the CuAAC of P(PgMA) scaffolds and mannose azide. 196

Figure 96: Example of ^{1}H NMR analysis. ^{1}H NMR spectrum of P(PgMA)4 after CuAAC reaction with mannose azide in DMSO at ambient temperature using N-(ethyl)-2-pyridylmethanimine as the copper ligand. Assigned peaks are from the resultant glycopolymer. 197

Figure 97: Example of ^{1}H NMR analysis in D_2O. ^{1}H NMR spectrum of P(PgMA)4 after CuAAC reaction with galactose azide in DMSO at ambient temperature using N-(ethyl)-2-pyridylmethanimine as the copper ligand. Assigned peaks are from the resultant glycopolymer, P(galactoseMA)3. 199

Figure 98: FT-IR of galactose azide and galactose polymers synthesised using P(PgMA) scaffolds and galactose azide. 200

Figure 99: MWDs from DMF GPC of the series of p(galactoseMA) polymers synthesised from deprotected P(TMSPgMA) polymers (P(PgMA)). 201

Figure 100: ^{1}H NMR of PMMA macro RAFT agent, and hydroxyethyl terminated PMMA after thiol-ene reaction. 203

Figure 101: One pot nucleophilic removal of dithiobenzoate group to yield a thiol and subsequent phosphine catalysed Michael addition to hydroxyethyl acrylate. 3D plots of UV wavelength (nm) and retention time in GPC (mins) with the colour intensity representative of UV absorption. Inset is the colour of the polymers before and after reaction. (Left) PMMA macroRAFT agent. (Right) after reaction with hydroxyethyl acrylate in the presence of DMPP. 204

Figure 102: MALDI-TOF spectrum of PMMA made using RAFT agent1 and AIBN. 205

Figure 103: MALDI-TOF spectrum of resultant PMMA after thiol-ene Michael addition with hydroxyethyl acrylate. Distribution: 68.05 + (100.12n) + 149.03 + 22.99, where n = 13, m/z = 1541.63 g.mol^{-1} 205

Figure 104: FT-IR spectra of thio mannose, P(PgMA)6, and P(PgMA)6 after thiol-yne reaction and dialysis to remove low molecular weight molecules. 208

Figure 105: ^{1}H NMR spectrum of P(PgMA)6 after radical thiol-yne click with thio mannose. 208

Figure 106: $CHCl_3$ GPC of P(TMSPgMA)6 and resultant starP(TMSPgMA)1 polymer after reaction with crosslinker1. Ratio of crosslinker1 to macroRAFT agent, P(TMSPgMA)6, = 4. 211

Figure 107: CuAAC of starP(PgMA)1 polymer with mannose azide, catalysed by triazole containing TBTA under an inert atmosphere of N_2. 212

Figure 108: Partial ^{1}H NMR spectrum between 7.0 and 9.0 ppm for the reaction of mannose azide with starP(PgMA)2. 212

Figure 109: DMF GPC spectra of starP(PgMA)2 before and after the CuAAC reaction with mannose azide. 213

Figure 110: IR spectra of starP(PgMA)2 alkyne bearing polymer, mannose azide and starP(PgMA)2 after CuAAC with mannose azide. 214

Figure 111: $CHCl_3$ GPC of P(TMSPgMA)6 and resultant starP(TMSPgMA) polymer after reaction with crosslinker1. Ratio of crosslinker5 to macroRAFT agent, P(TMSPgMA)6, was 4. Also showing "exploded" starP(TMSPgMA) after reaction with tributylphosphine. 216

Figure 112: ^1H NMR of starP(TMSPgMA) before and after reaction with TBAF. Green boxes highlight the area of the spectra where TMS and alkyne peaks are located. 217

Figure 113: FT-IR spectrum of starP(PgMA)2 217

Figure 114: ^1H NMR of starP(PgMA)2 after CuAAC with mannose azide in DMSO-d6. 218

Figure 115: ^1H NMR spectrum of P(TMSPgMA-co-$C_{12\text{-}15}$MA) made using RAFT agent1 and AIBN at 65 ^oC. 220

Figure 116: GPC molecular weight distribution of linear P($C_{12\text{-}15}$MA-co-TMSPgMA), and after crosslinking with crosslinker1 to form starP($C_{12\text{-}15}$MA-co-TMSPgMA) 222

Figure 117: $CHCl_3$ GPC of starP($C_{12\text{-}15}$MA-co-TMSPgMA) and after reaction to form Star(P($C_{12\text{-}15MA}$-co-PgMA) 223

List of Tables

Table 1: Examples of ATRP core-first initiators. 31

Table 2: Examples of RAFT core-first initiators. 33

Table 3: Examples of NMP core-first initiators. 34

Table 4: GPC results 3, 5, 8 and 21-arm star PMMA by both conventional GPC using a differential refractometer and linear PMMA standards to create a calibration curve, and by universal calibration using a differential refractometer and a four capillary viscometer 40

Table 5: The M_n, PDI and% arm incorporation of each star polymer (not including arm impurity) synthesised using PMMA 1 as a macro RAFT agent. Arm incorporation was determined by deconvolution of GPC spectra. ł Determined using conventional GPC against PMMA standards. * Determined using Universal calibration. 74

Table 6: PMMA star polymers made by an arm-first route using crosslinker1 as cross-linking agent. GPC analysis of stars is over the entire molecular weight distribution, inclusive of unreacted arm. ł Determined using conventional GPC against PMMA standards. * Determined using universal calibration. Mark-Houwink exponent is averaged over the entire molecular weight distribution. Conversions were determined by ^{1}H-NMR. Arm incorporation determined by deconvolution of GPC spectra. 78

Table 7: PMMA star polymers made by an arm-first route using crosslinker 3 as cross-linking agent. GPC analysis of stars is over the entire molecular weight distribution, inclusive of unreacted arm. ł Determined using conventional GPC against PMMA standards. * Determined using Universal calibration. Mark-Houwink exponent is averaged over the entire molecular weight distribution. Conversions were determined by ^{1}H-NMR. Arm incorporation determined by deconvolution of GPC spectra. 79

Table 8: PMMA star polymers made by an arm-first route using crosslinker 2 as cross-linking agent. GPC analysis of stars is over the entire molecular weight distribution, inclusive of unreacted arm. ł

Determined using conventional GPC against PMMA standards. * Determined using universal calibration. Mark-Houwink exponent is averaged over the entire molecular weight distribution. Conversions were determined by ^{1}H-NMR. Arm incorporation determined by deconvolution of GPC spectra. 81

Table 9: Crystallographic data for 2-cyanoprop-2-yl dithiobenzoate 98

Table 10: Results from the synthesis of star polymers via an arm-first procedure using RAFT polymerisation. The number average molecular weight, PDI were determined using conventional GPC against PMMA standards. Conversions were determined by ^{1}H NMR. Arm incorporation was determined by deconvolution of GPC spectra. 126

Table 11: Polymerisations used to determine the chain transfer constant for RAFT agent 3 during the co-polymerisation of $C_{12\text{-}15}$MA and MMA. 130

Table 12: Summary of macro-RAFT agents formed using batch and feed processes in mineral oil to be used in star formation 140

Table 13: Summary of oil soluble star polymers synthesised using macro-RAFT4. 144

Table 14: Selected examples on different combinations of click reactions and polymerisation techniques to synthesise glycopolymers. 162

Table 15: Summary of alkyne polymer scaffolds synthesised for further modification, by polymerisation reactions of TMSPgMA and deprotection of TMS groups 187

Table 16: Table of mannose polymers synthesised from series of P(PgMA) polymers. M_n and PDI are calculated from DMF GPC analysis.% click was calculated using comparison of backbone protons and triazole proton peak integrals in ^{1}H NMR. 198

Table 17: Table of galactose polymers synthesised from series of P(PgMA) polymers. M_n and PDI are calculated from DMF GPC analysis.% click was calculated using comparison of backbone protons and triazole proton peak integrals in ^{1}H NMR. 201

List of Schemes

Scheme 1: Important mechanisms in ATRP. 'R-X' is an halogen initiator reacting with a transition metal complex '$M^nX_nL_m$', wherein M is a transition metal in oxidation state n, complexed by n halogen species, X, and m neutral ligands, L. 7

Scheme 2: Important mechanisms present in RAFT polymerisation. 'I' is an initiator, P_n is a polymer of n units, P_m is a polymer of m repeat units. R is a leaving group on the RAFT agent and Z is a group used to control the reactivity of the RAFT agent. 9

Scheme 3: Reaction scheme of nitroxide mediated radical polymerisation, utilising a stable nitroxide radical to mediate polymerisation. 10

Scheme 4: Various reactions that have been termed "click" reactions. 12

Scheme 5: Controlled radical polymerisation methods for core-first star synthesis. 35

Scheme 6: Core-first polymerisation of stars by method b using RAFT and NMP initiators. 36

Scheme 7: General synthesis of multi functional initiator from the esterification of alcohols with a tertiary bromide functionalised acid bromide. 38

Scheme 8: Polymerisation of MMA from a trifunctional initiator to form a 3 arm PMMA star, CFStar1. 〰 = PMMA 38

Scheme 9: Synthesis of 3-arm initiator from 1,1,1-tris (hydroxymethyl) ethane 53

Scheme 10: Polymerisation of MMA using 1,1,1- tris(methyl-O-isobutyryl bromide) ethane initiator. 54

Scheme 11: ATR Polymerisation of methyl methacrylate using 1,2,3,4,6-penta-O-isobutyryl bromide-α-D-glucose initiator. 55

Scheme 12: ATR polymerisation of MMA using lactose based 8-arm initiator. 56

Scheme 13: ATR Polymerisation of MMA using β-CD based 21-arm initiator. 57

Scheme 14: General reaction scheme for star formation using core-crosslinking. ⬬ = initiating species, X= propagating chain end, 〰 = polymer, R_1 varies depending on crosslinker used. 70

Scheme 15: Synthesis of 2-cyanoprop-2-yl dithiobenzoate (RAFT agent 1), and 4-cyanopentanoic acid dithiobenzoate (RAFT agent 2), by first synthesising bis(thiobenzoyl) disulfide. 72
Scheme 16: Polymerisation of MMA with RAFT agent 2 and ACVA in toluene at 65 ^{o}C. 73
Scheme 17: RAFT polymerisation of PMMA star polymers by a core-crosslinking method. Target DP of MMA was 100, and AIBN was added with crosslinker after high conversion of monomer to yield a star architecture..... 75
Scheme 18: Arm-first star polymer synthesis using t-butyl peroxy-2-ethylhexanoate, (Trigonox 21S) as a peroxide radical source, with a RAFT agent 3, and $C_{12\text{-}15}$MA and MMA as monomers. 114
Scheme 19 Reaction scheme for the synthesis of $C_{12\text{-}15}$MA / MMA copolymer stars by an arm-first route..... 118
Scheme 20: Reaction of oil soluble macro-RAFT agent with crosslinker 1 to form star polymers..... 140
Scheme 21: Various synthetic routes to glycopolymers using ATRP and CuAAC employed by Haddleton et al. 166
Scheme 22: The synthesis of glycopolymers via cobalt catalysed - catalytic chain transfer polymerisation and click reactions by Haddleton et al..... 169
Scheme 23: The synthesis of glycopolymers via ROP of ε-caprolactone (CL) and 2-bromo-ε-caprolactone (BrCL) blocks, modification of the bromo moieties to azides, and CuAAC click. 171
Scheme 24: The synthesis of a 4-vinyl-1,2,3-triazole glycomonomer (top) and RAFT polymerisation (bottom)..... 172
Scheme 25: Synthesis of glycopolymers by combination of cationic ring opening polymerisation of 2-oxazoline and thiol-ene click reaction. 174
Scheme 26: Synthesis of hyperbranched glycopolymers using RAFT polymerisation and CuAAC click reactions (left) or thiol-yne click reactions (right). 175
Scheme 27: Synthesis of hyperbranched glycopolymers by RAFT using an alkyne functional RAFT agent and CuAAC click. 176

Scheme 28: RAFT polymerisation of PgMA, in the presence of AIBN and RAFT agent 1, in toluene at 65 °C, under nitrogen. 178

Scheme 29: Synthesis of trimethylsilyl propargyl methacrylate (TMSPgMA) from 3-trimethylsilyl propyn-1-ol and methacryloyl chloride. 179

Scheme 30: Reaction scheme of RAFT polymerisation of TMSPgMA in the presence of AIBN and RAFT agent 1 in toluene at 60 °C. 180

Scheme 31: Removal of TMS groups from P(TMSPgMA) using TBAF to yield alkyne bearing polymer, P(PgMA). 188

Scheme 32: Synthesis of mannose and galactose azide using DMC in a one-step process.[37,204] 192

Scheme 33: CuAAC reaction of P(PgMA) and mannose azide with tris[(1-benzyl-1H-1,2,3-triazol-4-yl)methyl]amine (TBTA) as the ligand for the copper catalyst to yield P(mannoseMA) polymer 193

Scheme 34: CuAAC reaction of P(PgMA) and mannose azide with N-(ethyl)-2-pyridylmethanimine as the ligand for the copper catalyst. 196

Scheme 35: CuAAC reaction of P(PgMA) and galactose azide with N-(ethyl)-2-pyridylmethanimine as the ligand for the copper catalyst. 198

Scheme 36: Phosphine catalysed thiol-ene reaction of hydroxyethyl acrylate and dithiobenzoate group of PMMA synthesised using RAFT agent 1. 203

Scheme 37: Synthesis of 2'- thioethyl -O-α-D-mannopyranoside. Reagents and conditions: a) 2-Bromoethanol, BF_3OEt_2, -20 °C to ambient temperature, b) KSAc, Acetone, reflux 60 °C, c) CH_3ONa (cat.), CH_3OH, ambient temperature. 206

Scheme 38: Reaction of P(PgMA) with 2'- thioethyl -O-α-D-mannopyranoside to yield glycopolymer 207

Scheme 39: Reaction of P(TMSPgMA) macroRAFT agent with crosslinker1 to form a core-crosslinked star polymer, starP(TMSPgMA)1. 210

Scheme 40: Reaction of starP(TMSPgMA)1 with TBAF to remove TMS groups to make alkyne bearing star polymer, starP(PgMA). 211

Scheme 41: Synthesis of N,N′-bis(methacryloyl)cystamine from cystamine dihydrochloride. 215

Scheme 42: Reaction scheme for the core-crosslinking reaction with macroRAFT agent P(TMSPgMA)6 and crosslinker10. 215

Scheme 43: CuAAC of starP(PgMA)2 with mannose azide using N-(ethyl)-2-pyridylmethanimine as the ligand for the copper catalyst. 218

Scheme 44: Reaction scheme for the copolymerisation of $C_{12\text{-}15}$MA and TMSPgMA using RAFT agent 1. 220

Scheme 45: Chain extension of P(C12-15MA-co-TMSPgMA) with crosslinker1 to form core-crosslinked star polymer. 221

Scheme 46: Deprotection of starP($C_{12\text{-}15}$MA-co-TMSPgMA) using TBAF to yield starP($C_{12\text{-}15}$MA-co-PgMA). 222

Scheme 47: Synthesis of acetylated mannose. Prepared as described by Geng and co-workers,[35,199] and Watt et al.[240] 231

Scheme 48: Synthesis of bromo-sugars from acetylated sugars. (b) - Prepared as described by Rama Rao et al.[234] 232

Scheme 49: Synthesis of acetylated thio mannose from bromine intermediate. Prepared as described by Grandjean et al.[235,236] 233

Scheme 50: Deprotection of thio sugars as described by Grandjean and co-workers.[198,235,236] 234

List of Abbreviations

ACVA	4,4'-azobis(4-cyanopentanoic acid)
AIBN	azoisobutylnitrile
AM	acrylamide
AN	acrylonitrile
ATR	atom transfer radical
ATRP	atom transfer radical polymerisation
Br-CL	2-bromo-ε-caprolactone
$C_{12\text{-}15}MA$	long chain alkyl methacrylate
CCTP	cobalt catalysed chain transfer polymerisation
CD	cyclodextrin
CF	core-first
CL	ε-caprolactone
Con A	Concanavalin A
Conv.	conversion
CPADB	(4-cyanopentanoic acid)-4-dithiobenzoate
CPDB	2-cyanoprop-2-yl dithiobenzoate

CROP	cationic ring-opening polymerisation
CRP	controlled/living radical polymerisations
CTA	chain transfer agent
CuAAC	copper (I)-catalysed azide-alkyne cycloaddition
DEGDMA	di(ethylene glycol) dimethacrylate
DEGMA	diethylene glycol methacrylate
DMSO-d6	deuterated dimethylsulfoxyde
DIPEA	diisopropylethylamine
DMAEMA	2-(dimethylamino)ethyl methacrylate
DMC	2-chloro-1,3-dimethylinidazolonium chloride
DMF	*N,N*-dimethyl formamide
DMPP	*dimethyl phenyl phosphine*
DMSO	dimethyl sulfoxide
dn/dc	specific refractive index increment
DP	degree of polymerisation/kinetic chain length
DRI	differential refractive index
EGDMA	ethylene glycol dimethacrylate

f	functionality (number of arms)/ initiator efficiency
FRP	free radical polymerisation
FT-IR	Fourier transform infrared
g^{I}	intrinsic viscosity reduction factor
g	radius of gyration contraction factor
GPC	gel permeation chromatography
HEA	hydroxyethyl acrylate
I	initiator
LCST	lower critical solution temperature
LRP	living radical polymerisation
M	monomer/ mass
MA	methyl acrylate
MALDI	matrix assisted laser desorption ionisation mass spectroscopy
MALLS	multi angle laser light scattering
MBL	mannose binding lectin
MMA	methyl methacrylate
MMA	methyl methacrylate

M_n	number average molecular weight
M_p	peak molecular weight
MTSHEMA	methyl-1-triethylsiloxy-1-propenyloxy)-ethyl methacrylate
MW	molecular weight
M_w	weight average molecular weight
MWCO	molecular weight cut off
MWD	molecular weight distribution
NMP	nitroxide-mediated polymerisation
NMR	nuclear magnetic resonance
OEGMA	oligo(ethylene glycol) methacrylate
PDI	polydispersity index
PgMA	propargyl methacrylate
PIB	poly(isolbutylene)
PMMA	poly(methyl methacrylate)
P(PgMA)	poly(propargyl methacrylate)
ppm	parts per million
PS	polystyrene

RAFT	reversible addition fragmentation chain transfer
R_g	radius of gyration
RI	refractive index
ROMP	ring opening metathesis polymerisation
ROP	ring-opening polymerisation
S	styrene
SEC	size exclusion chromatography
SEM	scanning electron microscopy
SET-LRP	single electron transfer living radical polymerisation
SSI	shear stability index
TBAF	tetra-*n*-butylammonium fluoride
TBTA	tris-(benzyl-triazolylmethyl)amine
TEA	triethylamine
TEGDMA	tri(ethylene glycol) dimethacrylate
TEM	transmission electron microscopy
TEMPO	(2,2,6,6-Tetramethylpiperidin-1-yl)oxyl
THF	tetrahydrofuran

TMM-LRP	transition metal mediated living radical polymerisation
TMS	trimethylsilyl
TMSPgMA	trimethylsilyl propargyl methacrylate
UV	ultraviolet
VAc	vinyl acetate
V_h	hydrodynamic volume
VI	viscosity index
VM	viscosity modifier

Acknowledgments

The number of people to whom I am indebted for their kind donation of time and effort in teaching me and supporting my learning is so very large that, if I were to include them all, my acknowledgements would be longer than my first chapter. That said, I shall mention a few that have helped me in such a way that I feel their contribution is too great not to mention.

I am very grateful to Professor Haddleton for giving me this opportunity. To me Professor David Haddleton is a source of great inspiration; embodying the true spirit of scientific investigation and also its endeavour to find innovative solutions to every-day problems, large or small. His positive encouragement, never-ending support and "just do it" mentality has made my time spent studying for a PhD at Warwick both a pleasure and rewarding.

I would like to thank Timothy Smith, my industrial supervisor, and his colleagues at Lubrizol for their invaluable contributions and guidance throughout my research.

The selfless sacrifice of time by the post-docs and other researchers of polymer chemistry in the Warwick Chemistry Department, of various research groups, has taught me not only chemistry (I hope), but also much about the pursuit of common goals and teamwork. I am humbled to know that I have shared these corridors over the last 3 years with so many talented and kind hearted people; I thank you all.

The final thank you is to my girlfriend, Natalie and my mum, dad, and brothers for their constant loving support.

Abstract

The objective of this thesis was to investigate the synthesis of well defined star polymers utilising controlled radical polymerisation techniques for potential use as viscosity modifiers in Engine oils.

Recent developments in the characterisation of star polymers using multi-detector GPC was investigated by first synthesising a series of star polymers using a core-first technique and ATRP. Core-first initiators were used to initiate the polymerisation of PMMA star polymers which were then analysed using multi-detector GPC. Using Zimm and Stockmayer theory the functionality, *f*, (number of arms) of the resultant star polymer was estimated over the MWD of the polymer using GPC with in-line viscometry. A variation in functionality with molecular weight was seen, which disagrees with the limited other literature in the field.

The GPC technique was then used to determine the functionality of star polymers synthesised using RAFT polymerisation and an arm-first technique to yield star PMMA with a high M_w and PDI. Varying the divinyl species and the ratio of [crosslinker] to [macroRAFT agent] was seen to control the functionality and molecular weight of the star formed. Varying the amount of monomer present at the point of crosslinking was seen to have little contribution to the star polymer formed when the ratio of [MMA] to [macroRAFT agent] was under 10.

Switching RAFT agents from 2-cyanoprop-2yl dithiobenzoate (CPDB) to an oil soluble trithiocarbonate, for the RAFT polymerisation of long chain alkyl methacrylate gave hybrid polymerisation kinetics. Through a monomer feed system, controlling the ratio of [monomer] to [RAFT agent] throughout the reaction, polymers of narrow PDI were synthesised and subsequently crosslinked to form oil soluble star polymers.

Applying the techniques used for the synthesis of core-crosslinked star polymers using RAFT chemistry to different area of polymer chemistry, glycopolymers; a series of linear mannose and galactose bearing glycopolymers have been synthesised. Trimethylsilyl propargyl methacrylate

(TMSPgMA) has been polymerised to varying DP, between 20 and 200, using CPDB as the RAFT agent. Subsequent deprotection of the propargyl groups has yielded a series of alkyne bearing linear polymers. Using a CuAAC reaction to “click” mannose and galactose azide to the polymer scaffolds yielded well defined sugar bearing polymers. A P(TMSPgMA) macroRAFT agent was crosslinked using different crosslinkers to giving a high molecular weight, alkyne bearing, star polymer.

Declaration

Experimental work contained in this thesis is original research carried out by the author, unless otherwise stated, in the Department of Chemistry at the University of Warwick, between October 2008 and October 2011. No material contained herein has been submitted for any other degree, or at any other institution.

Results from other authors are referenced in the usual manner throughout the text.

Signed: _____ Date:_____

James Adam Burns

Chapter 1

Introduction

1.1 Star polymers

Branching in polymer chemistry is very common, occurring inherently or by design; with this branching giving both positive and negative material properties. For example, in commercial polymerisation of ethylene simple chain transfer reactions cause both short and long chain branching. Branching can also be introduced intentionally through the addition of di-functional monomers, such as divinylbenzene or di(meth)acrylates, into the polymerisation formulation. Introducing branching in a controlled manner allows access to higher architecture polymers with a wide variety of properties. For example, branched polymers generally exhibit unusual dilute solution properties, with lower viscosity and lower hydrodynamic properties than their linear equivalents.[1-5]

A typical type of branched polymer, a star polymer, has a 3 dimensional structure consisting of multiple linear polymers (arms) emanating from a central moiety (core). The structural density of star polymers decreases as we move further from the central moiety, along the arms, towards the exterior surface of a globular star. Dendrimers, which are often compared to star polymers as their more precise and uniform analogues, actually have the inverse property of having greater structural density towards the periphery of the structure, and lowest density at the core. It should also be noted that star polymers are generally considered easier to synthesise than dendrimers, which are only realised by laborious multistep synthesis.

The earliest published synthesis of star polymers was by Flory *et al*. in 1948, though this type of synthesis would become much easier in the ensuing decade with the advent of living polymerisation techniques. In 1956, Morton and co-workers used the much-improved control offered by anionic living polymerisation to synthesise well defined four arm polystyrene stars by terminating the living styrene polymer with a

tetrachlorosilane core.[6] When lithium is used as the counter-ion, the polar head group readily undergoes a metathesis reaction with electronegatively substituted silanes:

$$SiCl_4 + 4Polymer\ Li \rightarrow Si\ Polymer_4 + 4LiCl$$

This work led to increased interest in star polymers and set the precedence for the use of anionic living polymerisation and chlorosilanes for their preparation. Divinylbenzene (DVB) was first used as a crosslinking agent by Milkovich in 1964, whereby poly(styrene-*b*-isoprene) was linked using a preformed poly alkene DVB core; though the yield was very low.[7] In 1969, Worsfold *et al*. optimised the star formation of polystyrene stars using the preformed DVB globule route by varying the ratio of DVB to head group to yield stars with up to 15 arms.[8]

The advent of living radical polymerisation techniques such as atom transfer radical polymerisation (ATRP), reversible fragmentation chain transfer (RAFT) polymerisation and nitroxide mediated polymerisation (NMP), has enabled novel and often facile routes to star polymers with many different monomers which contain polar and functional groups which might be incompatible with carbanions. Synthesis using "living" polymerisation is often categorised into two general routes. The first is "*core-first*", whereby a multifunctional initiating species is formed and used to initiate polymerisation from the same core to, ideally, form a star with the same number of arms as initiating sites. The second general route is the so-called "*arm-first*" approach, whereby the living polymer (arm) is reacted with a multifunctional quencher or core-crosslinked with a multifunctional linking agent.

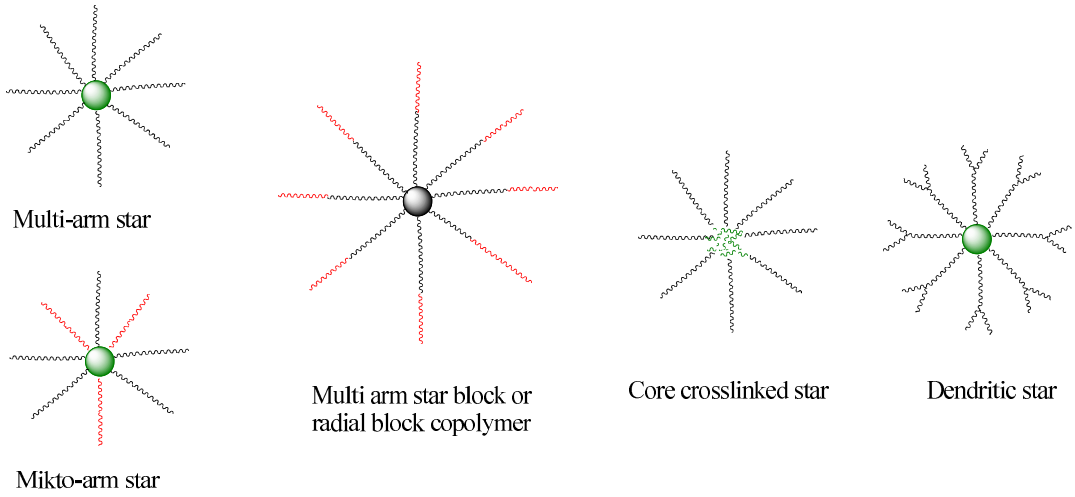

Figure 1: Different subcategories polymer star architecture

Within the concept of star polymers, a variety of architectures exist which can be realised in different ways. It is possible to form star block copolymers, figure 1, through polymerisation of block copolymer arms before crosslinking, or indeed by chain extension from a core-first star provided there is high enough retention of dormant chain end groups. It is also possible to form mikto-arm star polymers, figure 1, for instance, by retention of the dormant chain end groups in the core of a core-crosslinked polymer for further polymerisation of a secondary linear polymer arm. Some elements of these techniques have been used in ionic polymerisation; however, the advent of controlled radical polymerisation has made these routes more accessible.

1.2 Controlled radical polymerisation (CRP)

To understand CRP it is necessary to first understand some of the mechanisms of free radical polymerisation (FRP).

1.2.1 Free radical polymerisation (FRP)

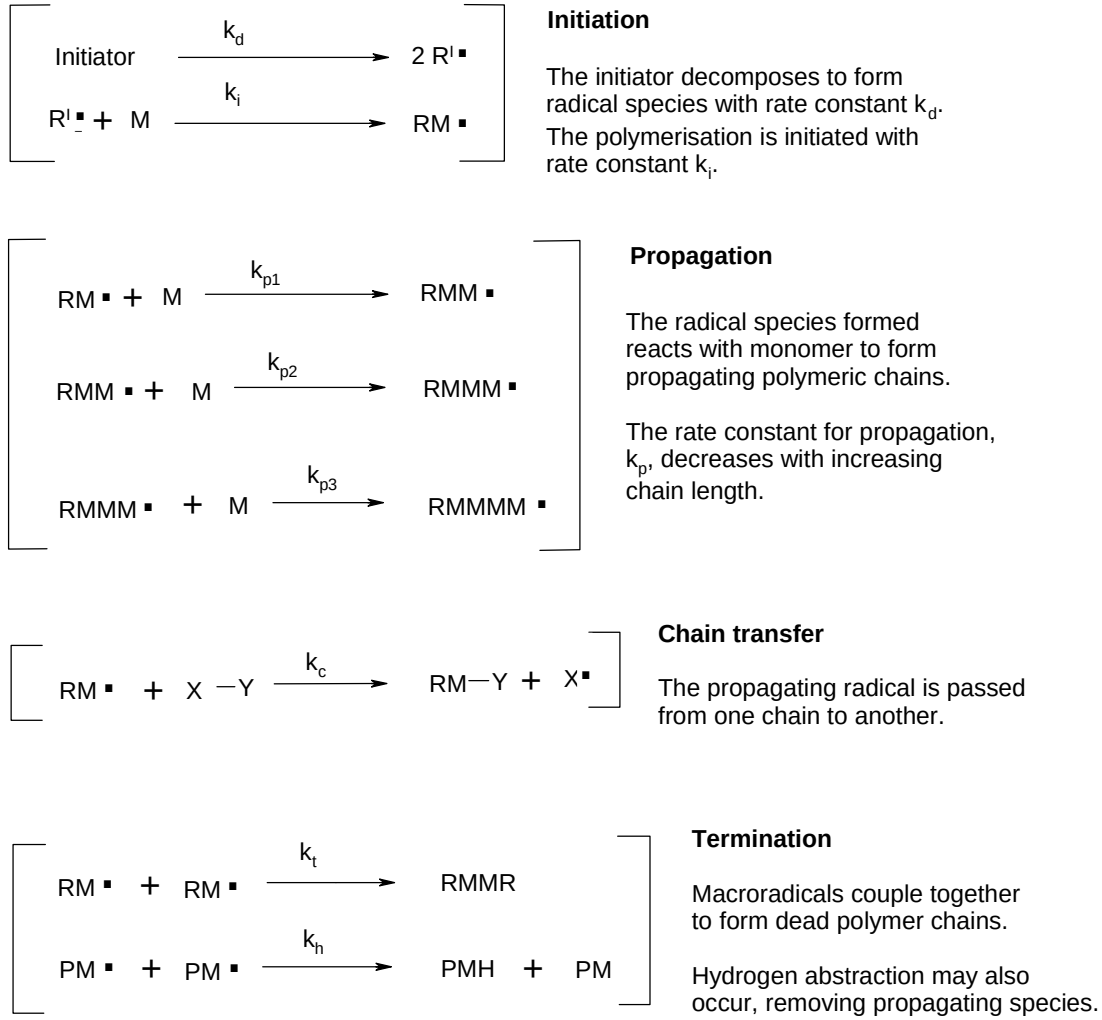

Figure 2: Reaction scheme for free radical addition polymerisation, initiation, propagation, chain transfer and termination.

FRP is a well-established synthetic route to a diverse range of polymers for many industries and applications. The tolerance of many functional groups and ability to polymerise a wide variety of monomers, acrylates, methacrylates, styrenes and vinyl chlorides especially make FRP very suitable for this application.[9,10] The different mechanisms involved in FRP are well established, figure 2. Bimolecular coupling, disproportionation, and chain transfer feature prominently in free radical

polymerisation. These processes prevent the control of the molecular weight and the polydispersity (PDI) of the polymers, and do not allow chain extension of the polymers as it is not a controlled process.

Controlled radical polymerisation (CRP) differs from conventional FRP as it minimises the rate of termination by controlling the concentration of radicals in the system. Within CRP there are several techniques used to create the "living" conditions. Whilst the precise mechanism of each reaction may differ, the fundamental principle of each technique is similar. A propagating radical species is reversibly formed, allowing polymer chains to propagate. The deactivation process keeps the concentration of radicals low, greatly reducing the rates of radical–radical termination and hydrogen abstraction so that chain growth is uninhibited.

The widely used controlled radical polymerisation techniques are ATRP, RAFT and NMP. Each has its own advantages and disadvantages. These are carefully considered when deciding which technique to utilise in polymer synthesis throughout this project. The general mechanisms of each are outlined below.

1.2.2 Atom Transfer Radical Polymerisation (ATRP)

The controlled radical technique ATRP was developed independently in the research groups of Sawamoto and Matyjaszewski.[11-13] These groups used ruthenium(II) and copper(I) catalysts respectively, though the use of copper (I) halides has been prevalent in the literature since.

The mechanism of ATRP in its simplest form can be thought to proceed as follows: the polymerisation is initiated by abstraction of a halogen atom from an initiating species by copper(I) stabilised by ligands.

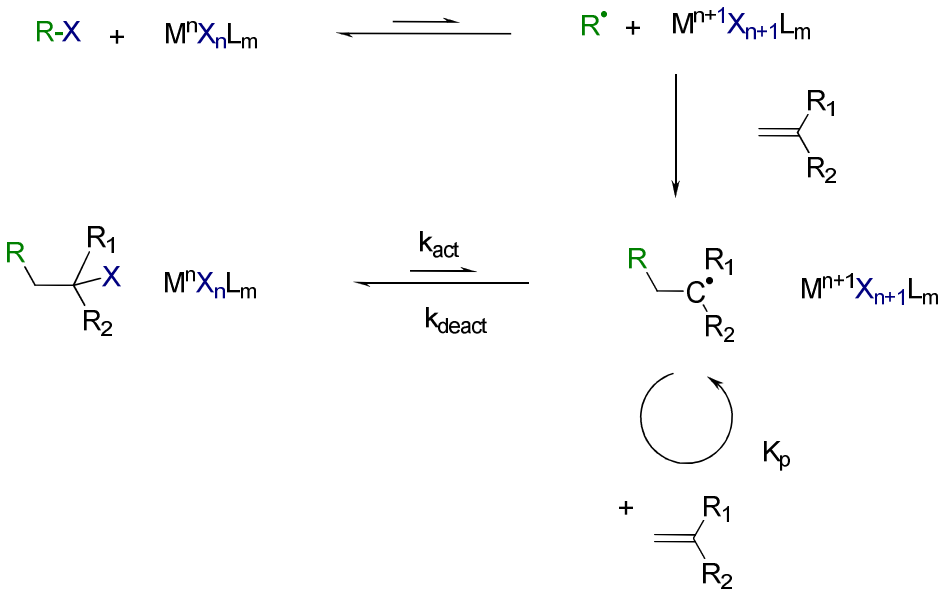

Scheme 1: Important mechanisms in ATRP. 'R-X' is an halogen initiator reacting with a transition metal complex '$M^nX_nL_m$', wherein M is a transition metal in oxidation state n, complexed by n halogen species, X, and m neutral ligands, L.

A dynamic equilibrium is then established between the propagating chain and the halogen-capped dormant chain. This dynamic equilibrium, which favours a capped chain end, minimises termination affording pseudo-living polymerisation conditions, scheme 1.

1.2.3 Reversible Addition Fragmentation chain Transfer (RAFT) polymerisation

Reversible Addition Fragmentation Transfer (RAFT) polymerisation was invented in the laboratories of CSIRO in Australia and Rhodia in France, with the first publication by Moad and Rizzardo of CSIRO in 1998.[14]

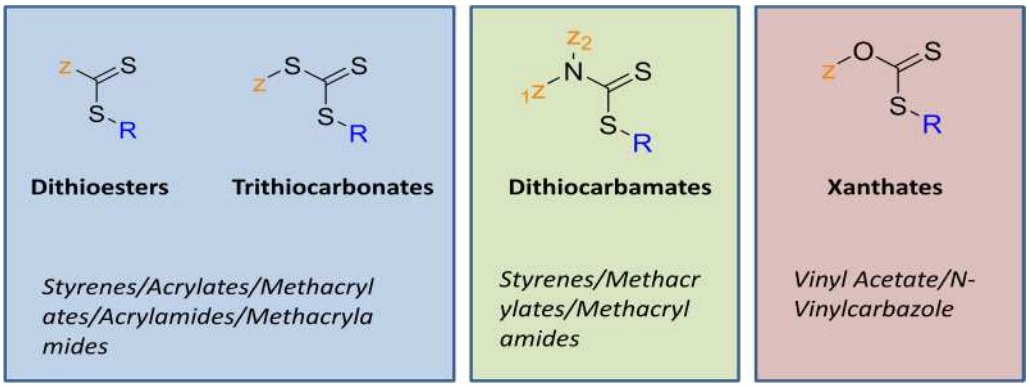

Figure 3: General groups of RAFT agents and groups of monomers that they are suitable for the polymerisation thereof.

This polymerisation technique uses thiocarbonyl thio RAFT chain transfer agents of the form ***[RS(Z)C=S]*** to facilitate living radical polymerisation. The effectiveness of the RAFT agent at polymerising a monomer depends on the ***R*** and ***Z*** groups. The ***R*** group must be a good free radical leaving group compared to the attacking radical $P_n^{\cdot}$, and be able to reinitiate polymerisation. Modifying the Z group, it is possible to activate and deactivate the thiocarbonyl bond and modify the stability of the intermediate radicals.

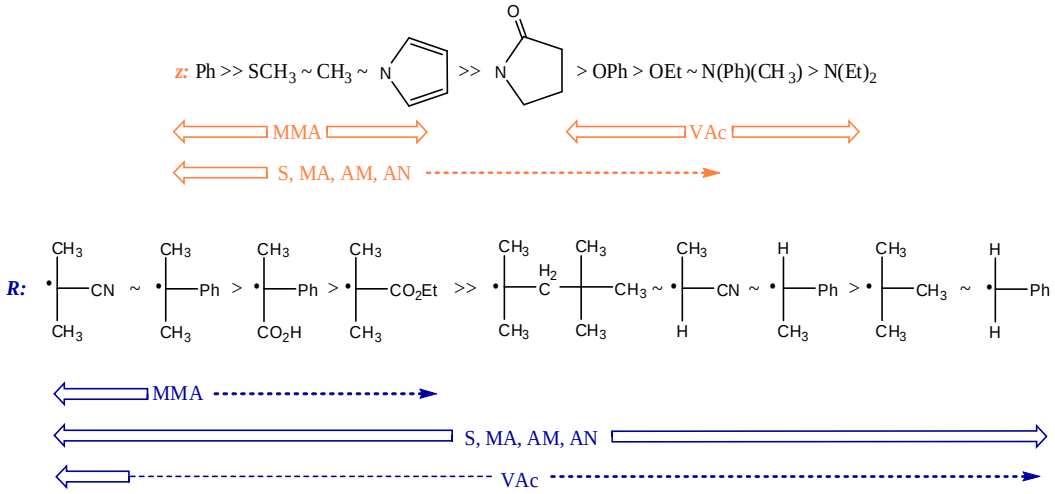

Figure 4: From reference.[15] Guidelines for the selection of RAFT agents for some general polymerisations. For the z group, addition rates decrease and fragmentation rates increase from left to right. The R group fragmentation rates decrease from left to right. Dashed line indicates partial control (i.e. control of molecular weight but poor PDI). MMA = methyl methacrylate, S = styrene, MA = methyl acrylate, AM = acrylamide, AN = acylonitrile, VAc = vinyl acetate.

This gives RAFT polymerisation versatility as tailoring the RAFT agent allows the polymerisation of many different types of monomers. There are four main types of RAFT agents; dithioesters, trithiocarbonates, dithiocarbamates and xanthates. These groups are suited to the polymerisation of certain monomer groups due to differing Z groups, figure 3. The choice of RAFT agent to use for each monomer is aided by previous research, which has been summarised in thorough reviews of the research area.[15-17] The effect of changing the Z and R group of the RAFT agent on the resultant RAFT agent's ability to polymerise a particular monomer has been summarised effectively by the inventors, figure 4.

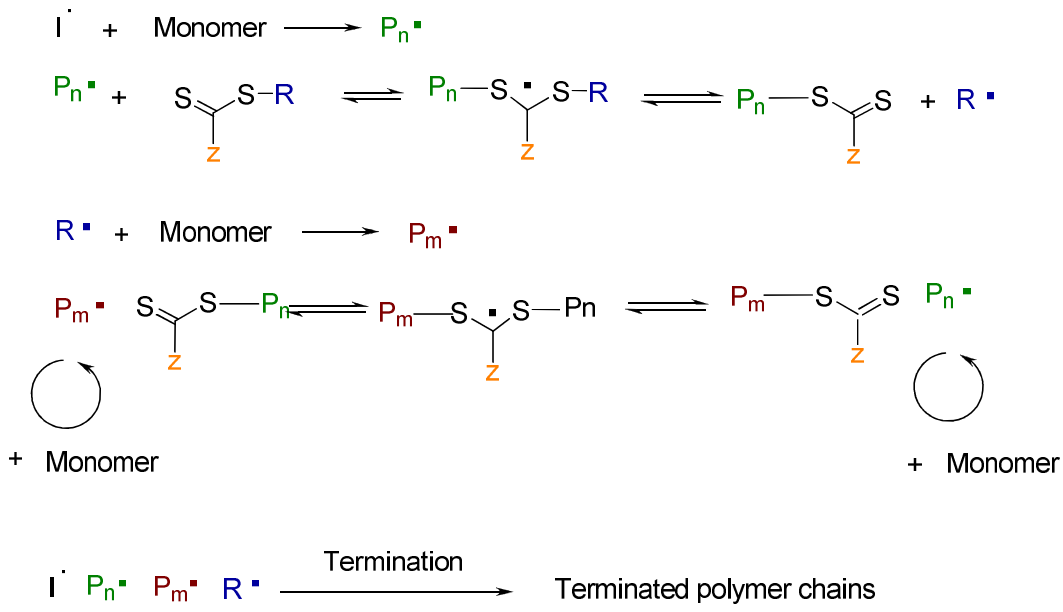

Scheme 2: Important mechanisms present in RAFT polymerisation. 'I' is an initiator, P_n is a polymer of n units, P_m is a polymer of m repeat units. R is a leaving group on the RAFT agent and Z is a group used to control the reactivity of the RAFT agent.

RAFT is thought to proceed *via* the general mechanism shown in scheme 2;[15] where a radical formed from a radical initiator propagates to form an initial propagating oligomer/ polymer, P_n. This radical can then react with a thiocarbonyl bond in a RAFT

agent, entering the RAFT pre-equilibrium, where this species can fragment to re-release the initial propagating polymer, P_n, or to yield a new radical, R. This new radical is then able to propagate, yielding a new oligomer/ polymer, P_m. A radical can then react with the thiocarbonyl bond of the RAFT agent, which again fragments to yield a new radical leaving group which can propagate.

With respect to star polymer synthesis, RAFT polymerisation has two sub-mechanisms of the core-first methodology. Depending on how the RAFT agent is attached to the core, the star synthesis is said to proceed by a ***Z*** group or ***R*** group mechanism. These mechanisms, their advantages, and disadvantages are discussed in chapter 2.

1.2.4 Nitroxide Mediated Polymerisation (NMP)

The third living radical technique is NMP, sometimes termed stable free radical polymerisation (SFRP). The controlled radical polymerisation of bulk styrene initiated by benzoyl peroxide was patented by Solomon and Rizzardo[18] and described by Georges[19] and Hawker[20] with a stable nitroxide radical, TEMPO, used as a mediating agent.

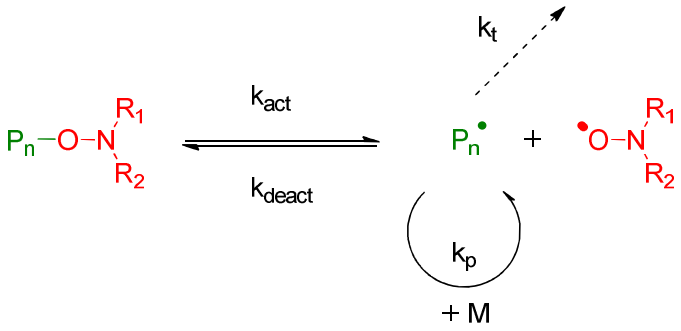

Scheme 3: Reaction scheme of nitroxide mediated radical polymerisation, utilising a stable nitroxide radical to mediate polymerisation.

The nitroxide radical is able to bind reversibly to the propagating polymer chain, end-capping the propagating polymer radical and preventing irreversible radical-radical termination reactions. This control of termination allows the molecular weight to be targeted by simply altering the ratio of initiator to monomer to determine the degree of polymerisation of the resultant polymer. NMP has been shown to provide a suitable method for the polymerisation of a variety of monomers.[21-25]

1.3 Click Chemistry

The concept of "*click chemistry*", a definition for a select number of highly efficient organic reactions that meet certain criteria, was introduced by Sharpless in 2001 and has captured the attention of synthetic chemists in many fields of chemistry.[26,27] According to the criteria drawn by Sharpless, a click reaction should be "modular and wide in scope, highly efficient, generate inoffensive or no by-products, be stereospecific, use readily available starting materials, use benign or no solvent, and require simple purification techniques".

The principle of a simple and highly efficient click reaction is advantageous towards post polymerisation modification; a route which has proven effective in the synthesis of polymers with functional groups incompatible with a particular polymerisation technique. It has recently been suggested that further requirements are desired of a reaction if it is to be applied in polymer chemistry.[28] These requirements are that the reactions should proceed with equimolarity, and should be able to be purified on a large scale. Under this more rigid definition, several "click" reactions discussed would not be considered "click" reactions, simply as efficient coupling reactions.

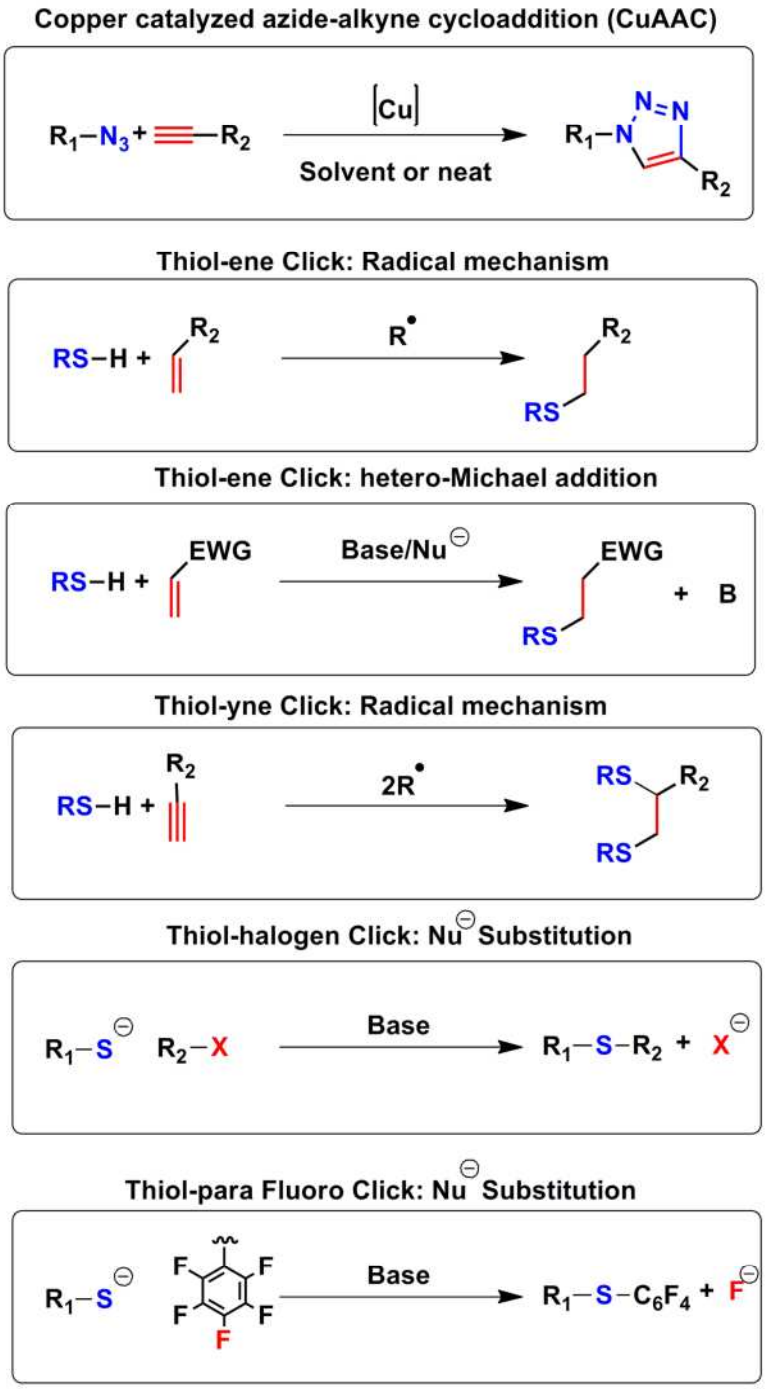

Scheme 4: Various reactions that have been termed "click" reactions.

One of the most widely employed click reactions has been the copper catalysed azide-alkyne cycloaddition (CuAAC) reaction.[22,29-31] The combination of the CuAAC reaction and transition metal-mediated living radical polymerisation has been inevitable since

they both use a similar catalyst and could even be conducted in a one-pot reaction.[32,33] Synthesis of functional polymers using the CuAAC click reaction have been demonstrated by a number of research groups, including Haddleton *et al*. and Stenzel *et al.*, which are discussed in chapter 5.[34,35] In general, a well-defined and functional backbone has been prepared using various polymerisation techniques and azide functional moieties have been clicked onto the backbone. This allows for the preparation of functional polymers in a more controlled manner by means of backbone length or co-monomer ratios. In a practical sense, it can be challenging to structurally characterise a polymer with certain functional groups (e.g. glycopolymers), therefore analysis of the precursor scaffold can give important information about the resulting functionalised polymer.

Alternatively, thiol based click reactions have attracted attention in the last 5 years due to the commercial availability of a wide range of thiols.[36] The versatility of thiol click reactions has been demonstrated by preparing tailor-made macromolecular architectures varying from telechelic homopolymers to highly complex dendritic structures.[37-41] Post polymerisation modification has afforded the synthesis of polymers using reactions of thiols with various functional groups such as alkenes, alkynes, *para*-fluoro phenyl and halides.[37] Most of these reactions are highly efficient and provide high yields under the employed conditions, scheme 4. In the case of thiol-ene and thiol-yne click reactions, it is possible to use UV-light and a photo-initiator to provide a radical source during the click reaction.[42,43] The remaining thiol-ene click reactions however, are either catalysed by base or are nucleophilic in nature and proceed under ambient conditions.[44-46] In terms of synthesis, it is relatively easy and versatile to obtain polymers with alkene, alkyne, *para*-fluoro, and halide pendant or terminal groups, which can then undergo thiol click chemistry.

1.4 References

(1) Roovers, J.; Hadjichristidis, N.; Pispas, S.; Pitsikalis, M.; Iatrou, H.; Vlahos, C. In *Branched Polymers I*; Springer Berlin / Heidelberg: 1999; Vol. 142, p 71.

(2) Roovers, J.; Burchard, W. In *Branched Polymers II*; Springer Berlin / Heidelberg: 1999; Vol. 143, p 113.

(3) Roovers, J.; McLeish, T.; Milner, S. In *Branched Polymers II*; Springer Berlin / Heidelberg: 1999; Vol. 143, p 195.

(4) Graham, S.; Cormack, P. A. G.; Sherrington, D. C. *Macromolecules* **2004**, *38*, 86.

(5) Magnusson, H.; Malmström, E.; Hult, A.; Johansson, M. *Polymer* **2002**, *43*, 301.

(6) M. Morton, T. E. H., S. D. Gadkary, F. Bueche, *J. Polym. Sci.* **1962**, *57*, 471.

(7) Milkovich, R.; CIPO, Ed.; Shell Oil Company: Canada, 1965; Vol. 716645.

(8) Worsfold, D. J.; Zilliox, J.-G.; Rempp, P. *Can. J. Chem.* **1969**, *47*, 3379.

(9) Matyjaszewski, K.; Davis, T. P. *Handbook of Radical Polymerisations*; J. Wiley & Sons Pub., 2003.

(10) Odian, G. *Principles of Polymerisation*; 4th ed.; J. Wiley & Sons Pub., 2004.

(11) Kato, M.; Kamigaito, M.; Sawamoto, M.; Higashimura, T. *Macromolecules* **1995**, *28*, 1721.

(12) Wang, J.-S.; Matyjaszewski, K. *Macromolecules* **1995**, *28*, 7901.

(13) Wang, J.-S.; Matyjaszewski, K. *J. Am. Chem. Soc.* **1995**, *117*, 5614.

(14) Chiefari, J.; Chong, Y. K.; Ercole, F.; Krstina, J.; Jeffery, J.; Le, T. P. T.; Mayadunne, R. T. A.; Meijs, G. F.; Moad, C. L.; Moad, G.; Rizzardo, E.; Thang, S. H. *Macromolecules* **1998**, *31*, 5559.

(15) Moad, G.; Rizzardo, E.; Thang, S. H. *Aust. J. Chem.* **2005**, *58*, 379.

(16) Moad, G.; Rizzardo, E.; Thang, S. H. *Aust. J. Chem.* **2006**, *59*, 669.

(17) Moad, G.; Rizzardo, E.; Thang, S. H. *Aust. J. Chem.* **2009**, *62*, 1402.

(18) Solomon, D. H.; Rizzardo, E.; Cacioli, P.; USPatent, Ed. 1986; Vol. 4581429.

(19) Georges, M. K.; Veregin, R. P. N.; Kazmaier, P. M.; Hamer, G. K. *Macromolecules* **1993**, *26*, 2987.

(20) Hawker, C. J. *J. Am. Chem. Soc.* **1994**, *116*, 11185.

(21) Grubbs, R. B. *Polymer Reviews* **2011**, *51*, 104.

(22) Lang, A. S.; Neubig, A.; Sommer, M.; Thelakkat, M. *Macromolecules* **2010**, *43*, 7001.

(23) Ott, C.; Hoogenboom, R.; Schubert, U. S. *Chem. Commun.* **2008**, 3516.

(24) Hoogenboom, R.; Popescu, D.; Steinhauer, W.; Keul, H.; Möller, M. *Macromol. Rapid Commun.* **2009**, *30*, 2042.

(25) Rigolini, J.; Grassl, B.; Billon, L.; Reynaud, S.; Donard, O. F. X. *J. Polym. Sci., Part A: Polym. Chem.* **2009**, *47*, 6919.

(26) Kolb, H. C.; Sharpless, K. B. *Drug Disc. Today* **2003**, *8*, 1128.

(27) Kolb, H. C.; Finn, M. G.; Sharpless, K. B. *Angew. Chem., Int. Ed.* **2001**, *40*, 2004.

(28) Barner-Kowollik, C.; Du Prez, F. E.; Espeel, P.; Hawker, C. J.; Junkers, T.; Schlaad, H.; Van Camp, W. *Angewandte Chemie International Edition* **2011**, *50*, 60.

(29) Slavin, S.; Burns, J.; Haddleton, D. M.; Becer, C. R. *Eur. Polym. J.* **2010**, *47*, 435.

(30) Singh, I.; Zarafshani, Z.; Heaney, F.; Lutz, J.-F. *Polym. Chem.* **2010**.

(31) Semsarilar, M.; Ladmiral, V.; Perrier, S. *Macromolecules* **2010**, *43*, 1438.

(32) Mantovani, G.; Ladmiral, V.; Tao, L.; Haddleton, D. M. *Chem. Commun.* **2005**, 2089.

(33) Lutz, J. F.; Borner, H. G.; Weichenhan, K. *Macromolecules* **2006**, *39*, 6376.

(34) Ladmiral, V.; Mantovani, G.; Clarkson, G. J.; Cauet, S.; Irwin, J. L.; Haddleton, D. M. *J. Am. Chem. Soc.* **2006**, *128*, 4823.

(35) Geng, J.; Lindqvist, J.; Mantovani, G.; Haddleton, D. M. *Angew. Chem., Int. Ed.* **2008**, *47*, 4180.

(36) Hoyle, C. E.; Lowe, A. B.; Bowman, C. N. *Chem. Soc. Rev.* **2010**, *39*, 1355.

(37) Campos, L. M.; Killops, K. L.; Sakai, R.; Paulusse, J. M. J.; Damiron, D.; Drockenmuller, E.; Messmore, B. W.; Hawker, C. J. *Macromolecules* **2008**, *41*, 7063.

(38) Pounder, R. J.; Stanford, M. J.; Brooks, P.; Richards, S. P.; Dove, A. P. *Chem. Commun.* **2008**, 5158.

(39) Willcock, H.; O'Reilly, R. K. *Polym. Chem.* **2010**, *1*, 149.

(40) Jones, M. W.; Mantovani, G.; Ryan, S. M.; Wang, X.; Brayden, D. J.; Haddleton, D. M. *Chem. Commun.* **2009**, 5272.

(41) Moad, G.; Rizzardo, E.; Thang, S. H. *Polym. Int.* **2011**, *60*, 9.

(42) Hensarling, R. M.; Doughty, V. A.; Chan, J. W.; Patton, D. L. *J. Am. Chem. Soc.* **2009**, *131*, 14673.

(43) ten Brummelhuis, N.; Diehl, C.; Schlaad, H. *Macromolecules* **2008**, *41*, 9946.

(44) Syrett, J. A.; Jones, M. W.; Haddleton, D. M. *Chem. Commun.* **2010**, *46*, 7181.

(45) Lowe, A. B. *Polym. Chem.* **2010**, *1*, 17.

(46) Li, G.-Z.; Randev, R. K.; Soeriyadi, A. H.; Rees, G.; Boyer, C.; Tong, Z.; Davis, T. P.; Becer, C. R.; Haddleton, D. M. *Polym. Chem.* **2010**, *1*, 1196.

Chapter 2

Synthesis and characterisation of core-first PMMA star polymers

To investigate the use of multi-detector GPC for estimating the functionality (number of arms) on a star polymer, PMMA star polymers have been synthesised using ATRP and a core-first technique. Using multifunctional 3 arm, 5 arm, 8 arm and 21 arm initiators the polymerisation of MMA was seen to yield star polymers with narrow PDI, when the reaction was terminated at low conversion.

Using Zimm and Stockmayer theory and multi-detector GPC, the number of arms on each star polymer has been estimated using the reduction in intrinsic viscosity of a star polymer relative to a linear polymer equivalent.

2.1 Characterisation of star polymers

There are a number of techniques available for the determination of the molecular weight of polymers, from multi-angle laser light scattering (MALLS) and membrane osmometry as ways to determine absolute weight average (M_w) and number average (M_n) molecular weights respectively, to sedimentation equilibrium and matrix assisted laser desorption ionisation (MALDI) mass spectroscopy. However, the characterisation of star polymers and copolymers presents a challenge to one of the technologies most commonly used to analyse polymers, i.e. gel permeation chromatography (GPC).

2.1.1 Conventional GPC

The principle of GPC is that a dilute solution of analyte is introduced into a stream of solvent flowing through a column of packed beads and separated depending on the size of the analyte. The beads have pores of varying sizes around the size of the analyte, and the elution time of the analyte is proportional to the number of pores the analyte can enter.[47-50] An analyte with a smaller hydrodynamic volume can enter more pores and therefore elutes later.[51]

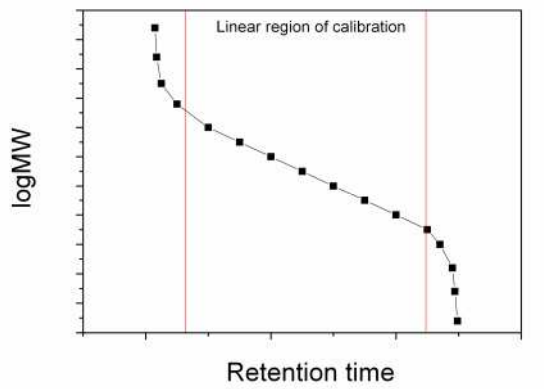

Figure 5: M_p of various linear calibration standards on a plot of logMW against retention time (retention volume) in the GPC. These plots are used as a calibration curve for conventional GPC.

In conventional GPC a concentration detector (e.g. a differential refractometer) is used to determine the varying concentration of polymer as it elutes from the size separating column, using equation 2.1. The elution time is related to the molecular weight of an analyte through a calibration and the calibration is usually made using linear narrow molecular weight standards, figure 5.

$$RI = B\,(dn/dc)\;c \qquad (2.1)$$

Where

RI is the refractive index

c is the concentration of polymer in sample

B is an instrumental constant

dn/dc is the change in the refractive index of the solution as a function of concentration. This value varies for each polymer-solvent pair under constant conditions.

As the GPC separates the polymer by the hydrodynamic volume in solution, any variation in architecture or chemistry between calibrant and polymer analyte will cause discrepancies and deviation from the calibration curve.[52,53] This is particularly problematic when analysing novel polymers and copolymers where the two constituent monomers have different refractive indices, although averaging of the dn/dc has been shown to be quite effective for some studies.[54] Likewise, different architectures can be difficult to analyse by conventional GPC.

Figure 6: Representation of the difference in root mean square radius of gyration of linear and star polymers of the same molecular weight.

Compared to their linear analogues with the same molecular weight, branched polymers usually have smaller dimensions leading to a reduced dilute solution viscosity. As branching increases, this relative reduction in viscosity becomes more pronounced.

The use of multiple detectors with GPC, such as MALLS and viscometry, can be used to observe these changes.[55,56]

2.1.2 Viscometry in GPC (Universal calibration)

It has been known for a long time that the use of a viscometer with GPC can be used to generate a "*universal calibration*"[52] which has been shown to give more accurate analysis of the molecular weight as it removes the need for the calibrant and polymer analyte to have the same chemistry and architecture.

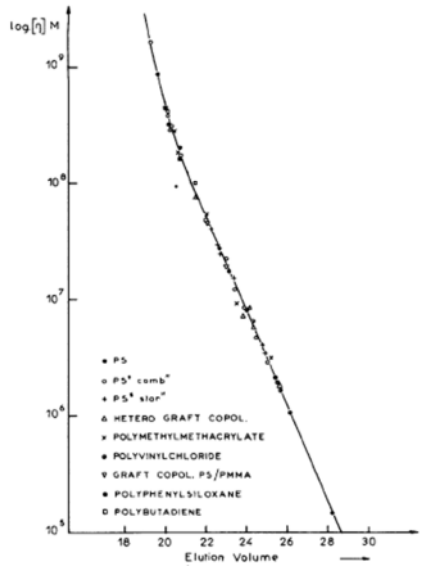

Figure 7: Plot of Log [η].MW against retention volume for polymers of different molecular weights/chemistries and architectures. Copied without editing from reference.[52]

The universal calibration is based upon Einstein's viscosity theory from his 1905 dissertation for the university of Zurich and subsequent corrections of 1911. This theory is used by Benoit and Grubisic in their seminal paper,[52] which is summarised below; using a simple form of Einstein's viscosity theory to show a relationship between viscosity and molecular weight. Modelling the polymer as hard spheres in dilute solution:

$$\eta_{sp} = 2.5 \frac{N_B V_\eta}{V} \qquad (2.2)$$

Where:

η_{sp} is the specific viscosity

N_B is the number of spheres

V_η is the volume of the spheres

V is the total volume

The volume of the spheres V_η is the effective hydrodynamic volume of the polymer in solution. Allowing the number of moles of polymer (n_B) to be $n_B = N_B/N_A$ then:

$$\eta_{sp} = 2.5 \frac{n_B V_\eta N_A}{V} \qquad (2.3)$$

Introducing a factor for the concentration into eqn. 2.3, using concentration, $c = n_B N_A/M$, where M is the molecular weight and N_A is Avogadro's number, gives:

$$\eta_{sp} = 2.5 \frac{n_B M}{V} \frac{V_\eta N_A}{M}$$

$$\eta_{sp} = 2.5c \frac{V_\eta N_A}{M}$$

$$\frac{\eta_{sp}}{c} = [\eta] = 2.5\frac{V_\eta N_A}{M} \quad (2.4)$$

Therefore, extrapolating to zero concentration to yield intrinsic viscosity, and assuming that the effective hydrodynamic volume is proportional to the mean it can be written that:

$$[\eta] = k\frac{V_h}{M} \text{ or } V_h = \frac{[\eta]M}{k} \quad (2.5)$$

[η] is the intrinsic viscosity

k is constant

V_h is the hydrodynamic volume of the polymer

As GPC separation is due to the size of the polymer in solution (provided there is no unwanted chemical interaction) use of the hydrodynamic volume of the polymer (log ([η].M)) vs. elution volume (figure 7), rather than the molecular weight (log(M)) should give a calibration independent of chemistry and architecture.[52,57,58] Therefore, this technique should give a closer representation of the molecular weight of a star polymer compared to conventional GPC.

2.1.3 Multi-angle laser light scattering (MALLS) in GPC

Light scattering is a powerful technique for the determination of the molecular weight of a polymer and can be used to determine the absolute weight average molecular weight, M_w. When electromagnetic radiation hits an atom or a molecule, the electrons emit the radiation in all directions.

$$R(\theta) = \frac{I_\theta r^2}{I_0} \tag{2.6}$$

I_θ is scattering intensity per unit of scattering volume.

I_0 is the intensity of incident light

r is the distance between the scattering volume and the detectors

The amount of scattered light is measured using detectors at varying angles to the incident light, and is proportional to the size of the analyte molecule, with larger molecules scattering more than smaller molecules. The amount of light scattered by a dilute solution of analyte at a given angle, θ, is termed the excess Raleigh ratio, R(θ), eqn. 2.6.

$$\frac{K^* c}{R(\theta)} = \frac{1}{M_w} \tag{2.7}$$

c is the concentration of the scattering volume.

$$K^* = \frac{4\pi^2 n_0^2 (dn/dc)^2}{\lambda_0^4 N_A} \tag{2.8}$$

N_A is Avogadro's number,

n_0 is the refractive index of the solvent,

λ_0 is the vacuum wavelength of the incident radiation,

(dn/dc) is the specific refractive index increment.

The excess Raleigh scattering and concentration of the solution can be used to determine the absolute molecular weight, M_w through the Raleigh-Gans-Debye approximation, eqn. 2.7.

The angular dependence of the scattered light and inverse absolute molecular weight, M_w^{-1} are related by a Zimm plot. By varying concentration of the polymer and angle of scattered light, the inverse absolute molecular weight, M_w^{-1}, is calculated by extrapolating to zero concentration and an angle of 0^o.[59] Using GPC-MALLS, the scattered light is detected at different angles for each eluting segment. When used in conjunction with a concentration detector it is possible to calculate the M_w and R_g for each integral slice of the GPC separation.

For star polymers, the radius of gyration has been related to the molecular weight by Daoud and Cotton's seminal paper[60] where they deduced a dependence of R_g on $N^{3/5}f^{1/5}$ where N is the number of segments in each arm. This led to the conclusion that for systems where N is constant this results in $R_g \propto M^{1/5}$.[61]

2.1.3.1 Radius of gyration contraction factor

By comparing the radius of gyration of a branched (star) polymer sample with a linear analogue at the same molecular weight, it is possible to resolve branching information.[62] The extent of the branching is described by the radius of gyration contraction factor, g,

$$g = \frac{< r_g^2 >_s}{< r_g^2 >_l} \qquad (2.9)$$

Where

$< r_g^2 >_s$ is the square mean radius of gyration of a star polymer

$< r_g^2 >_l$ is the square mean radius of gyration of a linear polymer of the same composition and molecular weight.

Mays and co-workers synthesised a range of highly branched PMMA polymers by varying the amount of ethylene glycol dimethacrylate (EGDMA) divinyl crosslinker used in the polymerisation. Then, using multi-detector GPC the radius of gyration contraction factor was investigated and seen to decrease with increasing branching.[63]

2.1.4 Mark-Houwink plots

The use of a capillary viscometer[64,65] allows determination of the intrinsic viscosity across the MWD of the polymer and is an easy way to produce a Mark-Houwink plot for a polymer from the Mark-Houwink equation, $[\eta] = KM^{\alpha}$. For a polymer with a constant amount of branching the contraction in solution is consistent, and the exponent of the Mark-Houwink equation will be reduced by a consistent amount.[66] Thus, a Mark-Houwink plot of a perfect core-first star polymer should result in a parallel line to the linear one, but shifted to lower viscosity. The Mark-Houwink exponent, α, depends on the structure of the polymer in solution. Its value can be in the range from 0 (solid sphere) to 2 (rigid rod).

Simon *et al*.[67] synthesised highly branched poly(methyl methacrylate) using 2-(2-methyl-1-triethylsiloxy-1-propenyloxy)-ethyl methacrylate (MTSHEMA) divinyl crosslinker. They then validated the use of multi-detector GPC to determine a Mark-Houwink plot, by separation of a highly branched polymer by preparative GPC. Using higher concentration light scattering experiments on the nine resulting relatively narrow PDI polymers gave the absolute M_w and viscosity measurements gave the intrinsic viscosity. Both the multi-detector GPC and the preparative GPC gave Mark-Houwink exponents in THF that are considerably lower than those for linear PMMA of

α = 0.40 (for linear PMMA, α= 0.688) highlighting the branched structure of the polymers.[67]

2.1.4.1 Intrinsic viscosity shrink factor

It has been shown that the use of intrinsic viscosity and ascertain an intrinsic viscosity shrink factor, g^I, defined in equation 2.10, can also be an effective and useful value.

$$g^I = \frac{[\eta]_s}{[\eta]_l} \qquad (2.10)$$

Where

$[\eta]_s$ is the intrinsic viscosity of a star polymer

$[\eta]_1$ is the intrinsic viscosity of a linear polymer of the same composition and molecular weight.

The radius of gyration contraction factor is predominantly used in models to quantify branching, however, the intrinsic viscosity is often more accessible. As viscosity has some dependence on the size of a molecule in solution,[68] there have been attempts to relate g^I back to the radius of gyration contraction factor, g, to allow its use in quantifying branching. Zimm and Stockmayer's work[62] has been used as the foundation for a number of investigations into dilute polymer solution properties.[55,69,70]

The relationship between g^I and g is currently disputed in the literature, but has been described by an exponential relationship $g^I = g^\varepsilon$, where ε can have a value of 1.5 based on Flory-Fox theory.[71] Zimm and Kilb calculated ε = ½, and argued that it was a universal value; however, it has been calculated experimentally as between 0.8 and 1 by Mays *et al*.[63] and also as 0.83 for PMMA by Millequant and co-workers.[68,69]

Complicating the argument further, several researchers have developed and used a different relationship between g' and g based on experimental data,[72-75] which takes the form:

$$g = [a + (1 - a)g'^{b}]\, g'^{c} \qquad (2.11)$$

Where

g is the radius of gyration contraction factor

g' is the intrinsic viscosity shrink factor

a, b and c are constants derived from experiment

This relationship has been particularly studied for PMMA, where Robello *et al*. have determined that for the above equation a= 0.2625, b= 1.0880 and c= 0.6087.[73]

2.1.5 Determining the functionality of star polymers

Determining the functionality of star polymers has been achieved in a variety of ways. Using the core-first methodology, the functionality is determined using ^{1}H NMR to ensure that all initiating sites on the core have initiated polymerisation, and hence the functionality of the star is estimated to be equal to the functionality of the core.

Using the arm-first approach the functionality can be determined during synthesis. A crude final product using this technique contains both star and unreacted arm polymers. Comparison of the M_n of the linear arms with the star polymer, and dividing the star molecular weight by the other is used to estimate the functionality.[76]

A novel technique for determining the functionality using multi-detector GPC has been used with varying success.[55,69,70] This approach, described below, has the advantage of allowing analysis of unknown polymers post-synthesis.

2.1.6 Determining the number of arms using multi-detector GPC

The relationship between the radius of gyration contraction factor and functionality (*f*) of the star polymer is dependent on the model used to simulate the star polymer. If the polymer is modelled as a singular core with arms of equal length, then Zimm and Stockmayer[62] have shown that the relationship takes the form:

$$g = \frac{3}{f} - \frac{2}{f^2} \qquad (2.12)$$

Robello *et al*. used this relationship to characterise 3, 5, 6 and 10 arm stars synthesised by ATRP using sulfonyl chloride initiators with defined functionality.[73] They found that the functionality, *f,* changed over the molecular weight distribution of the polymer, but at the M_p of the star polymer the functionality calculated by the above equation was within ± 1 of the initiator functionality.

2.2 Core-first polymers in literature

The possibility of attaching the appropriate initiating functionality to a multifunctional core to grow a star or dendritic polymer was recognised early for each form of living radical polymerisation. The compatibility of each polymerisation method with the functionality of the core and the monomer should determine which method is used. Importantly, the core-first route can yield star polymers with a precise number of arms, determined by the functionality of the core initiator.

2.2.1 Core-first stars by ATRP

Core-first synthesis can be achieved in ATRP through the synthesis of molecules with more than 2 active carbon-halogen bonds. Indeed, a large number of multifunctional initiators have been synthesised in the literature and used to form star polymers. A few examples of precursor ATRP initiators for star polymers are shown below.

Table 1: Examples of ATRP core-first initiators.

	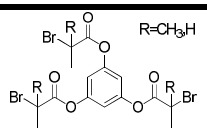	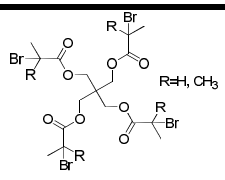	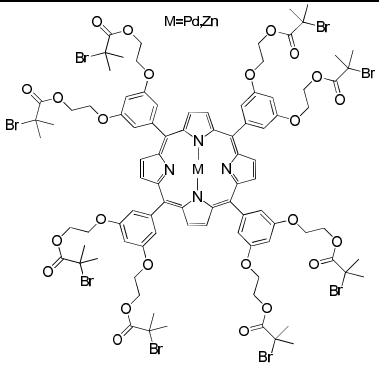
No. arms	3	4	4
REF	77-79	80	81

	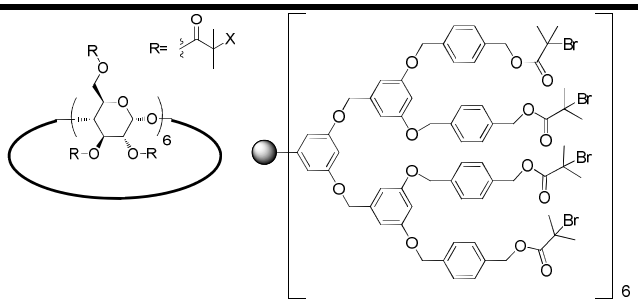	
No. arms	18	24
REF	[82]	[83]

One of the most common methods of core synthesis is via reaction with a corresponding polyol compound. The activated carbon halogen containing initiators can be utilised as they are, or converted to RAFT agents via an atom transfer radical addition (ATRA) reaction.[84]

2.2.2 Core-first stars by RAFT polymerisation

A variety of molecules have been modified into multifunctional chain transfer agents (CTAs), table 2. Commonly (aromatic) hydrocarbons, such as benzene or pentaerythritol, have been functionalised with trithiocarbonates and thiobenzoylthiomethyl RAFT groups for use as CTAs.[85-89] Ruthenium (II) bearing macrocycle derived CTAs and dendrimer derived CTAs have also been shown to be effective at RAFT star polymerisation.[90-92]

Table 2: Examples of RAFT core-first initiators.

	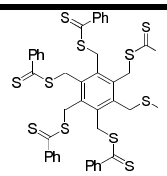	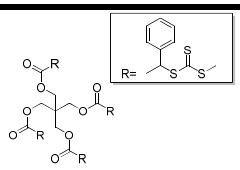
No. arms	6	4
REF	86,87,93	94
	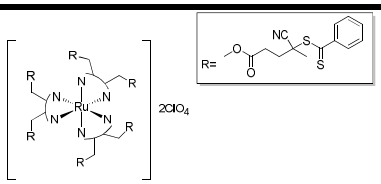	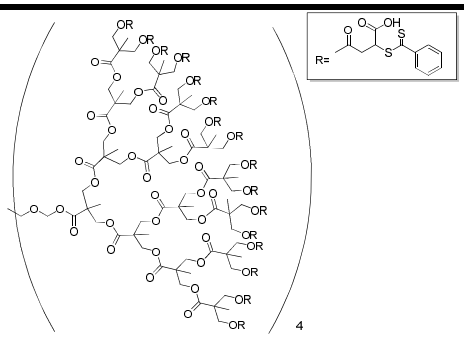
No. arms	6	64
REF	90-92	95,96

2.2.3 Core-first stars by NMP

For the NMP of core-first star polymers, the initiators are prepared by attaching an NMP initiating group to a central core. Multifunctional initiators have been synthesised from cores with different structures and composition depending on the number of arms and properties of the core required, table 3. Cores have been based on aromatics such as benzene or Mesitylene,[97-99] non-aromatic hydrocarbons,[100,101] cyclodextrins,[102] and even well defined dendrimers,[98,103-106] or hyperbranched polymers.[107] By using the core-first technique it is possible to have functionality in the stars, by synthesis of multifunctional initiators from functional precursor compounds, such as azobenzene,[108-110] porphyrin,[111] or metal containing initiators.[112]

The most commonly reported monomer used for the synthesis of star polymers by NMP is styrene, and styrene derived monomers like acetoxy styrene,[100,108,109] and 2,5-bis[(4-butylbenzoyl)oxy]styrene.[102,113] Other monomers used include acrylates,[106,113] acrylamides,[106] 4-vinyl pyridine,[103] and carbonate monomers.[111]

Table 3: Examples of NMP core-first initiators.

	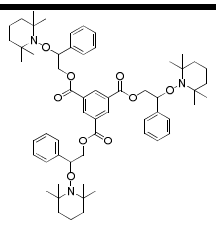	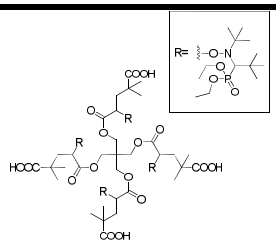	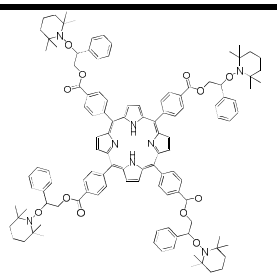
No. arms	3	4	4
REF	97	101	111
	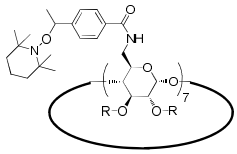	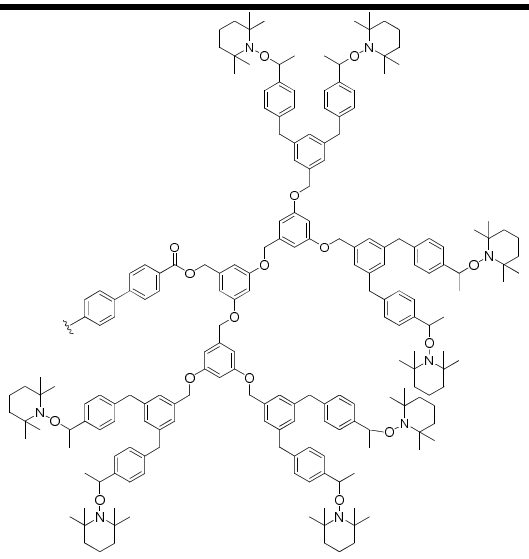	
No. arms	7	16	
REF	102	104	

The occurrence of star-star coupling has been shown in NMP star synthesis by Miura *et al*. for the polymerisation of styrene and 4-vinylpyridine[103,104] and Kukuchi for styrene from a modified cyclodextrin core[102] leading to formation of higher molecular weight products. In 2003, Hawker *et al*. investigated the extent of chain coupling in NMP.[105] Using a dendritic core NMP initiator and a chromophore bearing linear initiator combined in a polymerisation of styrene would yield star polymers and UV active linear polymers if no coupling termination was occurring. However, by following the reaction by UV detection GPC, UV active stars were seen to have formed by the chain-chain coupling of UV active linear polymers with star polymers. The authors concluded that most of the coupling occurred at the beginning of the polymerisation and that this was consistent with the persistent radical effect proposed by Fischer.[114]

Using ATRP, the polymer chain propagates from a central initiating core with the end capping moieties cleaving from the star to form a propagating radical on the core (method ***a***). RAFT and NMP can proceed in the same manner as seen in scheme 5.

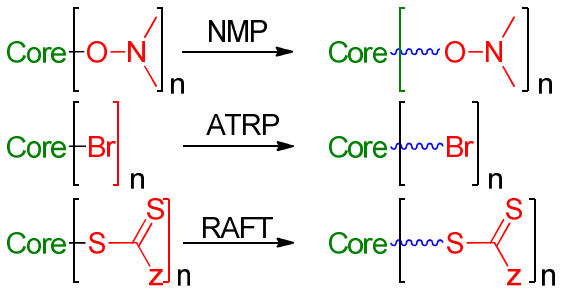

Scheme 5: Controlled radical polymerisation methods for core-first star synthesis.

However, RAFT and NMP can also form stars using a second approach (method ***b***), sometimes termed the 'Z-approach' in RAFT star polymerisation. In this approach the polymer chains activate by dissociation from the core to form a propagating linear polymer chain which then deactivates with recombination with a core, scheme 6.

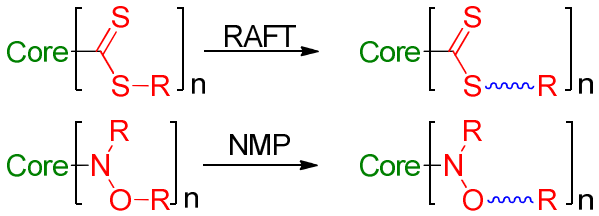

Scheme 6: Core-first polymerisation of stars by method b using RAFT and NMP initiators.

Each of these core-first star polymerisation strategies, within RAFT and NMP, has advantages and limitations. One limitation of method ***a*** is that the propagating radical on the core centre allows star-star coupling. Although this can be mediated by designing the appropriate experiment, it is possible to entirely circumnavigate this issue by using another method. In method ***b*** the propagating radical never exists on the core of the star polymer, removing the possibility of star-star coupling.

Table 3. Examples of RAFT and NMP method ***b*** core-first initiators.

	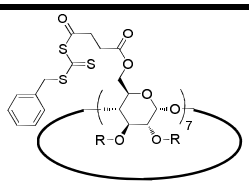	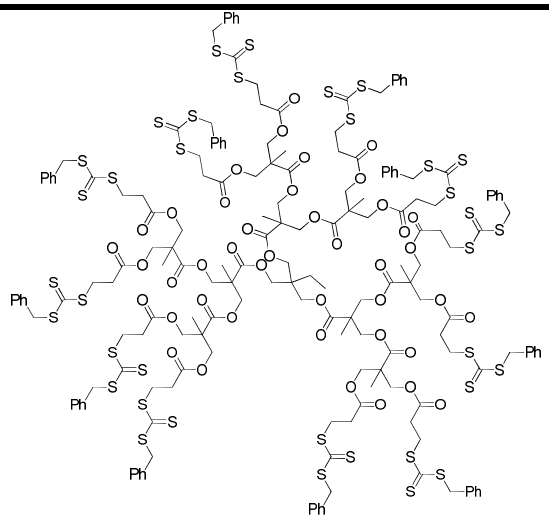
No. Arms	7	12
REF	115	116,117

Termination still occurs in method ***b***, however it is linear arm-arm termination forming dead chains which are always smaller than the star polymer. A possible disadvantage of method ***b*** is that the stars formed are inherently unstable; weakened by the C-O-N bond in NMP, and the C-S bond in RAFT. It has also been suggested that there is an upper limit of molecular weight of stars produced method ***b*** due to shielding of the core RAFT agent/nitroxide by large polymers attached to the core.

Method **a**, with ATRP, was used for the synthesis of core-first star polymers in this project. This route has the advantage of stable stars and avoids the complications that can arise from method **b**. However, conditions were chosen to minimise the possibility of star-star coupling in the reactions.[118-120]

2.4 Results and Discussion

2.4.1 Synthesis of core-first PMMA stars by ATRP

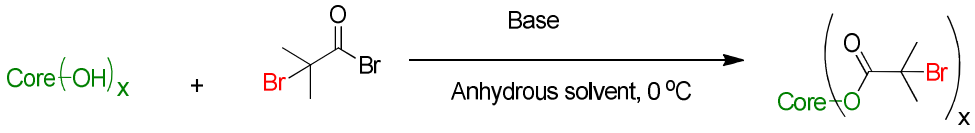

Scheme 7: General synthesis of multi functional initiator from the esterification of alcohols with a tertiary bromide functionalised acid bromide.

PMMA star polymers were synthesised using a well established core-first approach in ATRP. Core initiators were synthesised by esterification of polyols with 2-bromo-isobutyryl bromide in the presence of base, scheme 7. A 3-arm initiator was synthesised from 1,1,1 tris(hydroxymethyl) ethane by the esterification of three equivalents of 2-bromoisobutyryl bromide in anhydrous tetrahydrofuran (THF), with triethylamine (TEA) used as a base catalyst.

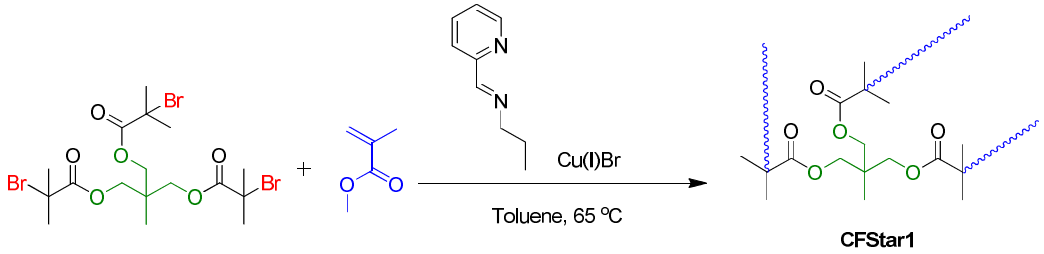

Scheme 8: Polymerisation of MMA from a trifunctional initiator to form a 3 arm PMMA star, CFStar1.
〰 = PMMA

CFStar1 was made by polymerisation of MMA using this initiator in toluene at 65 °C, scheme 8. The initiator, monomer, ligand and solvent were placed into a Schlenk tube and degassed by freeze-pump-thaw and filled with nitrogen to ensure the absence of

oxygen. The copper(I) bromide was added against a flow of nitrogen to start the reaction.

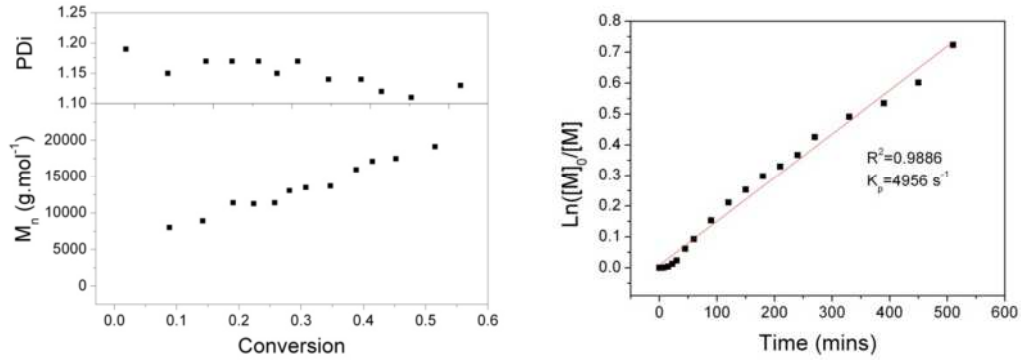

Figure 8 : Polymerisation of MMA using 3 arm initiator, by ATRP; (left) Molecular weight evolution with conversion, (right) Plot of ln($[M]_0/[M]_t$) against time as a kinetic plot.

Aliquots were taken periodically to allow the polymerisation to be monitored by ^{1}H-NMR and GPC throughout the reaction. The ATRP reactions were seen to progress in a pseudo living manner with molecular weight growth with conversion, PDI < 1.2, and a linear plot of ln($[M]_0/[M]_t$) against time. From the fit of the kinetic plot we obtain k_p = 4956 s^{-1}, figure 8. **CFStar2** was made similarly, using a 5-arm initiator derived from glucose with 1 equivalent of Cu(I)Br, and 2.1 equivalents of pyridineimine ligand per initiating site. The 8-arm initiator, made from lactose, was used to make the 8-arm star **CFStar3** which has also been used in this study. Finally, **CFStar4** has been polymerised using a 21-arm initiator, derived from β-cyclodextrin, figure 9.

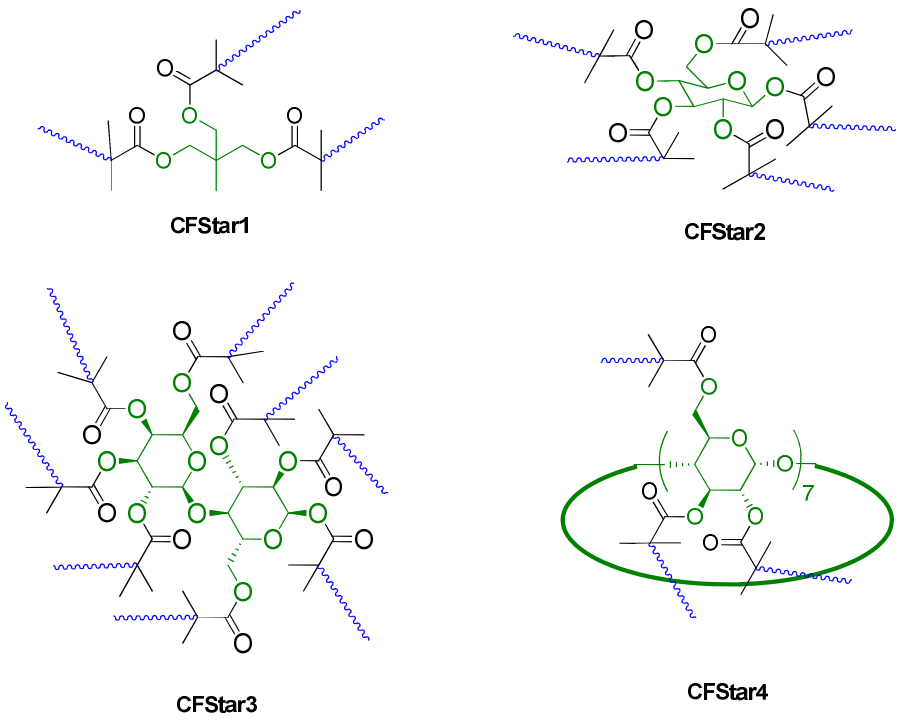

Figure 9: Star polymers synthesised using a core-first approach ATRP, using initiators with 3, 5, 8 and 21 initiating sites. ~~~ ***= PMMA***

Table 4: GPC results 3, 5, 8 and 21-arm star PMMA by both conventional GPC using a differential refractometer and linear PMMA standards to create a calibration curve, and by universal calibration using a differential refractometer and a four capillary viscometer.

Polymer	Functionality, *f*	Conventional GPC		Universal Calibration	
		M_n (g.mol^{-1})	PDI	M_n (g.mol^{-1})	PDI
CFStar1	3	15700	1.22	20300	1.51
CFStar2	5	19200	1.22	29200	1.45
CFStar3	8	34800	1.23	57100	1.67
CFStar4	21	21100	1.14	39800	1.29

Using the Universal calibration to analyse the polymers gives a higher M_n, M_w and PDI than the conventional GPC calibration, table 4. This is thought to be due to the increased density of the star polymer in solution resulting in larger retention times compared to the linear PMMA calibrants. Increasing the functionality causes an

increase in polymer density, which causes greater discrepancies between these two GPC calibration methods. This can be seen in table 1, where the M_n calculated by the two methods for the 3 arm star polymer differ 29%, and the discrepancies increase for the 5, 8 and 21-arm stars which are 52%, 64%, and 89% respectively.

Also of interest is the substantial apparent increase in PDI between conventional calibration and universal calibration. This was assumed at first to be due to an increase in band broadening;[121] an effect caused by lateral diffusion in 'dead' volume of the GPC, as a competitive process to the steric separation by columns. With the multi-detector GPC, the 'dead' volume is increased with the same steric separation, therefore the relative influence is greater than before and band broadening is increased. However, it is also inherent to the Universal calibration of branched materials. In conventional calibration, the calibration "curve" should be a straight line through the area of interest with a gradient, m_{con} and in universal calibration the calibration "curve" will be a straight line with a gradient, m_{univ}. It holds true for any given GPC column that $m_{univ} > m_{con}$ for a branched molecule. The gradient of the calibration curve is a function of the number of arms (branches) therefore the same peak shape and retention will not only have a higher molecular weight, but also greater relative difference between M_n and M_w.

2.4.2 Dilute solution properties of core-first PMMA stars

As described in section 2.1 it is possible to elucidate a great deal of information about a synthetic polymer using multi-detector GPC. Calculating the radius of gyration contraction factor can provide information about the structure of the polymer in solution. However, it has been shown that for polymers with high PDI, calculation of the bulk R_g for comparison with linear polymers is ineffective.[122] Conveniently, GPC

provides a method for rapidly fractionating a polymer solution and the use of MALLS allows the R_g to be determined for each eluting slice. One consideration to be noted is that for a randomly branched polymer, i.e. a star formed by core-crosslinking, the fractionation may not be complete. This is as the separation is based on hydrodynamic size. Core cross-linked star polymers can have very similar hydrodynamic volume but have different *f* and therefore different molecular weights. Therefore, it is possible that these polymers will not be separated on the chromatograph and will co-elute. Simon *et al.* showed that this co-elution does not occur for highly branched poly(methyl methacrylate-co- 2-(2-methyl-1-triethylsiloxy-1-propenyloxy)-ethyl methacrylate) using light scattering data.[67] Likewise, Radke *et al.* synthesised comb shaped polymers by anionic polymerisation and characterised them by multi-detector GPC, including viscometry and MALLS.[76] Using UV tagging of the side chains, they deduced that there was direct correlation between the number of side chains and the GPC elution. Therefore the branching was correlated to the molecular weight.

The analysis of the core-first star polymers by multi-detector GPC with MALLS provides information on the absolute M_w and the R_g of the eluting polymer fractions. However, the specific refractive index increment of PMMA in common GPC solvents is particularly low; the dn/dc of PMMA in $CHCl_3$ = 0.056 $mL.g^{-1}$ at T = 30 ^oC and λ_0 = 436 nm,[123] and in THF = 0.089 $mL.g^{-1}$ at T = 25 ^oC and λ_0 = 436 nm.[124,125] The inverse 2nd power dependence of light scattering on the specific refractive index increment of the analyte (eqn. 2.7, eqn. 2.8) hinders its use for PMMA in common GPC solvents at the low concentration needed for successful GPC.

The use of a capillary viscometer in-line on the GPC detector train allows the intrinsic viscosity of each fraction eluting from the GPC to be determined. A Mark-Houwink plot of log(η) against logMW has been produced for each of the polymers analysed.

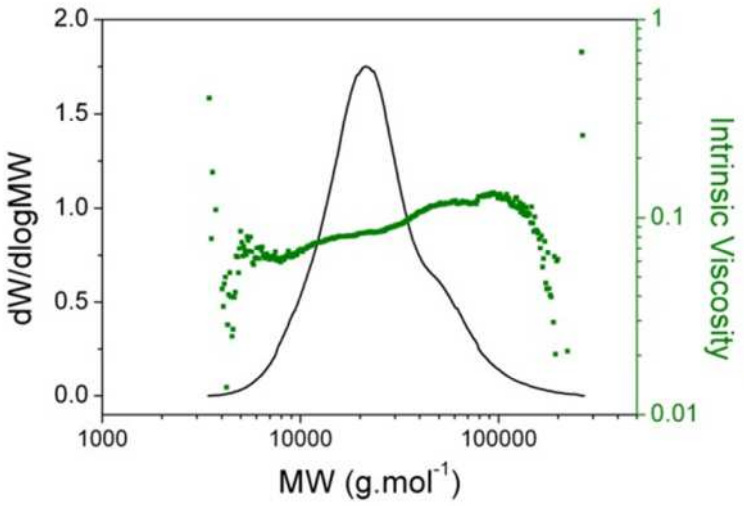

Figure 10: CFStar1, 3 arm star PMMA: From multi-detector GPC, green trace is the Mark-Houwink plot, black trace is the molecular weight distribution calculated by universal calibration, dW/dlogMW.

A Mark-Houwink plot for the 3 arm star polymer, **CFStar1**, shows that the intrinsic viscosity increases with molecular weight. The data is more uniform in areas of higher polymer concentration, but becomes more scattered and therefore less reliable at areas of low concentration, figure 10.

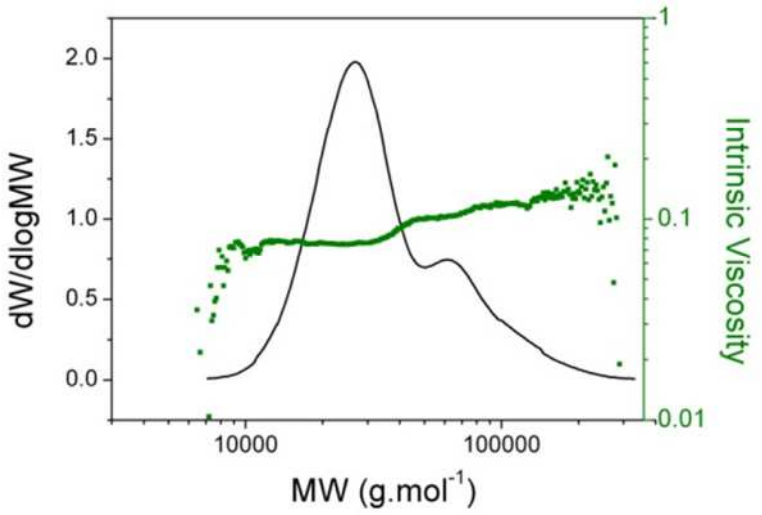

Figure 11: CFStar2, 5-arm star PMMA: From multi-detector GPC, green trace is the Mark-Houwink plot, black trace is the molecular weight distribution calculated by universal calibration, dW/dlogMW

CFStar2 has a bimodal MWD due to star-star coupling. This bimodal nature can be seen in the Mark-Houwink plot, which shows the transition from single star to aggregates at

approximately 40,000 g.mol^{-1}. The single star region shows a shallow increase in intrinsic viscosity over the MWD of the polymer, figure 11, and the high molecular weight region of the plot shows a step up to higher intrinsic viscosity that coincides with the star-star coupling shoulder on the MWD, figure 11.

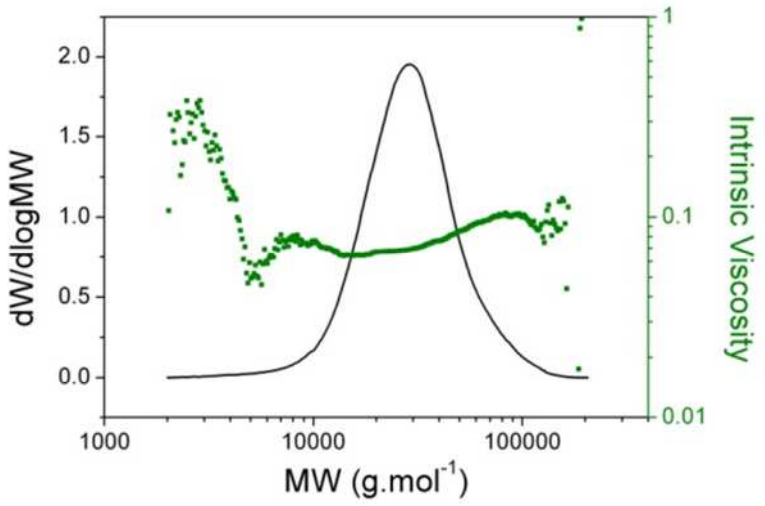

Figure 12 : CFStar3, 8-arm star PMMA: From multi-detector GPC, green trace is the Mark-Houwink plot, black trace is the molecular weight distribution calculated by universal calibration, dW/dlogMW.

The Mark-Houwink plot of **CFStar3** shows a decreasing intrinsic viscosity in the low molecular weight region, followed by a shallow increase in intrinsic viscosity over the remainder of the MWD, figure 12. The low molecular weight region however, is less reliable as the concentration of polymer is very low, therefore only high concentration areas were used for calculating the alpha value from the Mark-Houwink plot.

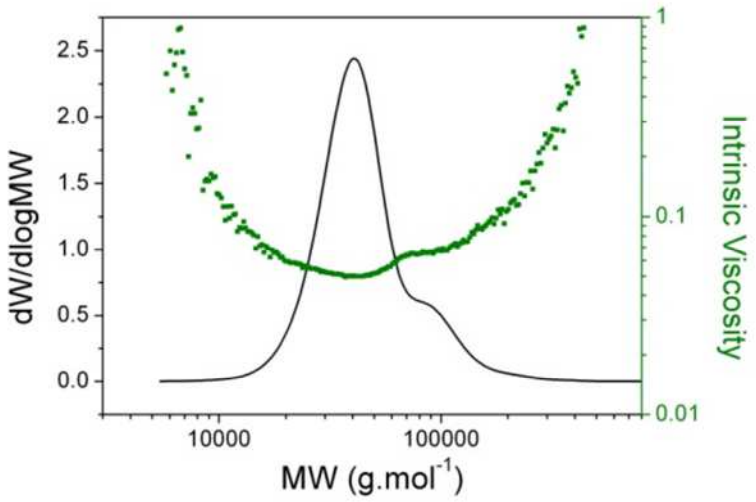

Figure 13: CFStar4, 21 arm star PMMA: From multi-detector GPC, green trace is the Mark-Houwink plot, black trace is the molecular weight distribution calculated by universal calibration, dW/dlogM.

CFStar4 has a much higher functionality than the other stars synthesised here. It shows a very interesting trend, where the intrinsic viscosity of the polymer decreases slightly with increasing MW over the MWD of the polymer, figure 13. In a similar fashion to **CFStar2**, **CFStar4**, has a high molecular weight shoulder ascribed to star-star coupling. The Mark-Houwink plot shows the same step in intrinsic viscosity as **CFStar2**. As in the 5-arm star, it coincides with the beginning of high molecular weight shoulder of the MWD, figure 13.

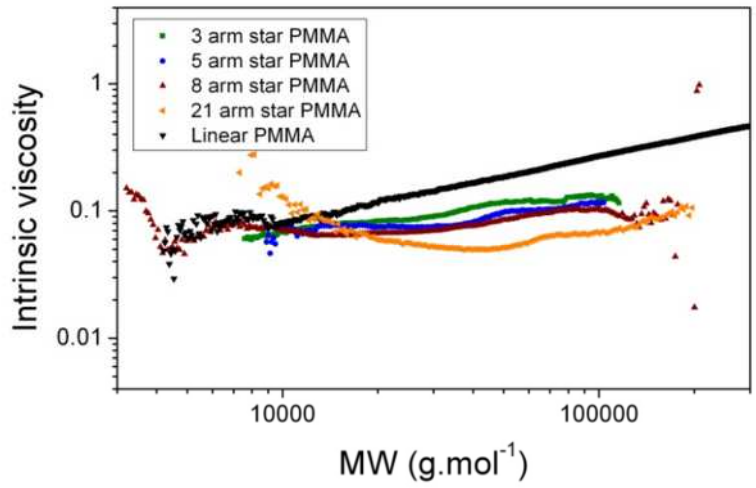

Figure 14: Mark-Houwink plots of linear PMMA, and 3, 5, 8 and 21 arm star PMMA

Overlaying the Mark-Houwink plots allows for a comparison of the effect molecular weight has on intrinsic viscosity of the various star polymers, figure 14. The Mark-Houwink plots for the star polymers shift to lower intrinsic viscosity with increasing functionality at the same molecular weights. This is expected as the polymers of the same molecular weight will contract in size with increasing functionality. Unexpectedly, there is also a decrease in the exponent, α, suggesting a change in architecture over the MWD. The decrease in α is more pronounced for the polymers with bimodal MWD, **CFStar2** and **CFStar4** suggesting that it could be related to the occurrence of star-star coupling.

The Mark-Houwink plots provide a lot of relative information about the differences in the star polymers; however, to elucidate any quantifiable data further analysis is required.

2.4.2.1 Quantifying the number of arms on PMMA core-first star polymers

The intrinsic viscosities of the star polymers and the linear polymer at the same molecular weight can be used to determine the intrinsic viscosity shrink ratio, g' for each integral slice of the MWD (eqn. 2.11). This shrink ratio can be useful as a further representation of the contraction of the star polymers in solution, however, it still only shows the contractions relative to the other stars; to quantify the functionality of the star polymers, it is necessary to convert g' to the radius of gyration contraction factor, g. This was carried out using a relationship derived from experiment in the literature (eqn. 2.12), using the parameters utilised by Robello *et al*.,[73] where a = 0.2624, b= 1.088 and c = 0.6087.

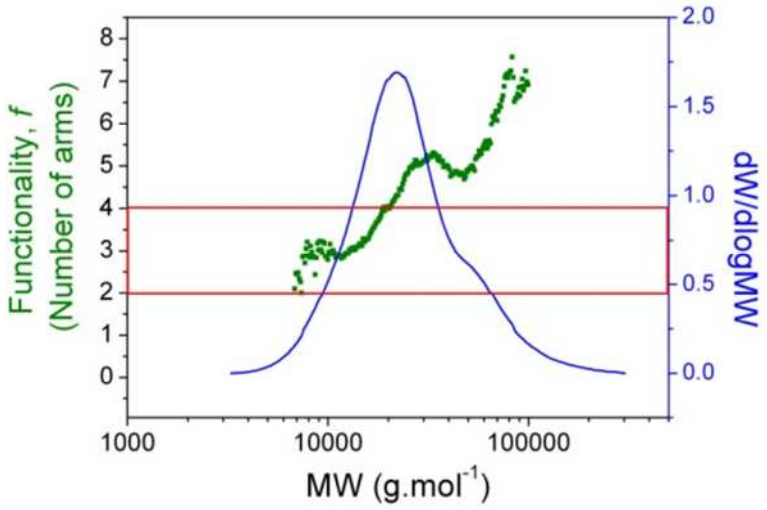

Figure 15: PMMA 3-arm star polymer: The estimated functionality, f, plotted over the distribution of the polymer, estimated from the radius of gyration contraction factor, g. The Zimm and Stockmayer solution for regular arm star polymers was used to relate g to f. The red box shows the functionality of the initiator ±1.

The functionality, *f*, was determined using Zimm and Stockmayer's quadratic solution for relating g and *f* for regular arm stars (eqn. 2.13) for a 3 arm star, **CFStar1,** figure 15. As expected, the data is seen to be most consistent at areas of high concentration of polymer close to the peak molecular weight (M_p) on the MWD. The functionality, f, increases with increasing molecular weight (MW), from 3 at low MW to 5 at high MW. At the M_p the functionality is approximately 4, one higher than the number of initiating sites on the multifunctional initiator. This could be accounted for by the star-star coupling which is evidenced by a high molecular weight shoulder on the MWD, figure 15.

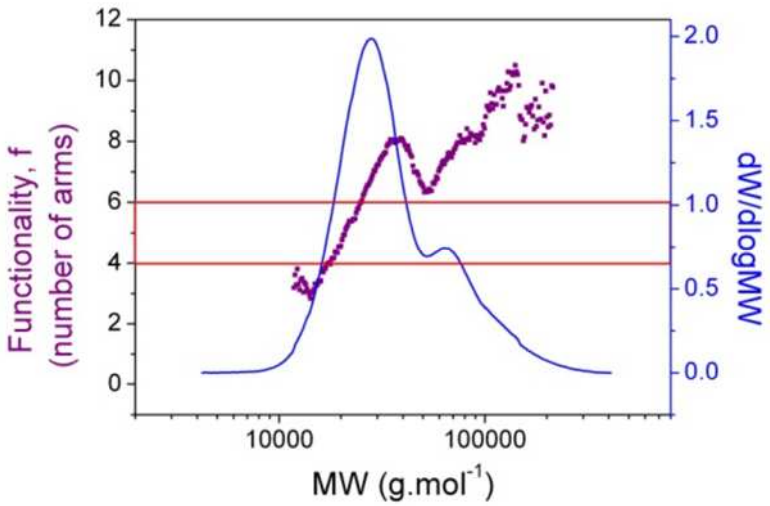

Figure 16: PMMA 5-arm star polymer: The estimated functionality, f, plotted over the distribution of the polymer, estimated from the radius of gyration contraction factor, g. The Zimm and Stockmayer solution for regular arm star polymers was used to relate g to f. The red box shows the functionality of the initiator ±1.

Using the analogous calculations to those used for **CFStar1,** the functionality was quantified for each slice of the MWD of **CFStar2,** figure 16**.** This polymer was synthesised using a 5-arm initiator, therefore the functionality of the PMMA polymer should be quantified to be close to 5. The functionality is seen to increase with the molecular weight, with the functionality at M_p quantified as 6. The increase in functionality over the MWD has been seen before by Robello *et al*. who report it to be due to imperfect initiator efficiency resulting in lower than expected functionality and star-star coupling resulting in higher than expected functionality.[73]

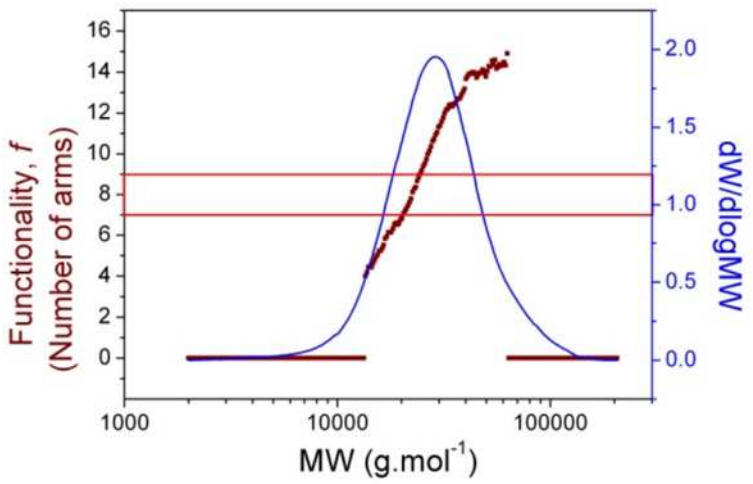

Figure 17: PMMA 8-arm star polymer: The estimated functionality, f, plotted over the distribution of the polymer, estimated from the radius of gyration contraction factor, g. The Zimm and Stockmayer solution for regular arm star polymers was used to relate g to f. The red box shows the functionality of the initiator ±1.

The functionality of the star PMMA made using an 8 arm initiator, **CFStar3,** has also been quantified, figure 17. The functionality here changes from 4 to 14 over the MWD, indicating that the initiator is inefficient at initiating every site, and that star-star coupling occurs. Interestingly, there is no shoulder on the polymer to indicate large quantities of star-star coupling.

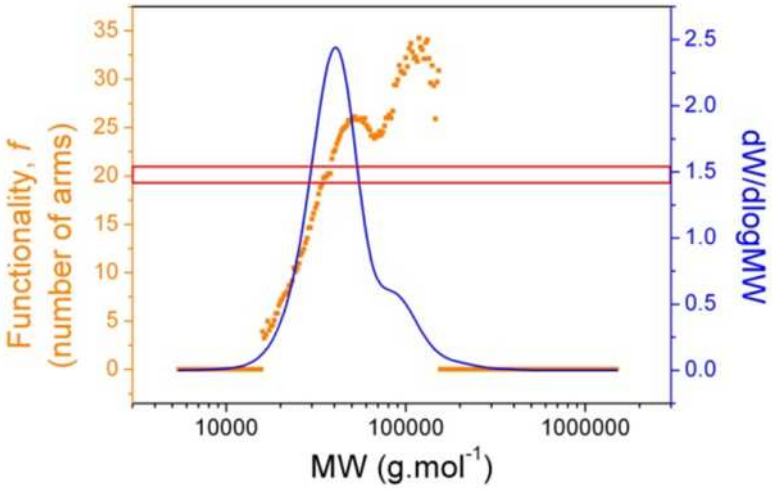

Figure 18 : PMMA 21-arm star polymer: The estimated functionality, f, plotted over the distribution of the polymer, estimated from the radius of gyration contraction factor, g. The Zimm and Stockmayer solution for regular arm star polymers was used to relate g to f. The red box shows the functionality of the initiator ±1.

It was expected that **CFStar4** would have a much higher functionality than the other PMMA star polymers as a 21-arm initiator was used in the synthesis. Using Zimm Stockmayer theory (eqn. 2.13) to quantify the functionality shows a wide range of functionality over the MWD of the polymer; from 4 to 27. The low functionality calculated at the lower MW of the MWD suggests that the initiator efficiency for each initiating site in the multi functional initiator is very variable, or termination is occurring early on in the reaction to leave low MW dead arms on the stars. As mentioned earlier, there is a high MW shoulder on the MWD of **CFStar4** evidencing star-star coupling. This can explain why the functionality exceeds the maximum of 21, related to the number of initiating sites on the star polymer.

This analysis has been carried out following the procedure outlined in the literature and recommended by the instrument manufacturers. It is apparent that the analytical procedure is far from perfect and some of the assumptions need to be questioned.

The use of multi-detector GPC with viscometry is still not commonly used in synthetic polymer chemistry research. Therefore this research, utilising branching information available from multi-detector GPC with narrow PDI PMMA star polymers synthesised using ATRP, is an important attempt to validate the technique reported in literature. The data here shows congruent data to that seen in literature, but it is this author's view that the changing functionality with molecular weight is inconsistent with the expected structure from core-first star polymerisation by ATRP.

2.5 Conclusions

Core-first stars have been made by ATRP of MMA using different well-defined multifunctional initiators. These stars were analysed using multi-detector GPC using a universal calibration and conventional GPC. Universal calibration was seen to estimate the MW more accurately than conventional GPC with respect to the values expected.

Although star-star coupling was seen to occur in the reaction, this was minimised by terminating the reactions at low conversions, below 50%. Interestingly, there is a visible change in the Mark-Houwink plots for these two polymer architectures, with a step up in the intrinsic viscosity. However, there is no evidence of a decrease in the gradient, α, which would be expected with coupling due to increased polymer density in solution. Comparison of the plots shows that at the same MW on the MWD of the polymers, the intrinsic viscosity is lower for a star with more arms.

Each star's functionality was determined using their intrinsic viscosity contraction factor (eqn. 2.11) and Zimm Stockmayer theory (eqn. 2.13), and seen to agree with the functionality of the core initiator at the M_p. At the highest concentration at the peak molecular weight, M_p, the functionality is approximately 4 for the 3-arm star (figure 15), 6 for the 5-arm star (figure 16), 8 for the 8-arm star (figure 17), and 21 for the 21-arm star (figure 18). The determination of functionality using this technique uses a number of approximations and assumptions, however, the error of ± 1 at the M_p was in agreement with a previous study of PMMA core-first star polymers by Robello and co-workers.[73]

The functionality of the stars was seen to change over their MWD, which is thought to be because of initiator efficiency, termination, and star-star coupling occurring in the reaction.

2.6 Experimental

2.6.1 Instruments

GPC was used to determine the molecular weight averages and the PDI of polymers using one of two systems. System 1, with a 390-LC Polymer Laboratories system equipped with a PL-AS RT/MT autosampler, a PL gel 3 µm (50 × 7.5 mm) guard column, two PL gel 5 µm (300 × 7.5 mm) mixed D columns (suitable for separations up to MW = 2.0×10^6 g.mol^{-1}), a differential refractometer, 4 capillary viscometer and MALLS were used. Solvent used was chloroform / triethylamine 95 : 5 (v/v) as the eluent with a flow rate of 1.0 mL.min^{-1}, unless otherwise stated. System 2 with a 390-LC Polymer Laboratories system equipped with a PL-AS RT/MT autosampler, a PL gel 3 µm (50 × 7.5 mm) guard column, two PL gel 5 µm (300 × 7.5 mm) mixed D columns (suitable for separations up to MW = 2.0×10^6 g.mol^{-1}), a differential refractometer, MALLS, and a photodiode array were used. Eluent used was tetrahydrofuran / triethylamine 95 : 5 (v/v) as the eluent with a flow rate of 1.0 mL.min^{-1}, unless otherwise stated. Calibrations were set using a single injection of narrow molecular weight PMMA standards (1000 – 1×10^6 g.mol^{-1}) of known concentration, with a minimum of 10 points to form the curve.

All ^{1}H and ^{13}C NMR spectra were recorded on Bruker DPX300, Bruker DPX400 and Bruker DRX500 spectrometers as solutions in deuterated nuclear magnetic resonance (NMR) solvents. Chemical shifts are cited as parts per million (ppm). The following abbreviations are used to represent multiplicities; s = singlet, d = doublet, t = triplet, q = quartet, m = multiplet.

FT-IR was recorded on a VECTOR-22 Bruker spectrometer using a Golden Gate diamond attenuated total reflection cell.

2.6.2 Materials

All materials were purchased from Sigma Aldrich at the highest available quality and used without further purification, unless otherwise stated.

Methyl methacrylate was de-inhibited by passing through an activated neutral aluminium oxide column prior to use. 5-arm, 8-arm initiator and 21-arm initiator were synthesised within the group and used as received. [126]

2.6.2.1 Synthesis of 1,1,1- tris(methyl-O-isobutyryl bromide) ethane

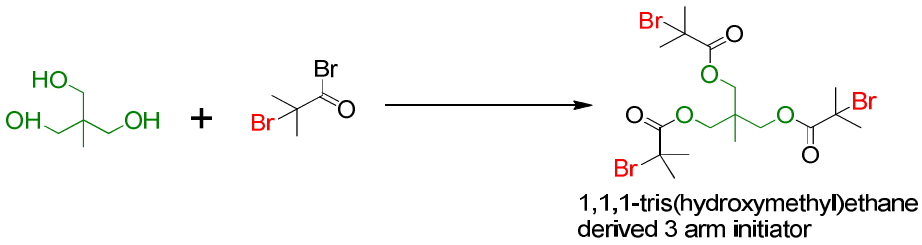

Scheme 9: Synthesis of 3-arm initiator from 1,1,1-tris (hydroxymethyl) ethane

1,1,1-Tris(hydroxymethyl) ethane (12.01 g, 100 mmol), triethylamine (56.20 mL, 350 mmol) and THF (200 mL) were placed into a round bottom flask and cooled to 0 ^{o}C in an ice bath. 2-Bromoisobutyryl acid bromide (41.70 mL, 330 mmol) was added dropwise with stirring over 30 minutes, and the reaction left over night at ambient temperature. The reaction mixture was filtered, and the filtrate passed through a column of basic aluminium oxide. The organic solution was washed with acidified water (pH 4.5, 2 x 300 ml) and dried with magnesium sulfate. The organic solvent was removed under reduced pressure.

FT-IR: 2975, 1732, 1461, 1389, 1265, 1153, 1102 cm^{-1};

^{1}H NMR ($CDCl_3$), δ (ppm): 4.20 (s, 6H, -COOC$\underline{H}_2$-), 1.98 (s, 18H, -C$\underline{H}_3$), 1.21 (s, 3H, C$\underline{H}_3$);

^{13}C NMR ($CDCl_3$), δ (ppm): 171.2 (-$\underline{C}$OO-), 66.6 (COO$\underline{C}H_2$), 55.4 (-C(CH_3)$_2$ Br), 39.7 ($\underline{C}(C_4H_8O_2Br)_3CH_3$), 30.7 (C($\underline{C}H_3$)Br), 17.1 ($C(C_4H_8O_2Br)_3\underline{C}H_3$);

2.6.3 ATR Polymerisation of methyl methacrylate 3 arm star polymer

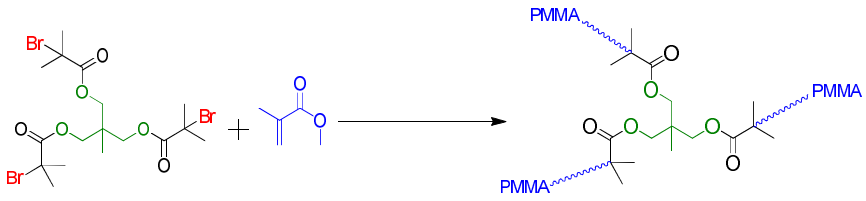

Scheme 10: Polymerisation of MMA using 1,1,1- tris(methyl-O-isobutyryl bromide) ethane initiator.

Methyl methacrylate (11.82 g, 118 mmol), 1,1,1-tris(hydroxymethyl)ethane derived initiator 1 (0.17 g, 0.30 mmol), *N-(*n-propyl)-2-pyridylmethanamine (0.26 g, 1.77 mmol) and toluene (10 mL) as the solvent, were placed in a dry Schlenk tube containing a magnetic stirrer. The tube was sealed with a rubber septum and subjected to five-freeze-pump thaw cycles to degas the solution. Copper (I) bromide (0.13 g, 0.89 mmol) was added to the degassed, frozen solution against a flow of nitrogen. The sealed tube was then immersed in an oil bath heated to 70 ^{o}C, and samples taken periodically using a degassed syringe for molecular weight and conversion analysis. At the end of the reaction, after 8 hours, the mixture was diluted with toluene (20 mL) and air was bubbled through for 1 hour. Neutral alumina (10 g) was added to the reaction mixture and stirred for 2 hours. The mixture was filtered, and the solution was

concentrated under reduced pressure. The polymer was precipitated in water/methanol to yield a white powder. Yield = 4.30 g. Conversion of the polymer was followed by comparing the decreasing singlet at 4.60 ppm (corresponding to the $C(O)OCH_2$ protons in the monomer) with the broad signal at 4.40 ppm increasing with time (corresponding to the $C(O)OCH_2$ protons in the polymer). M_n (GPC) = 15700 $g.mol^{-1}$; PDI (GPC) = 1.13; Conversion = 49%; Initiator efficiency = 94%

2.6.4 ATR Polymerisation of methyl methacrylate 5 arm star polymer

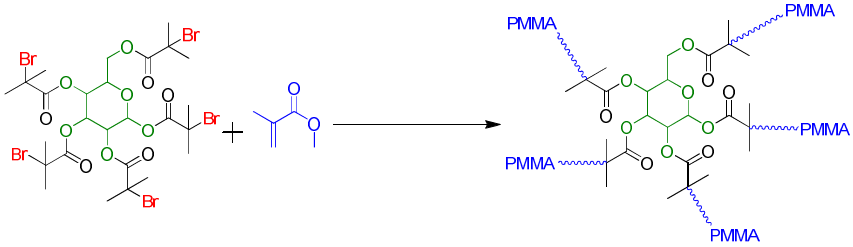

Scheme 11: ATR Polymerisation of methyl methacrylate using 1,2,3,4,6-penta-O-isobutyryl bromide-α-D-glucose initiator.

Methyl methacrylate (11.82 g, 118 mmol), 1,2,3,4,6-penta-O-isobutyryl bromide-α-D-glucose (0.28 g, 0.30 mmol), *N-(*n-propyl)-2-pyridylmethanamine (0.53 g, 3.60 mmol) and toluene (10 mL) as the solvent, were placed in a dry Schlenk tube containing a magnetic stirrer. The tube was sealed with a rubber septum and subjected to five-freeze-pump thaw cycles to degas the solution. Copper (I) bromide (0.26 g, 1.78 mmol) was added to the degassed, frozen solution against a flow of nitrogen. The sealed tube was then immersed in an oil bath heated to 70 ^{o}C, and samples taken periodically using a degassed syringe for molecular weight and conversion analysis. At the end of the reaction, after 3 hours, the mixture was diluted with toluene (20 mL)

and air was bubbled through for 1 hour. Neutral alumina (10 g) was added to the reaction mixture and stirred for 2 hours. The mixture was filtered, and the solution was concentrated under reduced pressure. The polymer was precipitated in water/methanol to yield a white viscous liquid. Yield = 4.16 g. Conversion of the polymer was followed by comparing the decreasing singlet at 4.60 ppm (corresponding to the $C(O)OCH_2$ protons in the monomer) with the broad signal at 4.40 ppm increasing with time (corresponding to the $C(O)OCH_2$ protons in the polymer). M_n (GPC) = 19200 $g.mol^{-1}$; PDI (GPC) = 1.22; Conversion = 56% by ^{1}H-NMR

2.6.5 ATR Polymerisation of methyl methacrylate 8 arm star polymer

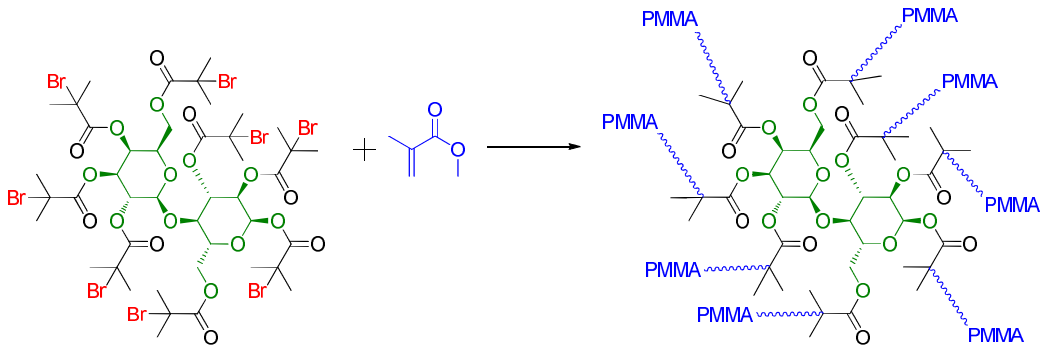

Scheme 12: ATR polymerisation of MMA using lactose based 8-arm initiator.

Methyl methacrylate (20.00 g, 199.98 mmol), lactose based 8 arm initiator (0.797 g, 0.52 mmol, 1 eq), *N*-(n-propyl)-2-pyridylmethanamine (1.26 g, 9.14 mmol, 2.2 eq) and toluene (20 mL) as the solvent, were placed in a dry Schlenk tube containing a magnetic stirrer. The tube was sealed with a rubber septum and subjected to five-freeze-pump thaw cycles to degas the solution. Copper (I) bromide (0.59 g, 4.16 mmol, 1.1 eq) was

added to the degassed, frozen solution against a flow of nitrogen. The sealed tube was then immersed in an oil bath heated to 70 ^{o}C, and samples taken periodically using a degassed syringe for molecular weight and conversion analysis. At 17% conversion, after 40 minutes, the mixture was diluted with toluene (20 mL) and air was bubbled through for 1 hour. Neutral alumina (10 g) was added to the reaction mixture and stirred for 2 hours. The mixture was filtered, and the solution was concentrated under reduced pressure. The polymer was precipitated in water/methanol to yield a white powder. Yield = 3.12 g. Conversion of the polymer was followed by comparing the decreasing singlet at 4.60 ppm (corresponding to the $C(O)OCH_2$ protons in the monomer) with the broad signal at 4.40 ppm increasing with time (corresponding to the $C(O)OCH_2$ protons in the polymer). M_n (GPC) = 34,800 g.mol^{-1}; PDI (GPC) = 1.23; Conversion = 17.3% by ^{1}H NMR.

2.6.6 ATR Polymerisation of methyl methacrylate 21 arm star polymer

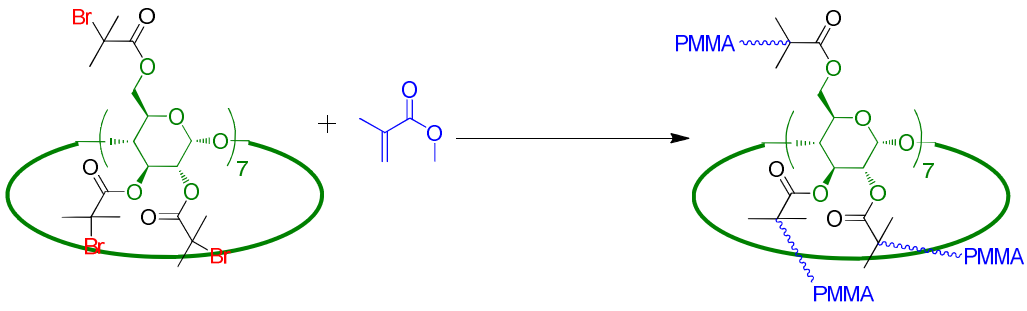

Scheme 13: ATR Polymerisation of MMA using β-CD based 21-arm initiator.

Methyl methacrylate (5.00 g, 49.94 mmol, 956 eqs), β-CD based 21 arm initiator (0.223 g, 0.052 mmol, 1eq), *N-(*n-propyl)-2-pyridylmethanamine (0.179 g, 1.10 mmol, 23.1 eq)

and toluene (5 mL) as the solvent, were placed in a dry Schlenk tube containing a magnetic stirrer. The tube was sealed with a rubber septum and subjected to five-freeze-pump thaw cycles to degas the solution. Copper(I) bromide (0.16 g, 1.21 mmol, 21 eq) was added to the degassed, frozen solution against a flow of nitrogen. The sealed tube was then immersed in an oil bath heated to 65^{o}C, and samples taken periodically using a degassed syringe for molecular weight and conversion analysis. At the 32% conversion, after 65 minutes, the mixture was diluted with toluene (5 mL) and air was bubbled through for 1 hour. The reaction solution was passed through a neutral alumina column and concentrated under reduced pressure. The polymer was precipitated in water/methanol to yield a white powder, and dried under vacuum. Yield = 1.45 g. Conversion of the polymer was followed by comparing the decreasing singlet at 4.60 ppm (corresponding to the C(O)OCH$_2$ protons in the monomer) with the broad signal at 4.40 ppm increasing with time (corresponding to the C(O)OCH$_2$ protons in the polymer). M_n (GPC) = 21,100 g.mol^{-1}; PDI (GPC) = 1.14; Conversion = 32.4% by ^{1}H NMR.

2.7 References

(47) Moore, J. C. *J. Polym. Sci., Part A: Gen. Pap.* **1964**, *2*, 835.

(48) Moore, J. C.; Hendrickson, J. G. *J. Polym. Sci., Part C: Polym. Symp.* **1965**, *8*, 233.

(49) Moore, J. C. *Separation Science* **1970**, *5*, 723.

(50) Striegel, A. M.; Yau, W. W.; Kirkland, J. J.; Bly, D. D. In *Modern Size-Exclusion Liquid Chromatography*; John Wiley & Sons, Inc.: 2009, p 18.

(51) Manfred J. R. Cantow, R. S. P., Julian F. Johnson, *J. Polym. Sci., Part A: Polym. Chem.* **1967**, *5*, 987.

(52) Grubisic, Z.; Benoit, H.; Rempp, P. *J. Polym. Sci., Polym. Lett. Ed.* **1967**, *5*, 753.

(53) Saunders, G. In *LC-GC Europe*; Advanstar Communications Inc.: 2004; Vol. 17, p 650.

(54) Liu, P.; Landry, E.; Ye, Z.; Joly, H.; Wang, W.-J.; Li, B.-G. *Macromolecules* **2011**, *44*, 4125.

(55) Saunders, G.; Cormack, P. A. G.; Graham, S.; Sherrington, D. C. *Macromolecules* **2005**, *38*, 6418.

(56) Fazeli, N.; Mohammadi, N.; Taromi, F. A. *Polym. Test.* **2004**, *23*, 431.

(57) G. Samay, M. K., J. Podescaronva, *Angew. Makromol. Chem.* **1978**, *72*, 185.

(58) Mourey, T. H.; Miller, S. M.; Balke, S. T. *J. Liq. Chromatogr. Relat. Technol.* **1990**, *13*, 435

(59) Zimm, B. H. *J. Chem. Phys.* **1948**, *16*, 1093.

(60) Daoud, M.; Cotton, J. P. *J. Phys. II* **1982**, *43*, 531.

(61) Held, D.; Müller, A. H. E. *Macromol. Symp.* **2000**, *157*, 225.

(62) Zimm, B. H.; Stockmayer, W. H. *J. Chem. Phys.* **1949**, *17*, 1301.

(63) Jackson, C.; Chen, Y.-J.; Mays, J. W. *J. Appl. Polym. Sci.* **1996**, *59*, 179.

(64) Haney, M. A. *J. Appl. Polym. Sci.* **1985**, *30*, 3037.

(65) Haney, M. A. *J. Appl. Polym. Sci.* **1985**, *30*, 3023.

(66) Roovers, J.; Zhou, L. L.; Toporowski, P. M.; van der Zwan, M.; Iatrou, H.; Hadjichristidis, N. *Macromolecules* **1993**, *26*, 4324.

(67) Simon, P. F. W.; Müller, A. H. E.; Pakula, T. *Macromolecules* **2001**, *34*, 1677.

(68) Bruno H. Zimm, R. W. K. *J. Polym. Sci.* **1959**, *37*, 19.

(69) Lesec, J.; Millequant, M. *Int. J. Polym. Anal. Charact.* **1996**, *2*, 305

(70) Balke, S. T.; Mourey, T. H.; Robello, D. R.; Davis, T. A.; Kraus, A.; Skonieczny, K. *J. Appl. Polym. Sci.* **2002**, *85*, 552.

(71) Flory, P. J. *Principles of Polymer Chemistry*; 16 ed.; Cornell University Press: Ithaca, 1953.

(72) Grest, G. S.; Fetters, L. J.; Huang, J. S.; Richter, D. *Adv. Chem. Phys.* **1996**, *94*, 67.

(73) Robello, D. R.; Andre, Alix; McCovick, T. A.; Mourey, T. H. *Macromolecules* **2002**, *35*, 9334.

(74) Weissmuller, M.; Burchard, W. *Polym. Int.* **1997**, *44*, 380.

(75) Burchard, W. *Adv. Polym. Sci.* **1999**, *143*, 113.

(76) Radke, W.; Müller, A. H. E. *Macromolecules* **2005**, *38*, 3949.

(77) Narrainen, A. P.; Pascual, S.; Haddleton, D. M. *J. Polym. Sci., Part A: Polym. Chem.* **2002**, *40*, 439.

(78) Pfaff, A.; Müller, A. H. E. *Macromolecules* **2011**, *44*, 1266.

(79) Castignolles, P.; Graf, R.; Parkinson, M.; Wilhelm, M.; Gaborieau, M. *Polymer* **2009**, *50*, 2373.

(80) Guillaneuf, Y.; Castignolles, P. *J. Polym. Sci., Part A: Polym. Chem.* **2008**, *46*, 897.

(81) Netopilík, M.; Kratochvíl, P. *Polymer* **2003**, *44*, 3431.

(82) Stenzel-Rosenbaum, M. H.; Davis, T. P.; Chen, V.; Fane, A. G. *Macromolecules* **2001**, *34*, 5433.

(83) Zhao, Y.; Chen, Y.; Chen, C.; Xi, F. *Polymer* **2005**, *46*, 5808.

(84) Wager, C. M.; Haddleton, D. M.; Bon, S. A. F. *Eur. Polym. J.* **2004**, *40*, 641.

(85) Mayadunne, R. T. A.; Jeffery, J.; Moad, G.; Rizzardo, E. *Macromolecules* **2003**, *36*, 1505.

(86) Barner-Kowollik, C.; Dalton, H.; Davis, T. P.; Stenzel, M. H. *Angew. Chem.* **2003**, *115*, 3792.

(87) Chaffey-Millar, H.; Stenzel, M. H.; Davis, T. P.; Coote, M. L.; Barner-Kowollik, C. *Macromolecules* **2006**, *39*, 6406.

(88) Nguyen, T. L. U.; Eagles, K.; Davis, T. P.; Barner-Kowollik, C.; Stenzel, M. H. *J. Polym. Sci., Part A: Polym. Chem.* **2006**, *44*, 4372.

(89) Stenzel-Rosenbaum, M.; Davis, T. P.; Chen, V.; Fane, A. G. *J. Polym. Sci., Part A: Polym. Chem.* **2001**, *39*, 2777.

(90) Chen, M.; Ghiggino, K. P.; Launikonis, A.; Mau, A. W. H.; Rizzardo, E.; Sasse, W. H. F.; Thang, S. H.; Wilson, G. J. *J. Mater. Chem.* **2003**, *13*, 2696.

(91) Chen, M.; Ghiggino, K. P.; Thang, S. H.; Wilson, G. J. *Angew. Chem., Int. Ed.* **2005**, *44*, 4368.

(92) Chen, M.; Ghiggino, K. P.; Thang, S. H.; Wilson, G. J. *Polym. Int.* **2006**, *55*, 757.

(93) Chong, Y. K.; Le, T. P. T.; Moad, G.; Rizzardo, E.; Thang, S. H. *Macromolecules* **1999**, *32*, 2071.

(94) Mayadunne, R. T. A.; Moad, G.; Rizzardo, E. *Tetrahedron Lett.* **2002**, *43*, 6811.

(95) Xu, J.; Luo, S.; Shi, W.; Liu, S. *Langmuir* **2005**, *22*, 989.

(96) Luo, S.; Xu, J.; Zhu, Z.; Wu, C.; Liu, S. *J. Phys. Chem. B* **2006**, *110*, 9132.

(97) Hawker, C. J. *Angew. Chem., Int. Ed.* **1995**, *34*, 1456.

(98) Chessa, G.; Scrivanti, A.; Matteoli, U.; Castelvetro, V. *Polymer* **2001**, *42*, 9347.

(99) Miura, Y.; Yoshida, Y. *Macromol. Chem. Phys.* **2002**, *203*, 879.

(100) Gopalan, P.; Zhang, Y.; Li, X.; Wiesner, U.; Ober, C. K. *Macromolecules* **2003**, *36*, 3357.

(101) Dufils, P.-E.; Chagneux, N.; Gigmes, D.; Trimaille, T.; Marque, S. R. A.; Bertin, D.; Tordo, P. *Polymer* **2007**, *48*, 5219.

(102) Kakuchi, T.; Narumi, A.; Matsuda, T.; Miura, Y.; Sugimoto, N.; Satoh, T.; Kaga, H. *Macromolecules* **2003**, *36*, 3914.

(103) Miura, Y.; Dote, H. *J. Polym. Sci., Part A: Polym. Chem.* **2005**, *43*, 3689.

(104) Miura, Y.; Dote, H.; Kubonishi, H.; Fukuda, K.; Saka, T. *J. Polym. Sci., Part A: Polym. Chem.* **2007**, *45*, 1159.

(105) Pyun, J.; Rees, I.; Frechet, J. M. J.; Hawker, C. J. *Aust. J. Chem.* **2003**, *56*, 775.

(106) Miura, Y.; Dairoku, M. *J. Polym. Sci., Part A: Polym. Chem.* **2007**, *45*, 4364.

(107) Hawker, C. J.; Frechet, J. M. J.; Grubbs, R. B.; Dao, J. *J. Am. Chem. Soc.* **1995**, *117*, 10763.

(108) Abdallah, D.; Ghani, M. A. A.; Cunningham, M. F.; Kazmaier, P. M.; Keoshkerian, B.; Buncel, E. *Can. J. Chem.* **2004**, *82*, 1393.

(109) Ghani, M. A. A.; Abdallah, D.; Kazmaier, P. M.; Keoshkerian, B.; Buncel, E. *Can. J. Chem.* **2004**, *82*, 1403.

(110) Erdogan, T.; Gungor, E.; Durmaz, H.; Hizal, G.; Tunca, U. *J. Polym. Sci., Part A: Polym. Chem.* **2006**, *44*, 1396.

(111) Beil, J. B.; Zimmerman, S. C. *Macromolecules* **2004**, *37*, 778.

(112) Miura, Y.; Yamaoka, K.; Mannan, M. A. *Polymer* **2006**, *47*, 510.

(113) Robin, S.; Guerret, O.; Couturier, J.-L.; Gnanou, Y. *Macromolecules* **2002**, *35*, 2481.

(114) Fischer, H. *Macromolecules* **1997**, *30*, 5666.

(115) Stenzel, M. H.; Davis, T. P. *J. Polym. Sci., Part A: Polym. Chem.* **2002**, *40*, 4498.

(116) Hao, X.; Nilsson, C.; Jesberger, M.; Stenzel, M. H.; Malmström, E.; Davis, T. P.; Östmark, E.; Barner-Kowollik, C. *J. Polym. Sci., Part A: Polym. Chem.* **2004**, *42*, 5877.

(117) Hao, X.; Malmström, E.; Davis, T. P.; Stenzel, M. H.; Barner-Kowollik, C. *Aust. J. Chem.* **2005**, *58*, 483.

(118) Castignolles, P. *Macromol. Rapid Commun.* **2009**, *30*, 1995.

(119) Angot, S.; Murthy, K. S.; Taton, D.; Gnanou, Y. *Macromolecules* **2000**, *33*, 7261.

(120) Cai-Yuan, P.; Lei, T.; De-Cheng, W. *J. Polym. Sci., Part A: Polym. Chem.* **2001**, *39*, 3062.

(121) Striegel, A. M.; Yau, W. W.; Kirkland, J. J.; Bly, D. D. *Modern Size-Exclusion Liquid Chromatography*; 2nd ed.; Wiley: Hoboken, New Jersey, 2009.

(122) Kilb, R. W. *J. Polym. Sci.* **1959**, *38*, 403.

(123) Kisakürek, D.; Baysal, B. M. *Polymer* **1984**, *25*, 693.

(124) Bodmann, O. *Makromol. Chem.* **1969**, *122*, 196.

(125) Cantow, H. J.; Bodmann, O. *Z Physik Chem (Frankfurt)* **1955**, *3*, 65.

(126) Wright, P. PhD thesis, University of Warwick, 2008.

Chapter 3

Synthesis and characterisation of arm-first PMMA star polymers

Star PMMA was synthesised using a core-crosslinking arm-first technique using RAFT chemistry. To allow the use of RAFT chemistry for the polymerisation of MMA, it was necessary to synthesise a suitable RAFT agent for methacrylates; 2-cyanoprop-2-yl dithiobenzoate (CPDB, ***RAFT agent1***) and 2-cyanoprop-2-yl dithiobenzoate (CPADB, **RAFT agent2**) were chosen.

Sequential addition of monomer and then a divinyl species, ethylene glycol dimethacrylate (EGDMA, **crosslinker1**), was seen to form star polymers. Varying the crosslinker used (**crosslinker1**, **crosslinker2 and crosslinker3**) and the ratio of crosslinker to RAFT agent, has been seen to control the size and yield of the star polymer formed.

A series of polymers of varying sizes have been analysed using a novel multi-detector GPC technique to determine the amount of branching (arms) in the polymer.

3.1 Introduction

3.1.1 Arm-first star synthesis

In this approach, linear polymer arms are prepared prior to being self-assembled to form the core. This can be done in different ways, including microgel formation after arm synthesis in the so called “core-crosslinking” method, or the use of highly efficient reactions and “click” reactions to form a multifunctional core.[127-131] Star formation can also be directed by self-assembly of amphiphilic diblock polymers prior to crosslinking.[132,133] The core-crosslinking technique has been widely used to form multi-arm star polymers.

Controlled radical polymerisation by RAFT,[133-139] NMP and TMM-LRP [140-145] allows for the formation of core cross-linked star polymers by linking reaction of linear arm polymers with divinyl compounds (or *via* a core-first approach through the polymerisation of vinyl monomers from living micro-gel cores). The resulting star polymers have nano-scale micro-gel cores protected from the external environment by many linear polymer arms radiating from the core.

Using TMM-LRP, they can be easily made by the reaction of propagating linear polymer chains with a divinyl crosslinker. This approach can give relatively narrow MWDs (PDI < 1.5) and high yield (arm incorporation > 90%) using TMM-LRP by selecting the appropriate crosslinking agent and reaction conditions, such as concentration of linear arm polymer, temperature and molar ratio of divinyl compound to propagating linear polymer. [140-144] This can be achieved by *in situ* crosslinking of propagating pre-polymers by the addition of divinyl crosslinker to propagating linear polymer solution or by polymerisation of a crosslinking agent using an isolated macroinitiator, method A in

figure 1. The latter is particularly useful as an easy route to mikto-arm star polymers.[146,147]

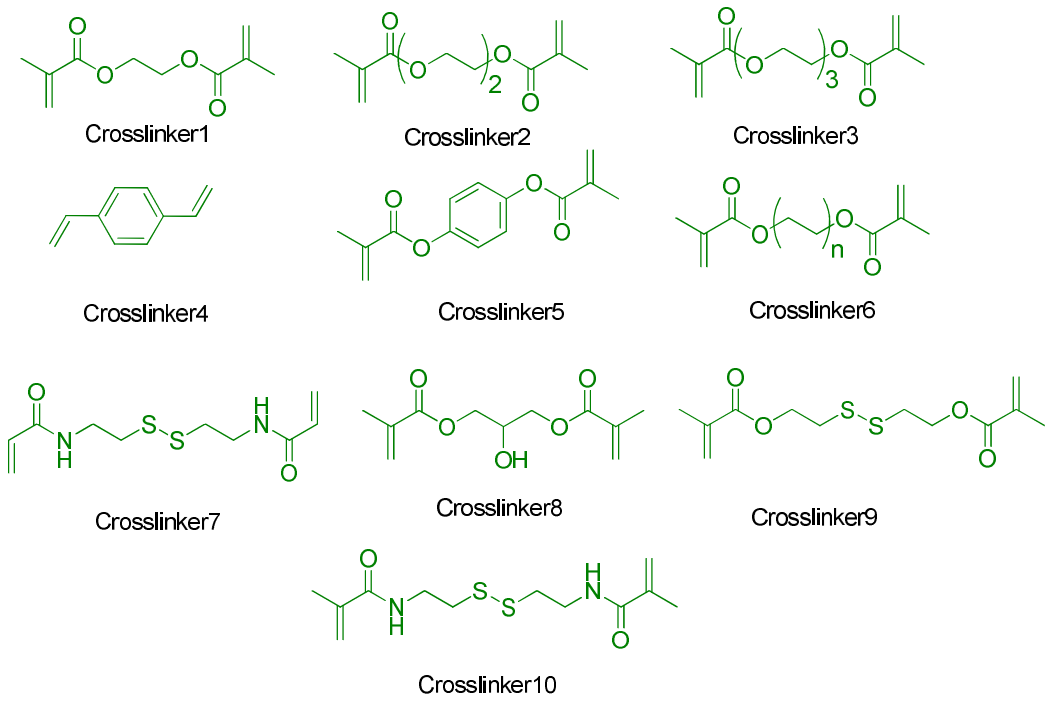

Figure 19: Cross-linking agents used in arm-first core cross-linked star polymer synthesis.

The star polymer yield, number of arms (*f*), absolute weight average molecular weight (M_w), radius of gyration (R_g) and intrinsic viscosity can be effectively controlled by varying the ratio of crosslinker to propagating polymer arm, concentration of arm polymer, degree of polymerisation of precursor arm polymer and species of divinyl compound.[140-145]

NMP has also been applied to the synthesis of star polymers with cross-linked cores by an arm-first approach. Solomon *et al*. synthesised 4-tert-butyl styrene star polymers crosslinked with **crosslinker 4**, figure 19, by NMP to form arm-first star polymers.[148] However, the optimal ratio of **crosslinker 4** to poly(styrene) macroinitiatior varied significantly depending on the applied conditions.[149-151] The strong covalent bond in

TEMPO based alkoxyamine has limited the composition of star polymers, and styrene based monomers have been prevalent in the star polymers formed using this controlled radical polymerisation technique.[152] With the development of more active second generation alkoxyamines, Hawker *et al.* expanded the utility of NMP to allow the synthesis of a series of star polymers with a cross-linked core and a range of arm compositions, including styrene, acrylates, vinyl pyridine, methacrylates and acrylamides.[153,154]

As is the case in TMM-LRP it is possible to introduce functionality to the arm-first star polymer. This can be achieved using functional nitroxides[155] or functional monomers/crosslinkers.[150,156]

RAFT chemistry has also been used to synthesise star polymers by an arm-first route, using a wide variety of RAFT agents, monomers and crosslinkers.[133,135-139] However, the use of RAFT has had limited success; the polymers typically yielded only provide narrow PDI at low arm incorporation. Typical high arm incorporation star polymers have high PDI (>>1.5).[135-138] Recently, careful choice of experimental conditions has been shown to optimise these reactions. In particular for RAFT the solvent/solubility of reagents has been shown to greatly affect the molecular weight distribution and efficiency of star formation.[134,157]

3.2 Results and Discussion

3.2.1 Arm-first core cross-linked PMMA stars by RAFT polymerisation

Multi-arm stars can be made in a variety of ways, as discussed in section 3.1.1. Here, the core-crosslinking approach has been used to synthesise multi arm star PMMA.

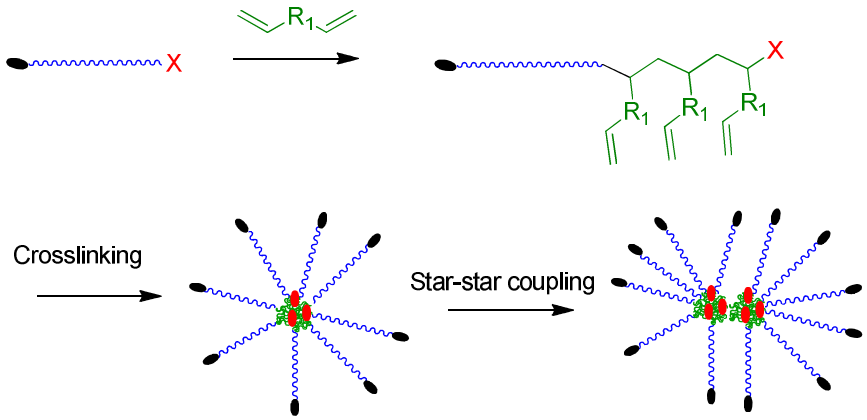

Scheme 14: General reaction scheme for star formation using core-crosslinking. = initiating species, X= propagating chain end, = polymer, R_1 varies depending on crosslinker used.

The core-crosslinking technique, scheme 14, was chosen as it has been shown to successfully synthesise multi arm star polymers in the literature using numerous controlled radical techniques. However, the synthesis of well controlled narrow PDI arm-first stars by RAFT had, until recently,[158] not been reported in the literature. As discussed in section 3.1.1 several factors affect the number of arms, conversion of arm to star, and PDI of the star formed. The effects of precursor polymer length, ratio of crosslinker to polymer, and overall concentration have been discussed in the literature. Mays[159] and Burchard[160] found that the number of arms increases with the ratio of crosslinker to polymer. Burchard and co-workers also noticed that increasing the arm length reduced the *f* of the resultant star polymer. However, for star polymers

produced by GTP Haddleton *et al*.[161] found that the number of arms is not related to the arm length. For the stars made by anionic polymerisation they emphasise the important role of the overall concentrations.[162] These factors are likely to effect the formation of star polymers by a core-crosslinking method using RAFT polymerisation.

Discussed here are some optimisation studies for the synthesis of core cross-linked star PMMA by RAFT. The factors investigated were the ratio of [crosslinker] / [RAFT agent] and the length of the spacer between the 2 vinyl groups in the crosslinker. Efforts were made to isolate these variables by keeping other potential factors constant. The resultant stars were then characterised by multi-detector GPC, analogously to the core-first stars discussed earlier in this chapter.

3.2.2 Synthesis of RAFT agents

As discussed in section 1.2.3 the selection of CTA is very important for control in RAFT polymerisation. To control the polymerisation of MMA, the R group of the RAFT agent must be have fast initiation of MMA. As MMA is a more activated monomer the Z group must also facilitate a high addition rate to the C=S bond of the thioester group, which is achieved by making it more electrophilic.[15]

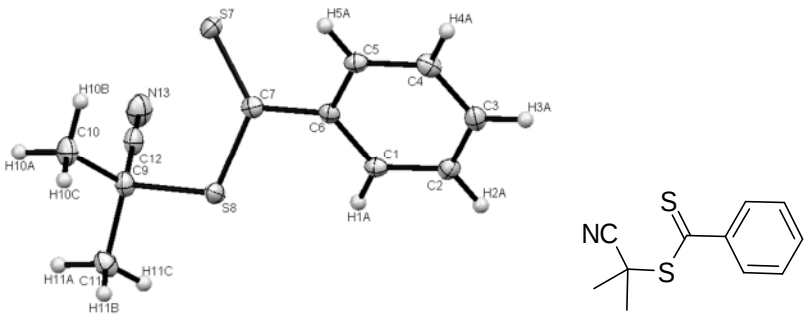

Figure 20: X-ray crystal structure of RAFT agent 1 2-cyanoprop-2-yl dithiobenzoate (RAFT agent 1).

2-Cyanoprop-2-yl dithiobenzoate (**RAFT agent 1**) has been reported to be particularly effective at controlling the polymerisation of methacrylates.[16,163] Therefore, it has been used here for the synthesis of arm-first star polymers. **RAFT agent 1** was synthesised, figure 20, by first synthesising a bis(dithiobenzoate) precursor and performing a radical addition reaction with an excess of AIBN in an inert atmosphere of argon, scheme 15, to yield a deep red crystalline solid. 4-Cyanopentanoic acid dithiobenzoate (**RAFT agent 2**) was synthesised using the same bis(thiobenzoyl) disulfide precursor and the thermal initiator ACVA to perform the radical addition, scheme 15.

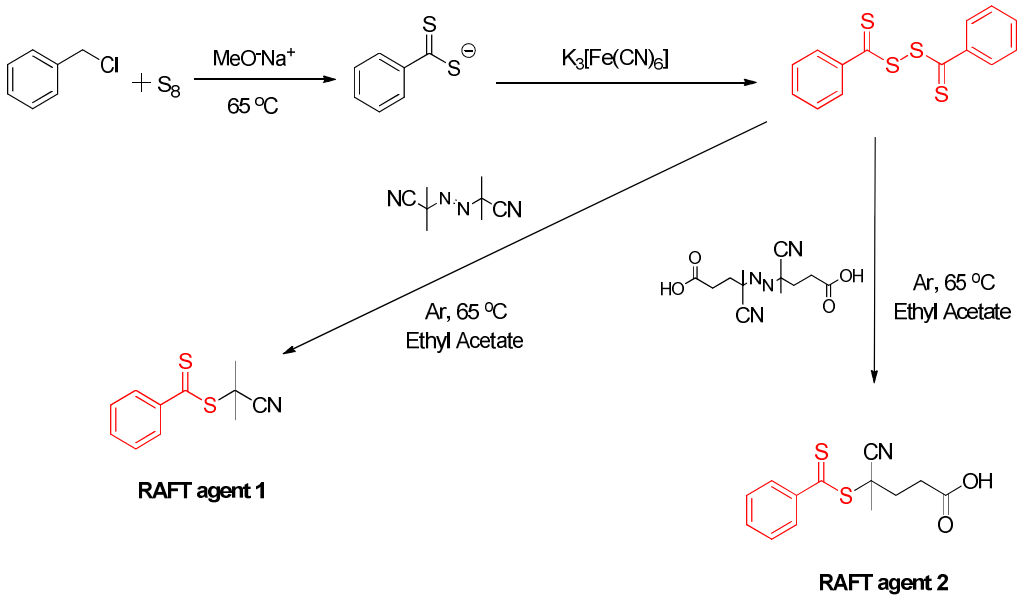

Scheme 15: Synthesis of 2-cyanoprop-2-yl dithiobenzoate (RAFT agent 1), and 4-cyanopentanoic acid dithiobenzoate (RAFT agent 2), by first synthesising bis(thiobenzoyl) disulfide.

3.2.3 The effect of monomer dilution on crosslinking

A study was carried out to determine whether the conversion of monomer at the time when the crosslinker is added affects the star formation. Firstly, an arm polymer was synthesised using **RAFT agent 2** and ACVA to polymerise methyl methacrylate in

toluene at 65 °C in the absence of oxygen, scheme 16. This polymer, **PMMA 1**, was isolated and utilised for a series of crosslinking reactions.

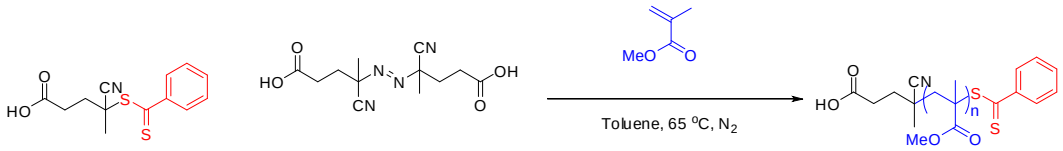

Scheme 16: Polymerisation of MMA with RAFT agent 2 and ACVA in toluene at 65 °C.

Here **PMMA 1** was used to study whether the presence of MMA effects the formation of the star architecture. Using **PMMA 1** as a macro-RAFT agent, four reactions with varying amounts of MMA, between 0 and 20 equivalents relative to RAFT end group, were carried out. Each of the reactions had 4 equivalents of **crosslinker 1** relative to the RAFT end group, and 0.1 equivalents of radical initiator, ACVA. They were reacted for 6 hours at 65 °C to yield star polymers.

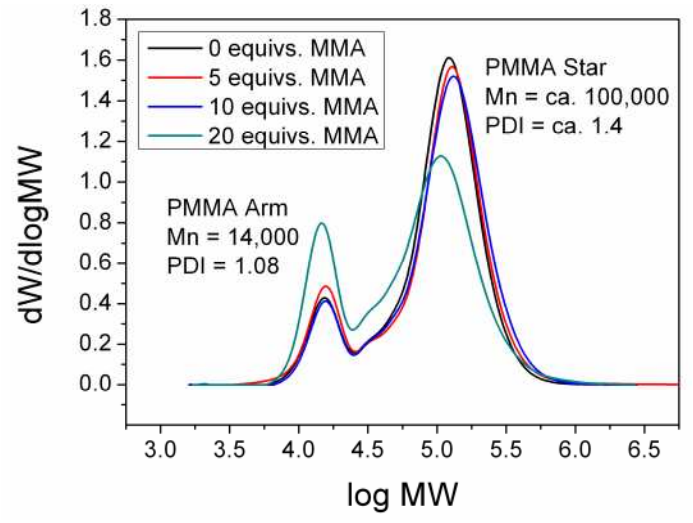

Figure 21: GPC chromatograms of polymers formed after reaction of a PMMA macro RAFT agent with 4 equivalents of crosslinker 1 and varying amounts of MMA.

When analysed by light scattering GPC, there was very little difference in the hydrodynamic volume of the stars in the reactions with fewer than 10 equivalents of MMA to **RAFT agent 1**. The star polymer synthesised with 0, 5 and 10 equivalents of MMA relative to **RAFT agent 1** have a M_n from kg.mol^{-1}, whereas the reaction with 20 equivalents of MMA gave a broader polymer, with lower arm incorporation into the star architecture, figure 21.

Table 5: The M_n, PDI and% arm incorporation of each star polymer (not including arm impurity) synthesised using PMMA 1 as a macro RAFT agent. Arm incorporation was determined by deconvolution of GPC spectra. ŧ Determined using conventional GPC against PMMA standards. * Determined using Universal calibration.

Reaction ID	Crosslinker	Ratio of [crosslinker1]/[RAFT]	Ratio of [MMA]/[RAFT]	Arm incorporation /%	M_n of Star /g. mol^{-1} ŧ	PDI of star ŧ	M_n of Star/. g mol^{-1} *	PDI of star *
M0	1	4	0	87	96900	1.37	115000	1.78
M5	1	4	5	85	102000	1.39	119000	1.90
M10	1	4	10	88	102000	1.45	120000	2.17
M20	1	4	20	72	80400	1.54	105000	1.96

The PDI of the resultant star polymer increases with the amount of MMA present in the reaction at the beginning, from 1.37 when no MMA is present to 1.54 when the ratio of [MMA] / [PMMA 1] is 20. From this study it was concluded that the polymerisation of arms should be such that there is less than 10 equivalents of MMA in the reactor before the crosslinker is added.

3.2.4 Arm-first star PMMA by RAFT using different crosslinkers

RAFT agent 1 was used to control the synthesis of PMMA star polymers. They were synthesised using an arm-first method, by sequential addition of MMA, followed by addition of a di-vinyl crosslinker, ethylene glycol dimethacrylate (**crosslinker 1**), di(ethylene glycol) dimethacrylate (**crosslinker 2**) or tri(ethylene glycol) dimethacrylate (**crosslinker 3**).

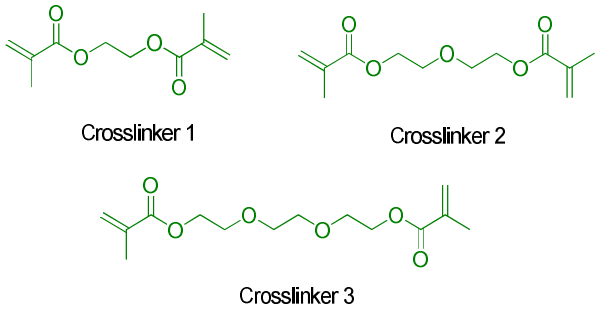

Figure 22: Crosslinkers used in this study. Crosslinker 1;ethylene glycol dimethacrylate, crosslinker 2;di (ethylene glycol) dimethacrylate and crosslinker 3; tri(ethylene glycol) dimethacrylate.

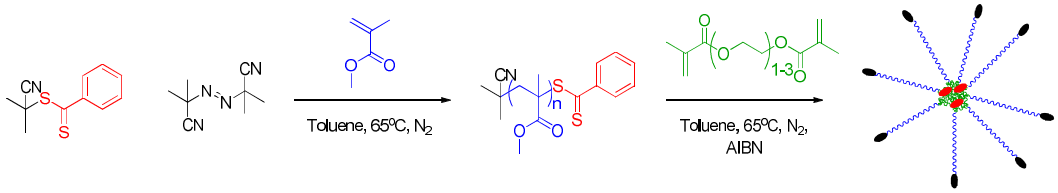

Scheme 17: RAFT polymerisation of PMMA star polymers by a core-crosslinking method. Target DP of MMA was 100, and AIBN was added with crosslinker after high conversion of monomer to yield a star architecture.

From the previous study, it was known that the linear PMMA arm should be polymerised to high conversion, generally over 90% monomer conversion, before addition of the crosslinker. By doing this, it is possible to limit the size of the cross-

linked core; the mono-vinyl monomer incorporated into the core dilutes the cross-linking and would lead to larger core sizes. It has also been seen that early addition of crosslinker can drive the formation of an insoluble gel.

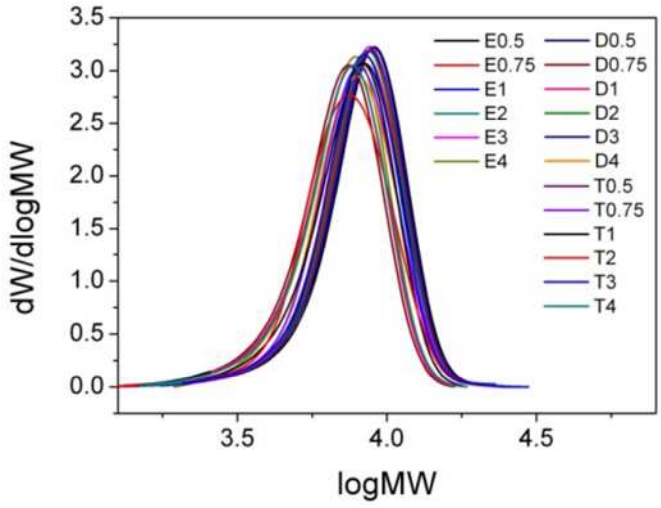

Figure 23: Molecular weight distributions from of 18 repeat polymerisations of MMA to form precursor arms. The target molecular weight was 10,000 g.mol^{-1} for each. Labelled with the crosslinker (E=EGDMA, D=DEGDMA, and T=TEGDMA) and the number denotes the number of equivalents relative to RAFT agent.

The polymerisation procedure involved dissolving RAFT agent, initiator and monomer in toluene in a sealed reactor with a magnetic stirrer. The reactor was then purged of oxygen by bubbling with nitrogen gas for 10 minutes. The target DP and molecular weight was 100 and 10,000 g.mol^{-1} respectively. The control of polymerisation of MMA by CPDB was good with PDI of around 1.1. The reaction was very reproducible, yielding linear PMMA arms of similar molecular weight (ca. 9,000 g.mol^{-1}) and PDI for over 18 reactions, figure 23. The MMA polymerisations were taken to high conversion, around 90%, table 6, table 7, and table 8, before the addition of different amounts of various crosslinkers. To minimise the effect of having monomer in the system, an effort was made to ensure the conversions of each of the precursor arms were as close as possible to each other.

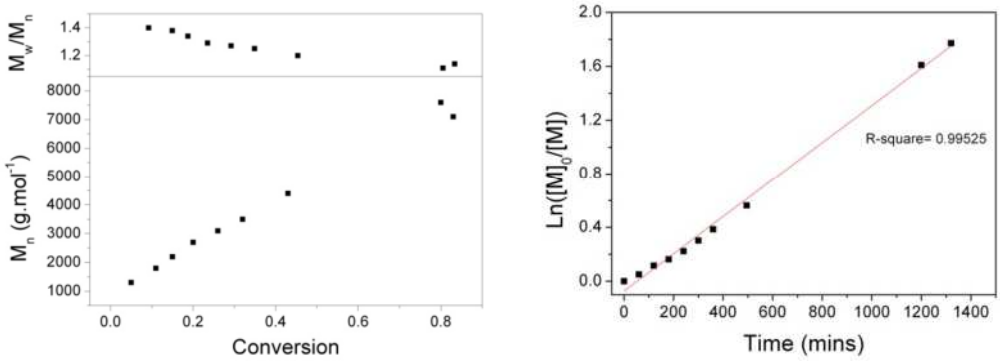

Figure 24: (left) M_n vs. conversion for polymerisation of MMA using CPDB in toluene at 65 ^{o}C. (right) first order kinetic plot showing ln($[M]_0/[M]_t$) vs. time.

The same volume of toluene was added to each reaction. Therefore the concentration of the polymer remained constant for all 18 polymerisations at 840 mg.mL^{-1}, only having slight variation due to small changes in monomer conversion and by the volume of crosslinker added.

3.2.4.1 Varying the ratio of [crosslinker 1] to [polymer]

PMMA star polymers have been synthesised using ethylene glycol dimethacrylate as a cross-linking agent. To yield different size star polymers, the ratio of [**crosslinker 1**]/[PMMA] was varied between 0.5 and 4, after preliminary results showed gel formation using a ratio greater than 4.

*Table 6: PMMA star polymers made by an arm-first route using crosslinker1 as cross-linking agent. GPC analysis of stars is over the entire molecular weight distribution, inclusive of unreacted arm. ł Determined using conventional GPC against PMMA standards. * Determined using universal calibration. Mark-Houwink exponent is averaged over the entire molecular weight distribution. Conversions were determined by ^{1}H-NMR. Arm incorporation determined by deconvolution of GPC spectra.*

Reaction ID	Conversion of MMA (arms) /%	Ratio of [crosslinker1]/[RAFT]	Conversion of MMA + crosslinker1 /%	Arm incorporation /%	M_n of Star /g.mol^{-1} ł	PDI of star ł	M_n of Star/ g.mol^{-1} *	PDI of star *	α
E0.5	91.4	0.5	94.2	12	9000	1.23	12700	1.34	0.292
E0.75	92.3	0.75	94.9	14	9200	1.26	12700	1.37	0.281
E1	94.7	1	91.2	16	9000	1.55	13700	1.65	0.275
E2	93.0	2	96.8	44	12500	1.55	20100	1.86	0.245
E3	90.5	3	95.8	67	18500	1.93	30900	2.99	0.186
E4	87.7	4	97.3	89	40700	3.48	52400	10.21	0.145

Analysing the polymers by GPC show that the greater the ratio of crosslinker to RAFT agent the higher the M_n, M_w, and PDI of the resultant star polymer, table 6 and figure 25.

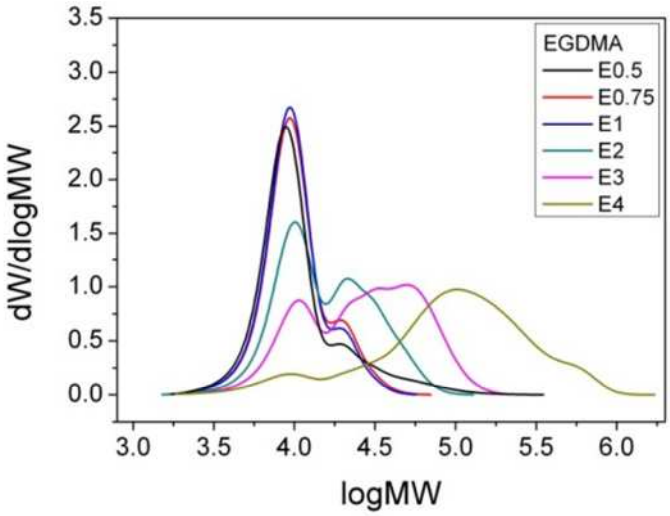

Figure 25: MWD of PMMA star polymers made using crosslinker 1 from the analysis by conventional $CHCl_3$ GPC.

Using 0.5 equivalents of **crosslinker 1** relative to **RAFT agent 1** added at 91% conversion of MMA did not crosslink the linear polymer significantly. A low concentration of high molecular weight species can be seen in the MWD, figure 25, and the best fit of the exponent of the Mark-Houwink plot of the whole polymer sample has been lowered significantly, table 6, compared with literature values of linear PMMA (α = 0.8). A ratio of **crosslinker 1** to **RAFT agent 1** of 0.75 and 1 yielded polymers with larger shoulders on the GPC chromatograms and further reduced the exponent of the Mark Houwink plots to α = 0.288 and 0.283, table 6. Increasing the [**crosslinker 1**]/ [**RAFT agent 1**] further to 2, 3 or 4 yields large multi-arm star molecules with reduced α values of 0.277, 0.256, and 0.233 respectively, table 6. Polymer **E4** is the largest star formed in the study with an M_w over 500,000 g.mol^{-1} and arm incorporation into star of 84%, table 6.

3.2.4.2 Varying the ratio of [crosslinker 3] to [polymer]

Table 7: PMMA star polymers made by an arm-first route using crosslinker 3 as cross-linking agent. GPC analysis of stars is over the entire molecular weight distribution, inclusive of unreacted arm. ł Determined using conventional GPC against PMMA standards. * Determined using Universal calibration. Mark-Houwink exponent is averaged over the entire molecular weight distribution. Conversions were determined by ^{1}H-NMR. Arm incorporation determined by deconvolution of GPC spectra.

Reaction ID	Conversion of MMA (arms) /%	Ratio of [crosslinker3]/[RAFT]	Conversion of MMA + crosslinker3 /%	Arm incorporation /%	M_n of Star /g mol^{-1} ł	PDI of star ł	M_n of Star/ g mol^{-1} *	PDI of star *	α
T0.5	93.3	0.5	95.4	6	8900	1.17	13000	1.23	0.303
T0.75	88.9	0.75	94.7	12	9000	1.22	12900	1.31	0.288
T1	86.9	1	94.3	12	8900	1.27	10400	1.35	0.283
T2	82.4	2	93.6	25	11200	1.38	16600	1.57	0.277
T3	86.3	3	93.7	39	12100	1.53	17800	1.88	0.256
T4	85.4	4	93.4	54	14400	1.87	18200	2.65	0.233

Crosslinker 3, TEGDMA, has previously been studied as a crosslinker by Sawamoto *et al.*,[164] who used it for the polymerisation of PMMA star polymers by Ru(II) catalysed polymerisation. In their study they noted a general trend that increasing the spacer length between vinyl moieties increased the crosslinker's efficiency. **Crosslinker 3** was the exception to the rule; the efficiency of **crosslinker 3** was significantly reduced relative to the smaller analogous dimethacrylate, **crosslinker 1** (EGDMA).

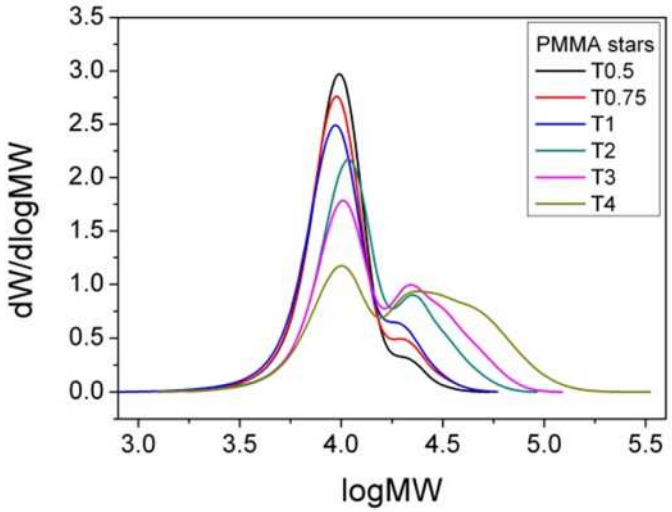

Figure 26: Conventional GPC analysis of PMMA star polymers made using crosslinker 3 as crosslinker.

The star polymers obtained here by RAFT polymerisation using **crosslinker 3** support the results of Sawamoto and co-workers. Use of **crosslinker 1** yielded larger star polymers relative to those made using **crosslinker3**. For example, comparing **E4** and **T4,** table 6 and table 7 respectively, we see that the M_n of the stars decrease from 40,700 $g.mol^{-1}$ to 14,400 $g.mol^{-1}$, with only the crosslinker as a variable.

3.2.4.3 Varying the ratio of [crosslinker 2] to [polymer]

Table 8: PMMA star polymers made by an arm-first route using crosslinker 2 as cross-linking agent. GPC analysis of stars is over the entire molecular weight distribution, inclusive of unreacted arm. ł Determined using conventional GPC against PMMA standards. * Determined using universal calibration. Mark-Houwink exponent is averaged over the entire molecular weight distribution. Conversions were determined by ^{1}H-NMR. Arm incorporation determined by deconvolution of GPC spectra.

Reaction ID	Conversion of MMA (arms) /%	Ratio of [crosslinker2]/[RAFT]	Conversion of MMA + crosslinker2 /%	Arm incorporation /%	M_n of Star /g mol^{-1} ł	PDI of star ł	M_n of Star/ g mol^{-1} *	PDI of star *	α
D0.5	92.0	0.5	93.7	2	8100	1.14	10800	1.19	0.301
D0.75	84.8	0.75	92.3	12	8800	1.24	10800	1.30	0.314
D1	88.3	1	93.7	19	8800	1.27	11100	1.34	0.301
D2	87.4	2	94.8	27	10700	1.37	14800	1.57	0.282
D3	93.2	3	97.0	40	12800	1.69	20300	2.17	0.252
D4	86.8	4	96.3	55	15200	1.9	20800	2.81	0.225

Commercially available, **crosslinker 2** has also been investigated as a crosslinker for this system, table 8. This crosslinker was chosen as it has a spacer length half way between **crosslinker 1** and **crosslinker 3.** As with the other crosslinkers increasing the ratio of [crosslinker] to [polymer] yielded larger star polymers. No formation of gel was seen to occur in the reactions, and all samples were soluble in toluene.

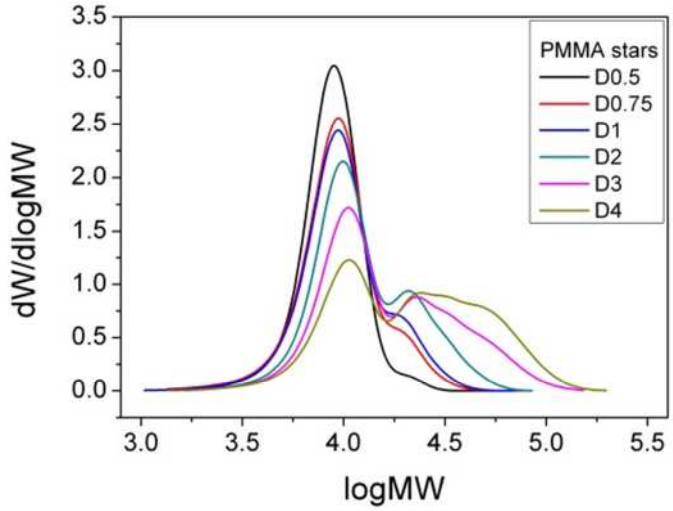

Figure 27: Conventional GPC analysis of PMMA star polymers made using crosslinker 2 as crosslinker.

When looking at the crosslinkers in the series of length of spacer, it can be seen that the efficiency of the crosslinker decreases as the length of the spacer increases. Comparing the GPC data for **E4**, **D4** and **T4** it is evident that the molecular weight of the resultant star polymer increases the shorter the spacer length between the vinyl groups. This is contradictory to the general trend observed by Sawamoto and co-workers in their research. [164] However, **crosslinker 3** was noted as having a surprisingly low efficiency, accounted for in the literature by a possible intramolecular cyclisation.[164]

Davis *et al.* recently carried out a study into crosslinker efficiency in star formation;[158] particularly focussing on the synthesis of narrow PDI water soluble star polymers. They suggest that the solubility of the crosslinker in the reaction mixture has a very strong influence on the arm incorporation and PDI of the resultant star polymer. Therefore the solubility/miscibility of **crosslinker 1**, **crosslinker 2** and **crosslinker 3** in the reaction solvent were investigated to see if a trend exists.

All three crosslinkers are liquids at room temperature and pressure, so their miscibility with toluene was considered. Taking 5 mL of each crosslinker into measuring cylinders, toluene was added slowly to see if a two phase system appeared. However, all crosslinkers were completely miscible with toluene.

3.2.5 Determining the functionality of core cross-linked star polymers

Stars made by the core-crosslinking approach differ significantly to those made by a core-first approach as they do not have a discrete number of arms and the product is a complex mixture. The molecular weight of the core-crosslinked polymer increases by addition of arms, increasing the amount of "branching" and changing the structure within the sample. As used before with core-first stars, it is possible to plot intrinsic viscosity vs. MW, in an analogous plot to the Mark-Houwink plot using multi-detector GPC, figure 28, figure 29 and figure 30.

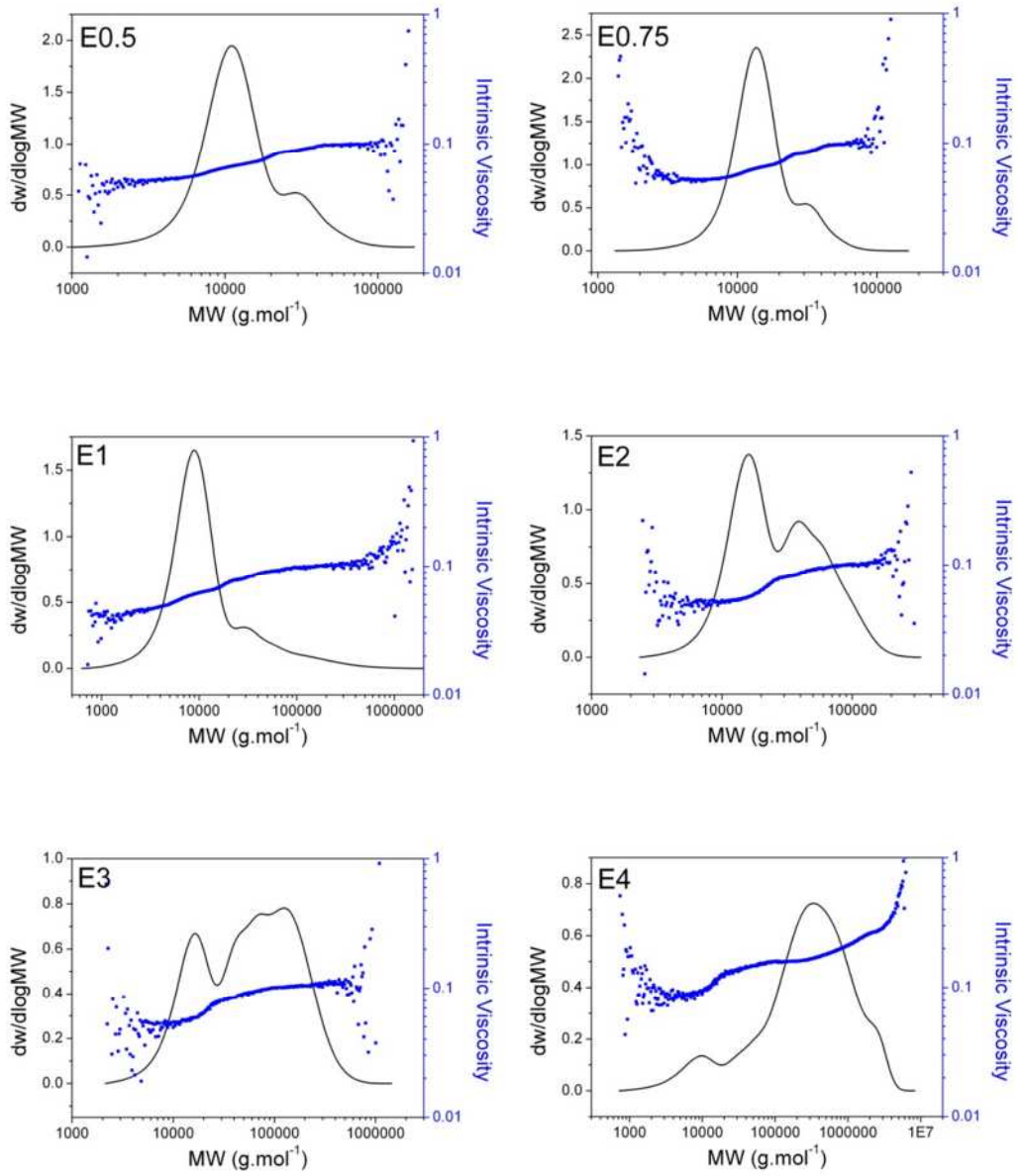

Figure 28. Mark-Houwink plots from multi-detector GPC. Polymers made using crosslinker 1 as crosslinker. Intrinsic viscosity data is plotted in blue and molecular weight distribution is plotted in black. The experiments are labelled such that the letter denotes the crosslinker (E=crosslinker 1, D=crosslinker 2, and T=crosslinker 3) used and the number is the ratio of crosslinker to PMMA arms.

There is a significant change in intrinsic viscosity at the same molecular weight for the different stars, highlighting the change in architecture between the polymer samples, figure 28.

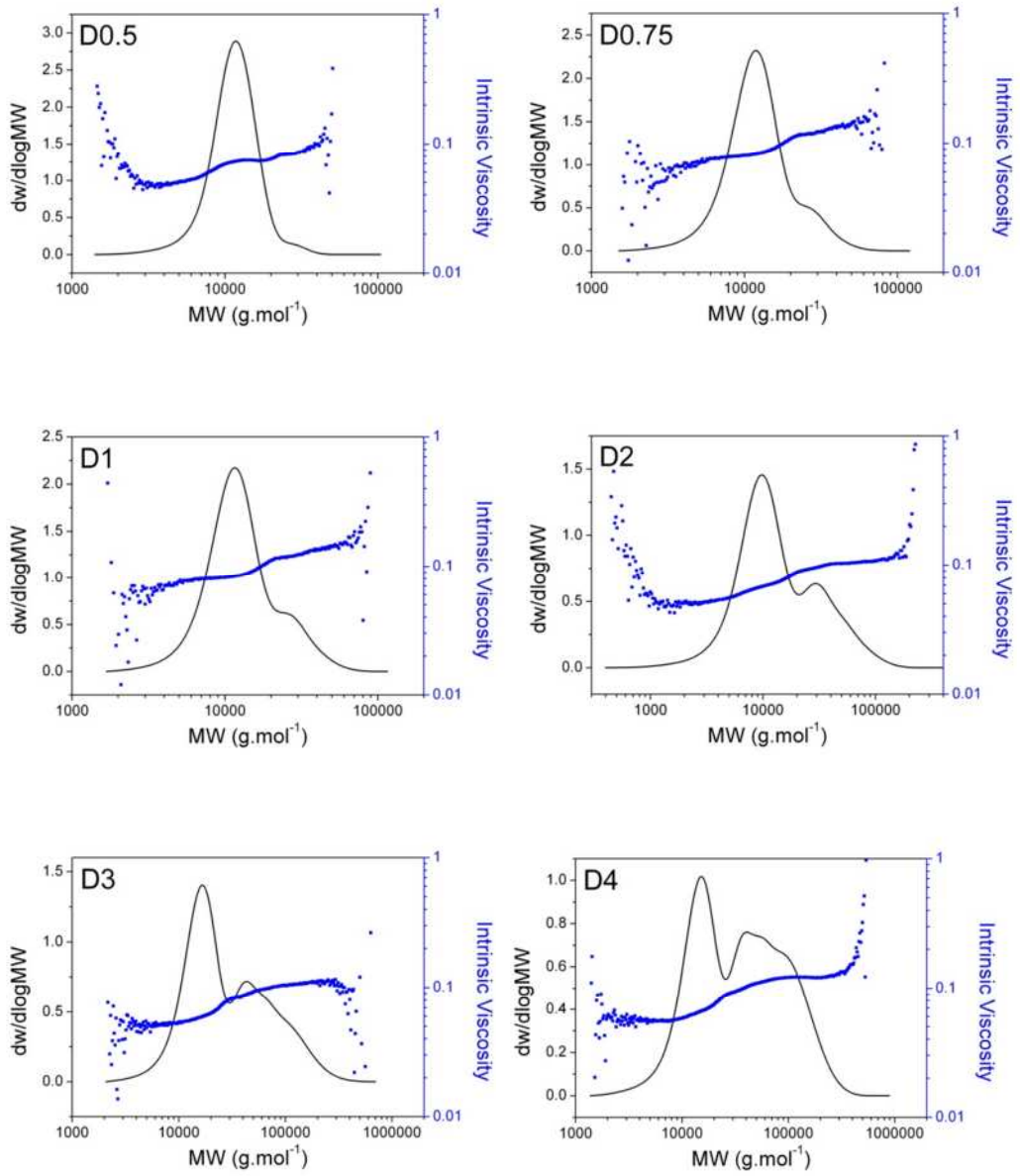

Figure 29: Mark-Houwink plots from multi-detector GPC. Polymers made using crosslinker2 as crosslinker. Intrinsic viscosity data is plotted in blue and molecular weight distribution is plotted in black. The experiments are labelled such that the letter denotes the crosslinker (E=crosslinker 1, D=crosslinker 2, and T=crosslinker 3) used and the number is the ratio of crosslinker to PMMA arms.

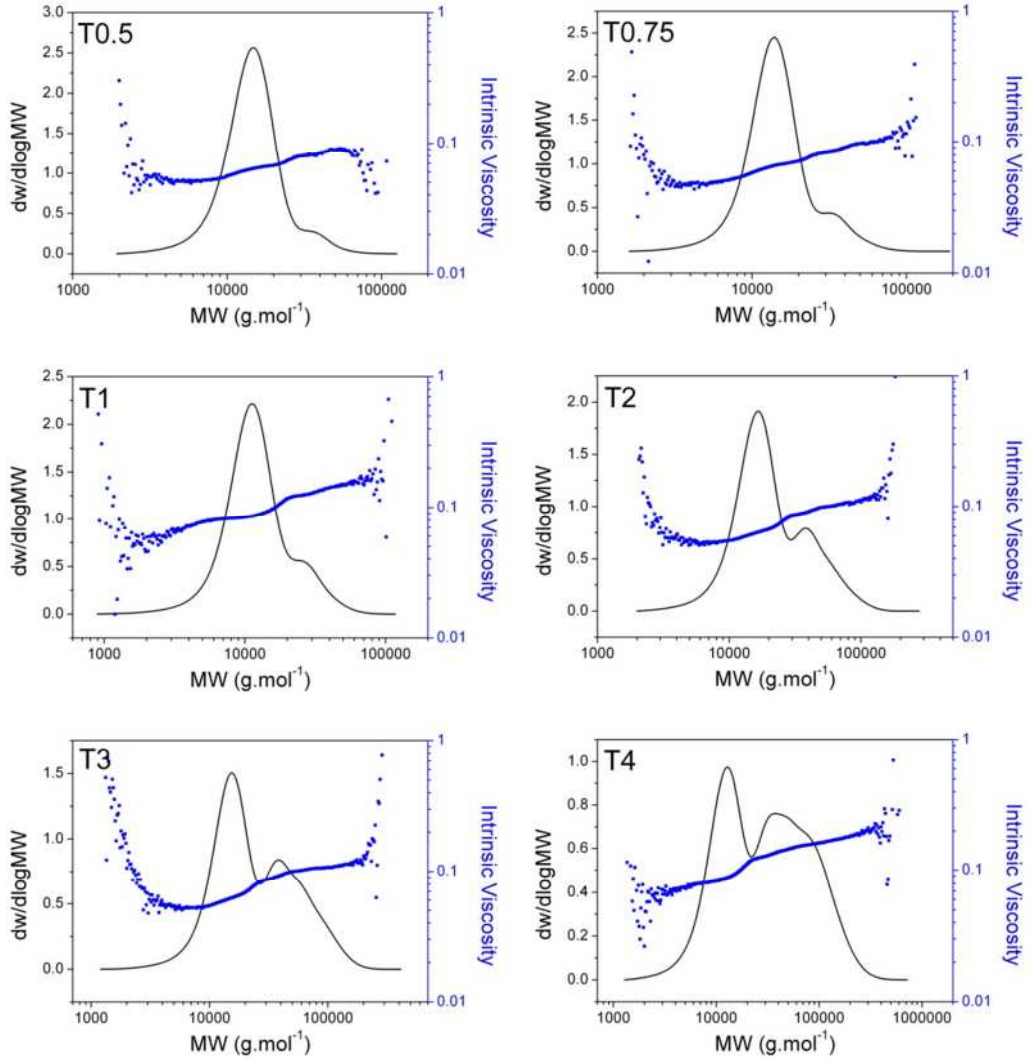

Figure 30: Mark-Houwink plots from multi-detector GPC. Polymers made using crosslinker3 as crosslinker. Intrinsic viscosity data is plotted in blue and molecular weight distribution is plotted in black. The experiments are labelled such that the letter denotes the crosslinker (E=crosslinker 1, D=crosslinker 2, and T=crosslinker 3) used and the number is the ratio of [crosslinker] to [PMMA arms].

A plot of log intrinsic viscosity vs. log molecular weight (analogous to a Mark-Houwink plot) should yield a smaller exponent, α.[165] By comparing the intrinsic viscosity of a star polymer sample with a linear polymer of the same molecular weight and composition it is possible to determine a value for the intrinsic viscosity contraction factor (g^{l}). As the viscosity is an effective measure of the hydrodynamic volume of the polymer in solution, it is possible to relate this value to an equivalent radius of gyration

contraction factor (g). By modelling the star polymer as a star shape, with a central singular point core and regular arm lengths, it is possible to calculate a value for the number of arms (*f*) [62] across the molecular weight distribution of the polymer. This model requires that a number of assumptions are made.

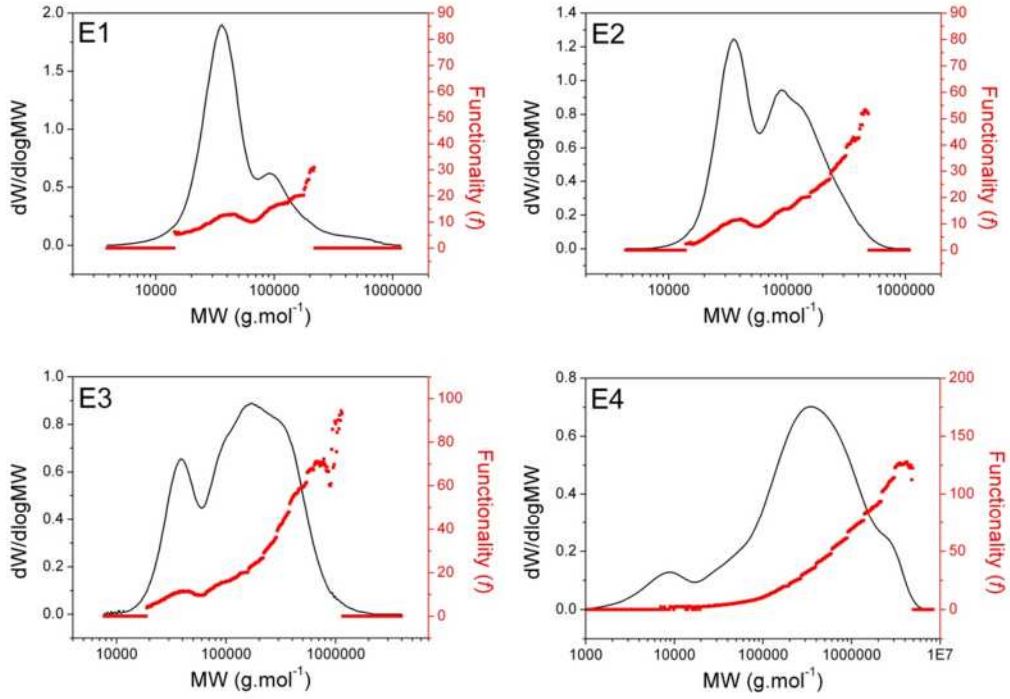

Figure 31: Calculated functionality for star polymers made using varying amounts of crosslinker 1 as crosslinker. The functionality is calculated based on the equation derived by Zimm and Stockmayer for stars with regular arm lengths: $g=(3/f)-(2/f^2)$, where f is the number of arms and g is the radius of gyration contraction factor.

The contraction factor is only valid for polymers of the same molecular weight and composition;[70,73] here we align the molecular weights of linear and star polymers by using a universal calibration on GPC. However, the compositions differ slightly as the stars have the addition of a crosslinker. It is assumed that the small amount of crosslinker used, and its location in the core of the star polymer means this should only be a small source of error.

Another potential problem with composition is the concentration calculations dependence on specific refractive indices of the polymer used. By changing composition, the dn/dc of the polymer changes and leads to changes in the calculated concentration. In the case of **crosslinker 1**, studied here, the molecule is very chemically similar to MMA, with similar dn/dc values of 0.057 for PMMA in chloroform at 30 ^{o}C, and 0.048 for P(EGDMA) in chloroform at 30 ^{o}C. Therefore, the effect of composition on concentration calculations from DRI measurement has been minimised.

As the molecular weight of the linear arms of these polymers is known, it is possible to estimate the number of arms using the molecular weight of the star polymer:

$$f = \frac{\mathrm{MW_{star}}}{\mathrm{M_{n,arm}}} \times \frac{\mathrm{conv_{MMA} X_{arm} m_{arm}}}{\mathrm{conv_{MMA} X_{arm} m_{arm} + m_X conv_X}} \qquad (3.1)$$

Where:

f is the functionality,

$conv_{MMA}$ is the conversion of the arms,

X_{arm} is the weight fraction of the arms,

m_{arm} is the mass of the arm,

m_X is the mass of the crosslinker and

$conv_x$ is the conversion of the crosslinker.

As the conversion of MMA approaches unity and the mass of the crosslinker << mass of arm, the functionality of the star can be simply described as:

$$f \approx \frac{\mathrm{MW_{star}}}{\mathrm{M_{n,arm}}} \qquad (3.2)$$

Estimating the functionality of the star polymer using this simple equation, can be used to evaluate the data calculated using the intrinsic viscosity contraction factor. As the molecular weight of the linear arm PMMA synthesised for these series of reactions is well defined (9,000 g.mol^{-1}) it is possible to use this equation to plot the estimated functionality against the molecular weight of the star polymers, figure 32.

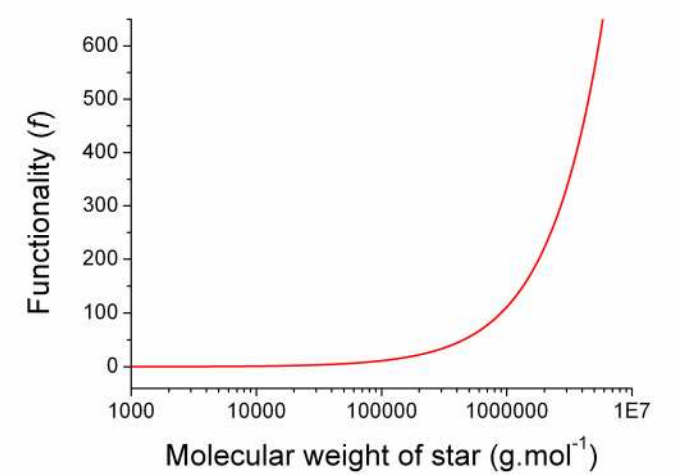

Figure 32: Plot of functionality (number of arms) against molecular weight of the star polymers. Using the equation $f \approx M_{n,star}/M_{n,arm}$ with a constant value of $M_{n,arm}$ calculated to be 9,000 g.mol^{-1} by GPC.

Comparing the simple function with the data acquired for some of the stars made using EGDMA as a crosslinker shows good correlation up to high molecular weight for each polymer. However, as the apparent functionality increases above 100 for the largest star polymer, made using a ratio of [**crosslinker 1**] / [**RAFT agent 1**] of 3, the data no longer fits.

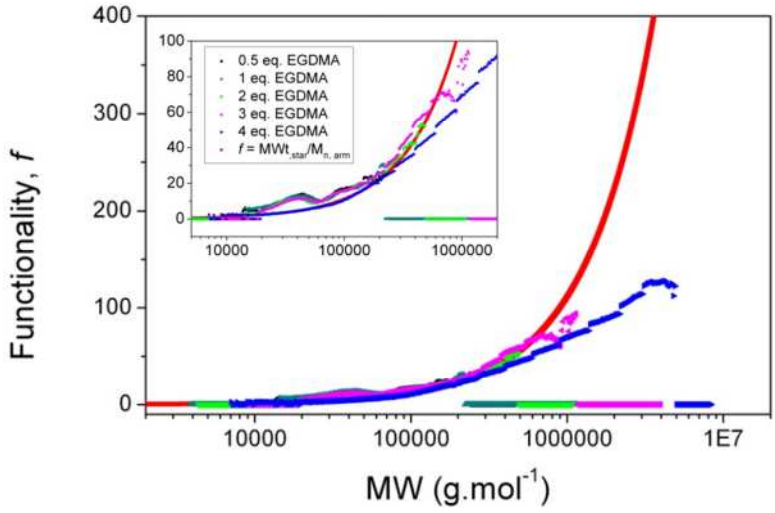

Figure 33: Plot of Functionality (number of arms) against molecular weight of star polymer. Star polymers have had their functionalities estimated using a contraction factor from the intrinsic viscosity of the star relative to a linear polymer. The functionality has been determined using a model relating the radius of gyration contraction factor (g) with the functionality of the star polymer: $g = (3f) - (2/f^2)$. Overlaid is the function $f = MW_{star}/M_{n,arm}$.

There are a number of factors that need to be investigated to determine why this deviation occurs. One of the many assumptions made in Zimm and Stockmayer's equations may have become invalid. For example, if star-star coupling were to occur late in the reaction, then the assumption of a single core may be invalid at the high molecular weight end of the MWD.

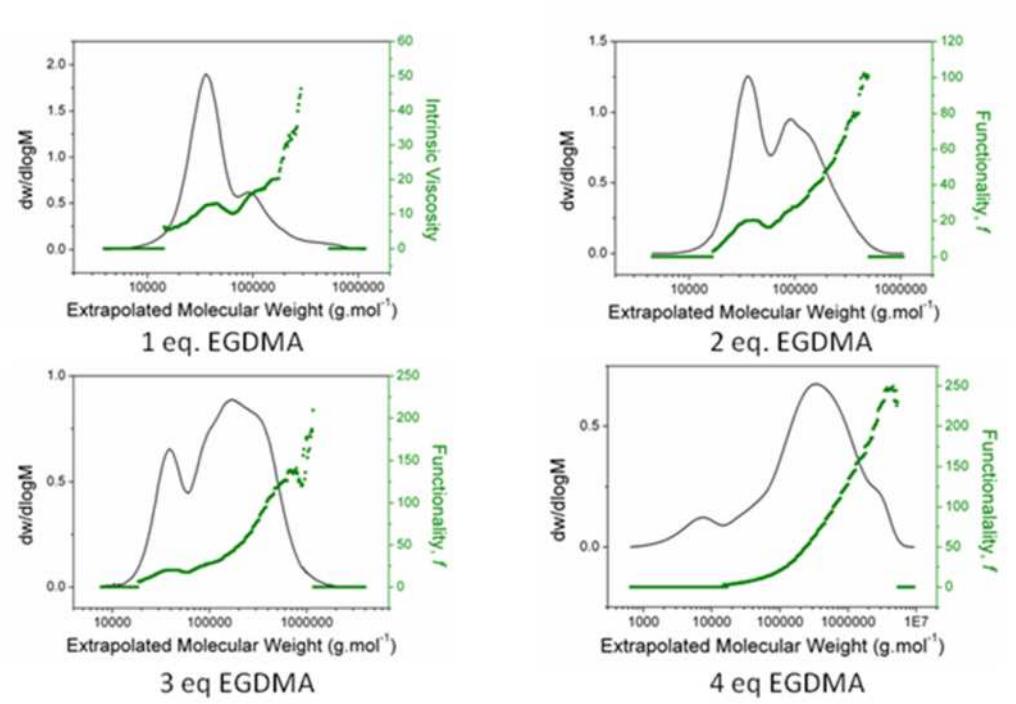

Figure 34: Calculated functionality for star polymers made using varying amounts of crosslinker1 as crosslinker. The number of arms is calculated based on the equation derived by Zimm and Stockmayer for irregular arm lengths: g= (3f)/ (f+1)^2, where f is the number of arms and g is the radius of gyration contraction factor.

Star polymers with a large number of arms, made *via* a core-first technique, are sometimes seen in the literature to be better modelled as having irregular arm lengths,[62] using the equation:

$$g = 3f/(f+1)^2, \qquad (3.3)$$

where:

g is the radius of gyration contraction factor,

f is the number of arms of the star polymer.

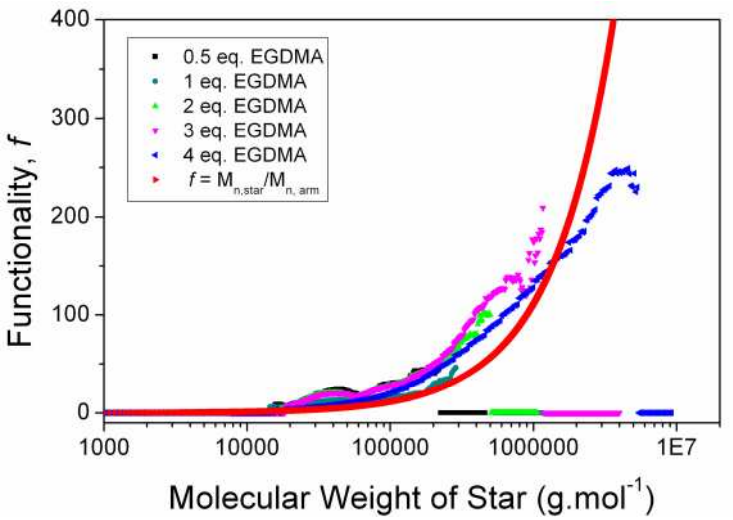

Figure 35: Plot of functionality (number of arms) against molecular weight of star polymer. Star polymers have had their functionalities estimated using a contraction factor from the intrinsic viscosity of the star relative to a linear polymer. The functionality has been determined using a model relating the radius of gyration contraction factor (g) with the functionality of the star polymer: $g = (3f)/(f+1)^2$. Overlaid is the function, $f = MW_{star}/M_{n,arm}$.

Analysing the same four star polymers to find the functionality using the equation for irregular arm lengths (eqn. 3.3) yielded results that deviate considerably from equation 3.2. The functionality calculated by the equation 3.3 was considerably larger over the entire molecular weight range of the polymer, figure 35. One exception was star polymer **E4** at very high molecular weight. Therefore, the equation for irregular arms is a worse model for the core-crosslinked PMMA star polymers than Zimm and Stockmayers equation for regular arm stars, equation 2.13.

3.3 Conclusions

PMMA with a star architecture has been synthesised using an arms first method, using RAFT chemistry. 2-Cyanoprop-2-yl dithiobenzoate (**RAFT agent 1**) and 4-cyanopentanoic acid dithiobenzoate (**RAFT agent 2**) were synthesised to control the polymerisation of MMA, and was seen to do so with good first order kinetics and linear molecular weight growth with conversion. The amount of MMA in the reaction at the point of crosslinking was seen to have little effect up to a ratio of [MMA] / [RAFT agent] of 1:10, therefore arm polymerisation was taken to 90% for subsequent reactions. The reaction was optimised by varying the ratio of [crosslinker] / [macroRAFT agent], and by changing crosslinker. The cross-linking efficiency of the crosslinker was seen to decrease with increasing ethylene glycol spacer length between the vinyl groups in the series **crosslinker 1**>**crosslinker 2**>**crosslinker 3**.

The series of broad PDI star polymers of varying size, made using the three crosslinkers, were analysed using multi-detector GPC to determine their MWD and also produce pseudo Mark-Houwink plots. The average exponent, α, of the plots were seen to be smaller for star polymers, and decreased for larger star polymers. Using the intrinsic viscosity shrink factor and Zimm and Stockmayer theory to determine the number of arms for four stars made using EGDMA as a crosslinker were shown to have functionalities varying from 10s to 100s of arms. Two models for analysing the star polymers were investigated. Using the regular arm length model derived by Zimm and Stockmayer was seen to be the most reliable model when compared to the simple method using the molecular weight of the star and arm polymers.

3.4 Experimental

3.4.1 Instruments

GPC was used to determine the molecular weight averages and the PDI of polymers using one of two systems. System 1, with a 390-LC Polymer Laboratories system equipped with a PL-AS RT/MT autosampler, a PL gel 3 µm (50 × 7.5 mm) guard column, two PL gel 5 µm (300 × 7.5 mm) mixed D columns (suitable for separations up to MW = 2.0×10^6 g.mol^{-1}), a differential refractometer, 4 capillary viscometer and MALLS were used. Solvent used was chloroform / triethylamine 95 : 5 (v/v) as the eluent with a flow rate of 1.0 mL.min^{-1}, unless otherwise stated. System 2 with a 390-LC Polymer Laboratories system equipped with a PL-AS RT/MT autosampler, a PL gel 3 µm (50 × 7.5 mm) guard column, two PL gel 5 µm (300 × 7.5 mm) mixed D columns (suitable for separations up to MW = 2.0×10^6 g.mol^{-1}), a differential refractometer, MALLS, and a photodiode array were used. Solvent used was tetrahydrofuran / triethylamine 95 : 5 (v/v) as the eluent with a flow rate of 1.0 mL.min^{-1}, unless otherwise stated. Narrow molecular weight PMMA standards (1.0×10^6 g.mol^{-1}) were used for calibration.

All ^{1}H and ^{13}C NMR spectra were recorded on Bruker DPX300, Bruker DPX400 and Bruker DRX500 spectrometers as solutions in deuterated NMR solvents. Chemical shifts are cited as parts per million (ppm). The following abbreviations are used to abbreviate multiplicities; s = singlet, d = doublet, t = triplet, q = quartet, m = multiplet.

FT-IR was recorded on a VECTOR-22 Bruker spectrometer using a Golden Gate diamond attenuated total reflection cell.

3.4.2 General method for calculating the percentage arm incorporation into stars when using an arm-first approach.

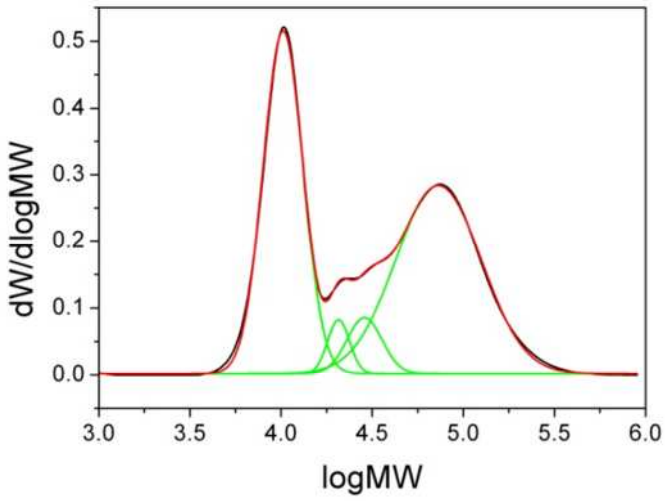

Figure 36: (Black) PMMA core-crosslinked star polymer MWD. (Green) four Gaussian curves calculated by Microcal Origin 8.0. (Red) Sum of the Gaussian curves.

The amount of arm incorporation into star was calculated by deconvolution of multimodal GPC traces using Microcal Origin 8.5.1, figure 36. The M_n, M_w and PDI of the component Gaussian distributions could be calculated along with the area of under the curve.

3.4.3 Materials

All materials were purchased from Sigma Aldrich at the highest available quality and used without further purification, unless otherwise stated.

The initiator 2,2,-azobisisobutyronitrile (AIBN) was re-crystallised from methanol before use. Methyl methacrylate, ethylene glycol dimethacrylate, di (ethylene glycol)

dimethacrylate and tri (ethylene glycol) dimethacrylate were de-inhibited by passing through an alumina column prior to use. The 5-arm, 8-arm and 21-arm initiators were synthesised within the group and used as received.

3.4.4 Synthesis of RAFT agent 1: 2-cyanoprop-2-yl dithiobenzoate

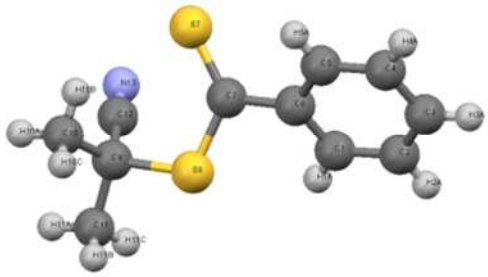

Figure 37: Ball and stick model of the X- crystal structure of RAFT agent 1.

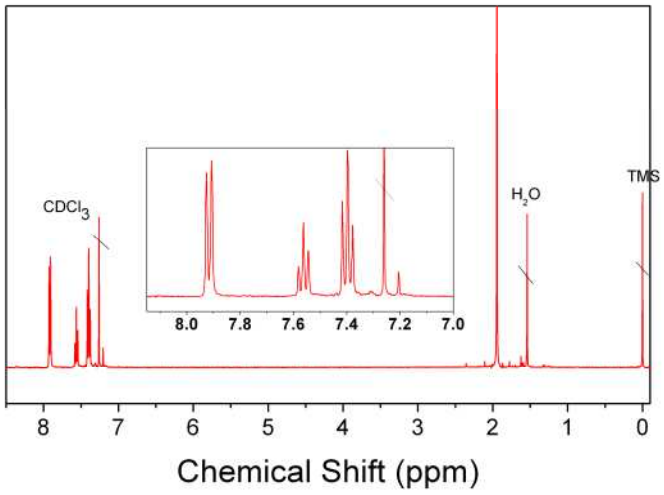

Figure 38: ^{1}H NMR of 2-cyanoprop-2-yl dithiobenzoate (RAFT agent 1).

Flower of sulfur (32.04 g, 1.00 mol) was added to a 3-neck round bottom flask and dissolved in methanol (200 mL) and sodium methoxide solution (25%) in methanol (200 mL). Benzyl Chloride (63.06 g, 4.98 $x10^{-1}$ mols) was added dropwise over a period of 3 hours at ambient temperature. The resultant brown solution was heated under reflux for 18 hours, and left to cool to ambient temperature. The white precipitate (sodium chloride) was removed by filtration and methanol removed under vacuum. The violet solid was dissolved in deionised water (400 mL) and washed with diethyl ether (4 x 150 mL). A final layer of diethyl ether was added, and the immiscible mixture acidified by dropwise addition of HCl solution (32%) until the ether layer was a deep purple and the aqueous layer was yellow. The ether layer was washed with deionised water (300 mL). Subsequently, a solution of NaOH (1 M) (300 mL) was added to extract the sodium dithiobenzoate into the aqueous media. The washing procedure was repeated a further 2 times to finally yield an aqueous solution of sodium dithiobenzoate.

Potassium ferricyanide (197.40 g, 6.01 x 10^{-1} mols) was dissolved in deionised water (600 mL) and added dropwise over 3 hours to the solution of sodium dithiobenzoate with vigorous stirring. The red precipitate formed was collected by filtration, and washed with deionised water until the supernatant become colourless. The crude solid bis(thiobenzoyl) disulfide was dried under vacuum, in the dark, at room temperature.

A mixture of AIBN (61.60 g, 3.75 x 10^{-1} mols) and bis(thiobenzoyl) disulfide (79.65 g, ca. 2.60 x 10^{-1} mols) in ethyl acetate (1.20 L) was degassed by purging with nitrogen and heated to 80 ^{o}C. After 18 h, the solvent was evaporated under vacuum, and the crude material was isolated with column chromatography with EtOAc : Hexane (4:1) as the mobile phase. After evaporation of the solvents, the 2-cyanoprop-2-yl dithiobenzoate was obtained as a red crystalline solid (yield 23%, recovery 26.5 g).

^{1}H NMR ($CDCl_3$), δ (ppm): 1.94 (s, 6H, 2xCH_3); 7.40 (t, 2H, J =7.7 Hz, *meta*-ArH); 7.56 (t, 1H, J=7.5 Hz, *para*-ArH); 7.91 (d, 2H, J = 7.5 Hz, *ortho*-ArH);

^{13}C NMR ($CDCl_3$), δ (ppm): 26.5 (2C, C(CN)($\underline{C}H_3$)$_2$); 41.8 (1C, $\underline{C}$(CN)(CH_3)$_2$); (C($\underline{C}$N)(CH_3)$_2$); 126.7 (2C, ortho-Ar); 128.69 (1C, para-Ar); 132.9 (2C, meta-Ar); 144.6 (1C, Ar);

FT-IR: 2976 (w), 2930 (w), 2231 (m), 1591 (m), 1444 (s),1434 (s), 1364 (w), 1313 (w), 1274 (w), 1236 (s), 1186 (w), 1079 (w), 1047 (s), 999 (w), 870 (s), 870 (s), 758 (s), 681 (s), 649 (m), 616 (m) cm^{-1};

CHN analysis: C, calculated 59.7%, found 60.0%; H, calculated 5.0%, found 5.0%; N, calculated 6.3%, found 6.3%;

Exact Mass Spectrometry (+ESI-MS) *m/z*: Calculated. 222.0406 (H^+), Found: 222.0405.

Table 9: Crystallographic data for 2-cyanoprop-2-yl dithiobenzoate

Compound reference	2-Cyanoprop-2-yl dithiobenzoate
Chemical formula	$C_{11}H_{11}NS_2$
Formula Mass	221.33
Crystal system	Triclinic
a/Å	6.39737(15)
b/Å	7.04977(18)
c/Å	13.6392(4)
α/°	97.076(2)
β/°	95.729(2)
γ/°	113.740(2)
Unit cell volume/Å^3	551.18(2)
Temperature/K	100(2)
Space group	*P*$\bar{1}$
No. of formula units per unit cell, *Z*	2
No. of reflections measured	9273
No. of independent reflections	2666
R_{int}	0.0210
Final R_1 values ($I > 2\sigma(I)$)	0.0230
Final $wR(F^2)$ values ($I > 2\sigma(I)$)	0.0637
Final R_1 values (all data)	0.0265
Final $wR(F^2)$ values (all data)	0.0647

3.4.5 Synthesis of RAFT agent 2: 4-cyanopentanoic acid dithiobenzoate

Bis(thiobenzoyl) disulfide was synthesised as for 2-cyanoprop-2-yl dithiobenzoate. A mixture of 4,4-azobis(4-cyanovaleric acid) (ACVA) (5.83 g, 2.08 x 10^{-2} mols) and bis(thiobenzoyl) disulfide (4.25 g, 1.39 x 10^{-2} mols) in ethyl acetate (80 mL) was degassed by purging with nitrogen and heated to 80^{o}C. After 20 h, the solvent was evaporated under vacuum, and the crude material was isolated with column chromatography with EtOAc:Hexane (9:1) as the mobile phase. After evaporation of the solvents, the 4-cyanopentanoic acid dithiobenzoate was obtained as a purple crystalline solid (yield 16%, 1.14 g).

^{1}H NMR ($CDCl_3$), δ (ppm): 1.95 (s, 6H, 2xCH_3); 2.54 (m, 2H, $\underline{C}H_2CH_2COOH$); 2.74 (m, 2H, $CH_2\underline{C}H_2COOH$); 7.40 (t, 2H, J = 7.7 Hz, meta-ArH); 7.56 (t, 1H, J = 7.5 Hz, para-ArH); 7.91 (d, 2H, J^2 = 7.8 Hz, ortho-ArH);

^{13}C NMR ($CDCl_3$), δ (ppm): 24.2 (1C, C(CN)($\underline{C}H_3$)); 29.5 (1C, $\underline{C}H_2COOH$); 33.1 (1C, $\underline{C}H_2CH_2COOH$); 53.1 (1C, $\underline{C}(CN)(CH_3)_2$); 118.4 (C($\underline{C}N$)$(CH_3)_2$); 126.7 (2C, ortho-Ar); 128.6 (1C, para-Ar); 133.1 (2C, meta-Ar); 144.5 (1C, Ar); 176.9 (1C, $\underline{C}OOH$);

FT-IR: 2904 (b), 1703 (s), 1590 (w), 1441 (s), 1429 (s), 1413 (s), 1307 (s), 1226 (s), 1184 (w), 1116 (m), 1078 (w), 1044 (s), 1026 (s), 999 (w), 937 (m, b), 869 (s), 762 (s), 688 (s), 647 (w) cm^{-1};

CHN analysis: C, calculated 55.9%, found 55.6%; H, calculated 4.7%, found 4.6%; N, calculated 5.0%, found 4.5%;

ESI-MS *m/z*: Calculated.280;0388 (H^+), Found:280.1.

3.4.6 Synthesis of PMMA1 macroRAFT agent

4-Cyanopentanoic acid dithiobenzoate (1.00 g, 3.60 mmols), ACVA (0.100 g, 0.360 mmols) and MMA (71.64 g, 716 mmols) were charged to large Schlenk reactor, equipped with a magnetic stirrer, and dissolved in toluene (100 mL). The reaction vessel was sealed with a septum and degassed by purging with nitrogen for 45minutes. The reaction was initiated by heating in an oil bath (65 ^{o}C) and aliquots were taken periodically to follow conversion by ^{1}H NMR. At 70% conversion of monomer the reaction was stopped by cooling with liquid nitrogen and dilution with toluene. The solution was concentrated under a stream of compressed air, and precipitated into hexane, yielding a pink powder, which was collected by filtration. Conversion of the polymer was followed by comparing the decreasing singlet at 4.60 ppm (corresponding to the C(O)OCH$_2$ protons in the monomer) with the broad signal at 4.40 ppm increasing with time (corresponding to the C(O)OCH$_2$ protons in the polymer). M_n (GPC) = 14,000 g.mol^{-1}; PDI (GPC) = 1.08; Conversion = 70%; Yield =52.1 g.

FT-IR: 2950, 1726, 1448, 1388, 1241, 1191, 1147, 988, 842, 750 cm^{-1};

^{1}H NMR ($CDCl_3$) δ (ppm), 0.7 - 2.1 (m, 5nH, backbone); 2.54 (bm, 2H, RAFT agent $\underline{C}H_2CH_2COOH$); 3.4 – 3.8 (m, 3nH, O –C$\underline{H}_3$); 4.0 - 4.4 (m, crosslinker); 7.37 (bm, 2H, RAFT agent *meta*-ArH); 7.52 (bm, 1H, RAFT agent *para*-ArH); 7.89 (bm, 2H, RAFT agent *ortho*-ArH).

3.4.7 General procedure for RAFT polymerisation of MMA arm-first star polymer

2-Cyanoprop-2-yl dithiobenzoate (3.99 x 10^{-2} g, 1.80 x 10^{-4} mols), AIBN (2.96 x 10^{-3} g, 1.80 x 10^{-5} mols) and MMA (1.80 g, 1.80 x 10^{-2} mols) were charged to a small reactor, equipped with a magnetic stirrer, and dissolved in toluene (1.25 mL). Mesitylene (0.54 g, 4.50 x 10^{-3} mols) was added as an inert NMR standard. The reaction vessel was sealed with a septum and degassed by purging with argon for 15 minutes. The reaction was initiated by heating in an oil bath (65 ^{o}C) and after 24 hours a sample was taken and degassed crosslinker (see table 1, 2 and 3) was injected into the reaction. The reaction was left for 14 hours before being cooled in an ice bath and sampled for analysis. The solution was concentrated under a stream of compressed air, and precipitated into hexane, yielding a pink powder, which was collected by filtration.

FT-IR: 2950, 1726, 1448, 1388, 1241, 1191, 1147, 988, 842, 750 cm^{-1};

^{1}H NMR ($CDCl_3$), δ (ppm): 0.7 - 2.1 (m, backbone); 3.4 – 3.8 (m, 3nH, O –C$\underline{H}_3$); 4.0 - 4.4 (m, crosslinker); 7.40 (bm, 2H, *meta*-ArH); 7.56 (bm, 1H, *para*-ArH); 7.91 (bm, 2H, *ortho*-ArH).

3.5 References

(15) Moad, G.; Rizzardo, E.; Thang, S. H. *Aust. J. Chem.* **2005**, *58*, 379.

(16) Moad, G.; Rizzardo, E.; Thang, S. H. *Aust. J. Chem.* **2006**, *59*, 669.

(62) Zimm, B. H.; Stockmayer, W. H. *J. Chem. Phys.* **1949**, *17*, 1301.

(70) Balke, S. T.; Mourey, T. H.; Robello, D. R.; Davis, T. A.; Kraus, A.; Skonieczny, K. *J. Appl. Polym. Sci.* **2002**, *85*, 552.

(73) Robello, D. R.; Andre, Alix; McCovick, T. A.; Mourey, T. H. *Macromolecules* **2002**, *35*, 9334.

(127) Liu, J.; Liu, H.; Jia, Z.; Bulmus, V.; Davis, T. P. *Chem. Commun.* **2008**, 6582.

(128) Dag, A.; Durmaz, H.; Hizal, G.; Tunca, U. *J. Polym. Sci., Part A: Polym. Chem.* **2008**, *46*, 302.

(129) Sinnwell, S.; Lammens, M.; Stenzel, M. H.; Du Prez, F. E.; Barner-Kowollik, C. *J. Polym. Sci., Part A: Polym. Chem.* **2009**, *47*, 2207.

(130) Feng, X.-S.; Pan, C.-Y. *Macromolecules* **2002**, *35*, 4888.

(131) Chan, J. W.; Yu, B.; Hoyle, C. E.; Lowe, A. B. *Polymer* **2009**, *50*, 3158.

(132) De, P.; Gondi, S. R.; Roy, D.; Sumerlin, B. S. *Macromolecules* **2009**, *42*, 5614.

(133) Jackson, A. W.; Fulton, D. A. *Chem. Commun.* **2010**, *46*, 6051.

(134) Syrett, J. A.; Haddleton, D. M.; Whittaker, M. R.; Davis, T. P.; Boyer, C. *Chem. Commun.* **2011**, *47*, 1449.

(135) Lord, H. T.; Quinn, J. F.; Angus, S. D.; Whittaker, M. R.; Stenzel, M. H.; Davis, T. P. *J. Mater. Chem.* **2003**, *13*, 2819.

(136) Zheng, G.; Pan, C. *Polymer* **2005**, *46*, 2802.

(137) Audouin, F.; Knoop, R. J. I.; Huang, J.; Heise, A. *J. Polym. Sci., Part A: Polym. Chem.* **2010**, *48*, 4602.

(138) Taton, D.; Baussard, J.-F. o.; Dupayage, L.; Gnanou, Y.; Destarac, M.; Mignaud, C.; Pitois, C. In *Controlled/Living Radical Polymerization*; American Chemical Society: 2006; Vol. 944, p 578.

(139) Taton, D.; Baussard, J.-F.; Dupayage, L.; Poly, J.; Gnanou, Y.; Ponsinet, V.; Destarac, M.; Mignaud, C.; Pitois, C. *Chem. Commun.* **2006**, 1953.

(140) Baek, K.-Y.; Kamigaito, M.; Sawamoto, M. *Macromolecules* **2001**, *34*, 215.

(141) Baek, K.-Y.; Kamigaito, M.; Sawamoto, M. *J. Polym. Sci., Part A: Polym. Chem.* **2002**, *40*, 2245.

(142) Gao, H.; Matyjaszewski, K. *Macromolecules* **2006**, *39*, 4960.

(143) Gao, H.; Matyjaszewski, K. *Macromolecules* **2006**, *39*, 3154.

(144) Deng, G.; Cao, M.; Huang, J.; He, L.; Chen, Y. *Polymer* **2005**, *46*, 5698.

(145) Peng, Y.; Liu, H.; Zhang, X.; Liu, S.; Li, Y. *Macromolecules* **2009**, *42*, 6457.

(146) Gao, H.; Matyjaszewski, K. *Macromolecules* **2006**, *39*, 7216.

(147) Gao, H.; Matyjaszewski, K. *J. Am. Chem. Soc.* **2007**, *129*, 11828.

(148) Abrol, S.; Kambouris, P. A.; Looney, M. G.; Solomon, D. H. *Macromol. Rapid Commun.* **1997**, *18*, 755.

(149) Gao, H.; Matyjaszewski, K. *Prog. Polym. Sci.* **2009**, *34*, 317.

(150) Adkins, C. T.; Harth, E. *Macromolecules* **2008**, *41*, 3472.

(151) Tsoukatos, T.; Pispas, S.; Hadjichristidis, N. *J. Polym. Sci., Part A: Polym. Chem.* **2001**, *39*, 320.

(152) Pasquale, A. J.; Long, T. E. *J. Polym. Sci., Part A: Polym. Chem.* **2001**, *39*, 216.

(153) Bosman, A. W.; Heumann, A.; Klaerner, G.; Benoit, D.; Fréchet, J. M. J.; Hawker, C. J. *J. Am. Chem. Soc.* **2001**, *123*, 6461.

(154) Bosman, A. W.; Vestberg, R.; Heumann, A.; Fréchet, J. M. J.; Hawker, C. J. *J. Am. Chem. Soc.* **2002**, *125*, 715.

(155) Narumi, A.; Satoh, T.; Kaga, H.; Kakuchi, T. *Macromolecules* **2001**, *35*, 699.

(156) Narumi, A.; Yamane, S.; Miura, Y.; Kaga, H.; Satoh, T.; Kakuchi, T. *J. Polym. Sci., Part A: Polym. Chem.* **2005**, *43*, 4373.

(157) Zheng, G.; Pan, C. *Macromolecules* **2005**, *39*, 95.

(158) Ferreira, J.; Syrett, J.; Whittaker, M.; Haddleton, D.; Davis, T. P.; Boyer, C. *Polym. Chem.* **2011**, *2*, 1671.

(159) Efstratiadis, V.; Tselikas, G.; Hadjichristidis, N.; Li, J.; Yunan, W.; Mays, J. W. *Polym. Int.* **1994**, *33*, 171.

(160) Eschwey, H.; Burchard, W. *Polymer* **1975**, *16*, 180.

(161) Haddleton, D. M.; Crossman, M. C. *Macromol. Chem. Phys.* **1997**, *198*, 871.

(162) Crossman, M. C.; Haddleton, D. M. *Macromol. Symp.* **1998**, *132*, 187.

(163) Sriprom, W.; James, M.; Perrier, S. b.; Neto, C. *Macromolecules* **2009**, *42*, 3138.

(164) Baek, K.-Y.; Kamigaito, M.; Sawamoto, M. *Macromolecules* **2000**, *34*, 215.

(165) Burchard, W. *Adv. Polym. Sci.* **1999**, *143*, 113.

Chapter 4

Synthesis of oil soluble star polymers for use as viscosity modifiers in engine oils

This chapter of research is focussed on the synthesis of star copolymers of long chain alkyl methacrylate and methyl methacrylate. A core-crosslinking arm-first technique was employed using an industrially pre-defined RAFT agent, ***RAFT agent 3****, to control the polymerisation. The target was to improve the yield of the polymer, i.e. to increase the arm incorporation into star.*

Using the results of the work from chapter 3 as a basis, stars were synthesised using batch polymerisation of arm polymer and subsequent crosslinking with a divinyl species. The polymerisation of methacrylates using ***RAFT agent 3*** *was seen to proceed with hybrid behaviour, and star polymers formed from the resultant macro-RAFT agents had broad PDI with low arm incorporation. The polymerisation was optimised by controlling the concentration of monomer using a feed system, and the narrow PDI resultant macro-RAFT agent used for a crosslinking study using* ***crosslinker 1****.*

The yield was seen to be higher when using the narrow PDI macro-RAFT agent (> 80%) and varying the equivalents of ***crosslinker1*** *and reaction time was studied to further improve the incorporation of arm into star polymer.*

4.1 Introduction

When considering mechanical lubrication, it is important to know that when two surfaces in motion are fully separated by a fluid, the friction is solely due to the viscosity of the liquid. Therefore if the lubricating oil is too viscous the efficiency of the mechanism decreases due to high friction. Alternatively, if it is not viscous enough the oil thickness between the moving parts will be too small which can cause wear to the mechanical parts. Therefore, for any given mechanical operation, the lubricating oil used has an optimum operating viscosity. This study is an investigation into the synthesis of viscosity modifiers (explained in section 4.1.1.1) for use in engine oils.

4.1.1 Viscosity

In general terms we consider something with high viscosity, such as honey, as being "*thick*" and something with low viscosity, such as water, as being "*thin*". This "*thickness*" or viscosity is defined as the resistance to flow, where the resistance arises from intermolecular forces and internal friction as the molecules move past each other.[166]

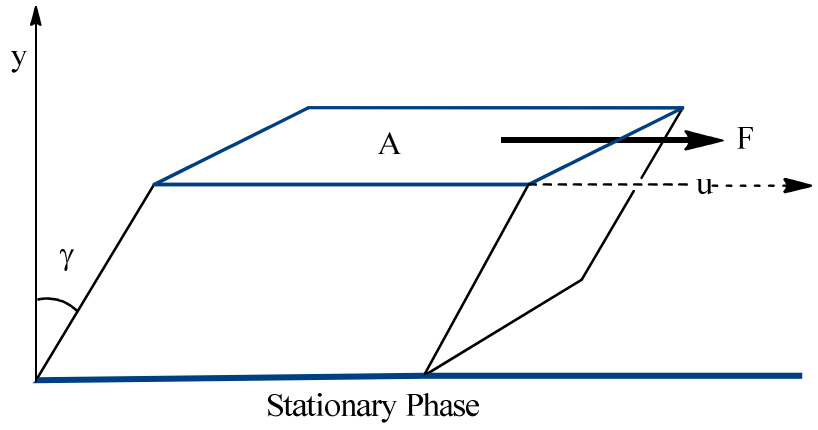

Figure 39: A fluid moving under a shear rate, $\dot{\gamma}$ ($\dot{\gamma}=d\gamma/dt$), and a shear stress, τ ($\tau = F/A$).

If we consider a liquid moving at a shear rate, $\ddot{\Upsilon}$, due to an applied shear stress of τ, the viscosity of the liquid is given by the ratio of the applied shear stress to the resulting shear rate, figure 39. Therefore if the shear stress is given by:

$$\gamma = \frac{du}{dy} \qquad (4.1)$$

where u is displacement in the x direction.

The shear rate is therefore given by:

$$\ddot{\Upsilon} = \frac{d}{dt}\frac{du}{dy} = \frac{dv_x}{dy} \qquad (4.2)$$

where v_x is velocity in the x direction.

The relationship between viscosity (η), shear stress (τ), and shear rate ($\ddot{\Upsilon}$) is given by:

$$\eta = \frac{\tau}{\ddot{\Upsilon}\,\ddot{\Upsilon}} \qquad (4.3)$$

For Newtonian fluids, the relationship between shear stress and shear rate is independent of shear rate and time, and only altered by temperature. However, non-Newtonian fluids can exhibit different shear stress, shear rate and time relationships. A fluid which thickens with time upon constant shear stress is termed "*thixotropic*", whereas a liquid which thins with time upon a constant shear stress is termed "*rheotropic"*. Non-Newtonian fluids can also be subdivided by their response to shear rate; a fluid which decreases in viscosity with increasing shear rate is termed "*shear thinning",* whereas a fluid which increases in viscosity with increasing shear rate is termed "*shear thickening"*. Polymer solutions are classed as non-Newtonian fluids.

4.1.1.1 Viscosity Modifiers

Within any commercial lubricating oil there are several important additives that contribute to its final properties; detergents, viscosity modifiers (VMs), anti-foam agents, and dispersants are but a few of the additives that allow tailoring of lubricating oils to specific requirements. The additives collectively are designed to improve the performance and durability of both the oil and the lubricated mechanical parts.

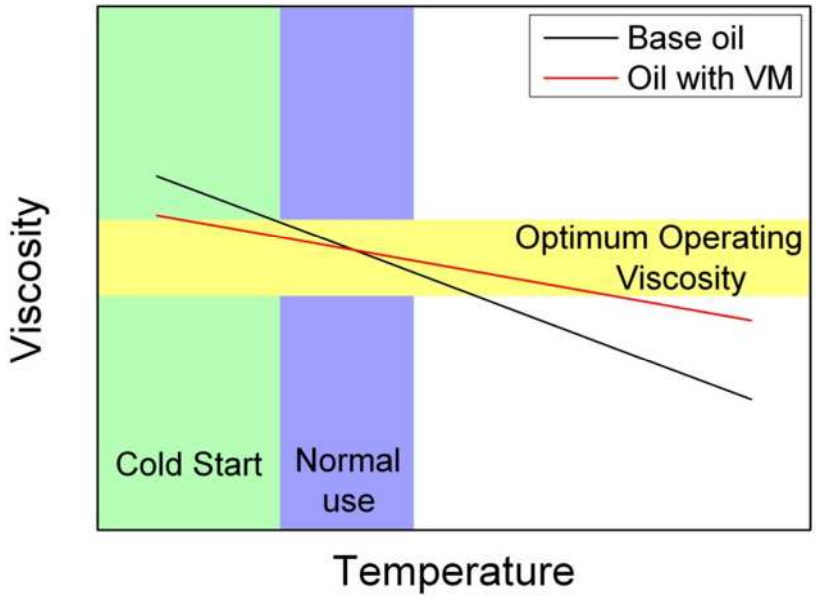

Figure 40: Plot of viscosity and temperature for a base oil, and an oil with a VM.

VMs (also known as viscosity index improvers) are designed to maintain a more consistent oil viscosity over a range of temperatures; this enables the oil to be within the optimum operating viscosity over a broad temperature range. To do this it must temper the inherent increase in oil viscosity with low temperature and/or the decrease in viscosity with high temperature, figure 40.

The viscosity of an oil comes from the interaction of the molecules trying to move past each other. Therefore, the addition of a spatially large polymer to the oil impedes the movement of the small oil molecules and increases the overall viscosity.

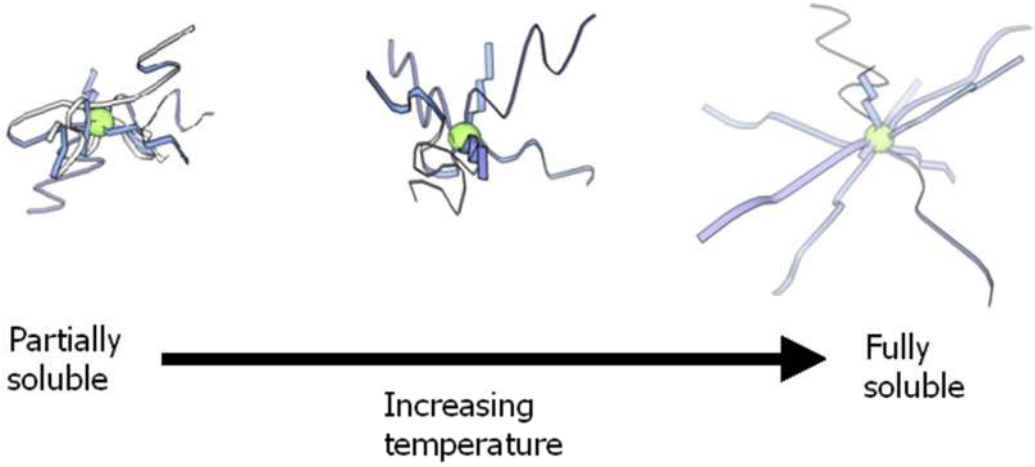

Figure 41: Cartoon describing the increase in volume with temperature of a star VM in solution. The green sphere represents the core of the star, and the blue ribbons represent the polymer arms.

The operation of a VM has been described as being due to the changing solubility of the VM with temperature.[167] At low temperatures it is partially solvaphobic, and contracted in solution. With increasing temperature a VM becomes more relaxed in solution increasing in volume and therefore improving its ability to increase the oil viscosity, figure 41. Without this temperature dependence on thickening ability the polymer additive would be referred to as a thickener.

VMs are described by several properties they possess. Their efficacy at tempering the viscosity change with temperature is described by the *Viscosity Index* (VI), and the polymer's ability to withstand high shear environments is described by the *shear stability index* (SSI).

The VI was adopted by the Society of Automotive Engineers as a standard after its inception by Dean and Davis[168] and extended use at the Standard Oil Company where they worked. The early form of the index was on a scale of 0 – 100, but the index has since been extended to accommodate oils with higher VI. A high VI is desired in a VM. This property is obtained from the kinematic viscosity measurements of the additives in oil at 40 ^{o}C and 100 ^{o}C.

The SSI is a measure of the ability of a VM to withstand a shear environment.

$$SSI = \frac{\eta_i - \eta_f}{\eta_i - \eta_0} \qquad (4.4)$$

where

η_i = initial oil viscosity

η_f = final oil viscosity after subjected to high shear conditions

η_o = viscosity of base oil blend with all additives except the VI improver

The size and the concentration of a polymer in solution determine the thickening ability of the polymer. Higher molecular weight VMs are advantageous commercially as they boast high VIs and they also allow the lowest treat rates. However, VMs require a fine balance of many performance characteristics to achieve the desired overall performance. Until recently there have been only two VM parameters that could be adjusted to reach the required performance characteristics: molecular weight and the polymer composition. High molecular weight VMs are desirable for their high VI but are also prone to mechanical shearing in an engine leading to less thickening and potential mechanical wear.[169] Therefore the molecular weight must be adjusted to give the highest VI possible while still meeting the shear stability requirements of an application. This trade-off makes it difficult to maximise both the VI and the shear

stability, where one is traditionally sacrificed for the other depending on the application.

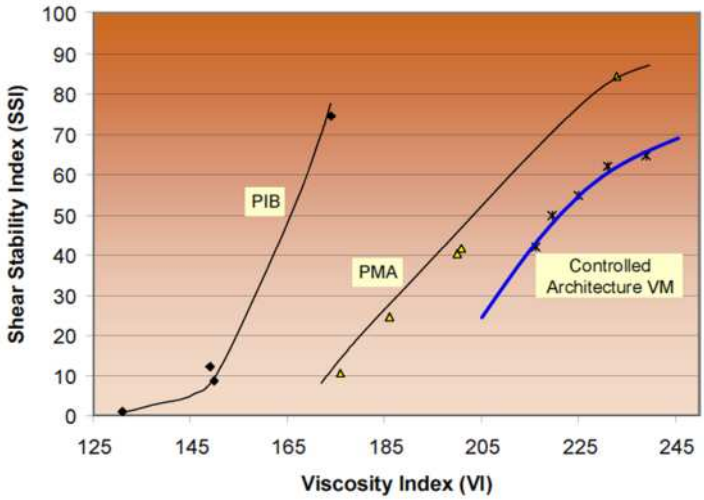

Figure 42: relationship between shear stability index and viscosity index for VMs of different compositions and architecture. PIB= linear poly(isobutylene), PMA = poly(long chain alkyl methacrylate), Controlled Architecture VM= higher architecture (e.g. Stars, hyper branched) poly(long chain methacrylate). Copied without editing from reference.[170]

Forces applied under shear deform the coiled structure of a polymer in solution. Under sufficient shear, polymer scission occurs at the point where the polymer is under most stress. When put under shear stress a linear polymer is seen to break at the centre of the polymer.[171-174] Thickening dependence on molecular weight of the VM means that halving the molecular weight of a VM or thickener will cause significantly reduced thickening.

It has been seen that star polymers have advantages over their linear counterparts in shear environments. Scission occurs near the core of the star, with loss of a polymer arm;[173] with high functionality (*f*) stars this would have little effect on the solution viscosity. The VM would remain active until many arms had been cut off, therefore it's predicted that increasing number of arms will increase the durability of the VM. Higher

architecture polymers, such as stars, have been promoted on a commercial basis in the oil additive business as they provide better combined shear stability and viscosity index properties than linear counterparts, figure 42.[170]

4.2 Results and Discussion

4.2.1 Synthesis of oil soluble core cross-linked star polymers

Long chain alkyl methacrylate VMs have been seen to exhibit a higher VI relative to hydrocarbon VMs, for example, poly(iso-butylenes) or ethylene/propylene copolymers.[175] Therefore, long chain alkyl methacrylate ($C_{12\text{-}15}$MA) has been used here for the study of arm incorporation into star polymers for potential use as VMs. The scope of this study was to optimise the arm incorporation into a star polymer made using commercially relevant feedstock and an industrially relevant process.

Arm-first synthesis of star polymers using a crosslinker is generally commercially favoured due to lower costs of associated with a crosslinker relative to a multifunctional initiator. It is commercially advantageous to understand the star formation and to control the arm incorporation into the star architecture. Some of the variables that effect the star formation have previously been studied within the Haddleton group and other research groups: equivalent amount of crosslinker, the reactivity of the crosslinker, the type of crosslinker,[140,176] and the percentage conversion of monomer when crosslinker is added to the reactor. Of particular interest is a study by Sawamoto and co-workers[140,141] looking at the effect of the distance between the reactive vinyl groups on the crosslinker for star synthesis using TMM-LRP. A general trend was observed that increased spacer length in a divinyl crosslinker resulted in an increase in molecular weight of the star polymer formed, and therefore

greater functionality, *f*. Their hypothesis was that the increased spacer length allowed the pendant crosslinker methacrylate groups to be more accessible, which increases the statistical likelihood of arm incorporation and/or star-star coupling. An exception to the rule was highlighted, triethylene glycol dimethacrylate (**crosslinker 3**) showed no star formation, whereas the shorter and chemically equivalent ethylene glycol dimethacrylate (**crosslinker 1**) was shown to form large star polymers. They argued that the larger crosslinker had a stable conformation with the vinyl groups very close together, promoting intra-molecular cyclisation.[140]

4.2.1.1 Synthesis of arms (batch process)

Oil soluble polymers have been synthesised here by co-polymerisation of $C_{12\text{-}15}$MA and MMA. The synthesis of star polymers by an arm-first approach requires a living or controlled polymerisation technique to allow reaction of many growing polymer chains with a crosslinker to form the star shape. Among the many benefits of RAFT is the ability to modify a RAFT agent to effectively control the polymerisation of (almost) any family of vinyl monomer. Trithiocarbonates can be made very easily from carbon disulfide, thiol compound and a bromine compound.[177] Commercial requirements mean it would be useful to be able to use a trithiocarbonate, **RAFT agent 3**, to control the polymerisation of $C_{12\text{-}15}$MA.

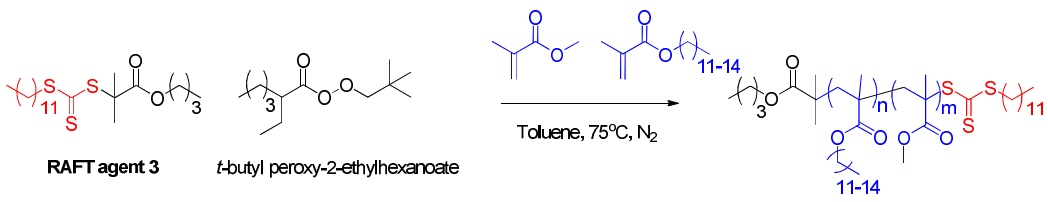

Scheme 18: Arm-first star polymer synthesis using t-butyl peroxy-2-ethylhexanoate, (Trigonox 21S) as a peroxide radical source, with a RAFT agent 3, and $C_{12\text{-}15}$MA and MMA as monomers.

The polymerisation kinetics of the arm synthesis, scheme 18, was followed by measuring conversion by ^{1}H NMR and molecular weight by GPC. The kinetics displayed some unusual reaction behaviour compared with an ideal RAFT polymerisation.

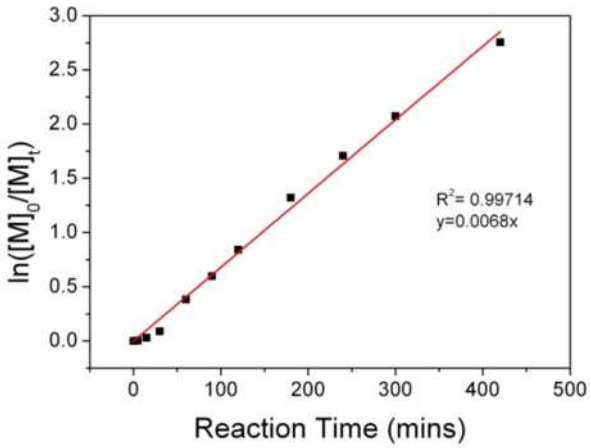

Figure 43: Plot of log ln($[M]_0/[M]_t$) against reaction time. A linear plot shows first order kinetics.

Hybrid behaviour, between controlled radical polymerisation (CRP) and traditional free radical polymerisation (FRP) was seen for the bulk reaction. A non-linear time dependence of ln($[M]_0/[M]_t$) was found, figure 43, indicating a decrease in radical concentration. This non-linear first order kinetic behaviour is commonly due to either the occurrence of termination in the polymerisation (e.g. disproportionation, chain coupling or non RAFT chain transfer reactions) or a decrease in initiator concentration; the decrease in initiator concentration could result from a steadily decreasing concentration of the radical source, *tert*-butyl peroxy-2-ethylhenxanoate (Trigonox 21S).

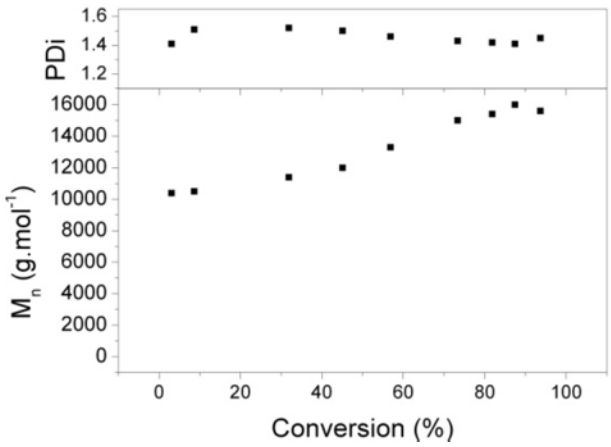

Figure 44: Molecular weight and PDI evolution with conversion for the bulk polymerisation of $C_{12\text{-}15}$MA / MMA copolymer using RAFT agent 3, targeting 10,600 g.mol^{-1}.

The polymerisation gave a polymer with high PDI close to the target molecular weight, 10,600 g.mol^{-1}, after very low conversion, figure 44. This is evidence that a non- RAFT free radical mechanism dominates the early part of the reaction. However, the relatively low molecular weight, suggests that the RAFT agent is behaving like a conventional chain transfer agent.[178] Once most of the **RAFT agent 3** has reacted, and the reaction enters the main equilibrium of the RAFT process, the molecular weight of the polymer increases with conversion of monomer to polymer.

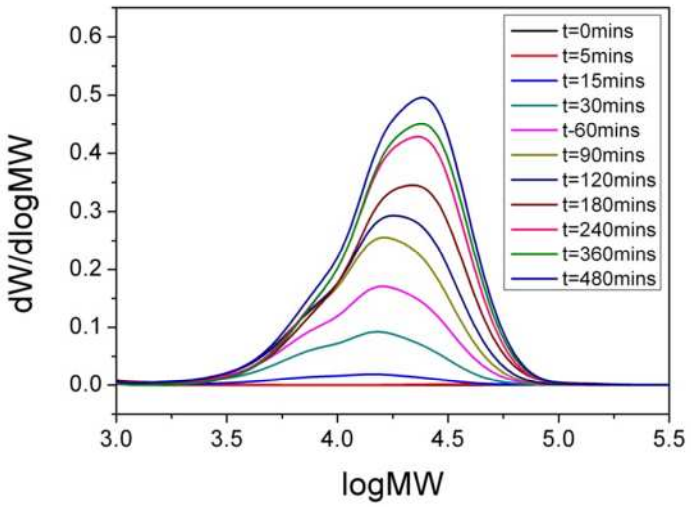

Figure 45: MWDs of polymers formed during the bulk co-polymerisation of $C_{12\text{-}15}$MA and MMA at different reaction times.

The higher than expected PDI of the polymer throughout the reaction (ca. 1.5), figure 44, supports the idea that **RAFT agent 3** behaves like a conventional chain transfer agent at low conversion. The MWD of the polymer is seen not to change much over the course of the reaction, figure 45. The multimodal distribution is seen to skew to the high molecular weight region at longer reaction times, which is likely due to reversible addition to the macro-RAFT agent.

4.2.1.2 Star formation by addition of crosslinker to arm polymerisation

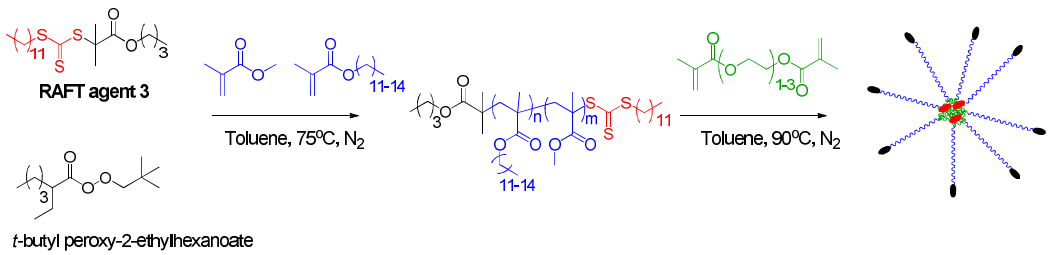

Scheme 19 Reaction scheme for the synthesis of $C_{12\text{-}15}$MA / MMA copolymer stars by an arm-first route.

This study aimed to improve the incorporation of arms into star polymer. One way that star formation can be effected is by investigating the crosslinker used. Sawamoto highlighted the dependence of crosslinker length on the efficiency of crosslinking.[140,141] By varying the length of the spacer between the vinyl moieties in the series of crosslinkers from EGDMA (**crosslinker 1**) < DEGDMA (**crosslinker 2**) < TEGDMA (**crosslinker 3**), increasing the length by one ethylene glycol repeat unit each time. By varying the relative amount of crosslinker added after arm synthesis, it was possible to optimise the conditions for the different cross-linkers to aid comparison.

A series of oil soluble star polymers were formed using **crosslinker 1**, **crosslinker 2** and **crosslinker 3**, using polymers formed in the bulk polymerisation process.

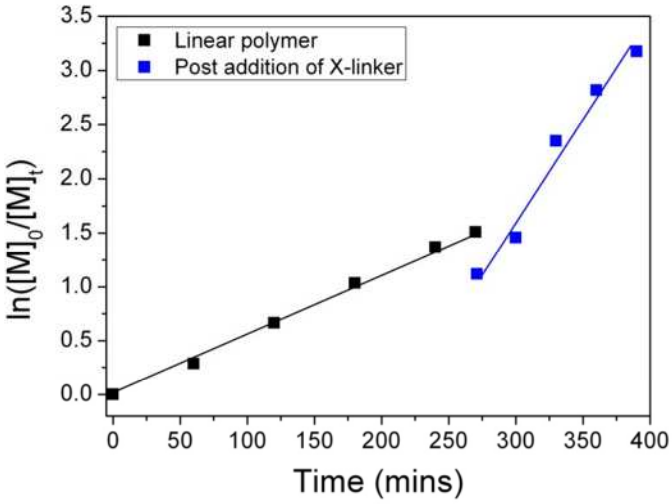

Figure 46: Kinetic plot for reaction E60. Co-polymerisation of $C_{12\text{-}15}$MA and MMA followed by addition of crosslinker 1 after 300 minutes

Copolymerisation of $C_{12\text{-}15}$MA and MMA was reproducible and showed first order kinetics, figure 46. After addition of **crosslinker 1**, the apparent rate of propagation was seen to increase, shown by the increase in gradient of the plot of $\ln([M]_0/[M]_t)$ against time, figure 46.

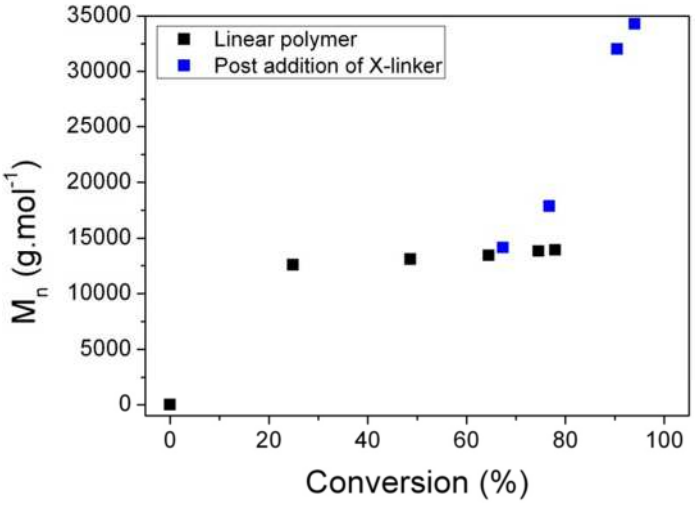

Figure 47: Reaction E60: Molecular weight evolution with conversion for the copolymerisation of $C_{12\text{-}15}$MA and MMA followed by the addition of crosslinker 1.

The evolution of the molecular weight during the polymerisation was followed using GPC and ^{1}H NMR showing that the molecular weight had increased to close to the target arm molecular weight after the first aliquot was taken at 20% conversion, in agreement with the earlier data for arm polymerisation, figure 44. After addition of crosslinker the molecular weight increased significantly, to yield a final polymer with molecular weight of more than double that of the linear arm, when the M_n of the entire molecular weight distribution was calculated by conventional GPC. The star polymers formed are considerably larger, however the high PDI multimodal peaks make deconvolution ineffective.

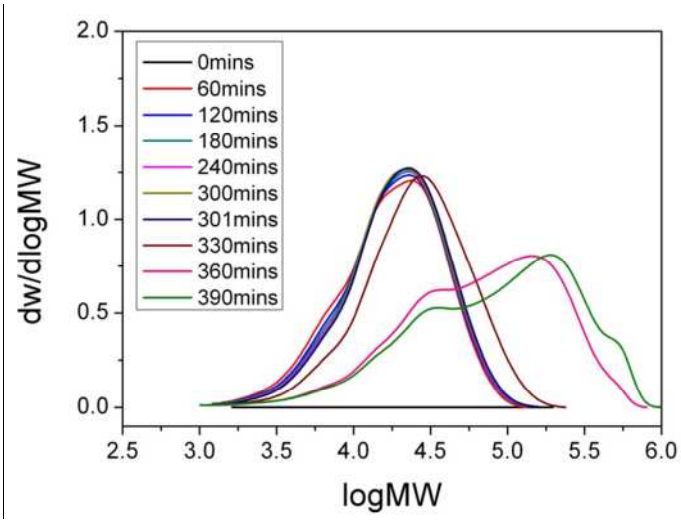

Figure 48: Reaction E60: Change in MWD with polymerisation time for the co-polymerisation of $C_{12\text{-}15}$MA and MMA followed by addition of crosslinker 1 after 300 minutes.

The MWD does not change significantly during the arm polymerisation, however, upon addition of **crosslinker 1** after 300 minutes the arms are chain extended with the crosslinker and a shift to higher molecular weight is seen at 330 minutes. Within an hour after crosslinker addition, a large high molecular weight shoulder is formed indicating star formation.

It was predicted that using **crosslinker 2**, with a longer spacer between the vinyl moieties would increase the efficiency of the star formation and yield larger star polymers, without the intramolecular cyclisation seen with **crosslinker 3**.[140]

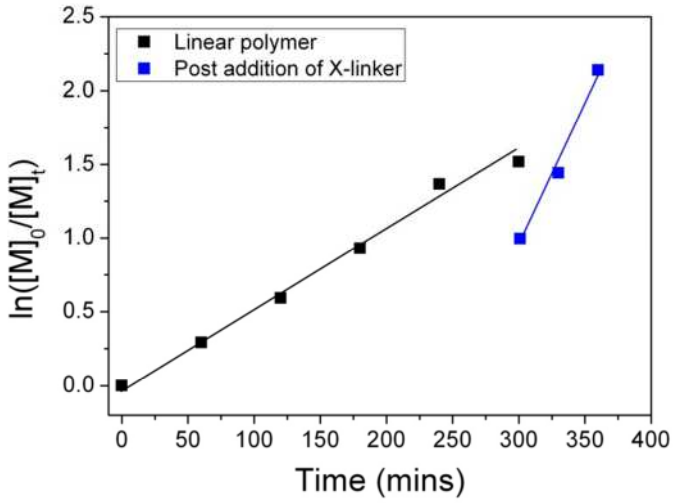

Figure 49: Kinetic plot for reaction D62. Co-polymerisation of $C_{12\text{-}15}$MA and MMA followed by addition of crosslinker 2 after 300 minutes

The addition of **crosslinker 2** after polymerisation of the monomer saw an increase in the apparent rate of propagation (conversion of the vinyl groups), figure 49.

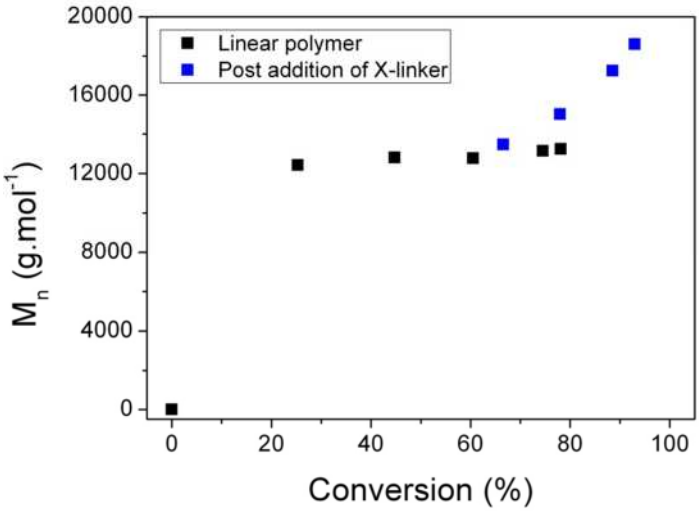

Figure 50: Reaction D62. Molecular weight evolution with conversion for the copolymerisation of $C_{12\text{-}15}$MA and MMA followed by the addition of crosslinker 2

However, the molecular weight increase after 90 minutes reaction of **crosslinker 2** (i.e. 390mins) was a lot less than that seen for **crosslinker 1;** the M_n of the final polymer = 18,600 $g.mol^{-1}$.

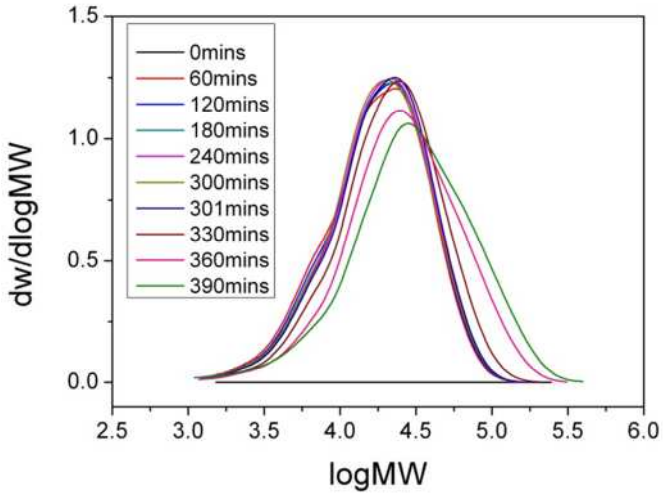

Figure 51: Reaction D62. Change in MWD with polymerisation time for the co-polymerisation of $C_{12\text{-}15}$MA and MMA followed by addition of crosslinker 2 after 300 minutes

The MWD of the polymer varied very little over the polymerisation of the monomer, with very small incremental increases in M_n with conversion after the initial polymer is formed. After addition of **crosslinker 2** after 300 minutes, chain extension can be seen to occur with an increase in M_n and a small shoulder appearing at the high molecular weight part of the distribution, figure 51.

TEGDMA**, crosslinker 3**, with the longest spacer in the series would be expected to have increased efficiency of star formation. However, it has been seen to form very small stars when using TMM-LRP to make methacrylate star polymers.[140]

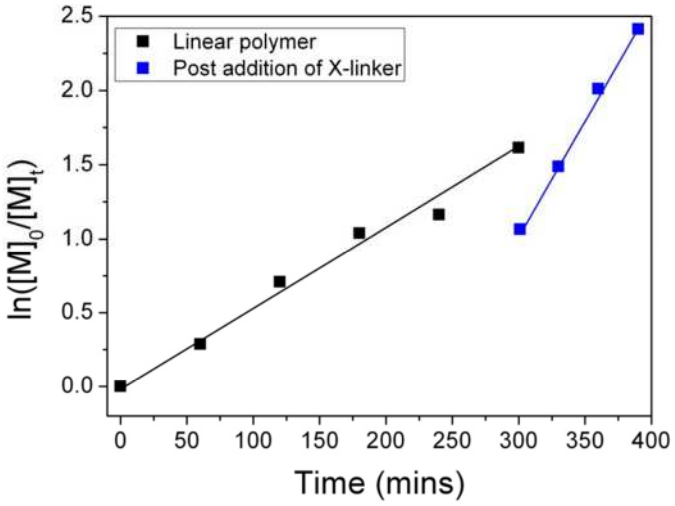

Figure 52: Reaction T63. Kinetic plot for reaction. Co-polymerisation of $C_{12\text{-}15}$MA and MMA followed by addition of crosslinker 3 after 300 minutes

The copolymerisation of the monomers is seen to proceed with pseudo first order kinetics as shown by a linear plot of $\ln([M]_0/[M]_t)$ against reaction time.

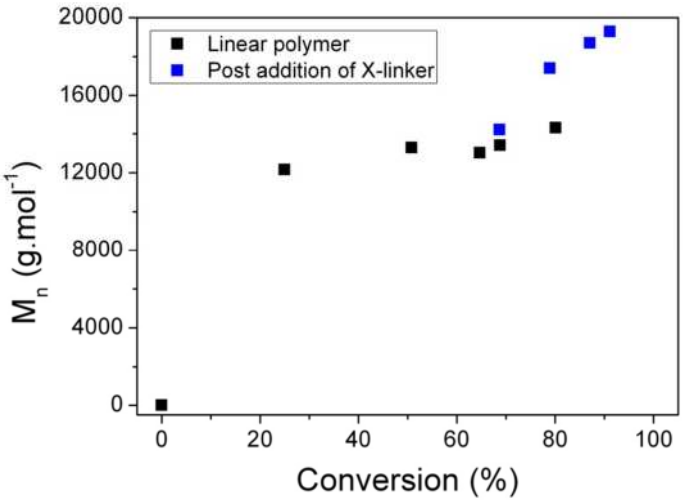

Figure 53: Reaction T63. Molecular weight evolution with conversion for the copolymerisation of $C_{12\text{-}15}$MA and MMA followed by the addition of crosslinker 3

The reaction data supports the other data suggesting high molecular weight polymer is formed early in the reaction with small growth in M_n over the course of the reaction.

Addition of 4 equivalents of **crosslinker 3** after 300 minutes led to the formation of increased molecular weight polymer. The increase in molecular weight expected from just chain extension due to the crosslinker is (4x286) 1144 g.mol^{-1} and extending by the remaining unreacted monomer at the time of crosslinker addition accounts for a further 3,000 g.mol^{-1} of chain extension. Therefore the increase in M_n of 6,000 g.mol^{-1} may be accounted for by chain extension with no star formation.

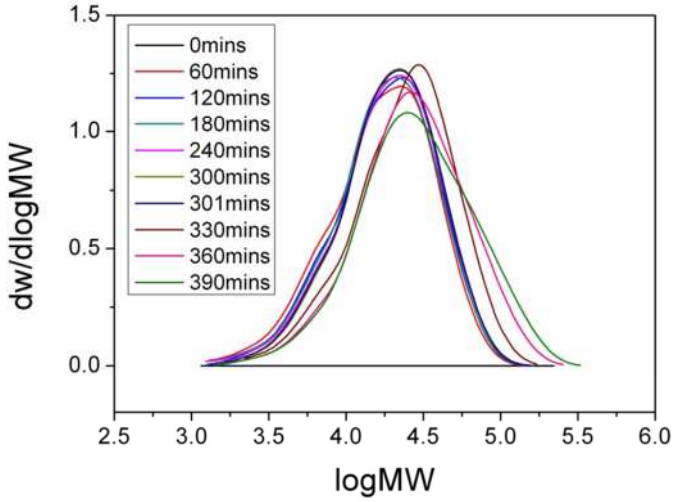

Figure 54: Reaction T63. Change in MWD with polymerisation time for the co-polymerisation of $C_{12\text{-}15}$MA and MMA followed by addition of crosslinker 3 after 300 minutes

The MWD of the polymer in reaction T63 moved to higher molecular weight 30 mins after addition of crosslinker, subsequent aliquots from the reaction show the MWD broadening with very little increase in M_n, figure 54.

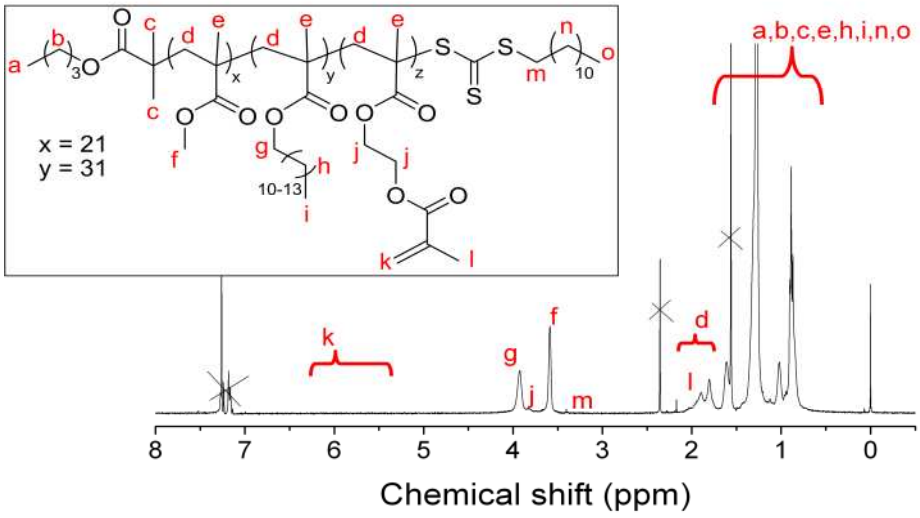

Figure 55: ^{1}H NMR of p($C_{12\text{-}15}$MA-MMA) statistical copolymer arms after reaction with crosslinker3. (inset) Possible structure of yielded polymer, with peak assigned. Note the apparent absence of vinyl peaks k.

If chain extension is occurring without star formation, it is hypothesised that a structure similar to that shown in figure 55 is formed; a structure with pendent vinyl groups from unreacted **crosslinker 3**.

The final polymer has relatively very small peaks at 5.5 and 6 ppm in the ^{1}H NMR that denotes the presence, in trace amounts, of vinyl groups, figure 55. This small amount is likely to be accounted for by a small amount of monomer being trapped in the polymer after precipitation; therefore it is unlikely that the polymer has the structure shown in figure 55.

Table 10: Results from the synthesis of star polymers via an arm-first procedure using RAFT polymerisation. The number average molecular weight, PDI were determined using conventional GPC against PMMA standards. Conversions were determined by ^{1}H NMR. Arm incorporation was determined by deconvolution of GPC spectra.

Reaction ID	Crosslinker	Ratio of [crosslinker]/[RAFT]	Conv. at addition /%	Arm M_n /g.mol^{-1}	Arm PDI	Final Conv. /%	Star M_n /g.mol^{-1}	Star PDI
E60	1	4	77.9	13900	1.76	95.8	34300	3.43
E61	1	4	76.6	14200	1.77	90.8	29800	2.85
E64	1	3	72.4	14400	1.72	93.6	40600	2.59
E65	1	6	67.5	14300	1.79	Gel	Gel	-
D62	2	4	78.1	13200	1.81	93.0	18600	2.34
D66	2	3	64.5	14700	1.77	88.9	26400	1.79
D69	2	3	68.8	13300	1.74	88.4	16400	1.95
T63	3	4	80.1	14300	1.71	91.1	19300	2.09
T67	3	3	73.3	14600	1.69	88.4	24000	1.56

In summary, the formation of star polymers using the high PDI Poly($C_{12\text{-}15}$MA-*co*-MMA) synthesised under batch conditions yielded low conversion of arms to stars for all crosslinkers. **Crosslinker 1** yielded broad PDI star polymers, with visibly low yield for arm conversion to star from GPC data. **Crosslinker 2** and **3** showed chain extension with little or no star formation. The series of reactions highlight the effect of changing crosslinker and the amount used. A summary of the reactions is shown in table 10 to allow easier comparison.

4.2.1.3 Optimisation of arm synthesis (feed process): RAFT polymerisation of methacrylates using trithiocarbonates

The batch process using **RAFT agent 3** to co-polymerise MMA and $C_{12\text{-}15}$MA star polymers with **crosslinker 1**, **2** or **3** saw a significant difference between the efficiencies of the crosslinkers. However the arm polymerisation was seen to proceed by a hybrid mechanism between FRP and RAFT. Further research into the literature revealed that this hybrid mechanism occurs during the RAFT pre-equilibrium (where the RAFT agent is converted to macro-RAFT agent) for other RAFT agent and monomer combinations.[93,178,179]

Schubert *et al.* observed hybrid behaviour in the synthesis of diethylene glycol methacrylate (DEGMA) and oligo(ethylene glycol) methacrylate (OEGMA) block copolymers using 2-cyano-2-butyl-dithiobenzoate (CBDB) as the RAFT agent; the apparent chain transfer coefficients for the polymerisations were calculated and their low value (<1) were reasoned to be the cause of the observed strange RAFT kinetics.[179] Davis and co-workers saw that at low temperatures polymerisation of MMA using the RAFT agent cumyl phenyldithioacetate displays reaction kinetics akin to that of a polymerisation using a conventional chain transfer agent. The chain transfer constant, C_s, for the "RAFT agent"/CTA was seen to increase with temperature, and polymerisation kinetics expected by a RAFT mechanism was observed at higher conversion (>50%). [178]

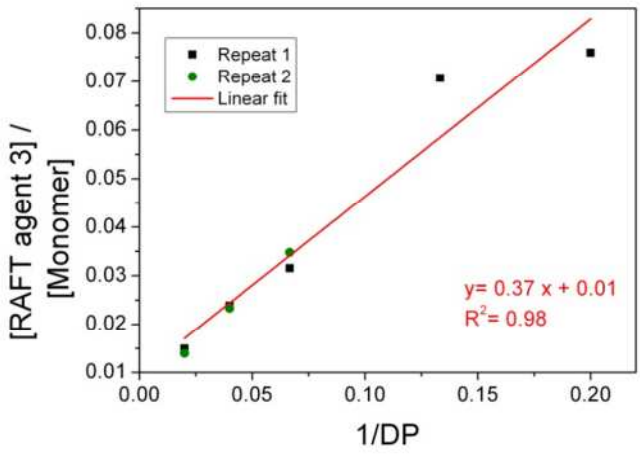

Figure 56: Mayo plot of [RAFT agent 3]/[Monomer] against 1/degree of polymerisation, where DP is calculated by M_n/m_0 where M_n is the number average molecular weight and m_0 is the average RMM of the monomer.

Thus the polymerisation of the long chain alkyl methacrylate monomer mixture using **RAFT agent 3** was investigated further to determine if the results coincided with the somewhat strange reaction kinetics seen in some RAFT systems in literature.

At low conversion the polymer formed in the polymerisation using **RAFT agent 3** is seen to be from a conventional chain transfer agent mechanism (i.e. non-reversible chain transfer). As a result, it is possible to use a Mayo plot to determine a chain transfer constant, C_s, for the CTA (*NB*: it is not usually possible to use the Mayo equation to determine a C_s for a RAFT agent, a value can only be determined for this instance as the RAFT agent is behaving like a conventional CTA for the polymerisation of these monomers). The Mayo equation takes the form:

$$\frac{1}{DP} = \frac{1}{DP_0} + C_s \frac{[RAFT\ agent\ 3]_0}{[monomer]_0} \qquad (4.5)$$

Where

$[RAFT\ agent\ 3]_0$ is the concentration of RAFT agent 3 at t=0,

[Monomer]$_0$ is the concentration of the monomer mixture at t=0.

The C_s is defined as:

$$C_s = \frac{k_{tr}}{k_p} \qquad (4.6)$$

Where

k_{tr} is the chain transfer coefficient,

k_p is the rate of propagation coefficient.

Hence, it is possible to obtain a value for the C_s by plotting the inverse of the number average degree of polymerisation, DP_n, against the ratio of RAFT agent 3 to monomer at the beginning of the reaction. The gradient provides the C_s, and the intercept with the y ordinate gives the inverse degree of polymerisation in the case with no transfer agent present in the reaction mixture. The degree of polymerisation was estimated using the M_n from GPC using the equation below.

$$DP_n = \frac{M_n}{m_0} \qquad (4.7)$$

Where

M_n is the number average molecular weight from GPC,

m_0 is the average molecular weight of the statistical mixture of monomers.

The co-monomer reagent feed mixture was polymerised using different ratios of RAFT agent to monomer to yield a polymer series, table 11. Importantly, the reactions were terminated at very low conversion (< 5%) to ensure that the ratio [**RAFT agent 3**] / [monomer] in the reaction is as close to the ratio [**RAFT agent 3**]$_0$ / [monomer]$_0$ as possible. Most reactions were stopped at very low conversion (< 2%), however the

small induction period seen in RAFT polymerisation and the high polymerisation rate made the termination of reactions with high [**RAFT agent 3**]$_0$ / [Monomer]$_0$ ratios very difficult. The data from each reaction provides a point for the Mayo plot, figure 56. The number average degree of polymerisation DP is determined using the M_n of the polymer / the average molar mass of the monomer mixture. This uses the assumption that the reactivity ratio for all of the methacrylates used = 1. From the data points an estimate of the C_s value is determined to be 0.49, which means that k_{tr} is smaller than k_p.

Table 11: Polymerisations used to determine the chain transfer constant for RAFT agent 3 during the co-polymerisation of $C_{12\text{-}15}$MA and MMA.

[RAFT agent 3] / [Monomer]	Conversion (%)	M_w (g.mol^{-1})	M_n (g.mol^{-1})	Conversion (%)	M_w (g.mol^{-1})	M_n (g.mol^{-1})
	Repeat 1			**Repeat 2**		
0.2	15.1	2700	2700	-	-	-
0.13	1.64	3600	2900	-	-	-
0.067	0.40	7600	6500	0.80	6600	5900
0.04	0.48	11600	8600	0.48	11500	8800
0.02	0.24	20700	13700	1.38	22100	14700
C_s		0.75	0.49		0.94	0.44

It has been argued that the M_w of the polymer calculated by GPC is more reliable than using M_n due to the large effects of peak and baseline selection on M_n.[180,181] Although M_n is the only direct measure of number average DP, the M_w of the polymer could be more reliable.[182] For a polymerisation dominated by chain transfer the $M_w = 2M_n$, therefore the number average DP can be calculated using the M_w using eqn. 4.8.

$$DP_n = \frac{M_w}{2m_0} \qquad (4.8)$$

Where:

M_w is the weight average molecular weight from GPC.

The relative rates of propagation and chain transfer to RAFT agent mean that a large excess of monomer in the reactor leads to propagation dominating, with the polymerisation showing kinetics similar to a free radical chain transfer mechanism. Once chain transfer to **RAFT agent 3** occurs, the main equilibrium of the RAFT mechanism proceeds as normal, with an incremental increase in molecular weight. Using this information, the following study was conducted to determine how this process can be manipulated to attain a narrow PDI polymer with high end group retention to be used as arms in the star polymer formation.

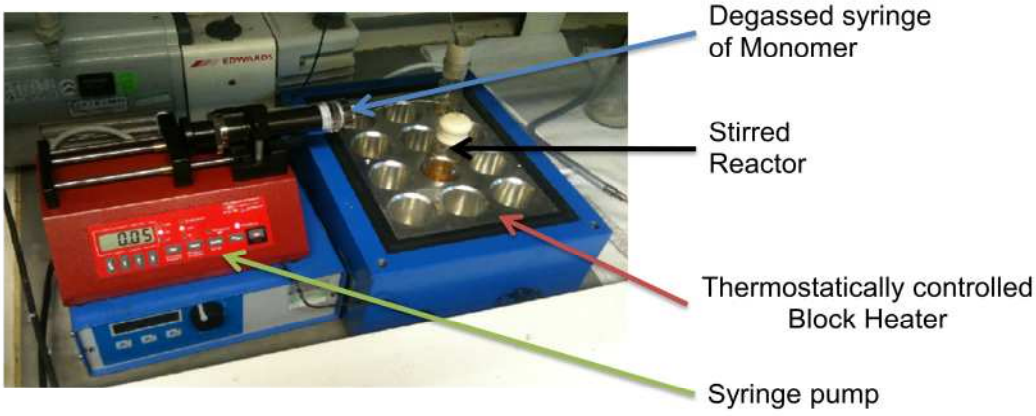

Figure 57: Labelled photograph of monomer feed system

The relative rates of propagation and chain transfer were changed by varying the concentration of monomer in solution, whilst keeping the concentration of RAFT agent constant. A feed system was set up to allow control of the amount of monomer present in the system, figure 57. A reaction vessel was charged with the RAFT agent, radical initiator and the solvent. Degassed monomer, with mesitylene to allow the reaction to be followed by ^{1}H NMR, was charged to a large gas-tight syringe and a percentage of the mixture transferred to the reaction vessel. The reaction was started and followed by ^{1}H NMR and GPC. At a minimum of 80% conversion of the initial monomer mixture, the remaining degassed monomer was pumped into the system at a rate that would keep the monomer at a relatively consistent concentration in the reactor. I.e. If the 12 mL of monomer is polymerised to 80% conversion in 300 minutes, the monomer was pumped in at 12 mL*0.8/ 300 minutes = 0.032 mL.min^{-1}.

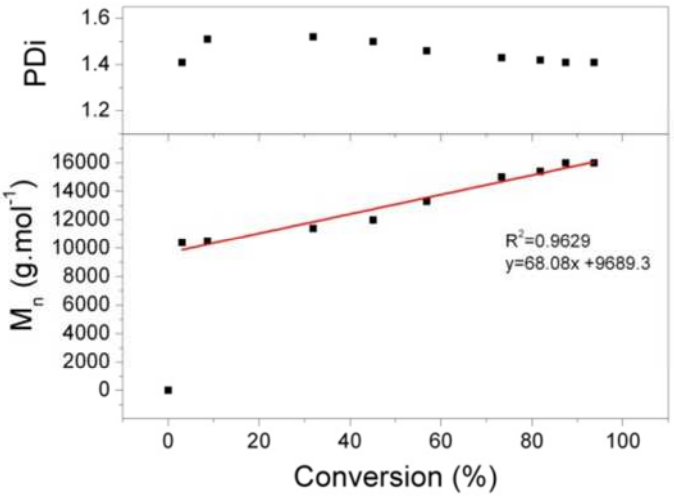

Figure 58: Molecular weight and PDI evolution with conversion for the bulk polymerisation (i.e. 100% monomer in reactor at the beginning of the reaction) of $C_{12\text{-}15}$MA / MMA copolymer using RAFT agent 3, targeting 10,600g.mol^{-1}. The red line shows the best fit of the data with linear equation shown below.

When all of the monomer is present in the reaction vessel at the beginning of the reaction (without any monomer feed system), the rate of propagation is predominant

over chain transfer and high molecular weight polymer is formed very early in the reaction. The M_n then increases slowly with conversion and the PDI decreases from 1.5 to about 1.4 by 90% conversion, figure 58. From the line of best fit of the data, the M_n of the polymer formed very early in the reaction can be estimated as 9,700 $g.mol^{-1}$.

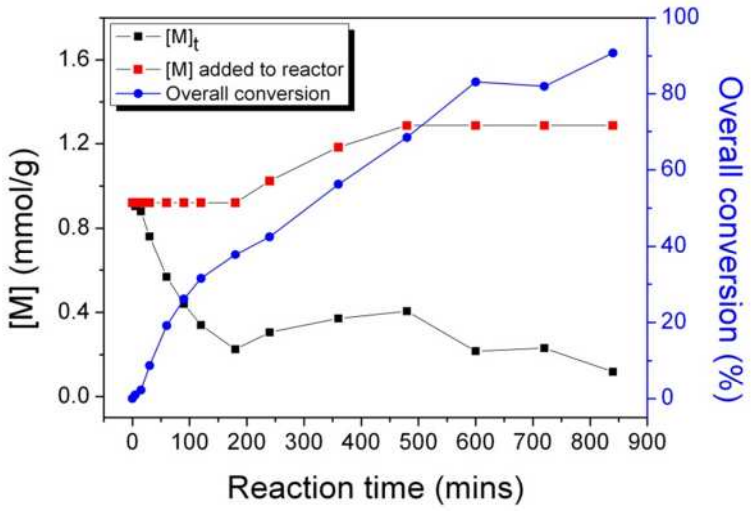

Figure 59: Plot showing the evolution of monomer concentration in the reactor, [M], with time when 50% of monomer is introduced at the beginning of the reaction, and the remaining 50% is fed at 0.3mL/min from 180minutes. Also shown is the concentration of monomer [M] added to the reactor and the overall conversion of the monomer.

The amount of monomer in the reactor at the beginning of the reaction was reduced to 50% of the total amount of monomer to be added. The remaining degassed monomer was added to the system using a syringe pump after the initial monomer had reached high conversion, at a rate of 0.03 mL/min. An internal standard, mesitylene, was added to the entire monomer mixture to allow the conversion to be followed by ^{1}H NMR.

The concentration of monomer in the reactor at the beginning of the reaction can be simply calculated from the masses of each component added. The evolution of monomer concentration is calculated based on the monomer feed and the conversion by ^{1}H NMR:

$$[M]_t = \frac{x(M_{m0} + tv_f)}{m_0 \,.\, M_{total}} \qquad (4.9)$$

Where:

$[M]_t$ is the concentration of monomer in the reactor at time, t, in mol/g

x is the conversion of monomer from ^{1}H NMR

M_{m0} is the mass of monomer in the reactor at t=0

v_f is the rate of monomer addition to the reactor in mass/min

M_{total} is the total mass of reagents in the reactor

For this study the concentration is determined using the unconventional units 'mol/g' as it provides a more accurate number than using an estimation of the volume. The concentration of monomer in solution is seen to drop from 0.921 mmol.g^{-1} to 0.226 mmol.g^{-1} over the first 3 hours of reaction, figure 59. The concentration of monomer remains at <0.4 mmol.g^{-1} for the remainder of the reaction, up to high overall conversion of monomer, figure 59.

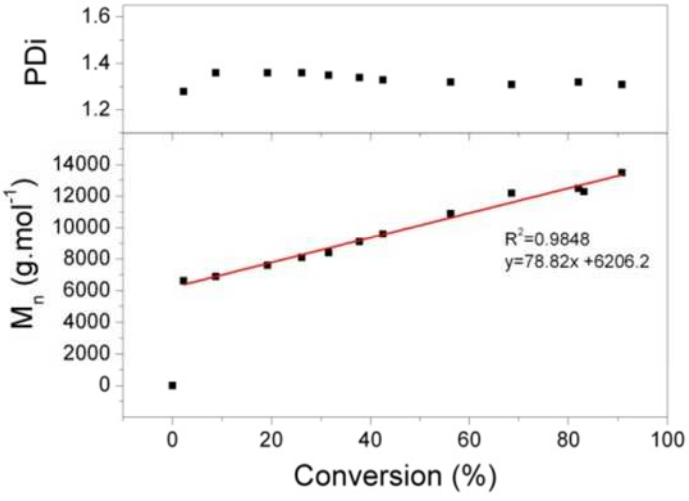

Figure 60: Molecular weight and PDI evolution with conversion for the polymerisation of $C_{12\text{-}15}$MA / MMA copolymer using RAFT agent 3, targeting 10,600 g.mol^{-1}. 50% of the monomer mixture was present in the reactor at the beginning of the reaction, with the rest fed into the reactor at 0.3 mL/min once the initial monomer present had reached 80% conversion. The red line shows the best fit of the data with linear equation shown below.

Reducing the amount of monomer in the reaction vessel at the beginning of the reaction to 50% of the monomer feedstock saw a dramatic improvement in the final polymer compared to the bulk reaction, where the PDI had decreased from 1.4 at the beginning of the reaction to just over 1.3 at over 90% conversion of monomer, figure 60. From the line of best fit of the M_n data, it was determined that the polymer formed very early on in the reaction was around 6,200 $g.mol^{-1}$. The final polymer remained close to the target molecular weight of 10,600 $g.mol^{-1}$. Assuming the concentration of RAFT agent is constant, and no RAFT agent is destroyed during the reaction, the greater control of PDI and molecular weight early in the reaction supports the hypothesis that controlling the relative rates of propagation and chain transfer can help push the reaction out of the pre-equilibrium and into the main equilibrium of RAFT. The RAFT mechanism is now seen to be more prevalent than the free radical mechanism during the pre-equilibrium.

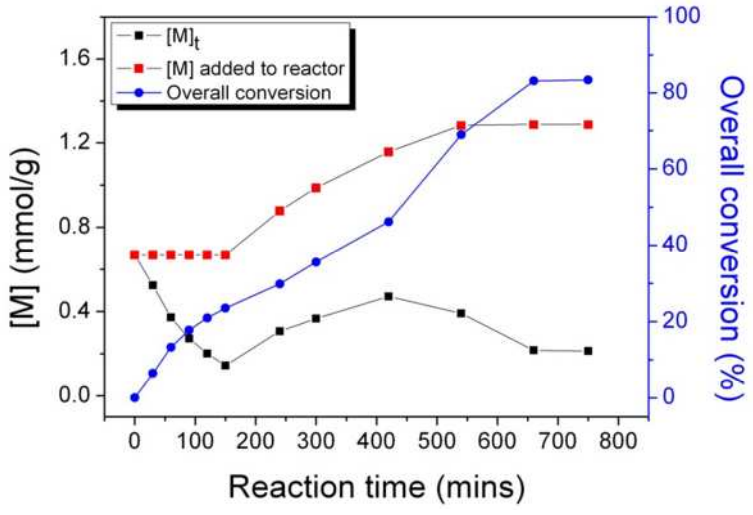

Figure 61: Plot showing the evolution of monomer concentration in the reactor, [M], with time when 30% of monomer is introduced at the beginning of the reaction, and the remaining 70% is fed at 0.3 mL/min from 150 minutes. Also shown is the concentration of monomer [M] added to the reactor and the overall conversion of the monomer.

Therefore, the concentration of monomer in the reactor at the beginning of the reaction was decreased further to 30% of the original bulk reaction, decreasing the concentration of monomer in the reactor to 0.668 mmol.g^{-1} at the beginning of the reaction. The monomer concentration decreased steadily over the course of the first 150 minutes of polymerisation to 0.144 mmol.g^{-1}, at which point the monomer began to be fed into the reactor faster than the propagation rate causing the concentration to increase steadily to 0.471 mmol.g^{-1}, figure 61.

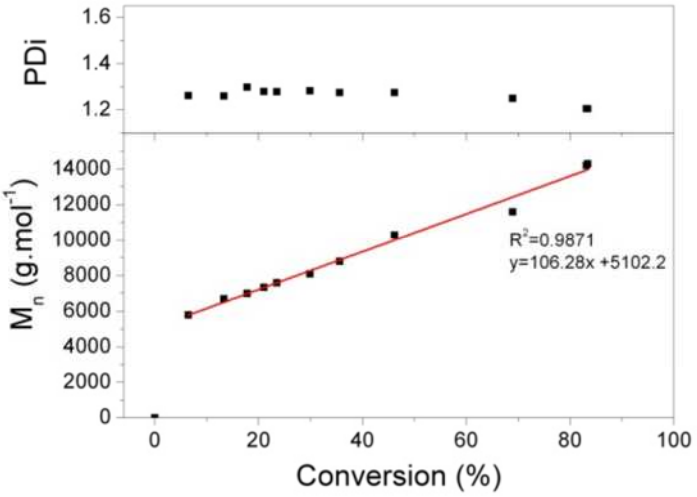

Figure 62: Molecular weight and PDI evolution with conversion for the polymerisation of long chain alkyl methacrylate / methyl methacrylate copolymer using RAFT agent 3, targeting 10,600 g.mol^{-1}. 30% of the monomer mixture was present in the reactor at the beginning of the reaction, with the rest fed into the reactor at 0.3 mL/min once the initial monomer present had reached 80% conversion. The red line shows the best fit of the data with linear equation shown below.

The PDI of the resultant polymer was lower than the either of the previous experiments; the PDI decreased from 1.3 to 1.2 over the course of the reaction, figure 62. The molecular weight growth with conversion was consistent with that of a RAFT mechanism, however, the polymer formed at very low conversion was still higher than expected; estimated to be around 5,100 g.mol^{-1}.

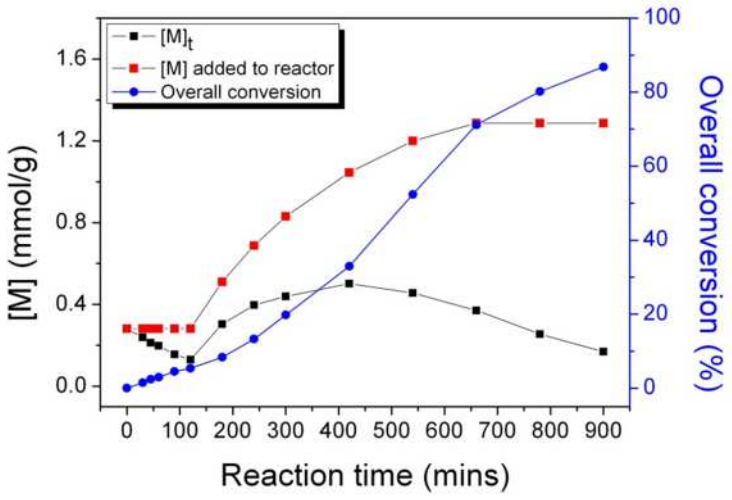

Figure 63: Plot showing the evolution of monomer concentration in the reactor, [M], with time when 10% of monomer is introduced at the beginning of the reaction, and the remaining 90% is fed at 0.3mL/min from 120 minutes. Also shown is the concentration of monomer [M] added to the reactor and the overall conversion of the monomer.

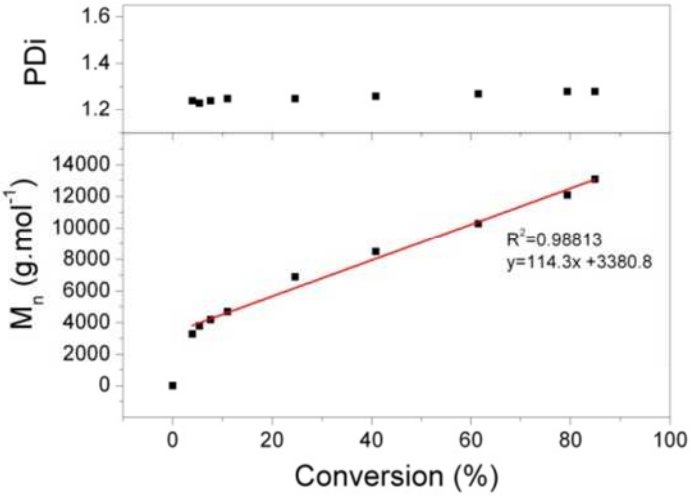

Figure 64: Molecular weight and PDI evolution with conversion for the polymerisation of $C_{12\text{-}15}$MA / MMA copolymer using RAFT agent 3, targeting 10,600 g.mol^{-1}. 10% of the monomer mixture was present in the reactor at the beginning of the reaction, with the rest fed into the reactor at 0.3 mL/min once the initial monomer present had reached 80% conversion. The red line shows the best fit of the data with linear equation shown below.

The amount of monomer in the reactor at the beginning of the reaction was reduced to 10% of the overall monomer mixture. This facilitated the synthesis of polymers exceeding the target molecular weight with PDI of approximately 1.2. The polymer formed very early in the reaction was seen to be low molecular weight, approximately 3,400 g.mol^{-1}.

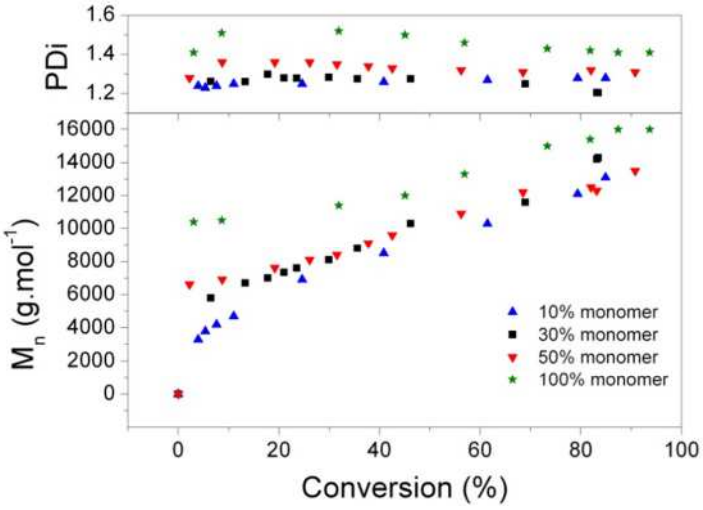

Figure 65: Change in molecular weight growth and PDI with conversion of monomer for a series of reactions containing various amounts of monomer at the beginning of the reaction. The remaining monomer was fed into the reactor at 0.03 mL/min after 80% of the initial monomer was consumed.

Comparing the data from these polymers, figure 65, it is seen that decreasing the amount of monomer in the reactor at the beginning of the polymerisation enabled greater control and led to low PDI polymer. The molecular weight of the polymer formed at the end of the reaction was consistently higher than the targeted 10,600 g.mol^{-1}. Therefore the RAFT agent efficiency, f_{RAFT}, is calculated by GPC to be 10,600/15,000 = 0.67.

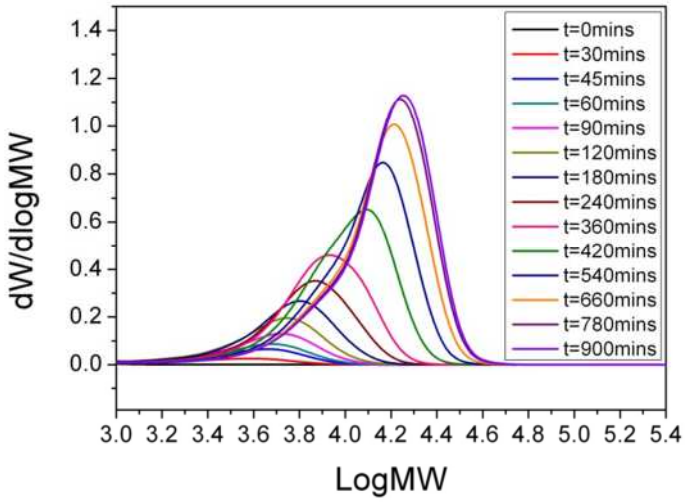

Figure 66: Evolution of the MWD during the polymerisation of $C_{12\text{-}15}$MA / MMA copolymer using RAFT agent 3, targeting 10,600 g.mol^{-1}. 10% of the monomer mixture was present in the reactor at the beginning of the reaction, with the rest fed into the reactor at 0.3 mL/min once the initial monomer present had reached 80% conversion.

Although the PDI of the polymer is significantly lower for the polymerisation where only 10% of the monomer is present at t = 0 mins, the MWD shows a low molecular weight tail indicative of termination occurring throughout the reaction, figure 66. Importantly for this project, the decrease in PDI is indicative of less termination and should increase the RAFT end group retention. Greater end group retention allows chain extension of these arm polymers with a crosslinker, thereby increasing arm incorporation.

Table 12: Summary of macro-RAFT agents formed using batch and feed processes in mineral oil to be used in star formation.

Reaction ID	$[RAFT]_0/[Monomer]_0$	% of total monomer in reactor at t=0	Rate of feed ($mL.min^{-1}$)	Final Conversion (%)	M_n ($g.mol^{-1}$)	PDI
Macro-RAFT1	0.020	100	0.03	93.6	15600	1.65
Macro-RAFT2	0.040	50	0.03	90.8	13500	1.31
Macro-RAFT3	0.067	30	0.03	83.4	14300	1.21
Macro-RAFT4	0.200	10	0.03	86.8	13,000	1.25

In summary, four distinct polymers were synthesised using the same reagents, by altering only the ratio of $[RAFT]_0/[monomer]_0$ by changing the amount of [monomer] in the reactor at the beginning of the reaction. The remaining monomer was fed into the reactor at 0.03 $mL.min^{-1}$ and the polymerisation terminated by cooling when high conversion (> 80%) was reached.

4.2.1.4Arm incorporation into star (yield)

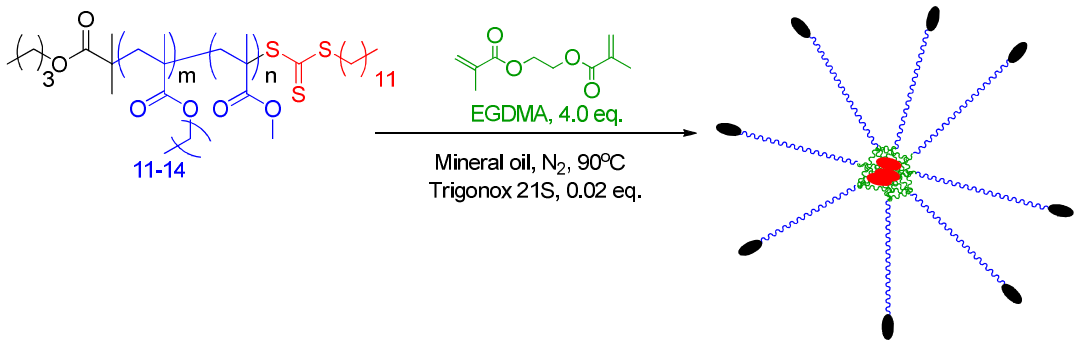

Scheme 20: Reaction of oil soluble macro-RAFT agent with crosslinker 1 to form star polymers

The optimised polymer arms with narrow PDI (**Macro-RAFT 4**) were crosslinked using a ratio of [**crosslinker 1] /** [**RAFT agent 3]** of 4, which was seen to be the optimal ratio in the MMA system, chapter 3. A small amount of peroxide initiator, t-butyl peroxy-2-ethylhexanoate, was added to the system to generate radicals to initiate the RAFT mechanism, scheme 20.

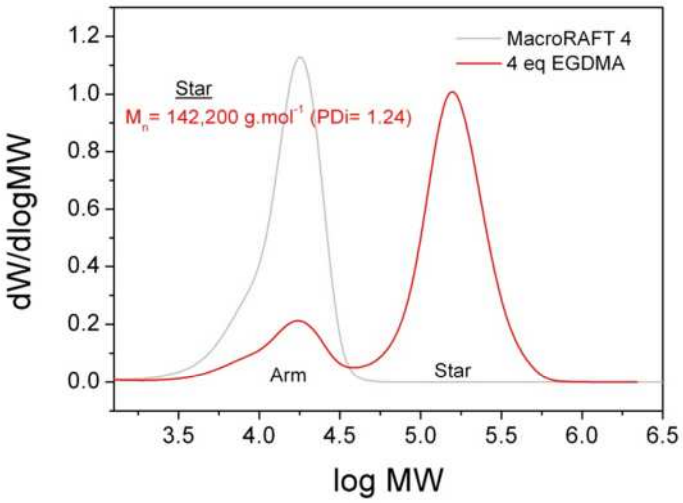

Figure 67: GPC spectra of macro-RAFT agent (arm) and after reaction for 3 hours at 90 ^{o}C with 4 equivalents of crosslinker 1 in the presence of Trigonox 21S radical initiator.

The deoxygenated solution was reacted for 3 hours at 90 ^{o}C, after which the resultant polymer was analysed by GPC and ^{1}H NMR. By GPC, the star polymer at low retention time was seen to have a narrow PDI (1.24) and a significantly higher M_n than the arm polymer (142,200 g.mol^{-1}), figure 67. De-convolution of the GPC chromatogram showed the arm incorporation into the star structure to be 81%. The 19% unincorporated arms could be due to termination leading to dead chains, in which case the arm synthesis needs to be improved further to minimise the number of dead arms. Otherwise, the crosslinking reaction needs to be investigated. The presence of the RAFT end group on

the polymer arm allows chain extension and is required for star formation by the core-crosslinking technique.

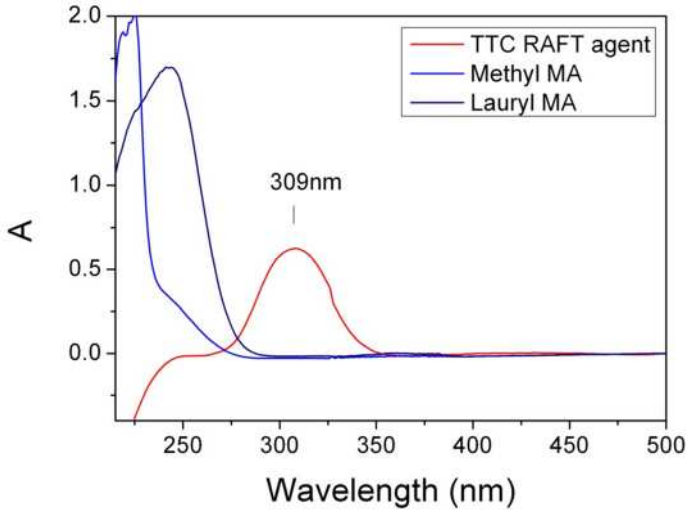

Figure 68: UV spectra of MMA, $C_{12\text{-}15}$MA and RAFT agent 3 in THF

It is possible to monitor the presence of the RAFT end group due to a characteristic absorption of light with a λ_{max} at 309 nm, figure 68. The absorption of the monomers were analysed using a UV spectrometer to see that the absorption was unique to the **RAFT agent 3** in this system, figure 68.

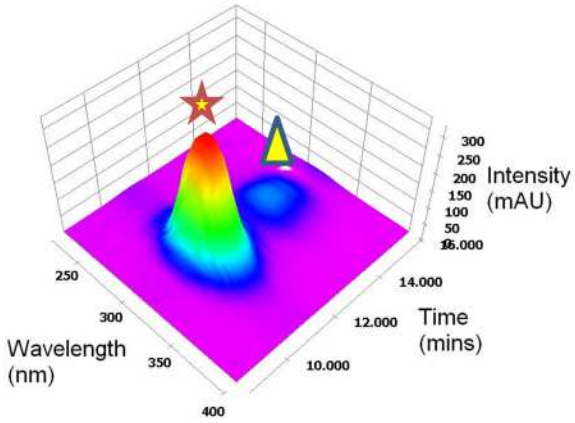

Figure 69: UV spectrum from photodiode array connected in series on the GPC detector train. Wavelength against retention time against intensity. (star) marks the star polymer. (triangle) marks the linear arm.

Analysis of the polymer using a photodiode array (PDA) detector in-line on the detector train of a THF GPC allows the UV absorption of an analyte to be investigated as it elutes from the GPC. The polymer formed after reaction of **Macro-RAFT 4** for 3 hours at 90 ^{o}C with 4 equivalents of crosslinker 1 in the presence of Trigonox 21S as a radical source was analysed to show the UV absorption of the polymer over its MWD. The polymer at low retention time (volume) correlating to high molecular weight star polymer shows a large absorption of UV light with a λ_{max} = 309 nm, figure 69.

4.2.1.5 Optimising the crosslinking reaction

The presence of small amounts of UV absorption at 309 nm at the low molecular higher retention volume on the GPC indicates that the limitation of arm incorporation is not due to the arm synthesis, but due to limitations in the crosslinking reaction. Therefore further investigations were carried out to determine which parameters are limiting the star formation. The star polymers formed in this study are summarised, table 13, and then discussed further below.

Table 13: Summary of oil soluble star polymers synthesised using macro-RAFT4.

Reaction ID	[macro-RAFT4] / [crosslinker]	Reaction time	2nd addition of crosslinker	2nd addition of initiator	3rd addition of crosslinker	3rd addition of initiator	M_n (g.mol^{-1})	PDI	Arm incorporation (%)
OilStar1	4	3	-	-	-	-	142200	1.24	81
OilStar2	4	6	-	-	-	-	136800	1.23	80
OilStar3	4	17	-	-	-	-	140700	1.23	79
OilStar4	5	3	-	-	-	-	Gel	Gel	Gel
OilStar5	4.5	3	-	-	-	-	158400	1.25	81
OilStar6	4.5	6	-	-	-	-	154900	1.24	81
OilStar7	4.5	17	-	-	-	-	158400	1.24	80
OilStar8	4.5	17+3	-	0.1	-	-	142800	1.24	81
OilStar9	4.5	17+3	0.5	0.1	-	-	208100	1.31	83
OilStar10	4.5	17+3+3	0.5	0.1	0.5	0.1	261300	1.31	83

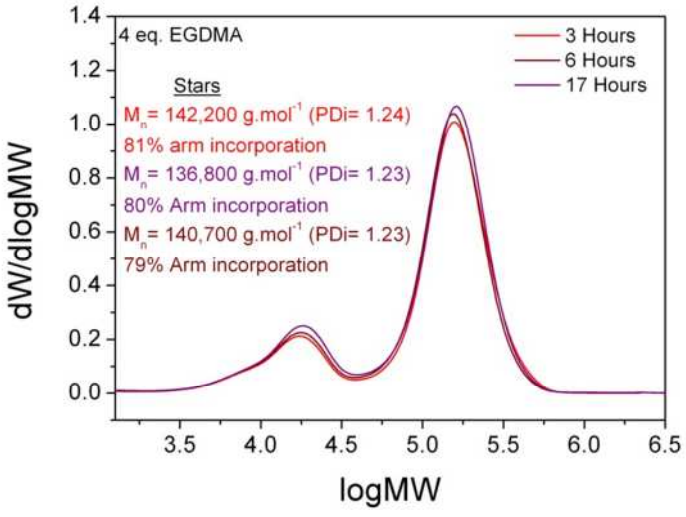

Figure 70: OilStar1, 2 and 3: GPC chromatograms of star polymers formed after reaction of macro-RAFT4 with 4 equivalents of crosslinker 1 for varying reaction times.

The star polymer formation was left for different reaction times of 3 hours, 6 hours and 17 hours. The radical source, Trigonox 21S, has a 1 hour half-life at 91 ^{o}C in chlorobenzene. Assuming a similar k_d and hence $t_{1/2}$ for mineral oil, this suggests that nearly 90% of the initiator is consumed in the 3 hour reaction time. The RAFT mechanism needs continued radical generation therefore it was hypothesised that star formation or star-star coupling shouldn't occur with longer reaction times. The reaction time was seen to have very little effect on the resultant star polymer. Reactions of 3 hours, 6 hours and 17 hours all yielded stars of around 140 kg.mol^{-1}, PDI = ca. 1.23, and star yield = ca. 80%, figure 70.

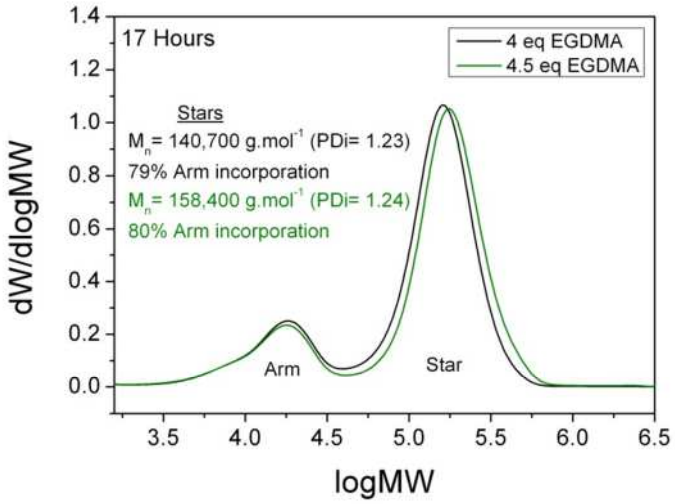

Figure 71: Comparison of OilStar3 and 7 - GPC of star polymers formed after reaction of macro-RAFT4 with 4 equivalents of crosslinker 1 and 4.5 equivalents of crosslinker 1.

The arm incorporation was not seen to increase with reaction time, therefore the reaction was repeated using a ratio of [**crosslinker 1**] / [**RAFT agent 3**] of 4.5. The resultant star polymer after 3 hours of reaction at 90 ^{o}C was over 10% larger than that made with a ratio of 4, at 158 kg.mol^{-1}. The arm incorporation into star remained unchanged though, figure 71.

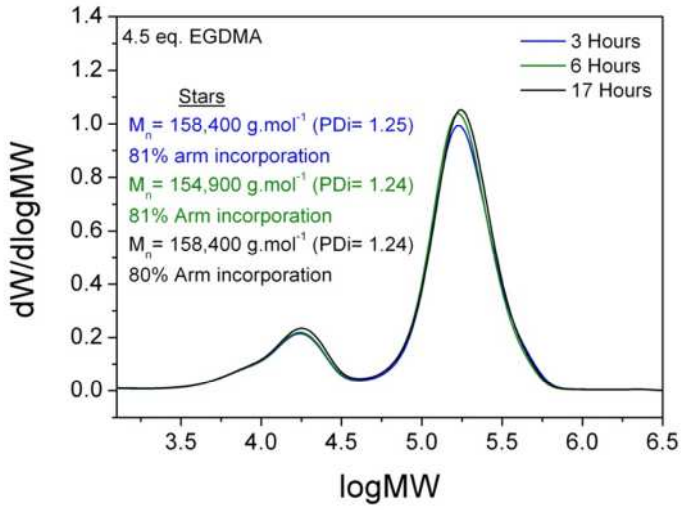

Figure 72: OilStar5, 6 and 7 - GPC of star polymers formed after reaction of macro-RAFT4 with 4.5 equivalents of crosslinker 1 relative to RAFT agent for varying reaction times.

As with the reactions with 4 equivalents of **crosslinker 1** compared with **RAFT agent 3**, the longer reaction times were seen to have little effect on the star polymer formation when 4.5 equivalents was used, figure 72.

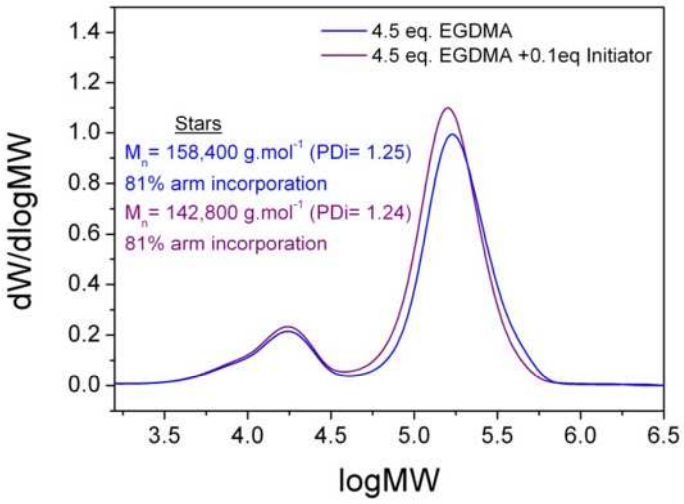

Figure 73: OilStar7 and 8 - GPC of star polymers formed after reaction of macro-RAFT4 with 4.5 equivalents of crosslinker 1 relative to RAFT agent for 17 hours. Overlaid with the polymer resulting from 2nd addition of initiator added after 17 hours and reacted for 3 hours.

It was hypothesised that the reaction time may not influence the star structure due to depletion of the radical source. Introducing 0.1 equivalents more Trigonox 21S after 3 hours of reaction, and leaving to react for a further 3 hours, led to no significant change in the yield of the resultant star polymer, figure 73. The molecular weight calculated by conventional GPC is reduced after further reaction with extra peroxide radical; this could be due to a contraction in the core.

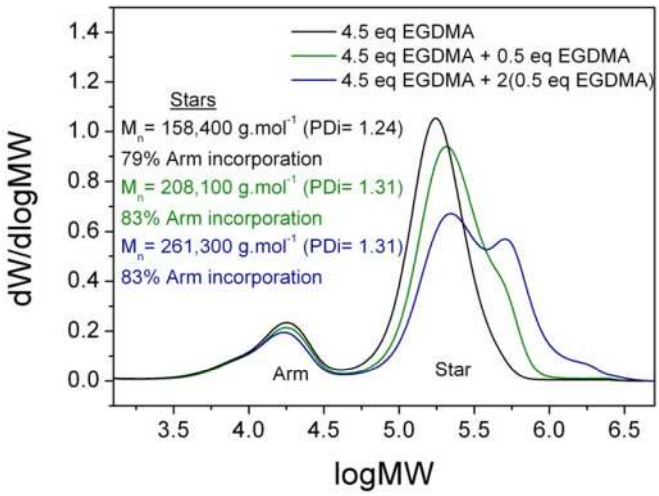

Figure 74: OilStar7, 9 and 10 - GPC of star polymers formed after reaction of macro-RAFT4 with 4.5 equivalents of crosslinker 1 relative to macro-RAFT4 for 17hours. Overlaid are the star polymers resulting after reaction with additional crosslinker1 and initiator after 17 hours, and further crosslinker1 and initiator after 20 hours.

The arm incorporation was not seen to increase with reaction time, or introduction of initiator therefore the reaction was repeated using a ratio of [**crosslinker 1**] / [**RAFT agent 3**] of 4.5. The repeat reaction showed very similar star polymer was formed after 3 hours reaction to the previous run, evidence of good reproducibility. To promote greater incorporation of arms into the star polymer, a further 0.5 equivalents of **crosslinker 1** and 0.1 equivalents of Trigonox 21S relative to [**RAFT agent 3**] at t=0. After 3 hours reaction the polymer was reanalysed by GPC showing a shift to higher molecular weight; the M_n of the star polymer was determined by conventional GPC to

be 208 kg.mol^{-1}. The PDI of the polymer formed was 1.31, an increase due to a high molecular weight shoulder on the MWD, figure 74. Further still, another addition of 0.5 equivalents of **crosslinker 1** and 0.1 equivalents of Trigonox 21S relative to [**RAFT agent 3**] at t=0 to the reactor was seen to increase the molecular weight further and saw a large increase in the relative size of the high molecular weight shoulder indicating significant amounts of star-star coupling, figure 74.

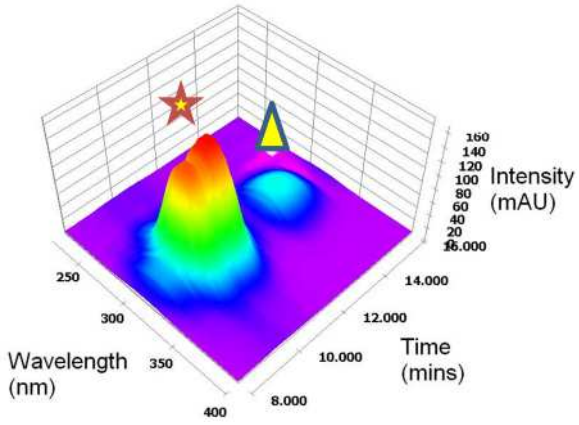

Figure 75: Oilstar10 - UV spectrum from PDA connected in series on the GPC detector train. Wavelength against retention time against intensity.

The high molecular weight star-star coupled polymer was seen to have a high UV absorbance at approximately 309 nm, indicating the presence of RAFT agent on the chain ends of the arms in the star. There was also an absorbance at the same wavelength at higher retention times corresponding to the molecular weight of the arm polymer, figure 75. This suggests that the arms are still active and therefore star-star coupling preferentially occurs over incorporation of the arms into the star.

4.3 Conclusions

RAFT co-polymerisation of $C_{12\text{-}15}$MA and MMA, using a C_{12}-trithio-butyl acrylate RAFT agent, **RAFT agent 3**, showed hybrid RAFT-FRP behaviour. The molecular weight can be targeted using the ratio of [RAFT agent] to [monomer]; however, relatively polydisperse polymers were produced.

Further reaction of the formed macro-RAFT agents with **crosslinkers 1, 2** and **3** showed chain extension and some star formation. Analysis of the stars by GPC showed that the crosslinker efficiency decreases with the series: **crosslinker 1** > **crosslinker 2** > **crosslinker 3**. This suggests that increasing the length of the ethylene glycol moieties separating the vinyl groups is detrimental to star formation. This could be due to cyclisation, and possibly suggests some form of phase separation or partial solubility. TEGDMA, **crosslinker 3**, yields no star polymer, and the increase in molecular weight can be accounted for by the addition of crosslinker, but without crosslinking. Analysis by ^{1}H NMR does <u>not</u> show evidence of unreacted pendent vinyl peaks. This supports the hypothesis of Sawamoto *et al*., that TEGDMA undergoes intramolecular cyclisation.[140]

As **RAFT agent 3** was seen to be working like a conventional CTA in the early stages of the polymerisation, it was possible to calculate a chain transfer constant, C_s, value for **RAFT agent 3** in the polymerisation of $C_{12\text{-}15}$MA and MMA. The C_s was calculated to be <1, which implies that $k_{tr} < k_p$.

By increasing the ratio of **RAFT agent 3** to monomer at the beginning of the reaction, with the remaining monomer fed into the reactor afterwards, it was seen that the PDI of the macro-RAFT agents can be decreased from 1.5 to 1.2.

Stars formed using the narrow PDI macro-RAFT agents were seen to produce stars of narrow PDI with high arm incorporation. Increasing reaction time or amount of crosslinker was seen to have a small increase in molecular weight of star polymer formed, but did not increase the percentage arm incorporation. Reaction of the star with further crosslinker was seen to preferentially form star-star coupling over incorporation of further arms. UV GPC analysis of the unreacted arms shows evidence of the RAFT end group's presence in the polymer. This suggests that the crosslinking reaction is still the limiting factor in increasing the arm incorporation, and it is not due to termination during the RAFT arm polymerisation. Using more crosslinker in star formation is seen to form larger stars, but does not increase arm incorporation into the star.

4.4 Experimental

4.4.1 Instrumentation

GPC was used to determine the molecular weight averages and the PDI of polymers using one of two systems. System 1, with a 390-LC Polymer Laboratories system equipped with a PL-AS RT/MT autosampler, a PL- gel 3 µm (50 × 7.5 mm) guard column, two PL-gel 5 µm (300 × 7.5 mm) mixed-D columns (suitable for separations up to MW = 2.0×10^6 g.mol^{-1}), a differential refractometer, 4 capillary viscometer and MALLS were used. Solvent used was chloroform / triethylamine 95 : 5 (v/v) as the eluent with a flow rate of 1.0 mL.min^{-1}, unless otherwise stated. System 2 with a 390-LC Polymer Laboratories system equipped with a PL-AS RT/MT autosampler, a PL- gel 3 µm (50 × 7.5 mm) guard column, two PL-gel 5 µm (300 × 7.5 mm) mixed-D columns (suitable for separations up to MW = 2.0×10^6 g.mol^{-1}), a differential refractometer, MALLS, and a photodiode array were used. Solvent used was tetrahydrofuran / triethylamine 95 : 5 (v/v) as the eluent with a flow rate of 1.0 mL.min^{-1}, unless otherwise stated. Narrow molecular weight PMMA standards (1.0×10^6 g.mol^{-1}) were used for calibration.

All ^{1}H and ^{13}C NMR spectra were recorded on Bruker DPX300, Bruker DPX400 and Bruker DRX500 spectrometers as solutions in deuterated NMR solvents. Chemical shifts are cited as parts per million (ppm). The following abbreviations are used to abbreviate multiplicities; s = singlet, d = doublet, t = triplet, q = quartet, m = multiplet.

FT-IR was recorded on a VECTOR-22 Bruker spectrometer using a Golden Gate diamond attenuated total reflection cell.

4.4.2 General method for calculating the percentage arm incorporation into stars when using an arm-first approach.

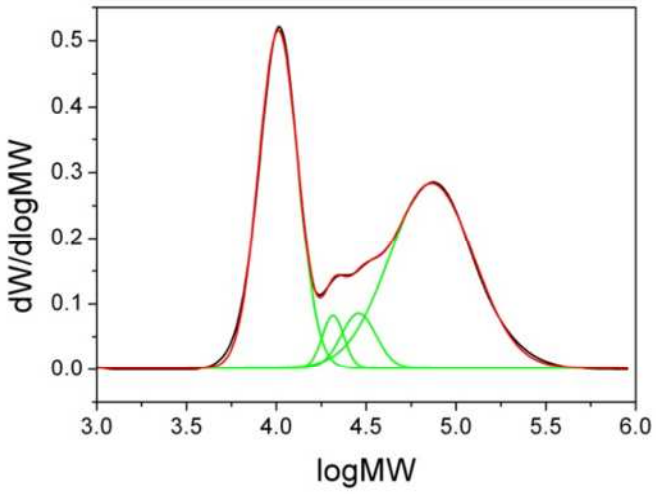

Figure 76: (Black) Core-crosslinked star polymer MWD. (Green) 4 Gaussian curves calculated by Microcal Origin 8.0. (Red) Sum of the Gaussian curves.

In the case of overlapping peaks, the amount of arm incorporation into star was calculated by deconvolution of multimodal GPC traces using MicroOrigin Origin 8.5.1 (figure 76) The M_n, M_w and PDI of the component Gaussian distributions could be calculated along with the area of under the curve.

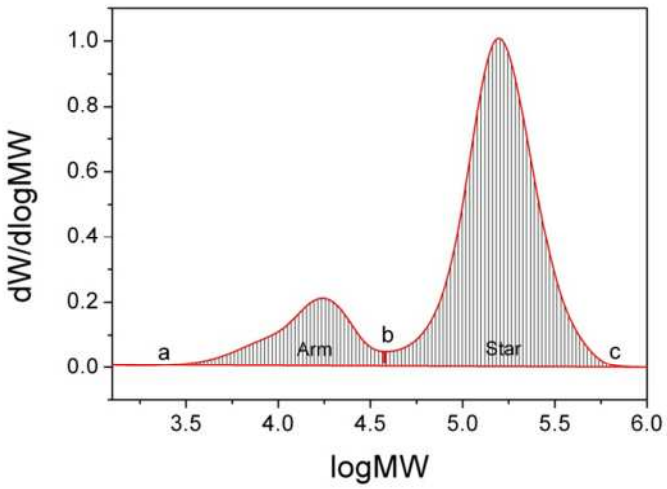

Figure 77: Example of a core-crosslinked star polymer MW, with the boundaries of the different polymer species marked a, b and c.

When the peaks are completely separated they are analysed separately, and the arm incorporation is determined using the equation:

$$\% = \frac{\int_c^b f_{GPC}}{\int_c^a f_{GPC}} . 100 \qquad (1.1)$$

Where

a,b, and c are exemplified in figure 77

f_{GPC} is the function of dW/dlogMW with logMW from the GPC chromatogram.

4.4.3 Materials

All materials were purchased from Sigma Aldrich at the highest available quality and used without further purification, unless otherwise stated.

The initiator 2,2,-azobisisobutyronitrile (AIBN) was re-crystallised from methanol before use. Methyl methacrylate, ethylene glycol dimethacrylate, di(ethylene glycol)

dimethacrylate and tri(ethylene glycol) dimethacrylate were de-inhibited by passing through an activated neutral aluminium oxide column prior to use. Long chain alkyl methacrylate, Trigonox 21S and **RAFT agent 3** were supplied by the Lubrizol Corporation, and used as received.

4.4.4 General procedure for arm-first star poly(C12-15MA-co-MMA) synthesis (batch reactions in toluene)

RAFT agent 3 (0.33 g, 0.78 mmols, 1 eq) and t-butyl peroxy-2-ethylhexanoate (0.055 g, 0.25 mmols, 0.32 eqs) were dissolved in toluene (5.4 mL) and added to a Schlenk tube containing MMA (1.67 g, 16.7 mmols, 21 eqs) and $C_{12\text{-}15}$MA (6.67 g, 24.3 mmols, 31 eqs) and toluene (10 mL). Mesitylene (2.00 g, 16.6 mmols, 20 eqs) was added as an ^{1}H NMR standard, and the reaction mixture was purged with nitrogen for 10 minutes. The reaction was initiated by heating in an oil bath (75 ^{o}C) and monitored by ^{1}H NMR and GPC. After reaction for 5 hours, degassed crosslinker was injected into the reaction and the system placed into an oil bath (90 ^{o}C). The reaction was monitored for a further 90-120 minutes, before being terminated by bubbling with air, and cooling in an ice bath.

4.4.5 General procedure for copolymerisation of C12-15MA and MMA (Bulk reaction in mineral oil)

RAFT agent 3 (0.510 g, 1.21 mmols, 1 eq) and t-butyl peroxy-2-ethylhexanoate (0.052 g, 0.242 mmols, 0.2 eqs) were dissolved in mineral oil (9.51 mL) and added to a reactor containing MMA (2.43 g, 24.2 mmols, 20 eqs) and $C_{12\text{-}15}$MA (10.00 g, 36.4 mmols, 30 eqs). Mesitylene (2.91 g, 24.2 mmols, 20 eqs) was added as an internal NMR standard,

and the reaction mixture was purged with nitrogen for 50 minutes. The reaction was initiated by heating in an oil bath (75 ^{o}C) and monitored by ^{1}H NMR and GPC. The reaction was taken to high conversion (> 80%) before being terminated by bubbling with air for 10 minutes, and cooling in an ice bath.

4.4.6 General procedure for copolymerisation of C12-15MA and MMA (Monomer feed reaction in mineral oil)

RAFT agent 3 (0.510 g, 1.21 mmols, 1eq) and t-butyl peroxy-2-ethylhexanoate (0.052 g, 0.242 mmols, 0.2 eqs) were dissolved in mineral oil (9.51 mL) and added to a stirred reactor. Methyl methacrylate (2.43 g, 24.2 mmols, 20 eqs), $C_{12\text{-}15}$ methacrylate (10.00 g, 36.4 mmols, 30 eqs) and Inert mesitylene (2.91 g, 24.2 mmols, 20 eqs) were purged with nitrogen for 15 minutes. A percentage of the oxygen free monomer mixture was transferred to the reactor, which was then purged with nitrogen for a further 15 minutes. The reaction was initiated by heating in an oil bath (75 ^{o}C) and monitored by ^{1}H NMR and GPC. At high monomer conversion (> 80%) the remaining deoxygenated monomer was fed into the reactor using a syringe pump at a rate of 0.03 mL/min. The reaction was monitored regularly and terminated at high overall monomer conversion, by bubbling with air for 10 minutes and cooling in an ice bath.

4.4.7 General procedure for arm-first star poly(C12-15MA-co-MMA) synthesis (Using Macro-RAFT agents)

An aliquot (10% of reaction mixture) of **macro-RAFT 4** (0.121 mmols) was placed into a reactor equipped with a stirrer bar. *Tert*-butyl peroxy-2-ethylhexanoate (0.0052 g,

0.0242 mmol, 0.2 eqs) and **crosslinker 1** (0.096 g, 0.485 mmol, 4 eq) were added to the reactor. The reaction mixture was purged by nitrogen gas for 15 minutes to remove oxygen and the reaction was started by heating in an oil bath (90 ^{o}C). After 3 hours the reaction was terminated by bubbling with oxygen and cooling in an ice bath, and analysed by ^{1}H NMR and GPC.

4.5 References

(93) Chong, Y. K.; Le, T. P. T.; Moad, G.; Rizzardo, E.; Thang, S. H. *Macromolecules* **1999**, *32*, 2071.

(140) Baek, K.-Y.; Kamigaito, M.; Sawamoto, M. *Macromolecules* **2001**, *34*, 215.

(141) Baek, K.-Y.; Kamigaito, M.; Sawamoto, M. *J. Polym. Sci., Part A: Polym. Chem.* **2002**, *40*, 2245.

(166) Newton, I. *The mathematical principles of natural philosophy*; Printed for Benjamin Motte: London, 1729.

(167) Selby, T. W. *A S L E Transactions* **1958**, *1*, 68.

(168) Dean, E. W.; Davis, G. H. B. *Chem Metall Eng* **1929**, *36*, 618.

(169) Lindhe, C. *Anal. Chem.* **1969**, *41*, 1463.

(170) Schober, B. J.; Vickerman, R. J.; Lee, O.-D.; Dimitrakis, W. J.; Gajanayake, A. In *Fuels & Lubes Asia* F&L Asia, Inc.: Seoul, Korea, 2008, p 1.

(171) Bueche, F. *J. Appl. Polym. Sci.* **1960**, *4*, 101.

(172) Buchholz, B. A.; Zahn, J. M.; Kenward, M.; Slater, G. W.; Barron, A. E. *Polymer* **2004**, *45*, 1223.

(173) Xue, L.; Agarwal, U. S.; Lemstra, P. J. *Macromolecules* **2005**, *38*, 8825.

(174) Odell, J. A.; Keller, A. *J. Polym. Sci., Part B: Polym. Phys.* **1986**, *24*, 1889.

(175) Callais, P.; Schmidt, S.; Macy, N. In *Powertrain & Fluid Systems Conference & Exhibition*; SAE: Tampa, FL, USA, 2004.

(176) Gao, H.; Min, K.; Matyjaszewski, K. *Macromolecules* **2009**.

(177) Skey, J.; O'Reilly, R. K. *Chem. Commun.* **2008**, 4183.

(178) Barner-Kowollik, C.; Quinn, J. F.; Nguyen, T. L. U.; Heuts, J. P. A.; Davis, T. P. *Macromolecules* **2001**, *34*, 7849.

(179) Pietsch, C.; Fijten, M. W. M.; Lambermont-Thijs, H. M. L.; Hoogenboom, R.; Schubert, U. S. *J. Polym. Sci., Part A: Polym. Chem.* **2009**, *47*, 2811.

(180) Moad, G.; Moad, C. L. *Macromolecules* **1996**, *29*, 7727.

(181) Heuts, J. P. A.; Kukulj, D.; Forster, D. J.; Davis, T. P. *Macromolecules* **1998**, *31*, 2894.

(182) Heuts, J. P. A.; Davis, T. P.; Russell, G. T. *Macromolecules* **1999**, *32*, 6019.

Chapter 5

Towards multi-arm star glycopolymers using a combination of RAFT and "click" chemistry

The work described in this chapter was started with the aim of synthesising water soluble sugar bearing multi-arm star polymers using the core-crosslinking technique applied in earlier work.

A review of the synthesis of glycopolymers in literature using controlled polymerisation techniques "click" reactions provides a background to the work presented.

A protected alkyne monomer has been synthesised and polymerised to varying chain lengths using RAFT polymerisation. These have been used as scaffolds for post polymerisation modification. Thio sugars and sugar azides have been synthesised and with the use of CuAAC and thiol-yne chemistry sugar bearing polymers have been synthesised.

Star glycopolymers have been synthesised through the crosslinking of a protected propargyl methacrylate macroRAFT agent. Using **crosslinker 10,** an "exploding" star glycopolymer has been synthesised that "explodes" in the presence of a reducing agent.

5.1 Introduction

Synthetic carbohydrate-containing macromolecules or *glycopolymers* have attracted increasing attention in various fields of science with particular interest to the biological sciences due to their excellent recognition properties.[183-185] Advances in synthetic chemistry have allowed for the preparation of well-defined and multi-functional glycopolymers in a relatively facile manner.[29,186] Carbohydrate units critically control the specific biological functions of cells and also play an important role in cell-cell recognition.[187,188] It is desirable to be able to control the chain length, composition and topology of glycopolymers since these factors determine the location and distance between the carbohydrates on the polymer chain.[189,190] Importantly, precise recognition properties can be achieved by an absolute control over the microstructure of the glycopolymer.

The synthesis of glycopolymers became popular in the 1990s with an effort towards biomimics, and most of the attempts were based on the polymerisation of monomers containing carbohydrate moieties.[191-194] These glycomonomers (sugar carrying monomers) were reported to be polymerised by free radical, controlled radical, anionic, cationic, ring opening and ring opening metathesis polymerisation (ROMP) techniques.[29,192,195,196] Until the last decade, there had been limited attempts to react functional polymeric backbones with a carbohydrate to obtain glycopolymers. A significant reason for this was the difficulty of introducing sufficiently reactive pendant groups onto the polymer backbone to react with carbohydrates. One successful attempt involved the modification of poly(vinyl alcohol) with 4-nitrophenyl carbonate groups to yield a reactive polymer backbone. The reactive nitrophenyl carbonate groups were transformed with glucosamine into glycopolymers, which were

subsequently investigated for their interaction with a commonly used plant lectin, Concanavalin A (Con A).[197]

Carbohydrates with various functionalities can be incorporated into polymers either by reacting onto a polymeric backbone or by polymerising preformed glycomonomers. Indeed, even with glycomonomer synthesis various click reactions have been recently utilised offering facile routes to glycomonomers. Moreover, sugars with azide, alkyne, and thiol groups have been reported for their use in the synthesis of glycopolymers *via* click reactions. Selected examples for the various combinations of click reactions and polymerisation techniques that are used to prepare glycopolymers are listed in table 14.

Table 14: Selected examples on different combinations of click reactions and polymerisation techniques to synthesise glycopolymers.

Click reaction	Polymerisation method	Backbone	Saccharide	Ref.
CuAAC	ATRP	Methacrylate	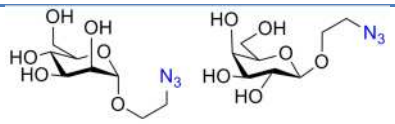	198
CuAAC	ATRP	Methacrylate	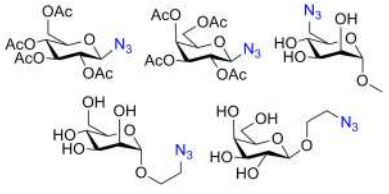	34
CuAAC	ATRP	Methacrylate	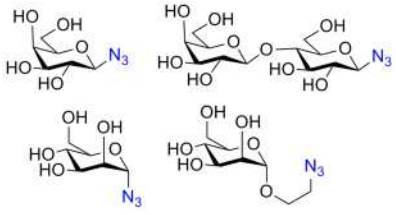	199

CuAAC	RAFT	Acrylate/Methacrylate	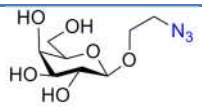	31
CuAAC	RAFT	4-Vinyl-1,2,3-triazole	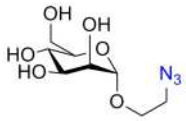	200
CuAAC	ROP	ε-Caprolactone	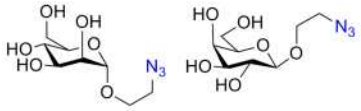	201
CuAAC	CCTP (Cobalt)	Methacrylate	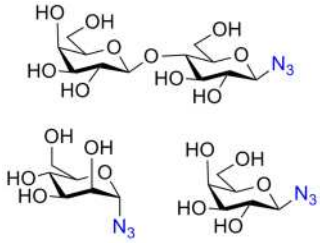	202
***p*-fluoro-thiol**	NMP	Pentafluorostyrene		203
Thiol-ene	Cationic	*N*-Acylalkyleneimine	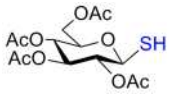	204
Thio-halogen	RAFT	Styrene		205
Thiol-ene	RAFT	Acrylate/Methacrylate	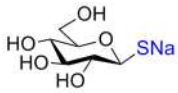	206
Thiol-yne	RAFT	Acrylate/Methacrylate		206
Thiol-ene	ROP	Ester	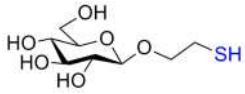	207

Some selected examples are shown here where clickable sugars are used either to synthesise glycomonomers, which lead to glycopolymers, or to directly click onto a polymeric backbone. The combination of different polymerisation techniques (*i.e.* FRP, RAFT, NMP, ATRP, cobalt catalysed chain transfer polymerisation (CCTP), and ROP) and selected click reactions are discussed.

5.1.1 Copper catalysed azide-alkyne cycloaddition (CuAAC)

The copper catalysed azide-alkyne cycloaddition (CuAAC) reaction has been influential in improving synthetic strategies in a range of subcategories including polymer chemistry, biochemistry, medicinal chemistry and surface chemistry. This has become increasingly popular due to advantages over other chemical transformations. The reaction is simple to perform, tolerates various conditions and functional groups, it is highly stereospecific and provides near quantitative conversions that eliminate purification steps.

The copper catalyst has a crucial role in the "click" process. Prior to copper reagents being used in the reaction, Huisgen and co-workers studied the azide-alkyne cycloaddition and realised that since organic azides are relatively reactive compounds, but also selective, they were able to undergo a dipolar cycloaddition reaction with alkynes and olefins.[208] However, this reaction is quite slow and results in a mixture of both 1,4- and 1,5- disubstituted 1,2,3-triazole regioisomers being formed with asymmetrically substituted alkynes. Meldal and Sharpless independently investigated and introduced copper reagents as a catalyst for this reaction which solved the previously mentioned problems associated with this reaction.[209,210] Through the use of a copper based catalyst, the reactions proceed faster at and below ambient temperature and with complete conversion to the 1,4-disubstituted 1,2,3-triazole product. An excellent tutorial review has been recently published by Fokin and Hein which provides extensive details into the CuAAC reaction and mechanism.[211] This type of click reaction has a major role in polymer chemistry since it provides a variety of new routes to synthesising glycopolymers.

Prior to the use of click chemistry the synthesis of sugar-monomers was hindered due to the number of synthetic steps necessary to protect functional groups and ensure

chemo- and stereoselectivity. The incorporation of the CuAAC process allows sugar monomers to be prepared with ease by the introduction of azide functionality. The original synthetic strategy first protects the hydroxyl groups on the sugar by acetylation, followed by the activation of the anomeric leaving group by a Lewis acid to selectively convert to a bromo group *via* a displacement.[212] The azide can then be introduced *via* nucleophilic substitution followed by deprotection to provide the sugar azide. It is now possible to carry out the azide functionalisation without the need to protect the hydroxyl groups *via* the use of a strong acid cation exchanger resin, simplifying the method further. Using these methods a variety of sugars have been functionalised with azides, which in conjunction with the CuAAC process broadens the synthetic scope of glycopolymers.[213] An additional facile method involves a one-pot direct synthesis of sugar azides reported by Shoda *et al.* with the reaction mediated by 2-chloro-1,3-dimethylimidazolinium chloride (DMC).[213] The reaction is carried out without any protection chemistry, since the DMC is able to directly activate the anomeric hydroxyl group, followed by intermolecular nucleophilic attack by the azide ion. The selectivity exists due to the lower pK_a value of the hemiacetal anomeric hydroxyl groups compared to that of the other hydroxyl groups present on the sugar. The aforementioned synthetic routes to sugar azides highlight the progress and ease of which sugar azides can be attained.

Transition metal mediated living radical polymerisation (TMM-LRP), also known as atom transfer radical polymerisation (ATRP), is a well established route to synthesise polymers which are well-defined with precise functionality.[214-217] Different functionalities can be introduced easily by taking advantage of the tolerance, which is given to functional groups by living radical polymerisation. By introducing functionality to the initiator this is then incorporated into the polymer chain with a simple linker

between the functional group and the initiator fragment to avoid any side reactions occurring during the polymerisation. The functionality remains intact on the α-chain end of the polymer. The chain length is controlled *via* rapid reversible deactivation of propagating radicals to keep their concentration low along with fast initiation to ensure all propagating species grow simultaneously. The deactivation of the propagating radicals is carried out by the copper(II) bromide-ligand complex.[218-220]

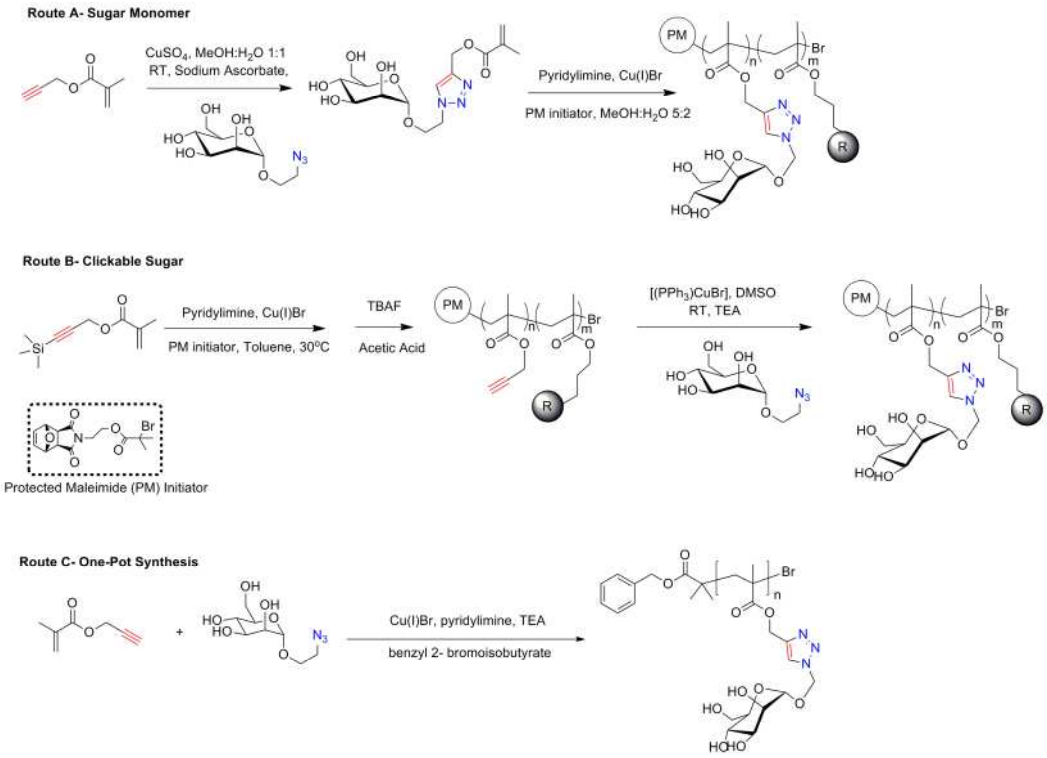

Scheme 21: Various synthetic routes to glycopolymers using ATRP and CuAAC employed by Haddleton et al.

Haddleton *et al.* reported a versatile synthetic strategy that generates a library of glycopolymers with exactly the same molar mass, PDI, and polymer architecture.[198] Moreover, a protected maleimide initiator was used that enables convenient conjugation to available thiol residues present in proteins after deprotection. These glycopolymers are suitable for probing interactions with mannose-binding lectin, whilst

omitting the effects of chain length or architecture. A combination of ATRP and CuAAC was implemented to create well-defined maleimide end-functionalised glycopolymers. One of the most attractive features of this work is the simplicity and efficiency in which a wide range of glycopolymers can be synthesised.

Three different synthetic strategies have been demonstrated to synthesise well defined glycopolymers, scheme 21. The first route (Route A) produces a sugar methacrylate monomer *via* CuAAC click reaction. This monomer is then polymerised by ATRP without the need to protect the hydroxyl groups present on the sugar molecule, which is typically required in glycopolymer synthesis.[221] Remarkably, the final step is to deprotect the maleimide end group can simply be carried out in a vacuum oven at 80 °C, avoiding the use of any organic solvents or further purification.

The second reported route to glycopolymers (Route B) reveals the advantages of using click chemistry. It involves the one step synthesis of a trimethylsilyl protected propargyl methacrylate (TMSPgMA). After polymerisation *via* ATRP, a deprotection step generates the reactive propargyl units providing a 'clickable' scaffold, onto which a variety of azide functional sugars can react. A final retro-Diels-Alder deprotection of the maleimide end-group was necessary for the polymer to undergo site specific conjugation to proteins. This synthetic route was optimised to ensure fewer steps were needed to synthesise sugar azides. In essence, it is possible to generate a library of polymers all containing the same macromolecular characteristics with the only difference being the sugar chosen to be 'clicked' onto the scaffold. Furthermore, Haddleton *et al.* successfully conjugated the glycopolymers onto bovine serum albumin (BSA) to create a glycoprotein mimic, which was shown to induce immunological behaviour *via* interaction with mannose binding lectin. Through the use of ATRP and

click chemistry a range of well defined functional glycopolymers were successfully synthesised and proven to show biological activity.

A third route has been investigated in which glycopolymers were synthesised *via* a one-pot process with simultaneous CuAAC and living radical polymerisation.[222] The mechanism for both of these processes is not yet fully understood, however, Haddleton *et al.* demonstrate that it is possible to have both reactions proceeding simultaneously in the same reaction mixture. Furthermore, by changing experimental conditions such as solvent, temperature and catalyst concentration it was possible to influence the rate of each process. This is an important feature of this work since any un-clicked alkyne groups may undergo side reactions *in situ* which would lead to a less controlled polymerisation. An additional advantage of this one-pot system is that there is no need to use sugar functional methacrylate monomers which can be prone to self-polymerise. This method is useful as it reduces the number of synthetic steps involved to make well defined glycopolymers.

Synthesis of chain end functional polymers with high fidelity has been challenging for polymer chemists. In the case of metal mediated living radical polymerisation, the polymer chain carries a terminal halide atom, which undergoes several activation-deactivation cycles. It should be noted that there is the possibility of side reactions in which loss of halide end groups leads to a loss of chain end fidelity.

Alternatively, CCTP is a versatile technique to produce ω–end functional polymers with a high chain end fidelity and controlled molecular weight. This technique benefits from the stability of the bis(boron difluorodimethylglyoximate) cobalt (II) (CoBF) catalyst in neutral aqueous media, allowing polymerisations of acidic monomers, which are unsuitable for anionic polymerisation. In anionic polymerisation these acidic monomers

would react rapidly with carbanions and eventually terminate the polymerisation. With monomers containing an α-methyl group termination and initiation occur principally by the chain transfer reaction from CoBF to the active centre. Thus products contain, invariably, an unsaturated end group. A vinyl terminated chain end allows facile modification of the polymer chain by a thiol-ene click reaction.

The combination of CCTP and click chemistry to synthesise glycopolymers has been recently reported by Haddleton *et al.,* in which a protected alkyne monomer is homopolymerised in the presence of CoBF and AIBN to yield protected alkyne polymers with vinyl end groups, scheme 22.[202] Various azide-sugars, *i.e.* mannose, galactose and cellobiose, were reacted with the alkyne groups of the glycopolymer after the removal of the deprotection groups. An attractive feature of this work is the ability of these polymers to undergo further functionalisation due to the ω-terminal vinyl group. It is well known that activated vinyl groups can undergo hetero-Michael reaction with thiols. This reaction has been termed as "base catalysed thiol-ene" click reaction since the process complies with the typical attributes of a click reaction. Moreover, the sugar azides can be clicked onto the polymer scaffold before or after the thiol-ene click chemistry has been performed. This allows a wide array of functionality to be introduced to the glycopolymers.

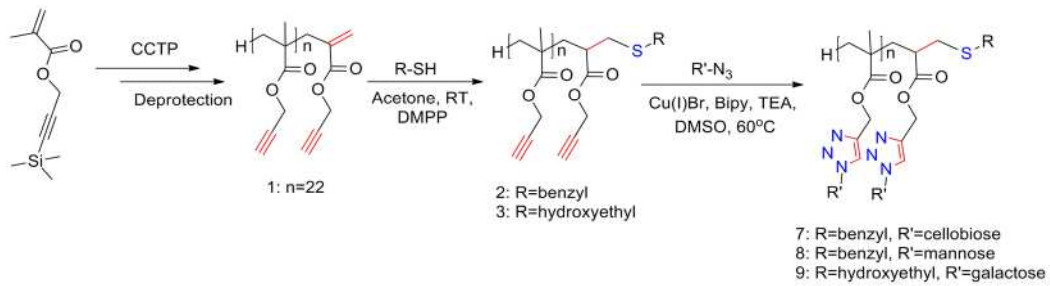

Scheme 22: The synthesis of glycopolymers via cobalt catalysed - catalytic chain transfer polymerisation and click reactions by Haddleton et al.

Ring opening polymerisation (ROP) gives access to a wider range of cyclic monomers which could not be polymerised by other techniques. This method of polymerisation is a chain polymerisation; however, the propagating rate constants are more akin to a step-growth polymerisation, making the molecular weight growth small in comparison to chain polymerisation of a monomer containing carbon-carbon double bonds. It is possible to control the molecular weight of polymers made *via* ring opening polymerisation due to its dependence on conversion and the ratio of monomer to initiator concentration.

Zi-Chen *et al.* demonstrated that amphiphilic biodegradable glycopolymers can be successfully synthesised *via* a combination of ROP and click chemistry.[223] In this paper, they synthesise a functional monomer, 2-bromo-ε-caprolactone, derived from successive modifications of cyclohexene. Addition to the alkene with *N*-bromosuccinimide was carried out to introduce bromine and alcohol functionalities. The alcohol group was initially converted to a ketone and subsequently to an ester *via* Baeyer-Villiger oxidation. The effort devoted to the synthesis and polymerisation of this type of monomer is worthwhile since the resulting glycopolymer is biodegradable. Block copolymerisation with poly(ε-caprolactone) macroinitiator is illustrated in scheme 23. Several more steps were required to introduce sugars and hence produce an amphiphilic block copolymer; involving the conversion of bromide groups to azides and then utilizing the CuAAC click reaction to attach alkyne functional sugars. Proof of aggregation as a result of interaction with lectin Con A was shown using atomic force microscopy (AFM) and transmission electron microscopy (TEM). When comparing with other synthetic routes to glycopolymers, the main drawback of this system is the time and effort required to produce a well-defined polymer. There is a great need to ensure all reactants are free from water and air to avoid deactivation of ionic initiators as well

as requiring relatively long reaction times and low temperatures due to the sensitivity of reactants. Nevertheless, it is a beneficial route to synthesise biodegradable glycopolymers, which could be of great importance in terms of biomaterial applications.

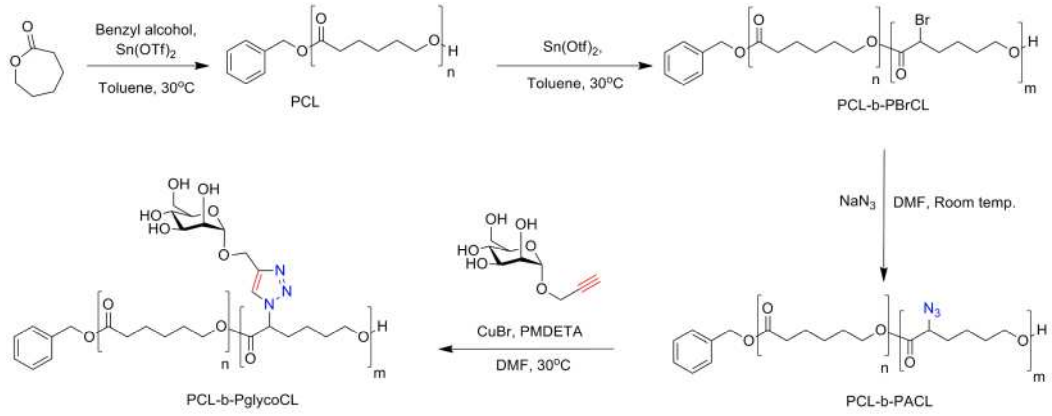

Scheme 23: The synthesis of glycopolymers via ROP of ε-caprolactone (CL) and 2-bromo-ε-caprolactone (BrCL) blocks, modification of the bromo moieties to azides, and CuAAC click.

RAFT polymerisation, used in a number of examples, is a well-established, versatile, route to the synthesis of well-defined polymer architectures.[16,224-226] In particular, it has been shown to be an effective route to hyperbranched polymers.[227-229] It provides control over the molecular weight, PDI and functionality and by changing the thiocarbonylthio chain transfer agent (RAFT agent), it is possible to polymerise a wide range of monomers. The RAFT agent has also been shown to be an effective route to introducing both α and ω functionality to polymers made by this technique.

Synthesis of RAFT agents with functionality on the re-initiating fragment allows the incorporation of α-functionality into a polymer. In addition, modification of the thiocarbonylthio RAFT end group can be used to easily introduce ω-functionality, summarised in a recent review by O'Reilly *et al.*[39] One issue which should be taken into

consideration is that the introduction of terminal functionality to polymers is usually no greater than 90% efficient; at the α terminus, this is due to initiation from the thermal initiator, whilst at the ω terminus termination during the reaction and loss of the RAFT agent end group can hinder complete end group modification. A review of many aspects of RAFT, including a comprehensive list of RAFT agents synthesised has been published by Moad and co-workers.[230]

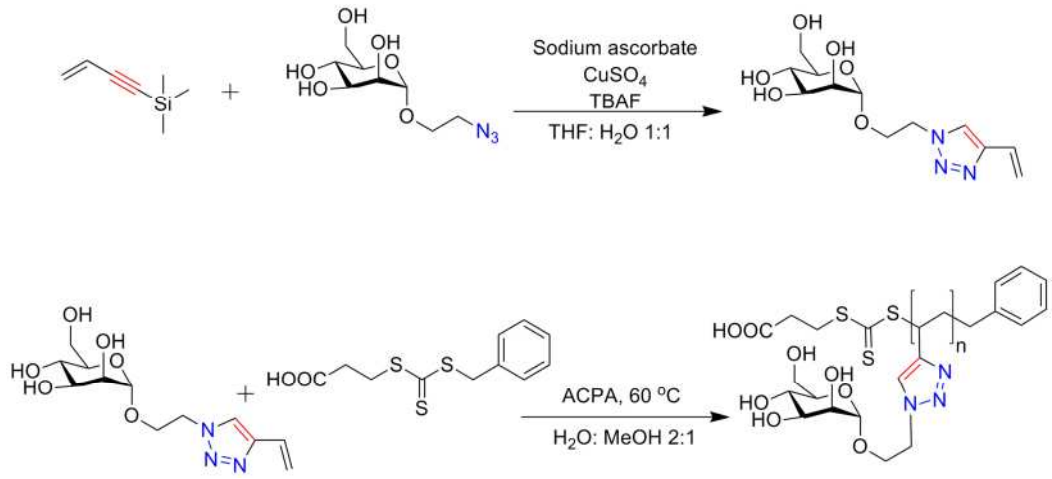

Scheme 24: The synthesis of a 4-vinyl-1,2,3-triazole glycomonomer (top) and RAFT polymerisation (bottom)

Stenzel *et al.* have reported the synthesis and RAFT polymerisation of a novel glycomonomer *via* CuAAC, belonging to an uncommon monomer class, scheme 24, [200] The 4-vinyl-1,2,3-triazole monomers are a relatively new class of monomers with good thermal properties.[231] Stenzel *et al.* show the facile synthesis of 2´-(4-vinyl-1,2,3-triazol-1-yl)ethyl-*O*-α-D-mannoside, from 2´-azidoethyl-*O*-α-D-mannoside and 4-trimethylsilyl-1-buten-3-yne. The azide-functional saccharide was easily synthesised without protecting groups. A disadvantage to this glycomonomer synthesis is the complex synthesis of 4-trimethylsilyl-1-buten-3-yne, which requires harsh conditions and led to low yields. To synthesise the glycomonomer, the deprotection of the alkyne by tetra-n-

butylammonium fluoride (TBAF) and CuAAC click reaction were carried out in a one-pot reaction, where the copper(I) was produced in situ by the reduction of $CuSO_4$ by sodium ascorbate.

The 4-vinyl-1,2,3-traizole monomer was polymerised by RAFT in water, with 4,4-azobis(4-cyanovaleric acid) used as the water soluble thermal initiator. The reactions were carried out in the presence of 3-(benzlsulfanylthiocarbonylsulfanyl) propionic acid (BSPA) as RAFT agent, to yield high molecular weight polymer with PDI < 1.25.

Poly[2'-(4-vinyl-1,2,3-triazol-1-yl)ethyl-*O*-α-D-mannoside)] macro RAFT agent was used to synthesise an AB block copolymer with *N*-isopropylacrylamide p(NIPAAm), which reversibly formed micelles above the LCST of the p(NIPAAm) block. The micelles formed were seen to have higher rates of binding to Con A in comparison to their linear counterparts, which highlights the potential effect that architecture can have on a glycopolymers recognition properties.

5.1.2 Thiol-ene click reactions

Thiol compounds react either *via* radical or catalysed processes under mild conditions with a multitude of substrates.[45] The radical addition of thiols to vinyl groups is a highly efficient technique used for polymerisations, curing reactions and for the modification of polymers.[232]

For thiol-ene chemistry to be used in glycopolymer synthesis, sugars must be functionalised with vinyl or thiol moieties. There are commercially available thio sugars, such as thio glucose; however, for many sugars it is still necessary for them to be synthesised from the native sugar. For the synthesis of thio mannose and thio

galactose, there have been several routes described in the literature. The most common route to thio sugars is *via* protected glycosyl halides.[233,234] Subsequent nucleophilic substitution with a sulfur nucleophile, such as potassium thioacetate or thiourea, yields a protected thio glycoside.[235,236] Other routes have potential to form thio sugars in fewer steps; Hayes *et al.* have shown the synthesis of 2'-thioethyl 2,3,4,6-tetra-*O*-acetyl-1-α-D-mannopyranoside using boron trifluoride etherate as a Lewis acid with a large excess of 1,2-ethane-dithiol, in 15% yield.[237] Davis and co-workers have published a simple synthesis of glycosyl thiols using Lawesson's reagent with the unprotected sugars.[238]

In 2007, Schlaad and co-workers first demonstrated a post-polymerisation modification of a well-defined poly[2(-3-isobutenyl)-2-oxazoline] that was synthesised *via* cationic ring opening polymerisation (CROP).[204] They have reacted various thiols including an acetylated thio glucose (2,3,4,6-tetra-*O*-acetyl-1-thio-*β*-D-glucopyranose) with the well-defined polymeric backbone by exposing to UV light, scheme 25. Photoaddition of thiols were performed in a 4 wt% solution of polymer in dry THF : methanol (1:1) under an argon atmosphere, and exposed to UV light for one day.

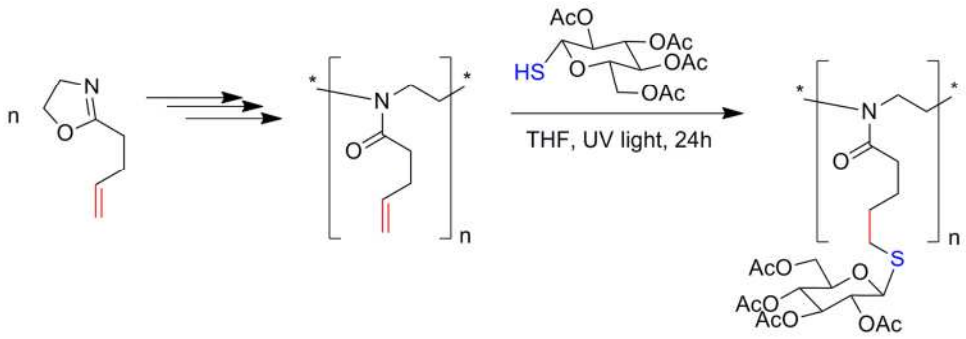

Scheme 25: Synthesis of glycopolymers by combination of cationic ring opening polymerisation of 2-oxazoline and thiol-ene click reaction.

A further study was reported by Stenzel *et al.* on the synthesis of thiol-linked *neo*glycopolymers by a combination of RAFT polymerisation and thiol-ene click reaction.[239] Block copolymerisation of di(ethylene glycol) methyl ether methacrylate (DEGMA) and 2-hydroxyethyl methacrylate (HEMA) was performed and followed by a post polymerisation modification of the hydroxyl groups of HEMA to clickable vinyl units. They have obtained thermoresponsive glycomicelles as a potential drug carrier.

5.1.3 Thiol-yne click reactions

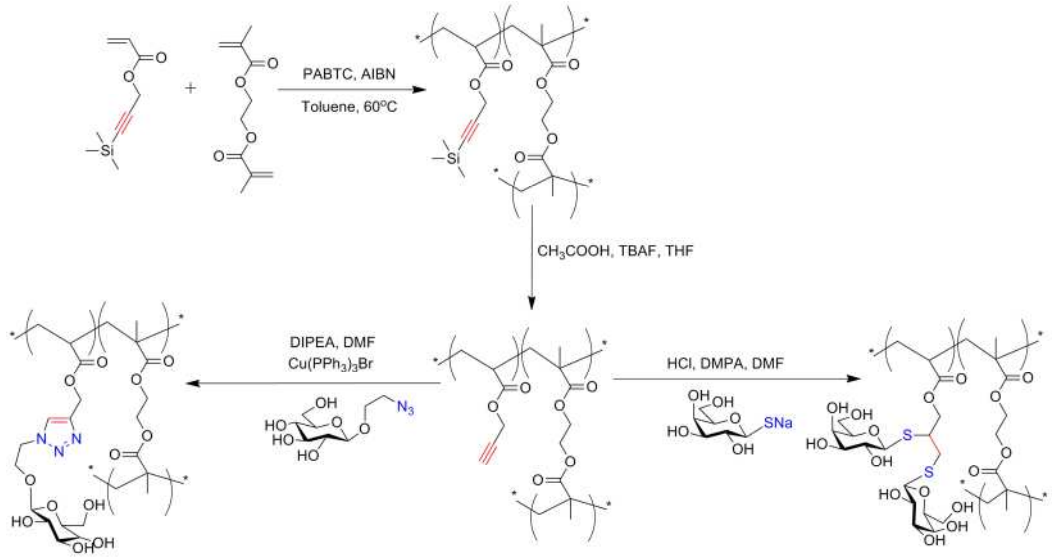

Scheme 26: Synthesis of hyperbranched glycopolymers using RAFT polymerisation and CuAAC click reactions (left) or thiol-yne click reactions (right).

Perrier *et al.* have reported the synthesis of hyperbranched glycopolymers using RAFT and a number of "click" reactions. Propionic acidyl butyl trithiocarbonate (PABTC), RAFT agent, was used to control the polymerisation of a protected alkyne acrylate in the presence of difunctional monomer, ethylene glycol dimethacrylate (EGDMA).[206] This was followed by a deprotection step to yield a hyperbranched scaffold with alkyne

functionality. The “clickable” scaffold was modified by two different routes, scheme 26. Firstly, by CuAAC of 2-azidoethyl-ß-D-galactopyranoside to the alkyne functionality on the polymer; this reaction was seen to reach 85% conversion. The second route was *via* radical addition of the thio glucose to the alkyne to yield bis-glucose functionality. The radical addition reaction was seen to reach 90% conversion, with a small amount of C=C bonds visible in the infra-red analysis and vinyl protons present in the ^{1}H NMR analysis. In summary, Perrier *et al.* have shown an effective route to synthesise hyperbranched glycopolymers. However, optimisation of the click reactions are necessary to avoid the possibility of crosslinking occurring between unreacted vinyl groups.

A further glycopolymer synthesis utilised unreacted pendant methacrylate groups present after the polymerisation of EGDMA in the absence of a monofunctional monomer. 2-Cyanoisopropyl dithiobenzoate RAFT agent was used to control the polymerisation and dimethyl phenyl phosphine (DMPP) was used to catalyse the hetero-Michael addition of thio glucose to the unreacted pendant methacrylate groups. This reaction yielded a hyperbranched glycopolymer with high conversion of click reaction in a relatively simple manner.

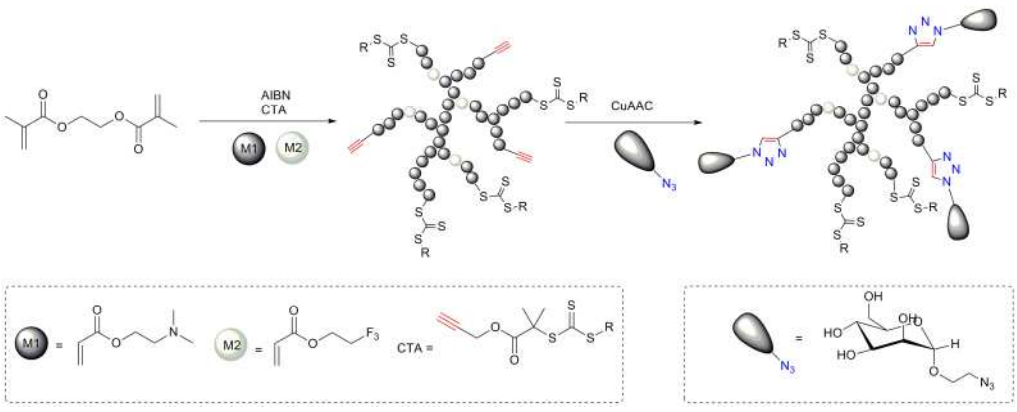

Scheme 27: Synthesis of hyperbranched glycopolymers by RAFT using an alkyne functional RAFT agent and CuAAC click.

Furthermore, Whittaker *et al*. demonstrate another efficient route to hyperbranched glycopolymers through the use of RAFT polymerisation and click chemistry, scheme 27.[240] They modify the chain transfer agent to incorporate alkyne groups into the polymer at the α-chain end. The polymer formed is a statistical copolymer of dimethylaminoethylacrylate (DMAEA) and trifluoroethyl acrylate (tFEA) with EGDMA as a crosslinker to give an alkyne functionalised hyperbranched polymer network. The CuAAC reaction was implemented to click azide functionalised sugars onto the polymer network. A nice feature of this work was the successful incorporation of a ^{19}F magnetic resonance imaging (MRI) contrast agent into the glycopolymer. Another striking feature was that the polymerisation was carried out without protection of the alkyne group on the RAFT agent. As has been discussed previously, alkynes are typically protected during polymerisation, with trimethylsilyl groups. This is to avoid unwanted side reactions; however, in this work no side reactions were reported. This enables synthesis of glycopolymers in only two steps with the added benefit of defined macromolecular properties due to the polymerisation method as well as incorporation of the MRI contrasting agent (tFEA).

5.2 Results and Discussion

5.2.1 Synthesis of polymer scaffolds for post polymer modification

The advent of the concept of "click" chemistry has seen a concerted effort from all areas of chemistry to draw on facile reactions to perform necessary chemical modifications. Using highly efficient chemistries to modify polymer backbones with tailored pendent, α and/or ω functionalities has become a popular research topic.[29,32,198,241-243] This is a perfect example of where "click" chemistry has opened up a field to new opportunities. A number of reactions have been determined to comply with the prerequisites set out by Sharpless and co-workers;[27] copper catalysed azide alkyne cycloaddition (CuAAC)[244] is currently the most widely used "click" reaction. By incorporation of either alkyne[34,245,246] or azide[247,248] moieties onto a polymer allows post-polymerisation introduction of chemical functionality. This holds two potential benefits: it can allow functionalities that may be incompatible with a particular polymerisation procedure to be introduced, whilst also allowing the synthesis of a library of compounds with the same scaffold size and properties, varying only by the chemical functionality that is introduced.

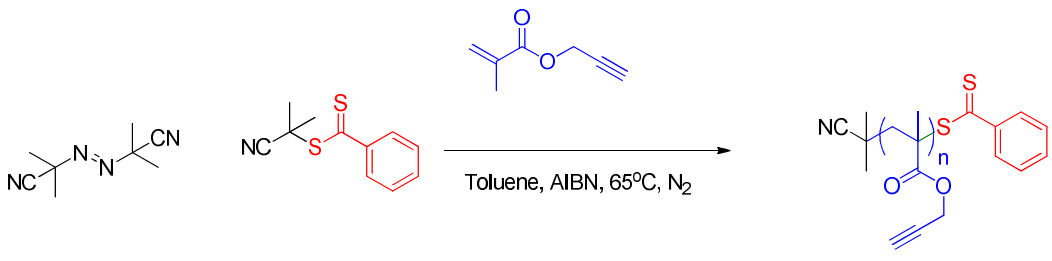

Scheme 28: RAFT polymerisation of PgMA, in the presence of AIBN and RAFT agent 1, in toluene at 65 °C, under nitrogen.

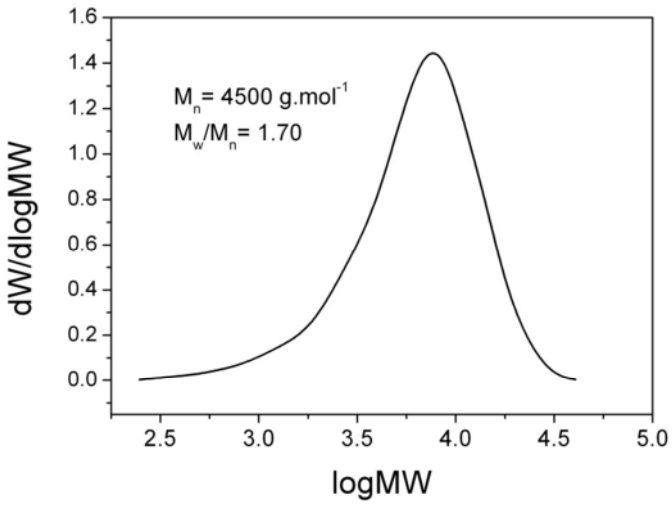

Figure 78: Molecular weight distribution of PgMA1. Synthesised using RAFT agent 1 and AIBN in toluene at 65 ^{o}C.

Although some reports have shown the polymerisation of commercially available unprotected alkyne monomers to form well defined polymers using polymerisation procedures such as RAFT-SET polymerisation;[249,250] the alkyne of the PgMA is generally prone to reaction with free radicals.[251] Therefore cross-linking reactions can occur, leading to networked polymers with broad PDIs, figure 78. Interestingly, neither cross-linking nor coupling has been seen to occur when alkyne moieties are incorporated on RAFT agents,[250,252,253] likely due to the low relative concentration of them in the reaction solution.

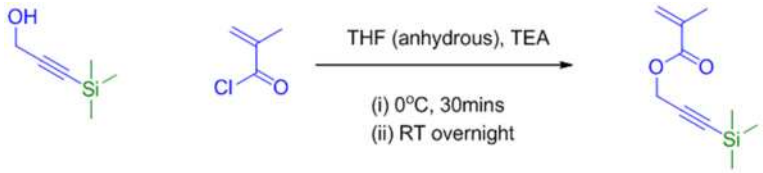

Scheme 29: Synthesis of trimethylsilyl propargyl methacrylate (TMSPgMA) from 3-trimethylsilyl propyn-1-ol and methacryloyl chloride.

The propargyl group can be protected from unwanted radical attack using a trimethylsilyl group, which can be easily removed post polymerisation. This allows the polymerisation of the alkyne bearing monomers, scheme 30. The protected monomer can be synthesised using Grignard chemistry, however, it is easier to perform an acylation reaction on the commercially available trimethylsilyl propyn-1-ol, scheme 29. This reaction proceeds in anhydrous conditions to high yield (*ca*.90%), and can be purified without chromatography. This monomer has been polymerised in the literature using a number of techniques, including transition metal-mediated radical polymerisation,[33,34,198,254] RAFT, [245,246,255] CCTP, [256] and NMP.[257]

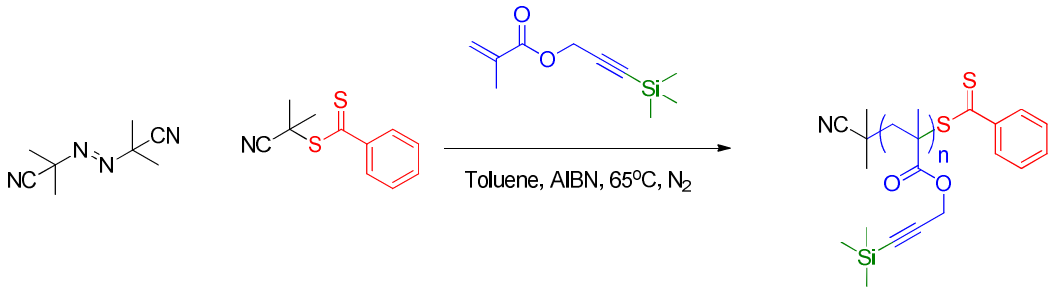

Scheme 30: Reaction scheme of RAFT polymerisation of TMSPgMA in the presence of AIBN and RAFT agent 1 in toluene at 60 °C.

Trimethylsilyl propargyl methacrylate (TMSPgMA), has been polymerised using **RAFT agent 1** and AIBN as the radical initiator in toluene, scheme 30. Similar methods using RAFT chemistry to synthesise functional polymers have been published by Stenzel and co-workers, highlighting the need for protection chemistry.[245,246,255]

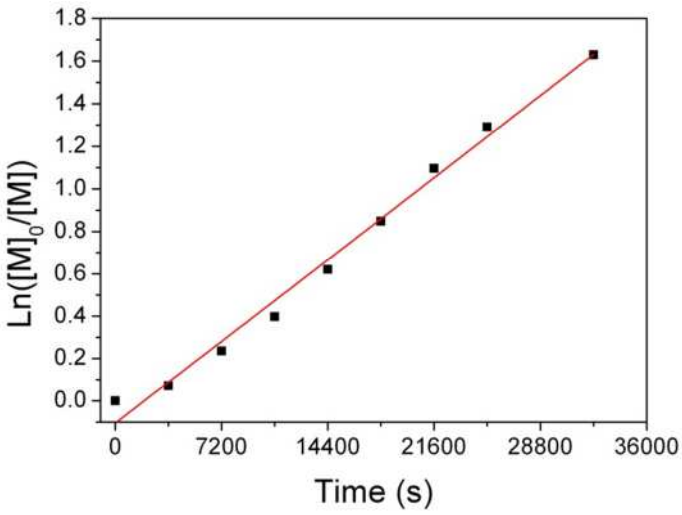

Figure 79: P(TMSPgMA)5. Polymerisation of TMSPgMA targeting a DP of 100, first order kinetic plot. .

With a targeted DP of 100, the polymerisation of TMSPgMA by **RAFT agent 1** was seen to proceed in a pseudo "living" manner, with linear molecular weight growth with conversion and polydispersities that decrease with conversion, figure 79. The apparent rate constants can be estimated, using the kinetic plot, figure 79. The slightly sigmoidal shape of the plots can be due to the decreasing concentration of radical source AIBN and/or termination occurring in the reaction. From the gradient of the kinetic plot, the apparent rate constant was calculated, k_{app}, = 5.36 x 10^{-5} s^{-1}.

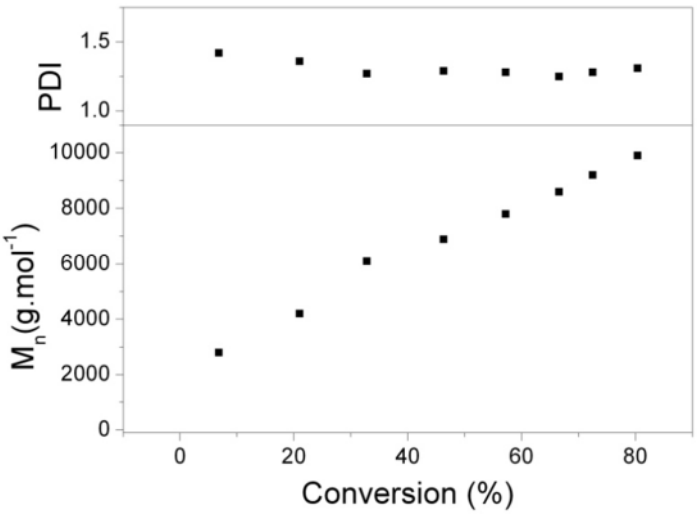

Figure 80: P(TMSPgMA)5. Polymerisation of TMSPgMA targeting a DP of 100. Evolution of M_n and PDI with percentage monomer conversion .

The M_n of the polymer increased with conversion, with low molecular weight polymer formed early in the reaction. The PDI of the polymer decreased from 1.5 at the beginning of the reaction to 1.25 at the end of the reaction.

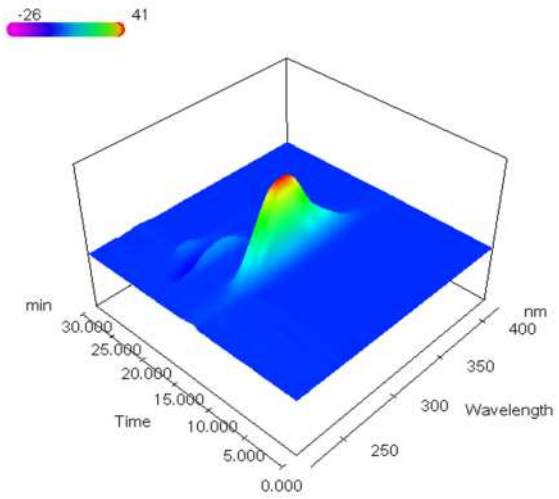

Figure 81: P(TMSPgMA)5. Polymerisation of TMSPgMA targeting a DP of 100. 3D plot of UV wavelength (nm) and retention time in GPC (mins) with the colour intensity representative of UV absorption.

The RAFT agent is intact on the end of the polymer chain over the molecular weight distribution of the polymer, as can be seen from the absorption of the thiocarbonyl group at λ =309 nm, at the retention time of the polymer on the GPC, figure 81. This wavelength is quite distinctive and the monomer, solvent and initiating groups do not absorb in this region of UV. This is only a qualitative measure of the RAFT agent presence on the polymer; however, quantification of this end group retention could be achieved if the extinction coefficient of the thiocarbonyl group is assumed to be the same in both small molecule and on the polymer, and the polymer concentration is accurately known.

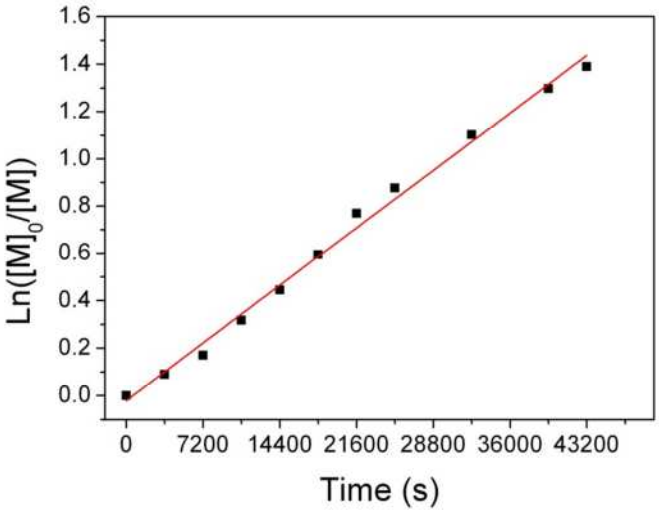

Figure 82: P(TMSPgMA)6. Polymerisation of TMSPgMA targeting a degree of polymerisation (DP) of 200, first order kinetic plot.

Increasing the ratio of [monomer] to [RAFT agent] allows control of the final polymer molecular weight. When targeting a DP of 200, the polymerisation of TMSPgMA by **RAFT agent 1** was seen to proceed in a pseudo "living" manner, figure 82. However, the sigmoidal nature of the plot increases, evidence of termination occurring in the reaction. Fitting the data to a straight line as before, the apparent rate constants can

be estimated, using the kinetic plot, figure 82, where the gradient of the kinetic plot gives the apparent rate constant, $k_{app} = 3.38 \times 10^{-5} s^{-1}$.

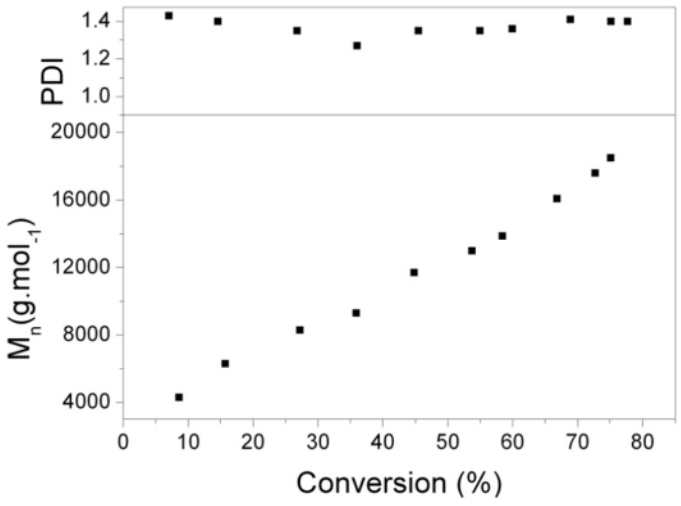

Figure 83: P(TMSPgMA)6. Polymerisation of TMSPgMA targeting a DP of 200. Evolution of M_n and PDI with percentage monomer conversion.

The M_n of the polymer was seen to increase with conversion of monomer, indicative of a living polymerisation. The polydispersity of the polymer was seen to remain low with PDI around 1.3-1.4 throughout the polymerisation.

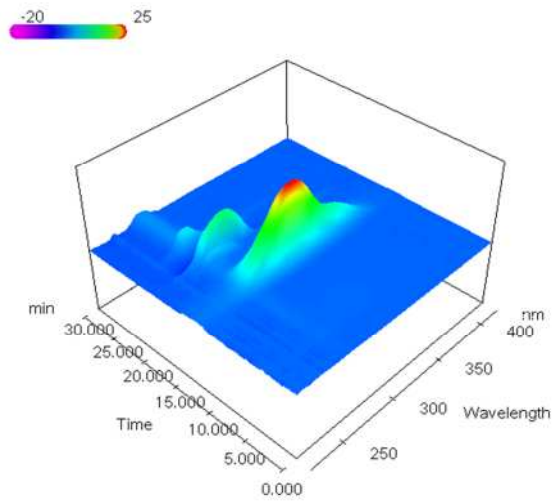

Figure 84: P(TMSPgMA)6. Polymerisation of TMSPgMA targeting a DP of 200. 3D plot of UV wavelength (nm) and retention time in GPC (mins) with the colour intensity representative of UV absorption.

The thiocarbonyl of the RAFT agent was seen to be present on the final polymer using PDA GPC, with an absorbance with a peak maximum at 309 nm at the retention volume of the polymer, figure 84.

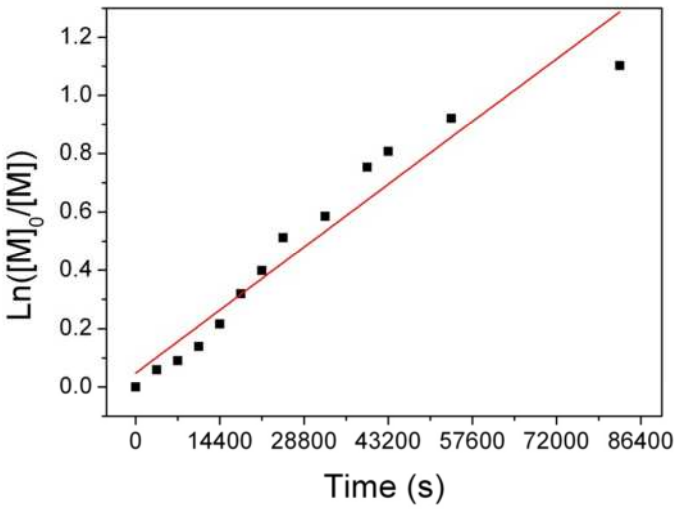

Figure 85: P(TMSPgMA)7. Polymerisation of TMSPgMA targeting a DP of 300. Plot of ln($[M]_0/[M]_t$) against time.

High molecular weight polymer was targeted by increasing the ratio of [RAFT agent] to [monomer] to 1:300. In a similar way to when targeting lower DP, the rate of propagation was determined from the gradient of a plot of $\ln([M]_0/[M]_t)$ against reaction time when pursuing a DP of 300, k_{app} = 1.50 x 10^{-5} s^{-1}. This was expected, as decreasing the amount of RAFT agent to target higher molecular weight the rate will lower the number of radicals being produced. The non-linear nature of the plot, figure 85, shows the changing number of radicals within the reaction, highlighting the presence of termination within RAFT polymerisation, and the decreasing supply of radical initiator as the reaction proceeds.

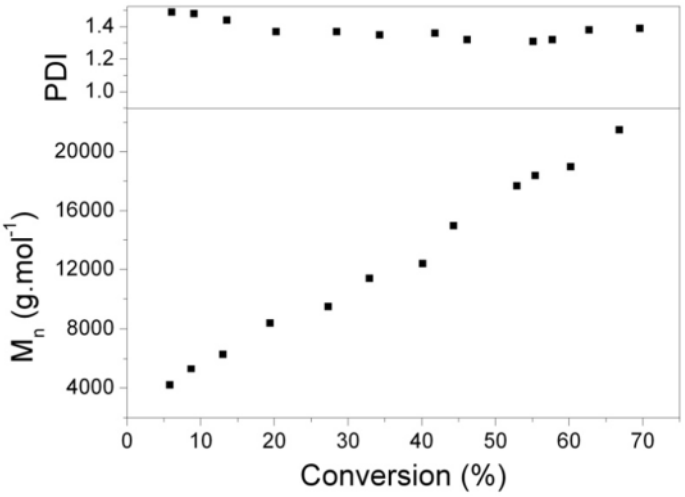

Figure 86: P(TMSPgMA)7. Polymerisation of TMSPgMA targeting a DP of 300. Evolution of M_n and PDI with monomer conversion.

The molecular weight of the polymer increases with conversion to high molecular weight. However, the PDI was seen to be high over the entire polymerisation.

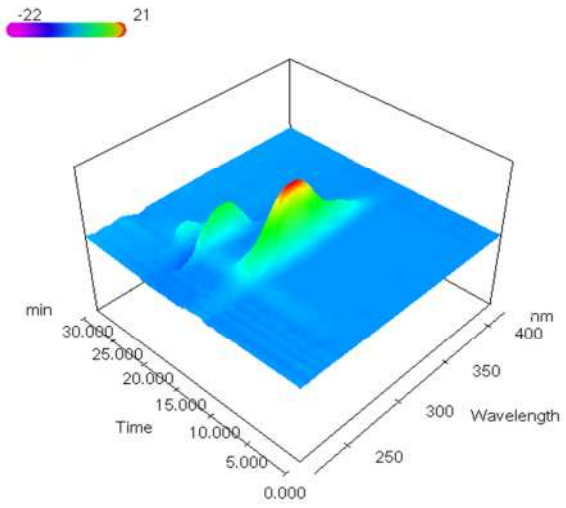

Figure 87: P(TMSPgMA)7. Polymerisation of TMSPgMA targeting a DP of 300. 3D plot of UV wavelength (nm) and retention time in GPC (mins) with the colour intensity representative of UV absorption.

The RAFT agent was intact on the end of the polymer chain over the molecular weight distribution of the polymer, as can be seen from the absorption of the thiocarbonyl group at a λ =309 nm, at the retention time of the polymer on the GPC.

Table 15: Summary of alkyne polymer scaffolds synthesised for further modification, by polymerisation reactions of TMSPgMA and deprotection of TMS groups

Polymer ID	Target DP	Conversion (%)	DP (NMR)	Protected M_n ($g.mol^{-1}$)	Protected PDI	Deprotected M_n ($g.mol^{-1}$)	Deprotected PDI
P(TMSPgMA)1	20	-	-	5200	1.18	4000	1.18
P(TMSPgMA)2	60	-	-	7500	1.18	6000	1.19
P(TMSPgMA)3	100	-	-	11200	1.21	9200	1.18
P(TMSPgMA)4	200	-	-	16500	1.26	13700	1.24
P(TMSPgMA)5	100	82	94	16700	1.22	12300	1.21
P(TMSPgMA)6	200	78	186	30200	1.31	25800	1.27
P(TMSPgMA)7	300	65	221	32000	1.38	-	-

RAFT polymerisation with **RAFT agent 1** was seen to control the polymerisation of TMSPgMA targeting varying degrees of polymerisation (DP) between 20 and 300, yielding polymers with the expected molecular weight and narrow PDI, table 15. **P(TMSPgMA)7** has a discrepancy between the conversion of monomer and the final polymer molecular weight. The number average molecular weight by ^{1}H NMR is larger than that estimated by GPC. One possible explanation is that the bulky trimethylsilyl group could allow the polymer to elute earlier from the GPC column than the PMMA standards and hence lower the determined molecular weight. From comparison of the reaction kinetics for targeting different DPs it is possible to see an increasing deviation from the ideal RAFT mechanism, shown by non first order kinetics, and comparatively high PDI. Therefore, no attempt was made to synthesise higher molecular weight linear P(TMSPgMA). **P(TMSPgMA)7** was not used for the further studies, but highlights the decrease in control of polymerisation of TMSPgMA by **RAFT agent 1** when targeting high molecular weight.

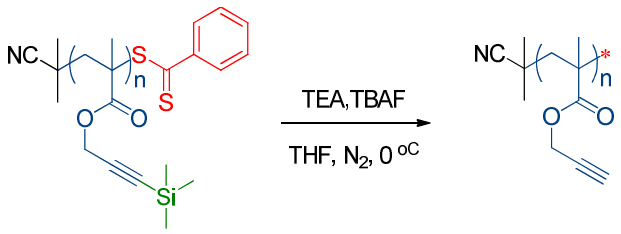

Scheme 31: Removal of TMS groups from P(TMSPgMA) using TBAF to yield alkyne bearing polymer, P(PgMA).

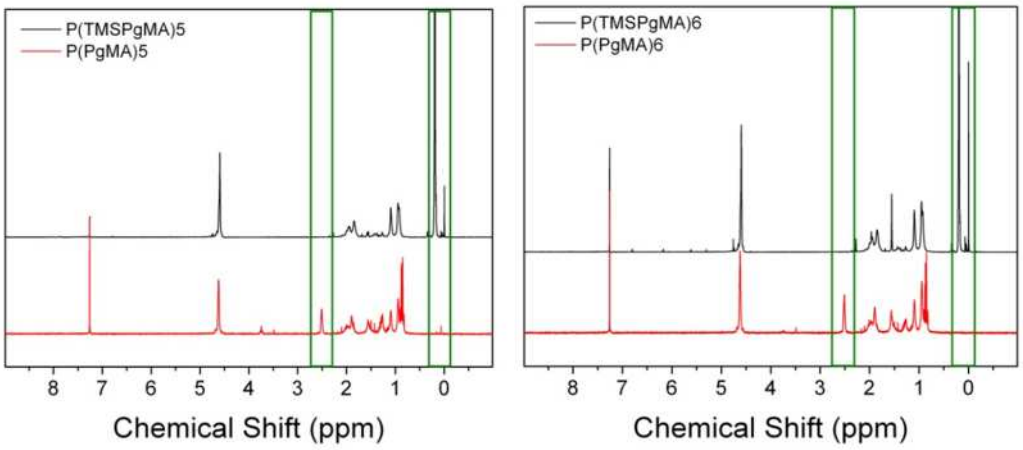

Figure 88: (Left) ^{1}H NMR of P(TMSPgMA)5 and after deprotection, P(PgMA)5. (Right) ^{1}H NMR of P(TMSPgMA)6 and after deprotection, P(PgMA)6. Green boxes highlght the chemical shift of where the alkyne and TMS protons appear in ^{1}H NMR.

These polymers were deprotected by treatment with tetra butyl ammonium fluoride to remove the trimethylsilyl protection groups, scheme 31. ^{1}H NMR showed that the de-protection proceeded to >99% completion, with the disappearance of the TMS peaks at 0.13 ppm, and appearance of a peak at 2.5 ppm corresponding to the alkyne proton for the polymer product, figure 88.

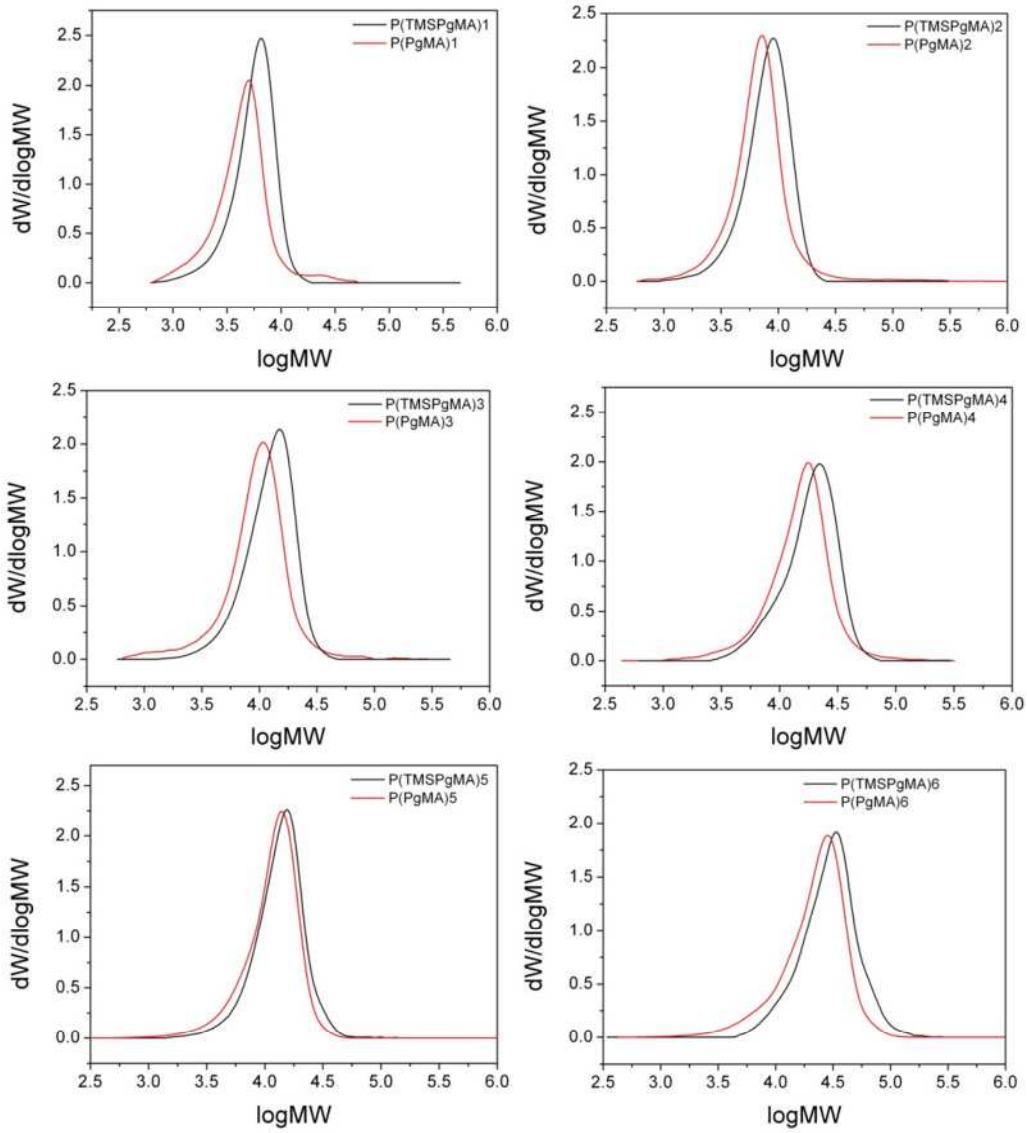

Figure 89: MWD from GPC of different P(TMSPgMA) before and after deprotection of the propargyl groups with TBAF to yield P(PgMA).

The removal of the TMS groups is further observed by the GPC chromatograms of the polymers in THF before and after reaction with TBAF, figure 89. The molecular weights, as determined by GPC, decreased after deprotection groups for each of the polymers.

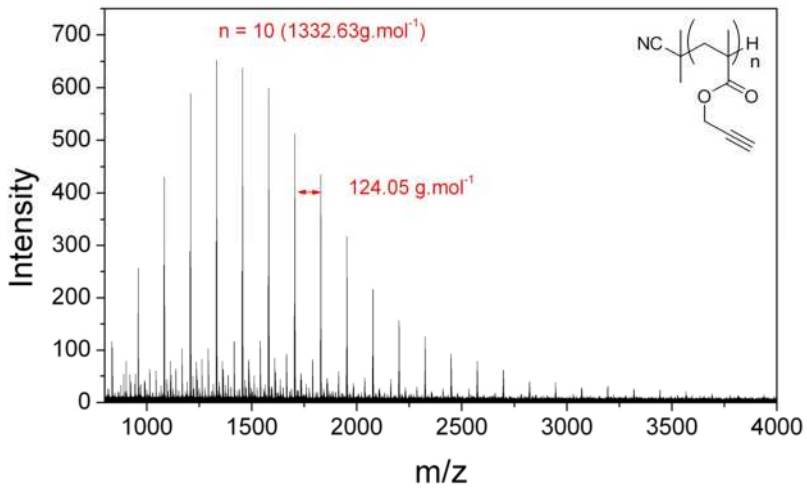

Figure 90: MALDI TOF spectrum of P(PgMA)1 (Matrix: trans-2-[3-(4-tert-Butylphenyl)-2-methyl-2-propenylidene]malononitrile (DCTB), salt: NaI, laser power: 30%)

The lowest molecular weight polymer was analysed by MALDI-TOF MS as further evidence of the polymer structure, figure 90. The mass spacing between the major peaks is 124.05 g.mol^{-1}, the mass of the alkyne bearing repeat unit (theoretical repeat unit mass = 125.0524 g.mol^{-1}). The largest peak at 1332.63 g.mol-1 corresponds to the alkyne polymer with a DP = 10 ((68.05 + (124.05n) + 1.00 + 22.99, where n = 10, m/z = 1332.54 g.mol^{-1}). This suggests that the major distribution of this polymer does not contain the RAFT agent dithioester, following reaction with TBAF. These alkyne polymer scaffolds have then been modified using a thio sugar and a sugar azide to form sugar bearing polymers.

5.2.2 Post polymerisation modification of poly(propargyl methacrylate) scaffolds

5.2.2.1 Synthesis of sugar azides

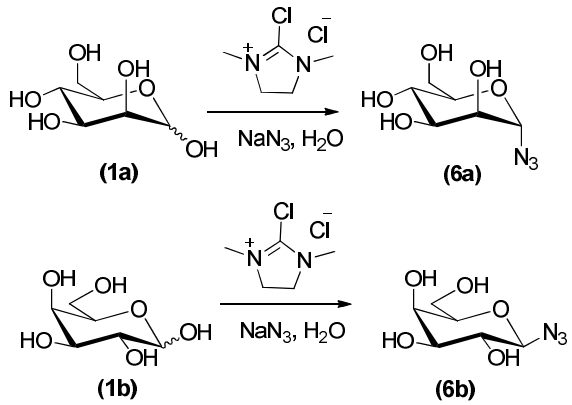

Scheme 32: Synthesis of mannose and galactose azide using DMC in a one-step process.[37,204]

A simple one-pot procedure was used for the preparation of sugar azides. Two sugars, mannose and galactose, were separately reacted with sodium azide in the presence of 2-chloro-1,3-dimethylimidazolinium chloride (DMC), in a 1-step reaction, with no column chromatography required, to form mannose and galactose azide respectively, scheme 32.[258,259]

5.2.3 CuAAC of sugar azides to linear poly(propargyl methacrylate) scaffold

5.2.3.1 CuAAC with mannose azide

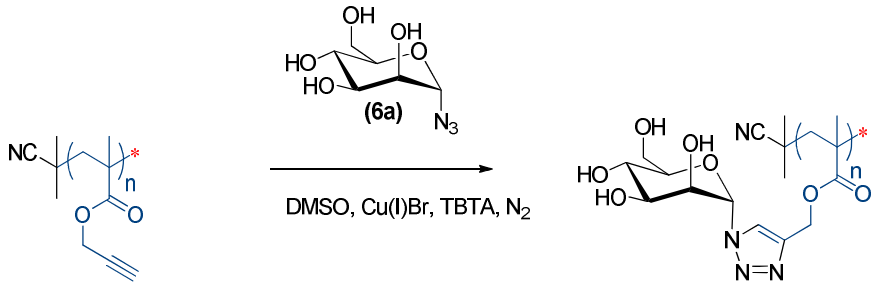

Scheme 33: CuAAC reaction of P(PgMA) and mannose azide with tris[(1-benzyl-1H-1,2,3-triazol-4-yl)methyl]amine (TBTA) as the ligand for the copper catalyst to yield P(mannoseMA) polymer

Mannose azide was reacted with the **P(PgMA)6** to how the feasibility of functionalising the scaffolds with sugar azides. Reaction conditions were taken from an optimisation study for the CuAAC of mono-saccharides to P(PgMA) by Haddleton *et al.;* tris[(1-benzyl-1*H*-1,2,3-triazol-4-yl)methyl]amine (TBTA) in DMSO was seen to be the fastest ligand/solvent combination which gave the fastest kinetics at ambient temperature and was therefore used in this study.[259] A 1.5 fold excess of mannose azide was used to ensure a complete reaction.

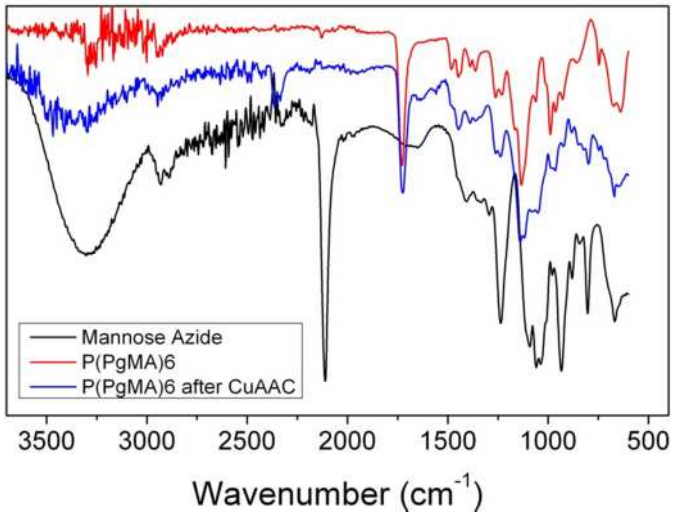

Figure 91: IR spectra for the reagents and product of the CuAAC of P(PgMA)6 and mannose azide.

The FT-IR spectrum of the product shows a broad peak at 3294 cm^{-1}, which is verification of the presence of the O-H peaks of the mannose, figure 91. It should be noted that the broad peak covers the smaller, sharper 3292 cm^{-1} peak of the alkyne C-H stretch, limiting the use of FT-IR for monitoring alkyne disappearance. The absence of the azide peak at 2100 cm^{-1} shows that the mannose azide reagent is removed by dialysis.

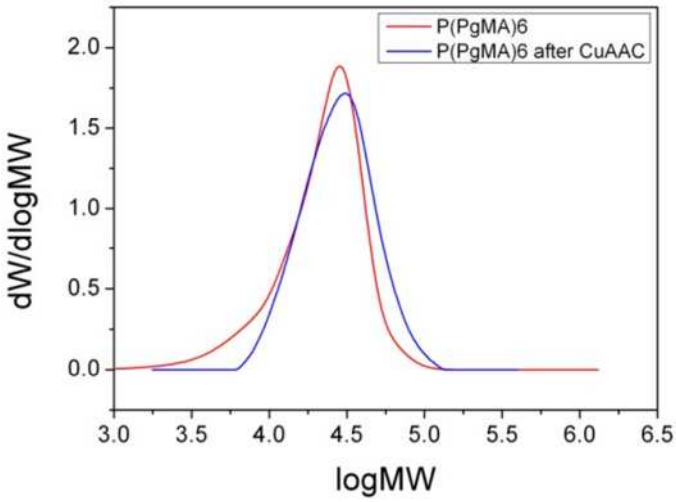

Figure 92: DMF GPC of P(PgMA)6 before and after CuAAC reaction with mannose azide.

The “clickable” polymer precursors and the polymer after reaction were analysed by GPC, using dimethylformamide (DMF) as the mobile phase, figure 92. By comparing the GPC data for the polymers, it is possible to see the increased molecular weight of the “clicked” polymer.

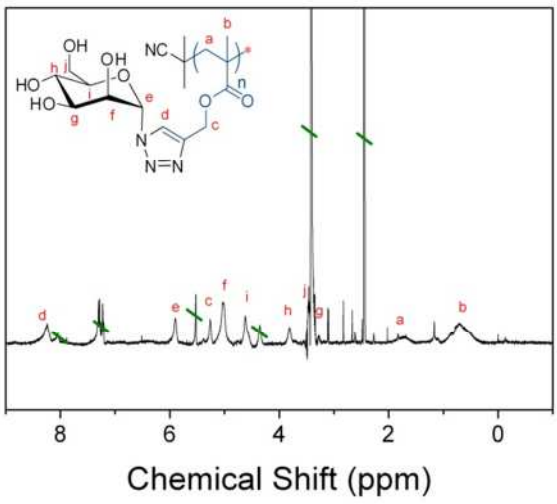

Figure 93: ^{1}H NMR spectrum of P(PgMA)6 after CuAAC reaction with mannose azide in DMSO at ambient temperature using TBTA copper complex as copper catalyst. Assigned peaks are from the resultant glycopolymer. Peaks for TBTA, DMSO and H_2O are also present.

The product was characterised by ^{1}H NMR, figure 93. However, the catalyst ligand, TBTA, was still present after purification by dialysis, due to its insolubility in H_2O for dialysis. The small scale reaction left a low yield of product; thus low concentration ^{1}H NMR analysis was shown to give a low resolution spectrum. However, important peaks can be located at 8 ppm, correlating with the triazole proton, present in the clicked glycopolymer. Although the resolution is low, and the baseline is noisy, it is possible to determine that the alkyne polymer was completely reacted by comparing the integral of the peak at 8 ppm with the 5 backbone protons between 0 - 2 ppm.

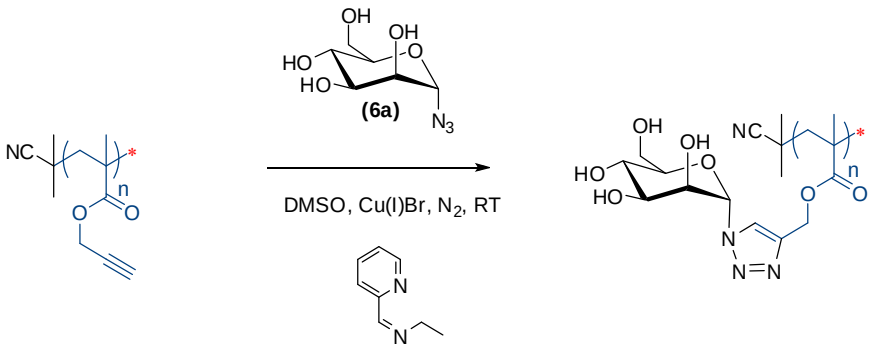

Scheme 34: CuAAC reaction of P(PgMA) and mannose azide with N-(ethyl)-2-pyridylmethanimine as the ligand for the copper catalyst.

To improve the reaction work up, this reaction was repeated, and further reactions were carried out, using *N*-(ethyl)-2-pyridylmethanimine as the ligand. The short chain pyridine imine ligand has greater water solubility than TBTA and was seen to be removed by dialysis after reaction. **P(PgMA)2**, **4** and **5**, linear alkyne scaffolds were reacted with mannose azide in deoxygenated DMSO. Reactions were left for long reaction times of 48 hours to allow complete reaction of alkyne polymers.

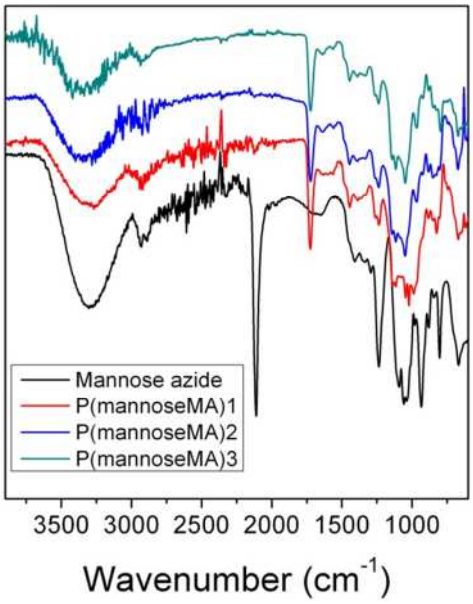

Figure 94: FT-IR of mannose azide and mannose polymers synthesised by the CuAAC of P(PgMA) scaffolds and mannose azide.

Resultant mannose polymers were characterised by IR, where the presence of the broad OH peaks and absence of the azide peaks from the mannose azide provide evidence for the successful click reaction. There is a small peak at 2300 cm^{-1} for **P(mannoseMA)2** and **3**, showing evidence of an alkyne C≡C stretch and incomplete CuAAC reaction.

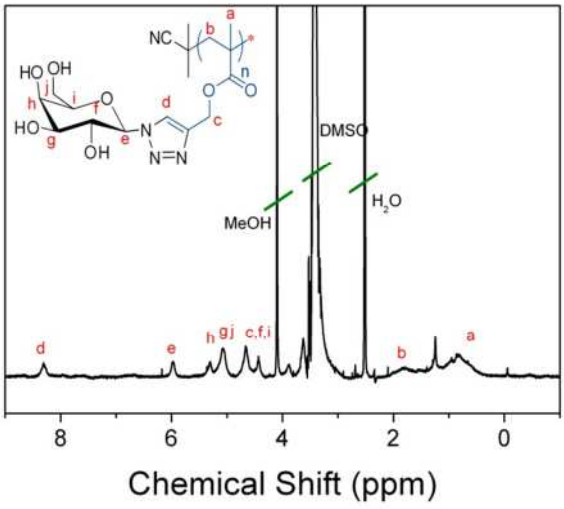

Figure 95: Example of ^{1}H NMR analysis. ^{1}H NMR spectrum of P(PgMA)4 after CuAAC reaction with mannose azide in DMSO at ambient temperature using N-(ethyl)-2-pyridylmethanimine as the copper ligand. Assigned peaks are from the resultant glycopolymer.

The extent of the CuAAC reaction was determined using the presence of the triazole peak at ca. 8 ppm in the ^{1}H NMR, figure 95. Comparison of the Integral of the triazole proton peak and the methyl of the backbone provided evidence of a high% conversion of alkyne to triazole (ca. 80%). It is thought that the small scale reactions, and low quantities of copper(I) bromide used in the reactions can make the reaction more susceptible to the catalyst being oxidised by trace amounts of oxygen in the deoxygenated reactors.

Table 16: Table of mannose polymers synthesised from series of P(PgMA) polymers. M_n and PDI are calculated from DMF GPC analysis.% click was calculated using comparison of backbone protons and triazole proton peak integrals in ^{1}H NMR.

Polymer ID	Precursor Polymer	Precursor M_n ($g.mol^{-1}$)	Precursor PDI	Glycopolymer M_n ($g.mol^{-1}$)	Glycopolymer PDI	% Click
P(mannoseMA)1	**P(PgMA)2**	6000	1.19	16700	1.45	>85
P(mannoseMA)2	**P(PgMA)4**	13700	1.24	23100	1.29	>75
P(mannoseMA)3	**P(PgMA)5**	12300	1.21	22700	1.30	>85

Using **P(PgMA)2**, **4** and **5** as linear alkyne scaffolds, mannose glycopolymers have been synthesised using mannose azide and the CuAAC click reaction, table 16. A large increase in molecular weight, as determined by conventional DMF GPC, is seen for the polymers before and after the click reaction; e.g. the M_n of **P(mannoseMA)2** was over double the M_n of the precursor polymer **P(PgMA)3**, however the PDI is also seen to increase from 1.19 to 1.45. This is likely a result of the incomplete click reaction.

5.2.3.2 CuAAC with galactose azide

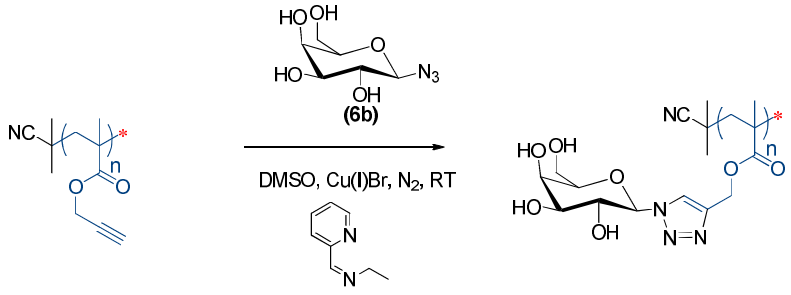

Scheme 35: CuAAC reaction of P(PgMA) and galactose azide with N-(ethyl)-2-pyridylmethanimine as the ligand for the copper catalyst.

To highlight the advantage of using preformed polymer scaffolds and post polymer modification, over polymerisation of functional monomers, analogous reactions to the mannose "click" reactions were carried out using galactose azide, scheme 35. This yielded polymers with congruent polymer properties (M_n, PDI, structure) to the mannose polymers synthesised in section 5.2.3.1, table 16 and table 17. This potentially allows direct comparison of the effects that changing between mannose and galactose has on the properties of the glycopolymers.

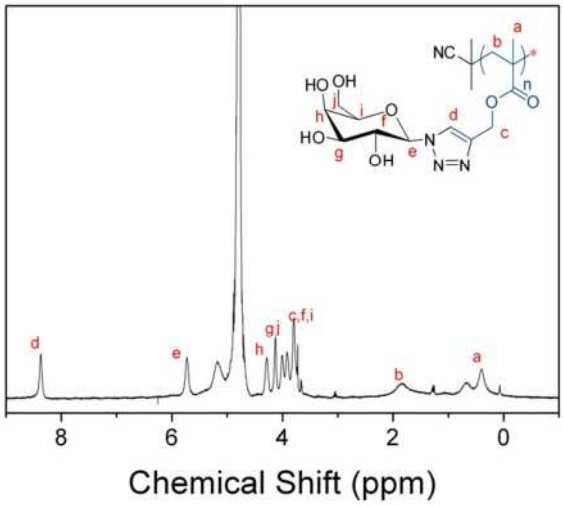

Figure 96: Example of ^{1}H NMR analysis in D_2O. ^{1}H NMR spectrum of P(PgMA)4 after CuAAC reaction with galactose azide in DMSO at ambient temperature using N-(ethyl)-2-pyridylmethanimine as the copper ligand. Assigned peaks are from the resultant glycopolymer, P(galactoseMA)3.

Characterisation of the polymers by ^{1}H NMR, allows for the determination of the conversion of alkyne to triazole, by monitoring the disappearance of the alkyne peak at 2.5 ppm. In all reactions, there is no evidence of a peak at 2.5 ppm. Further evidence for complete reaction is seen from the integration and comparison of the backbone methyl peaks to the triazole peaks, showing a ratio of 1 : 3.

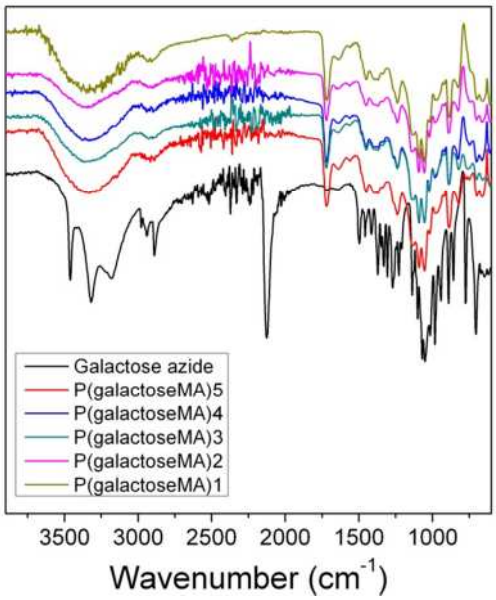

Figure 97: FT-IR of galactose azide and galactose polymers synthesised using P(PgMA) scaffolds and galactose azide.

The FT-IR of the galactose polymers show the presence of broad peaks at 3300 cm^{-1} corresponding to OH groups of the galactose. The absorption at ca. 1700 cm^{-1} shows the presence of the carbonyl bond from the methacrylate polymer. There is also a noteworthy absence of the absorption corresponding to azide in the polymers, showing that this must have undergone a reaction; this supports the ^{1}H NMR data that the CuAAC reaction has proceeded as expected.

Table 17: Table of galactose polymers synthesised from series of P(PgMA) polymers. M_n and PDI are calculated from DMF GPC analysis.% click was calculated using comparison of backbone protons and triazole proton peak integrals in ^{1}H NMR.

Polymer ID	Precursor Polymer	Precursor M_n ($g.mol^{-1}$)	Precursor PDI	Glycopolymer M_n ($g.mol^{-1}$)	Glycopolymer PDI	% Click
P(galactoseMA)1	**P(PgMA)2**	6000	1.19	9500	1.18	>80
P(galactoseMA)2	**P(PgMA)3**	9200	1.18	20400	1.17	>95
P(galactoseMA)3	**P(PgMA)4**	13700	1.24	25100	1.28	>95
P(galactoseMA)4	**P(PgMA)5**	12300	1.21	24900	1.25	>95
P(galactoseMA)5	**P(PgMA)6**	25800	1.27	42400	1.34	>95

The linear glycopolymers synthesised using galactose azide have been summarised, table 17. A large increase in molecular weight, as determined by conventional DMF GPC, is seen for the polymers before and after the click reaction; e.g. the M_n of **P(galactoseMA)3** was over double the M_n of the precursor polymer **P(PgMA)3**, however, the PDI is seen to remain low, 1.17, figure 98.

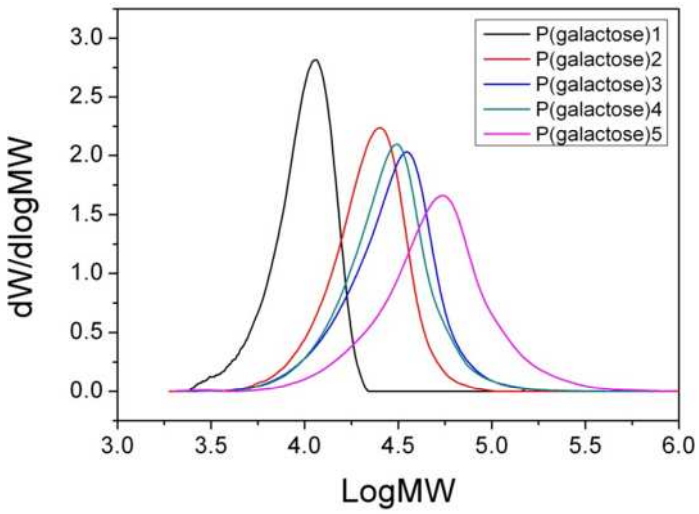

Figure 98: MWDs from DMF GPC of the series of p(galactoseMA) polymers synthesised from deprotected P(TMSPgMA) polymers (P(PgMA)).

The series of mannose and galactose glycopolymers were synthesised from the same precursors and therefore have identical backbone length and PDI. The precursors were synthesised using RAFT chemistry to polymerise linear alkyne scaffolds, and CuAAC to click mannose and galactose azides. As with ATRP, RAFT chemistry requires that the alkyne of PgMA is protected with TMS groups prior to polymerisation. The monomer synthesis and deprotection chemistry is simple and yields P(PgMA) polymers of targeted molecular weights and narrow PDI. CuAAC reaction between alkyne polymer and sugar azide is seen to react to completion in 48 hours. The use of TBTA has been shown in literature to be the most efficient catalyst,[259] however ethyl ligand was seen to be easier to remove from the reaction mixture, using dialysis, and was therefore preferred for this synthesis.

5.2.4 Thiol-yne "click" of thiol sugars to linear alkyne polymers

With the series of P(PgMA) polymers, thiol-yne chemistry was considered as alternative method of introducing sugar moieties. Thiol-yne chemistry has the potential advantage that 2 thiols can be reacted with a single alkyne. Therefore, a successful reaction with a thio sugar would yield a polymer with double the density of sugars along the backbone.

Using ATRP it has been shown how using a functional initiator to introduce α-functionality to a mannose glycopolymer could be used for targeted drug delivery.[185] With RAFT chemistry there are also ways to introduce terminal functionality.[260-264] It is also worth noting that, when using thiol-yne chemistry to functionalise P(PgMA), the dithiobenzoate group of the alkyne polymer scaffolds, P(PgMA) can also react under

the thiol-yne reaction conditions. Therefore, a method for the removal of the reactive dithiobenzoate groups of **RAFT agent 1** was investigated.

5.2.4.1 End group modification of PMMA made using RAFT Agent 1

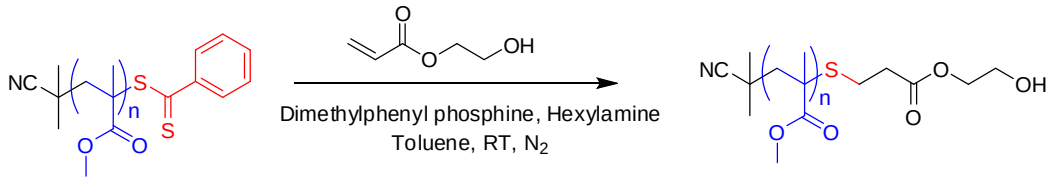

Scheme 36: Phosphine catalysed thiol-ene reaction of hydroxyethyl acrylate and dithiobenzoate group of PMMA synthesised using RAFT agent 1.

There are several methods for end group removal of RAFT agents in literature, nicely summarised in recent reviews by O'Reilly *et al*[39] and Moad *et al.*[239] For this work, a simple thiol-ene Michael addition was investigated for its application in the transformation of dithiobenzoate groups.[263,264]

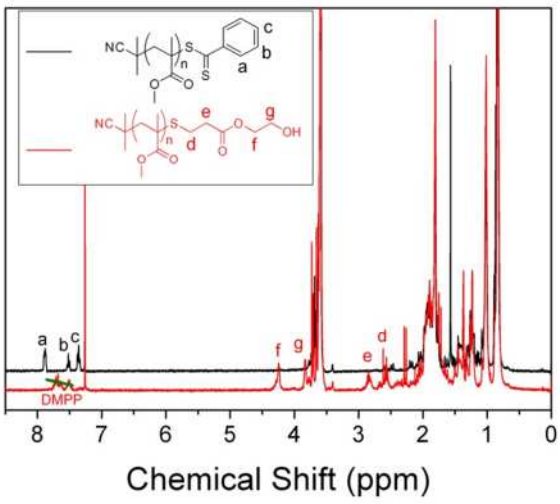

Figure 99: ^{1}H NMR of PMMA macro RAFT agent, and hydroxyethyl terminated PMMA after thiol-ene reaction.

The reaction was easily followed with disappearance of pink colour in solution, as the nucleophilic dimethylphenyl phosphine (DMPP) destroys the dithiobenzoate to leave a free thiol on the polymer chain end. The Michael addition has been studied extensively recently and been seen to proceed to completion within minutes.[206,259] Analysis of the polymer by ^{1}H NMR after twice precipitating the polymer into methanol to remove unreacted hydroxyethyl acrylate showed the presence of the hydroxyl ethyl groups next to the ester of the reacted hydroxyethyl acrylate, figure 99.

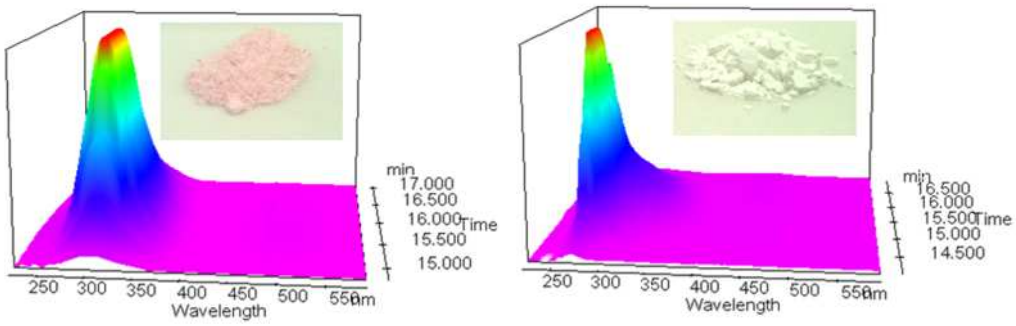

Figure 100: One pot nucleophilic removal of dithiobenzoate group to yield a thiol and subsequent phosphine catalysed Michael addition to hydroxyethyl acrylate. 3D plots of UV wavelength (nm) and retention time in GPC (mins) with the colour intensity representative of UV absorption. Inset is the colour of the polymers before and after reaction. (Left) PMMA macroRAFT agent. (Right) after reaction with hydroxyethyl acrylate in the presence of DMPP.

Analysis of the polymer using PDA GPC shows an absorption maximum at λ = 309 nm in the THF GPC trace of the PMMA macroRAFT agent, and an absence of that peak after the Michael addition, figure 100. Supporting this PDA data is an observed change in colour of the polymer from pink to white, figure 100.

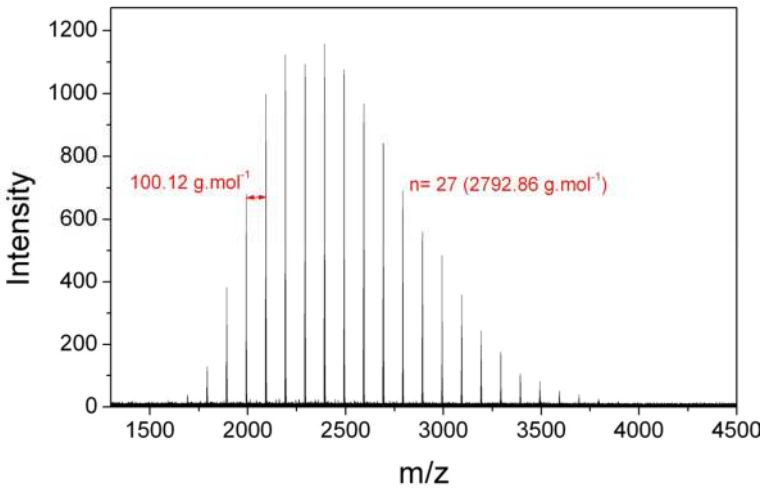

Figure 101: MALDI-TOF spectrum of PMMA made using RAFT agent1 and AIBN.

Looking at this PMMA by MALDI-TOF proved difficult due to the loss of dithiobenzoate RAFT end group during the ionisation process. The spectrum shows the major distribution of the polymer is due to the hydrogen terminated polymer, with no peak for the polymer with RAFT end group, figure 101. This suggested at first that the RAFT end group might be lost during the polymerisation.

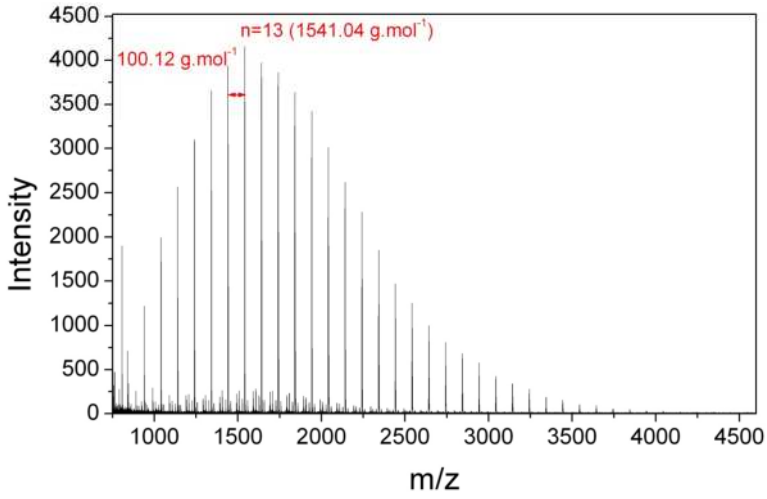

Figure 102: MALDI-TOF spectrum of resultant PMMA after thiol-ene Michael addition with hydroxyethyl acrylate. Distribution: 68.05 + (100.12n) + 149.03 + 22.99, where n = 13, m/z = 1541.63 g.mol^{-1}

However, upon reaction of the parent polymer with hydroxyethyl acrylate, *via* the highly efficient Michael addition, the major distribution of the product is now seen to be the HEA terminated polymer, figure 102. For example the largest peak at 1541.04 $g.mol^{-1}$ is within experimental error of the molecular weight expected from a DP of 13 (68.05 + (100.12n) + 149.03 + 22.99, where n = 13, m/z = 1541.63 $g.mol^{-1}$). This evidence supports the hypothesis that the dithiobenzoate group is removed during ionisation, and not lost during the polymerisation.

5.2.5 Synthesis of thio mannose

For the incorporation of thio sugars onto P(PgMA), the next step was the synthesis of sugars with thiol functionality. As discussed earlier in this chapter there are many different routes available for the synthesis of functional sugars, section.

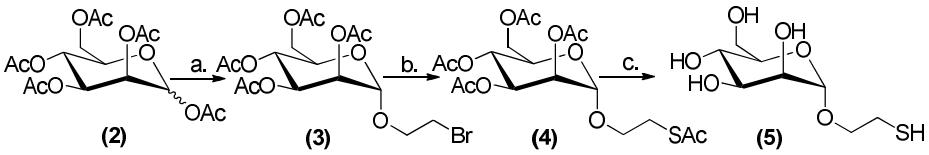

Scheme 37: Synthesis of 2'- thioethyl -O-α-D-mannopyranoside. Reagents and conditions: a) 2-Bromoethanol, BF_3OEt_2, -20 °C to ambient temperature, b) KSAc, Acetone, reflux 60 °C, c) CH_3ONa (cat.), CH_3OH, ambient temperature.

Thio mannose was synthesised following a commonly used procedure as discussed in section 5.1.2, scheme 37.[235,236] The monosaccharide was acetylated with acetic anhydride in the presence of a strong acid. The peracetylated manno-pyranose, was then treated with 2-bromoethanol in the presence of BF_3OEt_2 to give the corresponding bromide **(3)**. The desired thiol functional sugar **(5)** was obtained by conversion of the bromide intermediates into the corresponding thio acetate **(4)** and subsequent removal

of all the acetate protecting groups; 2'-thioethyl-*O*-α-D-mannopyranosidewas recovered in good yield.

5.2.5.1 Thiol-yne reaction of linear alkyne polymer scaffolds with 2'-thioethyl-*O*-α-D-mannopyranoside.

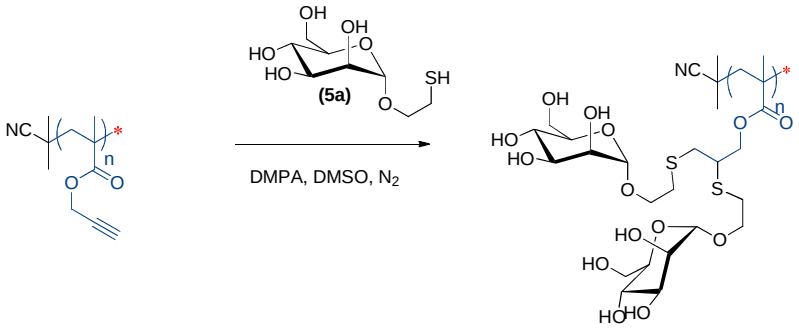

Scheme 38: Reaction of P(PgMA) with 2'- thioethyl -O-α-D-mannopyranoside to yield glycopolymer

Although removal of the RAFT end group was thought to be necessary, the reaction to remove the trimethylsilyl protection groups yielded a white solid polymer, where a pink colour would be the result of the C=S bond of **RAFT agent 1**. Therefore, the preparation of sugar polymers by thiol-yne click proceeded without further reaction of the RAFT end group. An alkyne polymer scaffold, **P(PgMA)6**, was modified using thio mannose and photo-initiator DMPA to yield a glycopolymer, scheme 38. After dialysis in MeOH : H_2O (20 : 80, MWCO 5,000 $g.mol^{-1}$),the resultant polymer was isolated by freeze drying.

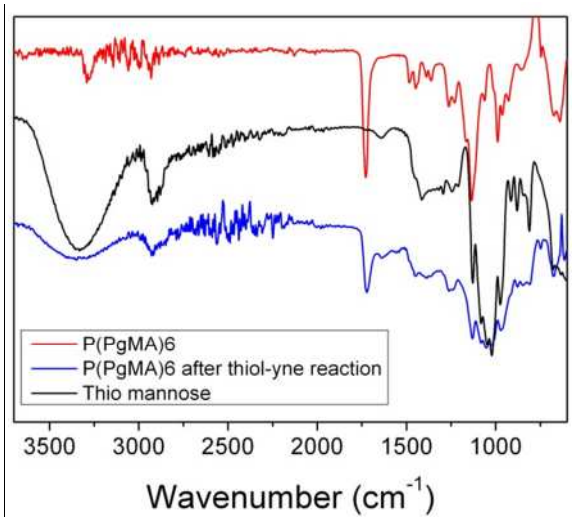

Figure 103: FT-IR spectra of thio mannose, P(PgMA)6, and P(PgMA)6 after thiol-yne reaction and dialysis to remove low molecular weight molecules.

Analysis of the FT-IR spectra of the precursor polymer, **P(PgMA)6**, and the polymer after radical reaction with an 10-fold excess of thio mannose, shows that the alkyne peak at 3239 cm^{-1} is no longer visible, and is replaced by a broad signal around 3300 cm^{-1}, corresponding to the OH groups on the mannose.

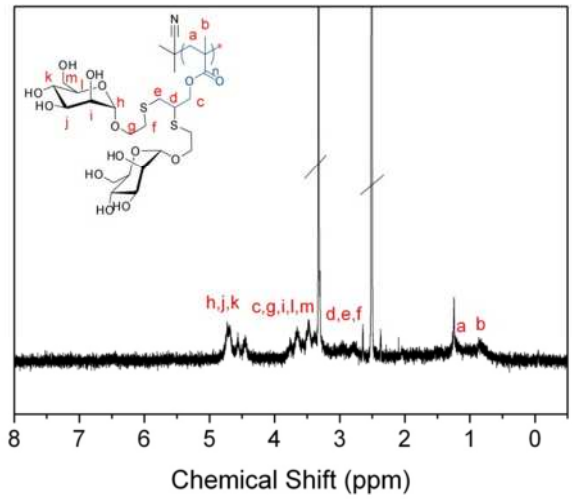

Figure 104: ^{1}H NMR spectrum of P(PgMA)6 after radical thiol-yne click with thio mannose.

Using ^{1}H NMR, it is possible to see the incorporation of sugars onto the polymer backbone. Thio mannose peaks are visible between 2.6 - 5.0 ppm. The spectrum does not show any alkene or alkyne peaks at between 5.5 - 6.5 ppm or at 1.5 ppm respectively. The low concentration of the analyte does not allow conclusive analysis of the conversion, however, in combination with the FT-IR spectra it can be concluded that a water soluble glycopolymer has been synthesised using RAFT chemistry and thiol-yne "click" chemistry.

Thiol-yne has the potential advantage over CuAAC that it does not use copper catalyst, which can often be difficult to remove in CuAAC, due to the copper binding triazole rings formed. Using radical addition to the alkyne also has the interesting property of increased sugar density on the resultant polymer as two thiols are able to add to each alkyne repeat unit.

However, these experiments show that the thiol-yne reaction does not go to completion, even given long reaction times. The synthesis of thio sugars was seen to be more challenging than the sugar azides, and the thiocarbonyl of any RAFT agent can be problematic. Therefore, thiol-yne chemistry is not a simple method for introducing thio sugar moieties to a P(PgMA) backbone synthesised by RAFT, and has several drawbacks relative to the simple CuAAC reaction.

5.2.6 Core-crosslinked glycol-star polymers

5.2.6.1 Synthesis of a core-crosslinked "clickable" P(PgMA) star scaffold

The polymers; **P(TMSPgMA)5,6** and **7;** were found to have RAFT end groups present using PDA-GPC, figure 81, figure 84 and figure 87.

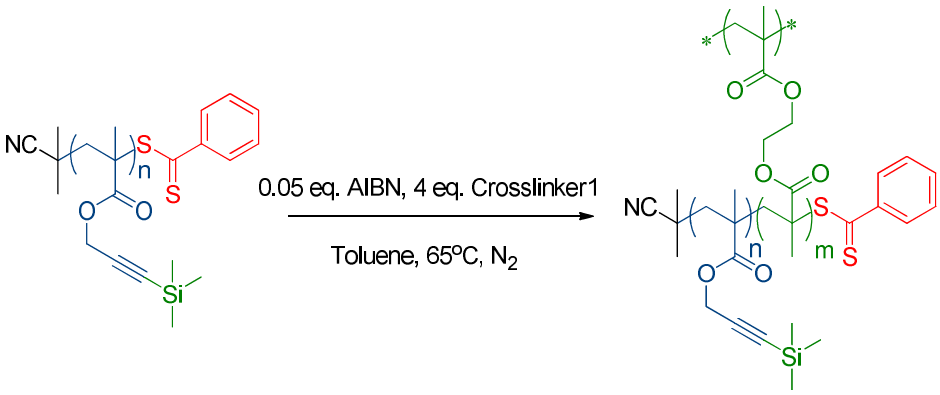

Scheme 39: Reaction of P(TMSPgMA) macroRAFT agent with crosslinker1 to form a core-crosslinked star polymer, starP(TMSPgMA)1.

This allowed chain extension of the polymers with a crosslinking species to form a core-crosslinked star polymer, scheme 39. The ratio of macroRAFT agent to **crosslinker1** was 1:4, as this was seen to provide star polymer in the previous studies. **P(TMSPgMA)6** was used in this study.

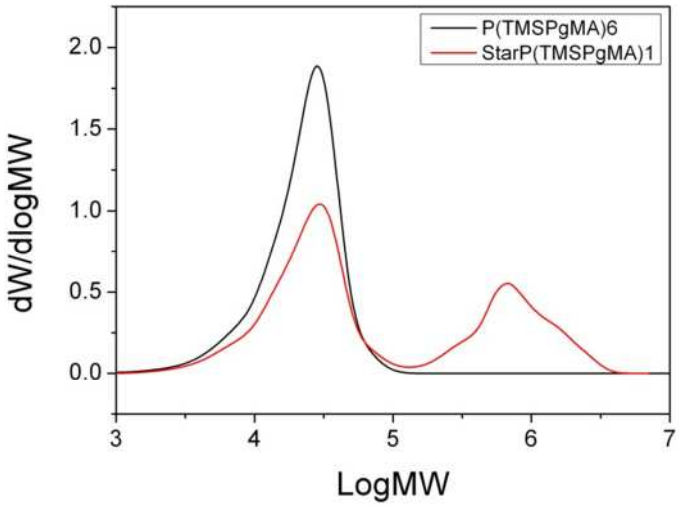

Figure 105: $CHCl_3$ GPC of P(TMSPgMA)6 and resultant starP(TMSPgMA)1 polymer after reaction with crosslinker1. Ratio of crosslinker1 to macroRAFT agent, P(TMSPgMA)6, = 4.

Efficient formation of star was not seen to occur after reaction with **crosslinker1**. **P(TMSPgMA)6** was seen to form a small high molecular weight peak in the MWD from the GPC analysis, figure 105.

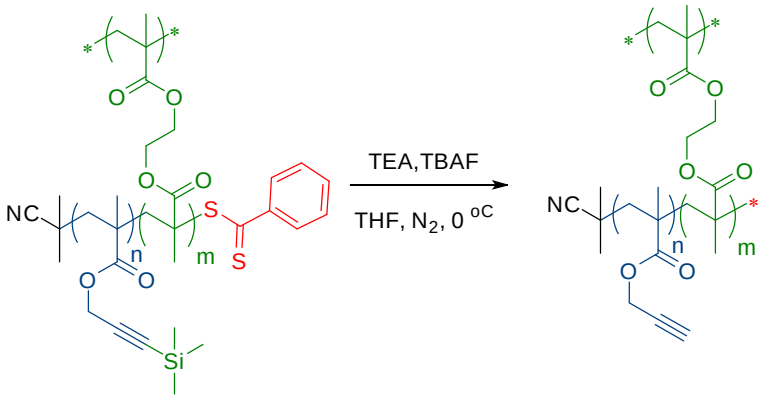

Scheme 40: Reaction of starP(TMSPgMA)1 with TBAF to remove TMS groups to make alkyne bearing star polymer, starP(PgMA).

StarP(TMSPgMA)1 was reacted with TBAF in the presence of TEA for the deprotection of the propargyl groups to yield **starP(PgMA)1**, scheme 40.This core-crosslinked star

with alkyne groups be used as a star polymer scaffold for CuAAC with functional azides to give star polymers with the given functionality.

5.2.6.2 CuAAC of sugar azides to core-crosslinked P(PgMA) star polymer

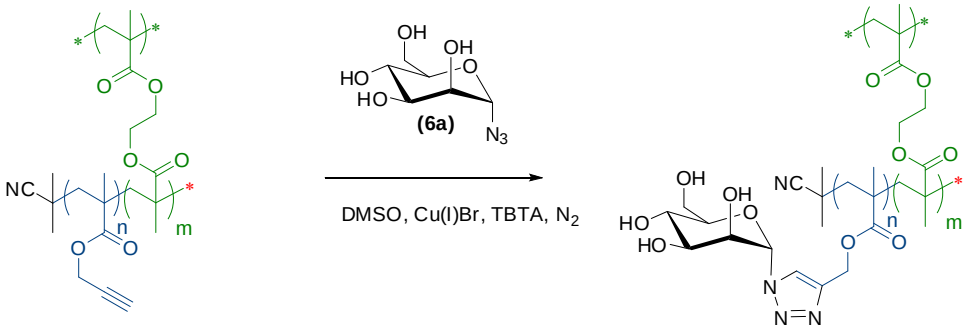

Figure 106: CuAAC of starP(PgMA)1 polymer with mannose azide, catalysed by triazole containing TBTA under an inert atmosphere of N_2.

The alkyne polymer **starP(PgMA)1** has been functionalised with mannose azide to give a water soluble polymer. Using TBTA as a ligand to solubilise the copper catalyst, an inert atmosphere was used to stabilise the Cu (I) catalyst.

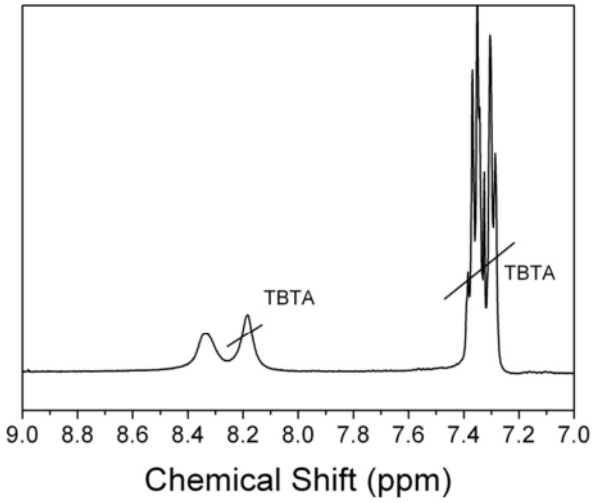

Figure 107: Partial ^{1}H NMR spectrum between 7.0 and 9.0 ppm for the reaction of mannose azide with starP(PgMA)2.

The reaction was seen to proceed by monitoring the appearance of the triazole proton in ^{1}H NMR, figure 107. The spectrum is complicated by the presence of a second triazole proton from TBTA ligand used for the catalysis. However, the broad polymer based triazole proton is clearly seen at 8.35 ppm, indicating that the cycloaddition reaction has occurred. Integrating this peak relative to alkyne peak at 2.5 ppm shows that the reaction has proceeded to approximately 50%. This reaction was left for 24 hours, as this was seen to work for the linear polymers. However, longer reaction times may be required due to the steric hindrance caused by the increased density of the polymer at the core.

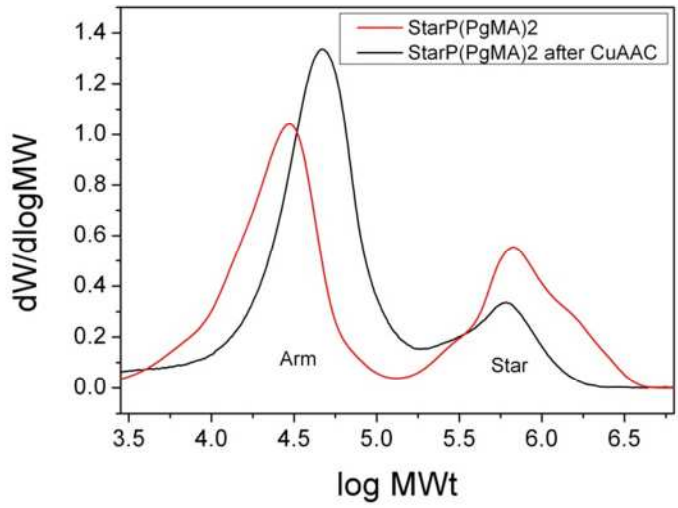

Figure 108: DMF GPC spectra of starP(PgMA)2 before and after the CuAAC reaction with mannose azide.

Analysis of the polymer by GPC shows that the hydrodynamic volume of the linear polymer has increased significantly. The star is seen to contract in solution. The star structure is still present after the CuAAC reaction, as seen by DMF GPC of the resultant polymer, figure 108.

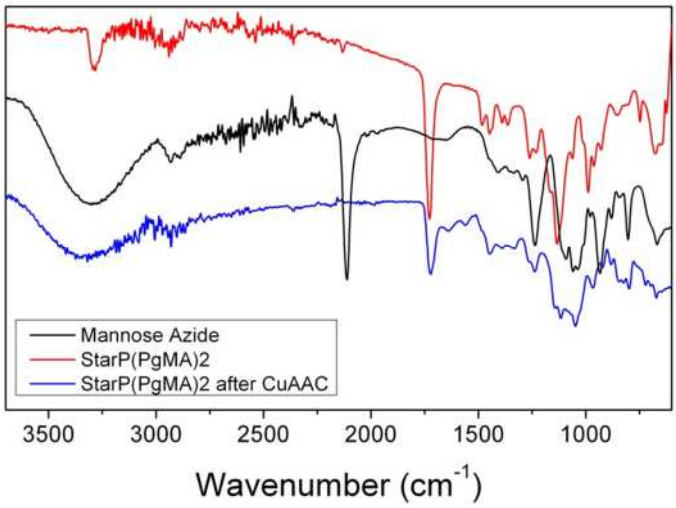

Figure 109: IR spectra of starP(PgMA)2 alkyne bearing polymer, mannose azide and starP(PgMA)2 after CuAAC with mannose azide.

Characterisation of the polymer by FT-IR shows the presence of the broad OH bond stretch at 3300 cm^{-1}. The absence of the azide peak of the mannose azide is also noteworthy, as it excludes the possibility of molecular sugar contamination of the glycopolymer sample.

The combination of these evidence suggest that the polymer has been partially clicked with mannose azide. The aim of the project at the beginning was to synthesise sugar bearing multi-arm star polymers, and this shows the promise of the method. However, the synthesis requires optimisation at several stages of the process, particularly at the crosslinking stage to form higher yield, better defined star architecture.

1.4.1 "Exploding" star polymers: mannose glycopolymer core-crosslinked star, with cleavable crosslinker

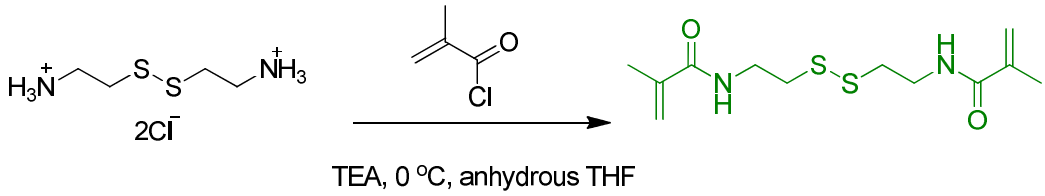

Scheme 41: Synthesis of N,N'-bis(methacryloyl)cystamine from cystamine dihydrochloride.

Recent research by Ferreira and co-workers showed the potential benefits of using a partially soluble crosslinker for synthesis of core-crosslinked star polymers.[265] In their research using *N,N'*-bis(acryloyl)cystamine (**crosslinker9**) as the crosslinking agent in toluene allowed the synthesis of very narrow PDI core-crosslinked star polymers in high yield. Using this work as inspiration, a methacrylamide crosslinker, *N,N'*-bis(methacryloyl)cystamine (**crosslinker10**), was synthesised from commercially available cystamine dihydrochloride, scheme 41.

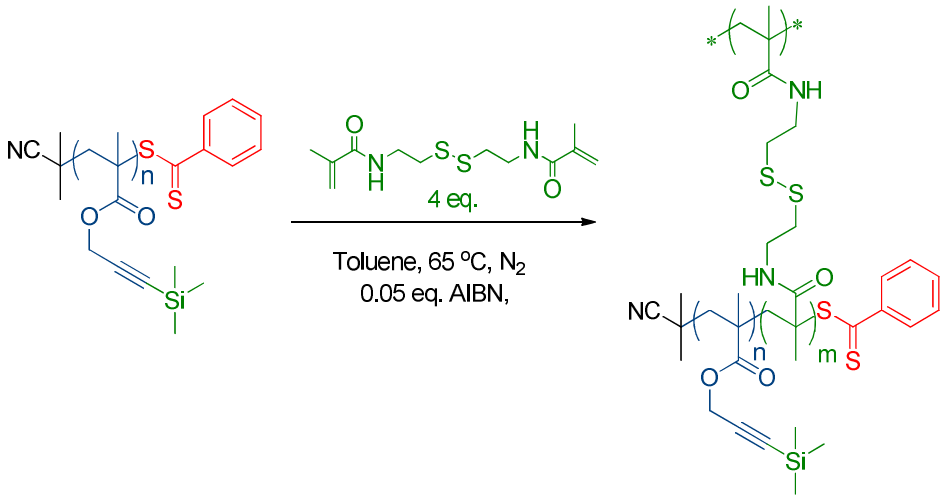

Scheme 42: Reaction scheme for the core-crosslinking reaction with macroRAFT agent P(TMSPgMA)6 and crosslinker10.

This crosslinker was then used in a crosslinking reaction with macroRAFT agent **P(TMSPgMA)6** to form star a core-crosslinked star polymer, scheme 42. AIBN was used as the initiator, in toluene, in which the dimethacrylamide crosslinker was sparingly soluble.

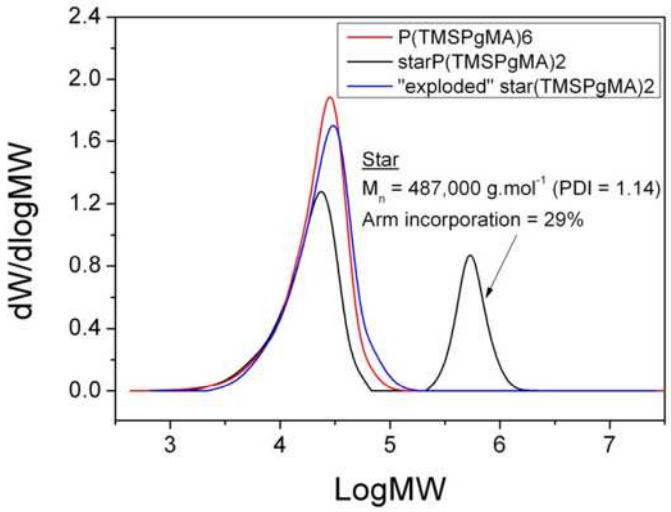

Figure 110: $CHCl_3$ GPC of P(TMSPgMA)6 and resultant starP(TMSPgMA) polymer after reaction with crosslinker1. Ratio of crosslinker5 to macroRAFT agent, P(TMSPgMA)6, was 4. Also showing "exploded" starP(TMSPgMA) after reaction with tributylphosphine.

Analysis of the resultant polymer by chloroform GPC shows a high molecular weight narrow PDI polymer formed after 4 hours, at which point the reaction was terminated. The yield was seen to be low; 29% of the arms were incorporated into star, figure 110.

In order to prove the expected star structure the disulfide bond in **crosslinker10** has been reduced using tributylphosphine. Reduction of the disulfide bond "explodes" the star polymer yielding the linear arm polymer, figure 110.

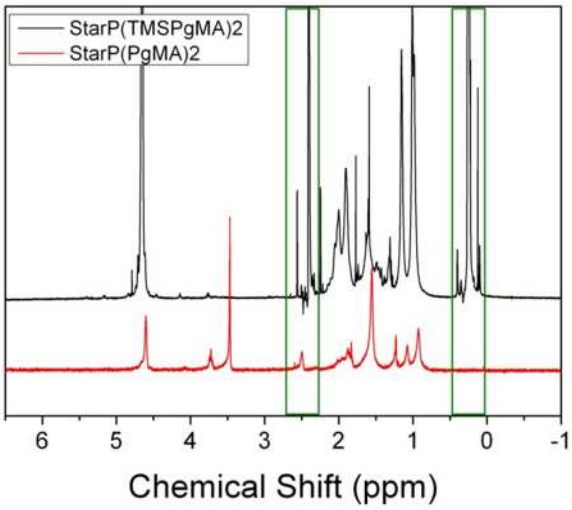

Figure 111: ^{1}H NMR of starP(TMSPgMA) before and after reaction with TBAF. Green boxes highlight the area of the spectra where TMS and alkyne peaks are located.

Removal of the trimethylsilyl protecting groups from the star using TBAF was seen to go to completion using ^{1}H NMR, figure 111; Comparison of the **starP(TMSPgMA)2** and **starP(PgMA)2** shows the presence and then absence of a large peak at ca. 0.13 ppm corresponding to the TMS groups. Similarly the alkyne proton peak is seen to appear around 2.5 ppm after deprotection.

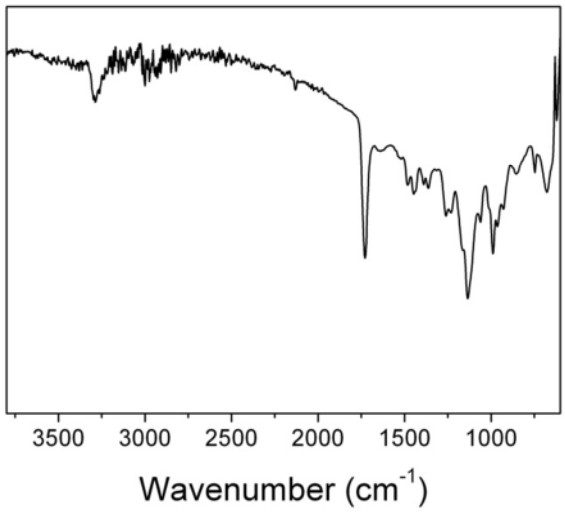

Figure 112: FT-IR spectrum of starP(PgMA)2.

The alkyne peak is also clearly visible, at 3286 cm^{-1} in the FT-IR spectrum of the **starP(PgMA)2**, figure 112.

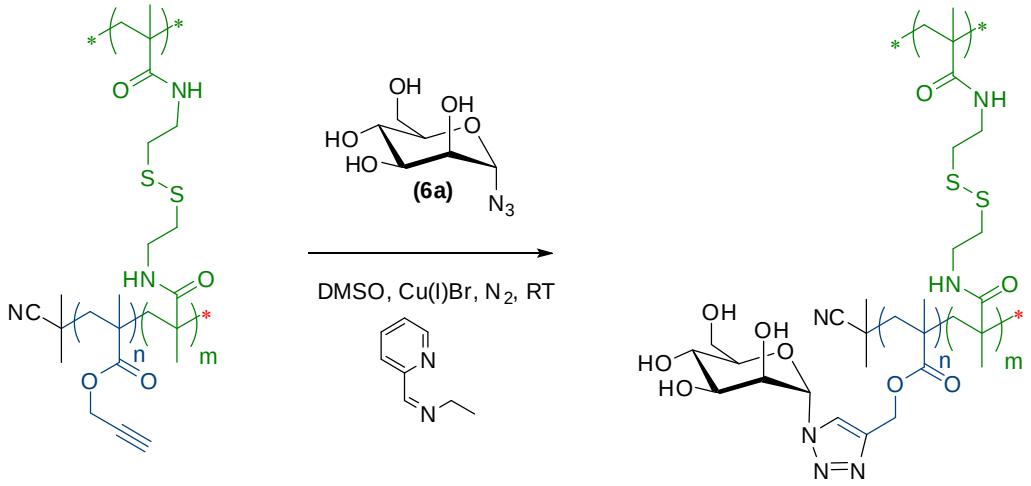

Scheme 43: CuAAC of starP(PgMA)2 with mannose azide using N-(ethyl)-2-pyridylmethanimine as the ligand for the copper catalyst.

Utilising the deprotected alkyne groups of **starP(PgMA)2,** a CuAAC reaction was performed with mannose azide to form a water soluble mannose star polymer with a cleavable core, scheme 43.

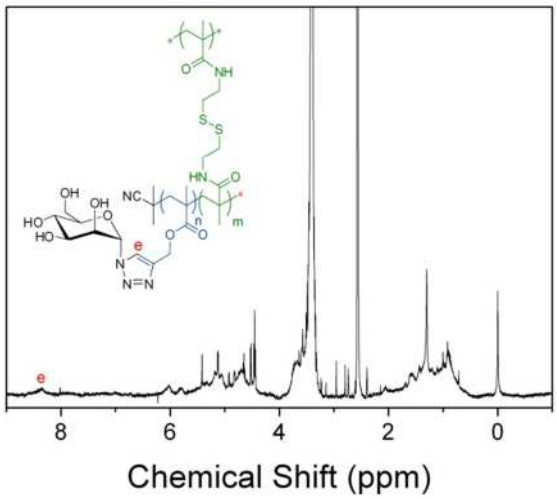

Figure 113: ^{1}H NMR of starP(PgMA)2 after CuAAC with mannose azide in DMSO-d6.

The reaction was left for 48 hours and the resultant polymer purified using dialysis. However, the polymer was seen to be insoluble in water. Analysis by ^{1}H NMR shows that click reaction was unsuccessful. A small peak at ca. 8 ppm shows the presence of a small amount of triazole formed on the polymer, figure 113.

These preliminary reactions highlight the potential of the synthesis of "exploding" glycopolymer star polymers. The final CuAAC reaction was not seen to proceed to give the water soluble glycopolymer. Due to the small scale of the reactions, culminating in the CuAAC reaction, it was not possible to easily repeat the final step. The synthesis and reduction of the disulfide bond of the **starP(PgMA)2** highlights the principle of an exploding star polymer, as has been seen in literature.[134,265] Further reactions are required to determine the viability of this route to star glycopolymers with a cleavable core.

1.4.2 Preliminary study into the synthesis of oil soluble "clickable" star polymers

Synthesis of statistical copolymers of "clickable" monomers with the oil soluble, C_{12-15}MA, is a facile route to introducing chemical functionality randomly along a polymer chain length. A number of monomers with functional groups that are capable of undergoing "click" reactions have been considered here for use in such a system. Other routes such as the unactivated vinyl group on commercially available allyl methacrylate could provide a moiety for post-polymerisation modification by radical thiol-ene chemistry, if it can be incorporated into the polymer backbone without reacting in the polymerisation to form a crosslinked network. As seen in the homopolymerisation of PgMA earlier in the chapter, PgMA can form polymers with broad PDI during RAFT

polymerisation. This is likely due to reaction with the reacts during RAFT polymerisation to form a polymer with a broad PDI.

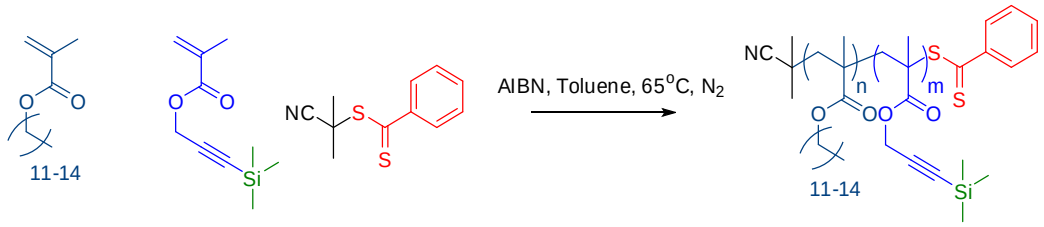

Scheme 44: Reaction scheme for the copolymerisation of $C_{12\text{-}15}$MA and TMSPgMA using RAFT agent 1.

A random copolymer of $C_{12\text{-}15}$MA and TMSPgMA was synthesised using a ratio of 95 : 5 of $C_{12\text{-}15}$MA : TMSPgMA. **RAFT agent1**, which has been shown to control the polymerisation of methacrylates effectively in chapter 3, was used to for the copolymerisation. AIBN was used as the radical source, as the decomposed product takes the same form as the R group of **RAFT agent 1**. The reaction was seen to proceed to >99% conversion by monitoring the disappearance of vinyl protons in ^{1}H NMR, figure 114.

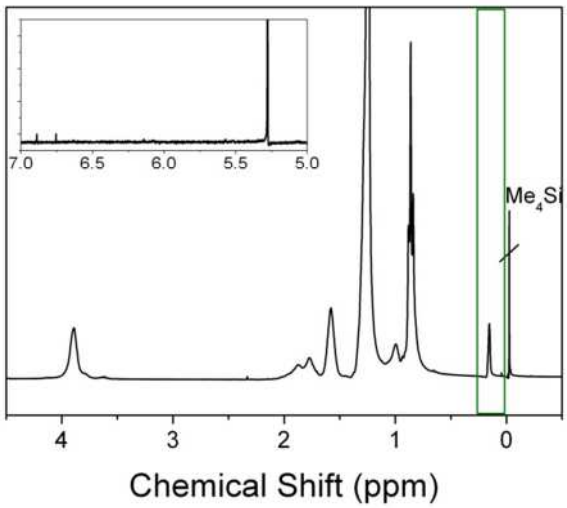

Figure 114: ^{1}H NMR spectrum of P(TMSPgMA-co-$C_{12\text{-}15}$MA) made using RAFT agent1 and AIBN at 65 °C.

The ^{1}H NMR of the P(TMSPgMA-*co*-$C_{12\text{-}15}$MA) is very complicated due to the monomer mixture, however, the TMS group was seen in the ^{1}H NMR after precipitation of the polymer at 0.13 ppm, indicating the incorporation of the TMSPgMA, figure 114. The sharp peak at 0.0 ppm is a reference for NMR, tetramethylsilane, and is not due to loss of protection groups. The reaction was taken to >95% conversion, therefore the ratio of different monomers in the copolymer is assumed to consistent with the ratio of each monomer in the reaction mixture, $C_{12\text{-}15}$MA : TMSPgMA (95 : 5).

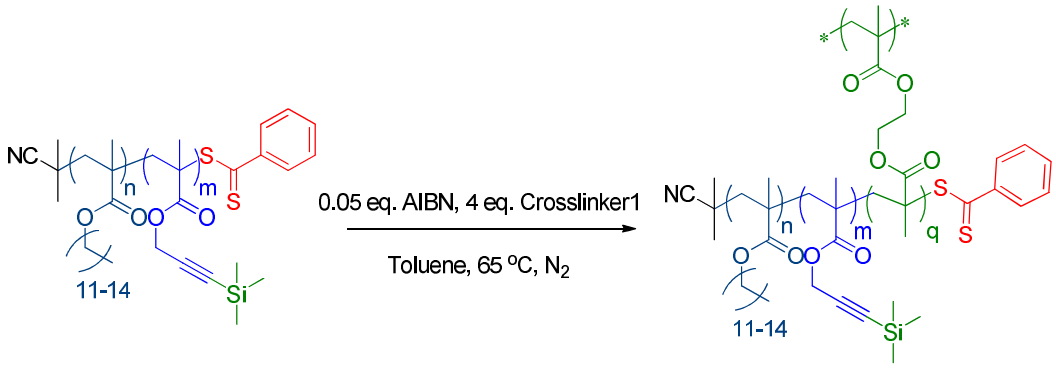

Scheme 45: Chain extension of P(C12-15MA-co-TMSPgMA) with crosslinker1 to form core-crosslinked star polymer.

In order to form a star polymer, the copolymer was chain extended using a ratio of 4:1 of **crosslinker1** to macroRAFT agent, scheme 45. AIBN was added to the degassed reactor to initiate the chain extension/ crosslinking reaction.

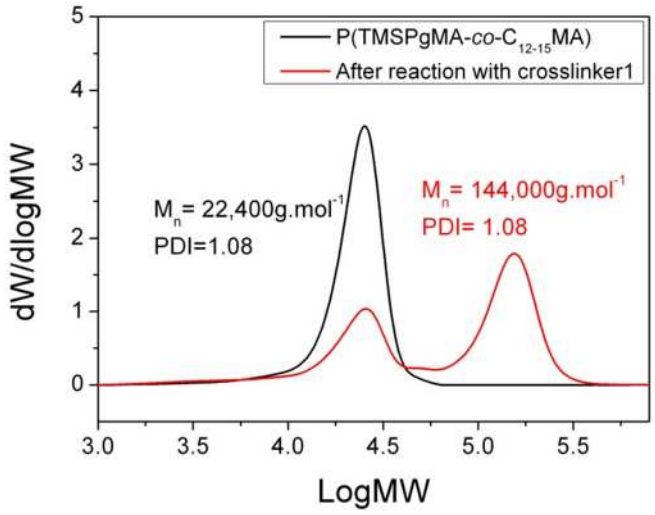

Figure 115: GPC molecular weight distribution of linear P(C_{12-15}MA-co-TMSPgMA), and after crosslinking with crosslinker1 to form starP(C_{12-15}MA-co-TMSPgMA).

After 5 hours, the crosslinker was consumed, and a star polymer was achieved, as seen by GPC, figure 115. Comparing the GPC of the precursor linear p(TMSPgMA-*co*-C_{12-15}MA) with the core-crosslinked polymer highlights a large increase in mass from 22 kg.mol^{-1} to 144 kg.mol^{-1}. The PDI of the resultant star polymer was very low, 1.08. The arm incorporation into star was of high yield; estimating the yield by comparison of the area under arm and star peaks in the MWD from GPC shows 65% arm incorporation into star.

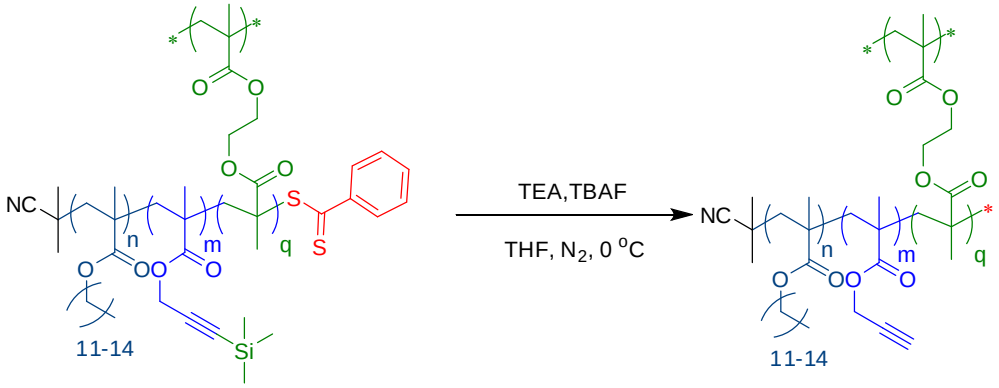

Scheme 46: Deprotection of starP(C_{12-15}MA-co-TMSPgMA) using TBAF to yield starP(C_{12-15}MA-co-PgMA).

StarP($C_{12\text{-}15}$MA-co-TMSPgMA) was dissolved in THF and reacted with TBAF to remove the TMS groups and yield an oil soluble alkyne polymer, scheme 46.

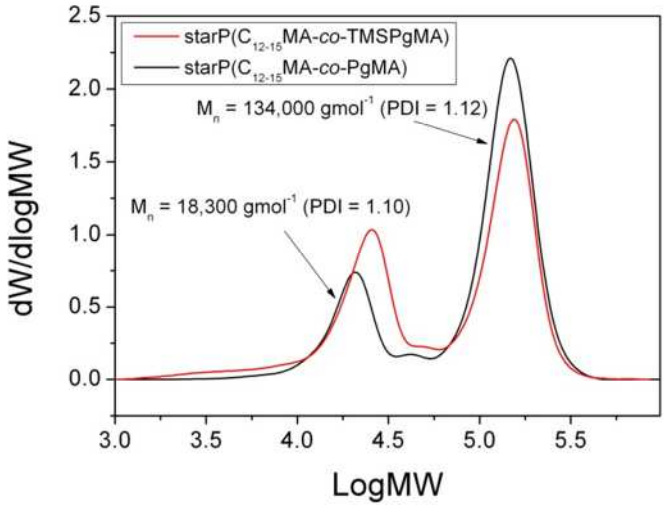

Figure 116: $CHCl_3$ GPC of starP($C_{12\text{-}15}$MA-co-TMSPgMA) and after reaction to form Star(P($C_{12\text{-}15MA}$-co-PgMA).

Evidence of the removal of TMS groups is seen in ^{1}H NMR, where the small peak at 0.13 ppm corresponding to the TMS groups is no longer present, and a new peak corresponding to the alkyne proton at 2.5 ppm appears after deprotection.

These reactions demonstrate the potential of this route to alkyne bearing oil soluble polymers with either linear or star architectures. The narrow PDI of the oil soluble star polymer is particularly promising.

5.3 Conclusions

Alkyne bearing polymers have been synthesised using RAFT chemistry. A protected monomer was seen to be required, and a series of polymers were synthesised using **RAFT agent 1**, with varying M_n and narrow PDI. When targeting high molecular weight the kinetic plot showed deviation from first order kinetics and an increase in PDI was seen in the final polymer. These polymers were deprotected to yield alkyne scaffolds for post polymerisation modification. The RAFT chemistry was seen to be as effective as in the synthesis of these alkyne scaffolds as literature routes using ATRP.

Mannose and galactose azide reacts with the P(PgMA) series of polymers to yield water soluble glycopolymers. A second route to introducing mannose and galactose groups to the polymers was attempted, using thiol-yne chemistry. Mannose was modified at the anomeric carbon to yield a thiol functional sugar; which was then reacted with **P(PgMA)6** to yield a glycopolymer in low yield. After dialysis the polymer was partially soluble in water and ^{1}H NMR and IR data showed partial functionalisation of the alkyne polymer by thio mannose. These results show the difficulty of thiol-yne chemistry in the modification of P(PgMA) polymers. Further investigation is needed, as the resultant polymer may have interesting properties due to the high density of sugars in proximity.

The P(TMSPgMA) polymer was crosslinked using **crosslinker 1** and a novel crosslinker, **crosslinker 10**. **Crosslinker 1** was seen to produce high molecular weight star polymer in low yield, deprotection and subsequent CuAAC with mannose azide yielded a star glycopolymer, with unreacted arms. Using **crosslinker 10,** star polymer with narrow PDI and a cleavable core was synthesised in low yield. This polymer was deprotected to yield an alkyne polymer and reacted with mannose azide in a CuAAC reaction. However the reaction was not seen to proceed to a high conversion of alkyne groups, possibly due to steric hindrance of the star. Finally, an oil soluble alkyne bearing star polymer

was synthesised by copolymerisation of long chain alkyl methacrylate with TMSPgMA and crosslinking with **crosslinker 1**. The deprotection of the TMS groups in the polymer was seen to be successful yielding an oil soluble alkyne bearing polymer for further reaction.

5.4 Experimental

5.4.1 Instrumentation

GPC was used to determinate the molecular weight averages and the PDi of polymers using one of two systems. System 2 with a 390-LC Polymer Laboratories system equipped with a PL-AS RT/MT autosampler, a PL gel 3 µm (50 × 7.5 mm) guard column, two PL gel 5 µm (300 × 7.5 mm) mixed-D columns (suitable for separations up to MW = 2.0×10^6 g.mol^{-1}), a differential refractometer, MALLS, and a photodiode array were used. Solvent used was tetrahydrofuran / triethylamine 95 : 5 (v/v) as the eluent with a flow rate of 1.0 mL.min^{-1}, unless otherwise stated. System 3, with a 390-LC Polymer Laboratories system equipped with a PL-AS RT/MT autosampler, a PL gel 3 µm (50 × 7.5 mm) guard column, two PL gel 5 µm (300 × 7.5 mm) mixed-D columns (suitable for separations up to MW = 2.0×10^6 g.mol^{-1}), a differential refractometer, 4 capillary viscometer and UV detector were used. Solvent used was DMF (0.05% LiBr) as the eluent with a flow rate of 1.0 mL.min^{-1}, unless otherwise stated. Calibrations were set using a single injection of narrow molecular weight PMMA standards (1000 – 1×10^6 g.mol^{-1}) of known concentration, with a minimum of 10 points to form the calibration curve.

All ^{1}H and ^{13}C NMR spectra were recorded on Bruker DPX300, Bruker DPX400 and Bruker DRX500 spectrometers as solutions in deuterated NMR solvents. Chemical shifts are cited as parts per million (ppm). The following abbreviations are used to abbreviate multiplicities; s = singlet, d = doublet, t = triplet, q = quartet, m = multiplet. *b* is used as a prefix to denote a broad peak.

FT-IR was recorded on a VECTOR-22 Bruker spectrometer using a Golden Gate diamond attenuated total reflection cell.

5.4.2 Materials

All reagents were purchased from Sigma Aldrich Company used without purification unless otherwise stated. Hydroxyethyl acrylate and propargyl methacrylate were passed through an alumina column to remove inhibitor before use. Long chain alkyl methacrylate ($C_{12\text{-}15}MA$) was supplied by the Lubrizol Corporation, and used without purification.

5.4.3 General procedure for RAFT polymerisation of propargyl methacrylate, P(PgMA)9

RAFT agent 1 (2.254×10^{-2} g, 1.018×10^{-4} mols), AIBN (1.673×10^{-3} g, 1.018×10^{-5} mols) and allyl methacrylate (0.643 g, 5.090×10^{-3} mols) were charged to reaction vessel, equipped with a magnetic stirrer, and dissolved in toluene (0.65 g). The reaction vessel was sealed with a septum and degassed by purging with nitrogen for 15 minutes. The reaction was initiated by heating in an oil bath (65 ^{o}C), and left to react for 8 hours. The solution was concentrated under a stream of compressed air, and precipitated into methanol: water (95 : 5), yielding a pink powder, which was collected by filtration.

FT-IR: 2957 (w), 2185 (w), 1733 (s), 1447 (w), 1250 (s), 1133 (s, b), 962 (w), 839 (s), 759 (s), 700 (w), 645 (m) cm^{-1};

^{1}H NMR ($CDCl_3$), δ (ppm): 7.50-8.00 (m, 5H, ArH); 4.50 – 4.80 (m, 2nH, OCH_2); 0.75 – 1.90 (m, backbone); 0.17 (*b*s, 9nH, $Si(CH_3)_3$);

^{13}C NMR ($CDCl_3$), δ (ppm): 0.0 (3nC, $Si(CH_3)_3$); (1C, backbone); 45.1 (1C, backbone); 53.2 (1C, OCH_2); 92.5 (1C, $C{\equiv}\underline{C}Si(CH_3)_3$); 98.7 (1C, $\underline{C}{\equiv}CSi(CH_3)_3$); 176.3 (1C, C=O).

5.4.4 Synthesis of trimethylsilyl propargyl methacrylate (TMSPgMA)

Methacryloyl chloride (30.57 g, 2.92 x 10^{-1} mols) in THF (30 mL) was added dropwise to an ice cold solution of 3-trimethylsilyl propyn-1-ol (25.00 g, 1.95 x 10^{-1} mols) and triethylamine (39.44 g, 3.90 x 10^{-1} mols) in THF (170 mL) over 2 hours. The reaction mixture was left to react for 16 hours at ambient temperature after addition. The reaction mixture was then filtered, and passed through a column of activated basic aluminium oxide. Volatiles were then removed under vacuum to yield a clear colourless liquid (Yield 38.23 g, recovery 97%).

FT-IR: 2961 (m), 2187 (w), 1723 (s), 1638 (m), 1452 (w), 1367 (w), 1315 (m), 1292 (m), 1251 (m), 1147 (s), 1105 (s), 970 (w), 942 (m), 839 (s), 760 (s), 700 (w), 664 (m) cm^{-1};

^{1}H NMR ($CDCl_3$), δ (ppm): 0.19 (s, 9H, $Si(CH_3)_3$); 1.97 (s, 3H, CH_3); 4.76 (s, 2H, OCH_2); 5.62 (s, 1H, -C=C(H)H); 6.17 (s, 1H, -C=C(H)H);

^{13}C NMR ($CDCl_3$), δ (ppm): 0.0 (3C, $Si(CH_3)_3$); 18.4 (1C, $CH_3C=CH_2$); 53.1 (1C, OCH_2); 93.1 (1C, $C\equiv CSi(CH_3)_3$); 127.2 (1C, $CH_3C=CH_2$); 135.8 (1C, $CH_3C=CH_2$); 166.6 (1C, C=O).

5.4.5 General procedure for RAFT polymerisation of trimethylsilyl propargyl methacrylate

RAFT agent 1 (0.113 g, 5.10 x 10^{-4} mols), AIBN (8.40 x 10^{-3} g, 5.10 x 10^{-5} mols) and trimethylsilyl propargyl methacrylate (10.00 g, 5.10 x 10^{-2} mols) were charged to Schlenk tube, equipped with a magnetic stirrer, and dissolved in toluene (8.77 mL). Mesitylene (1.22 g, 1.02 x 10^{-2} mols) was added as an inert NMR standard. The reaction vessel was sealed with a septum and degassed by purging with nitrogen for 30 minutes.

The reaction was initiated by heating in an oil bath (65 °C) and sampled regularly for NMR and GPC analysis. The solution was concentrated under a stream of compressed air, and precipitated into hexane, yielding a pink powder, which was collected by filtration.

FT-IR: 2957 (w), 2185 (w), 1733 (s), 1447 (w), 1250 (s), 1133 (s, b), 962 (w), 839 (s), 759 (s), 700 (w), 645 (m) cm^{-1};

^{1}H NMR ($CDCl_3$), δ (ppm): 7.50-8.00 (m, 5H, ArH); 4.50 – 4.80 (m, 2nH, OCH_2); 0.75 – 1.90 (m, backbone); 0.17 (*b*s, 9nH, $Si(CH_3)_3$);

^{13}C NMR ($CDCl_3$), δ (ppm): 0.0 (3nC, $Si(CH_3)_3$); (1C, backbone); 45.1 (1C, backbone); 53.2 (1C, OCH_2); 92.5 (1C, $C\equiv\underline{C}Si(CH_3)_3$); 98.7 (1C, $\underline{C}\equiv CSi(CH_3)_3$); 176.3 (1C, C=O).

5.4.6 Removal of trimethylsilyl protection groups

P(TMSPgMA) (500 mg, 2.55 mmol of trimethylsilyl groups) and acetic acid (0.22 mL, 3.8 mmol) were dissolved in THF (10 mL). Nitrogen was bubbled (ca. 10 min) and the solution was cooled to -20 °C. A 1 M solution of TBAF·$3H_2O$ in THF (0.32 mL, 3.2 mmol) was then added dropwise. The resultant mixture was stirred at this temperature for 30 min and then allowed to warm up to ambient temperature and stirred overnight. Amberlite IR-120 ion-exchange resin (ca. 2 g) was added and the resulting slurry stirred for 30 min. The resin was then filtered off and the resulting solution was concentrated under reduced pressure. The polymer was precipitated into petroleum ether to yield an off-white powder.

FT-IR: 3286 (w), 3000 (w), 1728 (s), 1447, 1362, 1261, 1135, 989, 747, 678, 621 cm^{-1};

^{1}H NMR ($CDCl_3$), δ (ppm): 4.62 (s, $C\underline{H_2}CH$), 2.51 (s, $CH_2C\underline{H}$), 0.80-2.10 (m, backbone).

5.4.7 Synthesis of sugar azides

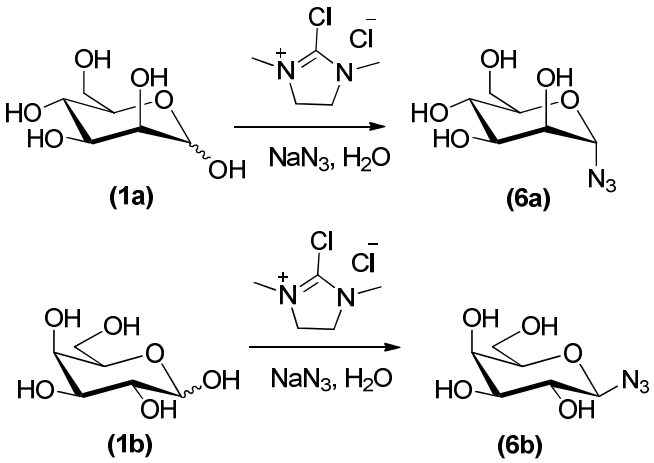

Scheme 32: Synthesis of mannose and galactose azide using DMC in a one-step process.[37,204]

D-(+)-Mannose (5.00 g, 27.8 mmol) and sodium azide, (20.0 g, 307.7 mmol) were dissolved in water (50 mL) and stirred at 0 ^{o}C for 15 hours. 2-Chloro-1,3-dimethylimidazolinium chloride (20.0 g, 106.8 mmol) was added slowly and reacted for 1 hour. Water was removed under reduced pressure, and the resultant solid was dissolved in ethanol (40 mL) with stirring. The remaining insoluble solid was removed by filtration and the filtrate was washed with ethanol. The sugar containing ethanol solution was passed through, an amberlite IR-120 column (amberlite was washed with ethanol first). Volatiles were removed under reduced pressure, and the product extracted with water (50 mL) / DCM (5 x 50 mL). Product was freeze dried to give a hygroscopic white solid. Yield = 4.80 g, recovery = 83%

FT-IR*:* 3303, 2607, 2593, 2473, 2331, 2110, 1236, 1059, 934, 803, 669 cm^{-1};

^{1}H NMR (DMSO-d6), δ (ppm): 3.34-3.52 (m, 5H), 3.67 (m, 1H), 4.28 (*b*s, 4 x OH), 5.35 (d, 1H, J = 1.89 Hz);

^{13}C NMR (DMSO-d6), δ (ppm): 90.2 (C1), 76.6 (C5), 70.2 (C2), 69.8 (C3), 66.4 (C4), 60.9 (C6).

5.4.7.1 Galactose azide

FT-IR: 3319, 2127, 1371, 1306, 1270, 1138, 1051, 983, 942, 891, 775, 705 cm^{-1};

^{1}H NMR (DMSO-d6), δ (ppm): 3.32 (m, 2H), 3.47 (m, 3H), 3.65 (d, 1H), 3.8-4.5 (*b*s, 4 x OH), 4.35 (d, 1H);

^{13}C NMR (DMSO-d6), δ (ppm): 90.9 (C1), 77.8 (C5), 73.4 (C2), 70.4 (C3), 68.3 (C4), 60.6 (C6).

5.4.8 Synthesis of thio mannose

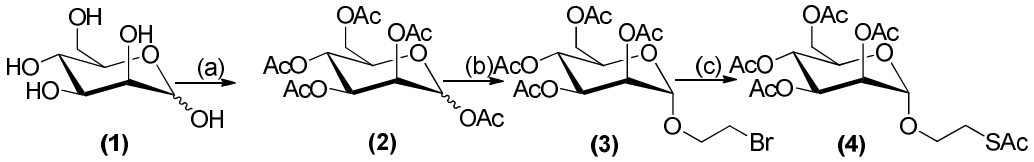

Scheme 37: Synthesis of 2'- thioethyl -O-α-D-mannopyranoside. Reagents and conditions: a) 2-Bromoethanol, BF3OEt2, -20 °C to ambient temperature, b) KSAc, Acetone, reflux 60 °C, c) CH3ONa (cat.), CH3OH, ambient temperature.

5.4.8.1 Synthesis of 1,2,3,4,6-Penta-O-acetyl- α-D-mannopyranoside

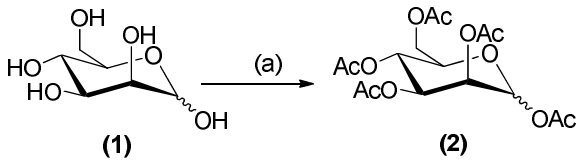

Scheme 47: Synthesis of acetylated mannose. Prepared as described by Geng and co-workers,[35,199] and Watt et al.[240]

D-Mannose (9.0 g, 49 mmol) was suspended in acetic anhydride (25 mL) and the resulting mixture was stirred for 5 min. Three drops of conc. sulfuric acid were added with evolution of heat. After cooling to ambient temperature, Dichloromethane (100 mL) was added and the resulting solution was stirred for 10 min. Then the reaction mixture was neutralised by adding a saturated solution of sodium bicarbonate (3×100 mL). The organic layer was then washed with water (2x200 mL) and dried over sodium sulfate, filtered and the volatiles removed under reduced pressure to give 1,2,3,4,6-penta-O-acetyl-α-D-mannopyranoside as a colourless viscous oil. Obtained 17.95 g. The crude product was used for further reactions.

5.4.8.2 2'-Bromoethyl 2,3,4,6-tetra-O-acetyl-α-D-mannopyranoside

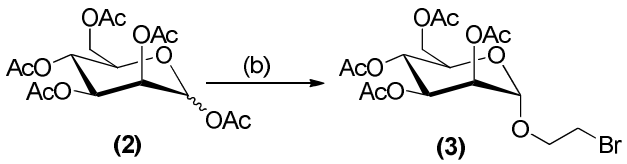

Scheme 48: Synthesis of bromo-sugars from acetylated sugars. (b) - Prepared as described by Rama Rao et al.[234]

A solution of boron trifluoride etherate (25.99 mL, 205.1 mmol) and 1,2,3,4,6-penta-O-acetyl-α-D-mannopyranoside (20.0 g, 51.2 mmol) and 2-bromoethanol (7.42 mL, 102 mmol) in dry dichloromethane (250 mL) was stirred in the dark under a nitrogen atmosphere for overnight. TLC analysis, using ethyl acetate/petroleum ether (1:2, v/v) as the developing solvent, showed that the reaction had gone to completion (starting material R_f 0.53, product R_f 0.63). 200 mL dichloromethane was added, then the

reaction mixture was neutralised by adding a saturated solution of sodium bicarbonate (3×100 mL) and the resulting solution was washed with water (2×200 mL). The combined organic layers were dried over magnesium sulfate, filtered and the volatiles removed under reduced pressure. The crude product was purified by flash chromatography (SiO_2, ethyl acetate/petroleum ether (1 : 4, v/v). The relevant fractions were combined and volatiles were removed under reduced pressure. Yield= 12.12 g, recovery = 50% as colourless crystals.

^{1}H NMR ($CDCl_3$), δ (ppm): 1.99 (s, 3H, CH_3); 2.05 (s, 3H, CH_3); 2.10 (s, 3H, CH_3); 2.15 (s, 3H, CH_3); 3.50 (m, 2H, *C*H_2Br); 3.85-3.99 (m, 2H, O*C*H_2); 4.10-4.15 (m, 3H, CHCH_2OAc); 4.27 (m, 1H, CH); 4.86 (d, *J* = 1.76 Hz, 1H, CH); 5.25-5.38 (m, 3H, 3×CH);

^{13}C NMR ($CDCl_3$) δ (ppm): 20.69 (1C, CH_3); 20.72 (1C, CH_3); 20.76 (1C, CH_3); 20.89 (1C, CH_3); 29.63 (1C, *C*H_2Br); 62.45 (1C, CH_2OAc); 66.02 (1C, CH); 68.51 (1C, CH); 68.97 (1C, CH); 69.03 (1C, CH_2CH_2O);69.45 (1C, CH); 97.76 (1C, $C_{anomeric}$); 169.81 (1C, $CH_3C(O)O$); 169.91 (1C, $CH_3C(O)O$); 170.07 (1C, $CH_3C(O)O$); 170.68 (1C, $CH_3C(O)O$);

Exact Mass Spectrometry (+ESI-MS) *m/z*: Calculated. 477.0367, Found: 477.0367.

5.4.8.3 2'-Acetylthioethyl 2,3,4,6-tetra-O-acetyl-α-D-mannopyranoside

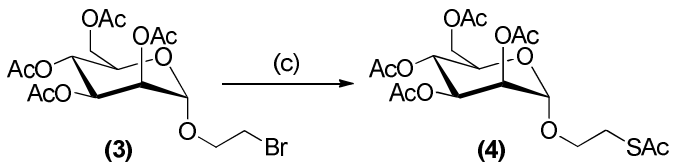

Scheme 49: Synthesis of acetylated thio mannose from bromine intermediate. Prepared as described by Grandjean et al.[235,236]

A solution of 2'-bromoethyl 2,3,4,6-tetra-O-acetyl-α-D-mannopyranoside (10.10 g, 22.2 mmol) in anhydrous DMF (50 mL) was treated with potassium thioacetate (14.48 g, 130 mmol) and the reaction mixture stirred at 50 °C overnight. TLC analysis, using ethyl acetate/petroleum ether (1:1, v/v) as the developing solvent, showed that the reaction had gone to completion (starting material R_f = 0.69, product R_f = 0.59). The reaction mixture was concentrated to dryness under reduced pressure, dissolved in DCM (30 mL) and then washed with deionised water (4×50 mL). The organic layers were dried over magnesium sulfate, filtered and the volatiles removed under reduced pressure. The crude product was purified by flash chromatography (SiO_2, ethyl acetate/petroleum ether (1:1, v/v). The relevant fractions were collected, combined and concentrated to dryness under reduced pressure. Yield = 9.20 g (recovery = 92%) of 2'-acetylthioethyl 2,3,4,6-tetra-O-acetyl-α-D-mannopyranoside as colourless crystals.

^{1}H NMR ($CDCl_3$), δ (ppm); 2.00 (s, 3H, CH_3); 2.06 (s, 3H, CH_3); 2.10 (s, 3H, CH_3); 2.16 (s, 3H, CH_3); 2.36 (s, 3H, CH_3); 3.13 (m, 2H, C$\underline{H_2}$SAc); 3.64 (m, 2H, C$\underline{H_2}$CH$_2$SAc); 4.14 (d, 3H, CHC$\underline{H_2}$OAc); 4.25 (1H, CH); 4.83 (d, *J* = 1.76 Hz, 1H, CH); 5.21-5.36 (m, 3H, 3 × CH);

Exact Mass Spectrometry (+ESI-MS) *m/z*: Calculated. 473.1094, Found: 473.1088.

5.4.8.4 2'- Thioethyl -O-α-D-mannopyranoside

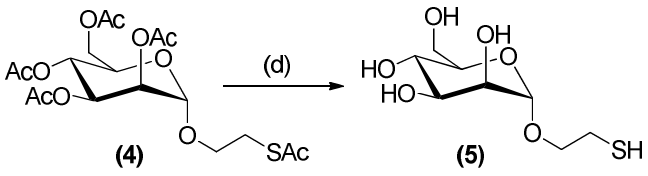

Scheme 50: Deprotection of thio sugars as described by Grandjean and co-workers.[198,235,236]

2'-Acetylthioethyl 2,3,4,6-tetra-*O*-acetyl-α-D-mannopyranoside **(12)** (8.01 g, 19.2 mmol) was dissolved in methanol (100 mL). Sodium methoxide (25% wt in methanol) (21.9 mL, 96.0 mmol) was added, the mixture was stirred at ambient temperature for 3 h. Amberlite IR-120 ion-exchange resin was added and stirred with the reaction mixture for 30 min. The resin beads were then decanted off and the resulting solution concentrated to dryness in reduced pressure. The sugar was dissolved in water and freeze-dried to yield a white solid Obtained 4.62 g (82%) of 2'-thioethyl-*O*-α-D-mannopyranoside as colourless crystals.

FT-IR: 3358 (bs), 2927, 2097, 1644, 1301, 1262, 1132, 1056, 976, 913, 881, 812 cm^{-1};

^{1}H NMR (D_2O), δ (ppm): 3.45 (m, 2H, CH_2N_3); 3.55-3.60 (m, 2H, $CH_2CH_2N_3$); 3.61-3.67 (m, 2H, CH_2OH); 3.67-3.91 (m, 4H, 4×CH); 4.92 (d, *J* = 1. 5 Hz, 1H, CH);

^{13}C NMR (D_2O), δ (ppm) 50.20 (1C, CH_2SH); 60.91 (1C, CH_2OH); 66.30 (1C, CH_2CH_2O); 66.68 (1C, CH); 69.97 (1C, CH); 70.39 (1C, CH); 72.89 (1C, CH); 99.81 ($C_{anomeric}$);

Exact Mass Spectrometry (+ESI-MS) *m/z*: Calculated: 263.0560, Found: 263.0560.

5.4.9 General procedure for CuAAC of sugar azides to poly (propargyl methacrylate)

Poly (propargyl methacrylate) (10 mg, 0.08 mmol of alkyne groups), mannose azide (20 mg, 0.10 mmol) and triethylamine (3 mg, 0.03 mmol) were dissolved in DMSO (2 mL). The solution was bubbled with nitrogen for 30 minutes and *tris*-(benzyltriazolylmethyl)amine (12 mg, 0.02 mmol) and copper(I) bromide (3 mg, 0.02 mmol) added. The reaction was stirred at ambient temperature for 24 hours. The

reaction was diluted with water (50 mL) and dialysed against deionised water (1 L). The resultant aqueous solution was freeze dried to yield a white solid.

5.4.10 Thiol-yne click reaction of thio mannose to poly(propargyl methacrylate)

P(PgMA)6 (20 mg, 0.16 mmol of alkyne groups), 2'- thioethyl -O-α-D-mannopyranoside (97 mg, 0.40 mmol) and 2,2-dimethoxy-2-phenylacetophenone (4 mg, 0.02 mmol) were dissolved in DMSO (2.5 mL). The solution was bubbled with nitrogen for 10 mins. The reaction was exposed to 365 nm UV light (36 W) to initiate the reaction and left to react for 24 hours. The reaction was diluted with water (20 mL) and dialysed using centrifuge dialysis. The resultant solid was dissolved in water and freeze dried to yield a white solid (15 mg, 76.6%).

5.4.11 Synthesis of N,N′-bis(methacryloyl)cystamine (crosslinker10)

Cystamine dihydrochloride (10 g, 44.4 mmol) was charged to a dry 3- neck flask in a nitrogen atmosphere and dissolved in anhydrous THF (20 mL). Triethylamine (8.99 g, 88.8 mmol) was added and the reaction cooled to 0 ^{o}C. Methacryloyl chloride (4.77 mL, 48.8 mmol) was added slowly over an hour. The reaction mixture was reacted for 1 hour at 0 ^{o}C, and then left to react at ambient temperature overnight. The resultant reaction mixture was filtered to remove through an alumina column to remove any acid formed, and purified by flash chromatography (SiO_2, ethyl acetate/petroleum ether (1:1, v/v), R_f = 0.20). The relevant fractions were collected, combined and

concentrated to dryness under reduced pressure. Yield = 8.45 g (Recovery = 66%) of *N*,*N*′-bis(methacryloyl)cystamine as a colourless powder.

FT-IR: 3331, 2922, 1652, 1610, 1534, 1434, 1295, 1210, 1184, 928, 646 cm^{-1};

^{1}H NMR ($CDCl_3$), δ (ppm): 6.45 (s, 2H, NH), 5.74 (s, 2H, C(H)$\underline{H_{cis}}$), 5.36 (d, J= 1.0 Hz, 2H, C(H)$\underline{H_{trans}}$), 3.65 (t, J= 6.7 Hz, 4H, NC$\underline{H_2}$), 2.89 (d, J = 6.8 Hz, 4H, SC$\underline{H_2}$), 1.97 (d, J = 0.8 Hz, 6H, CH_3);

^{13}C NMR ($CDCl_3$), δ (ppm): 18.65 (2C, $\underline{C}H_3$), 37.79 (2C, S$\underline{C}H_2$), 38.70 (2C, N$\underline{C}H_2$), 119.99 (2C, C=$\underline{C}H_2$), 139.74 (2C, $\underline{C}$=CH_2), 168.68 (2C, $\underline{C}$=O);

Exact Mass Spectrometry (+ESI-MS) *m/z*: Calculated. 311.0856 (Na+), Found: 311.0855.

5.4.12 General procedure for copolymerisation of "clickable" monomer with C12-15MA

RAFT agent 1 (0.0127 g, 5.09 x 10^{-5} mols), AIBN (8.36 x 10^{-4} g, 5.09 x 10^{-6} mols), trimethylsilyl propargyl methacrylate (0.050 g, 2.55 x 10^{-4} mols) and long chain alkyl methacrylate (1.331 g, 4.839 x 10^{-3} mols) were charged to reaction vessel, equipped with a magnetic stirrer, and dissolved in toluene (1.3 mL). The reaction vessel was sealed with a septum and degassed by purging with nitrogen for 15 minutes. The reaction was initiated by heating in an oil bath (65 ^{o}C) and reacted for 8 hours. The solution was concentrated under a stream of compressed air, and precipitated into methanol : ethyl acetate 80 : 20, yielding a pink viscous liquid, which was collected and dried. Yield 1.25 g.

5.4.13 Removal of TMS groups from P(C12-15MA-co-TMSPgMA)

P($C_{12\text{-}15}$MA-*co*-TMSPgMA) (500 mg, 2.55 mmol of trimethylsilyl groups) and acetic acid (8.3 mg, 0.14 mmol) were dissolved in THF (10 mL). Nitrogen was bubbled (ca. 10 min) and the solution was cooled to -20 °C. A 1 M solution of TBAF·$3H_2O$ in THF (0.14 mL, 0.14 mmol) was then added dropwise. The resultant mixture was stirred at this temperature for 30 min and then allowed to warm up to ambient temperature and stirred overnight. Amberlite IR-120 ion-exchange resin (ca. 5 g) was added and the resulting slurry stirred for 30 min. The resin was then filtered off and the resulting solution was concentrated under reduced pressure. The polymer was precipitated into ethyl acetate : methanol (20 : 80) to yield a pink viscous liquid.

^{1}H NMR ($CDCl_3$), δ (ppm): 4.6 (s, C(O)OC$\underline{H}_2$), 2.43 (s, $CH_2C\underline{H}$), 0.80-2.10 (m, backbone and pendant long alkyl chain protons).

5.5 References

(16) Moad, G.; Rizzardo, E.; Thang, S. H. *Aust. J. Chem.* **2006**, *59*, 669.

(27) Kolb, H. C.; Finn, M. G.; Sharpless, K. B. *Angew. Chem., Int. Ed.* **2001**, *40*, 2004.

(29) Slavin, S.; Burns, J.; Haddleton, D. M.; Becer, C. R. *Eur. Polym. J.* **2010**, *47*, 435.

(31) Semsarilar, M.; Ladmiral, V.; Perrier, S. *Macromolecules* **2010**, *43*, 1438.

(32) Mantovani, G.; Ladmiral, V.; Tao, L.; Haddleton, D. M. *Chem. Commun.* **2005**, 2089.

(33) Lutz, J. F.; Borner, H. G.; Weichenhan, K. *Macromolecules* **2006**, *39*, 6376.

(34) Ladmiral, V.; Mantovani, G.; Clarkson, G. J.; Cauet, S.; Irwin, J. L.; Haddleton, D. M. *J. Am. Chem. Soc.* **2006**, *128*, 4823.

(35) Geng, J.; Lindqvist, J.; Mantovani, G.; Haddleton, D. M. *Angew. Chem., Int. Ed.* **2008**, *47*, 4180.

(37) Campos, L. M.; Killops, K. L.; Sakai, R.; Paulusse, J. M. J.; Damiron, D.; Drockenmuller, E.; Messmore, B. W.; Hawker, C. J. *Macromolecules* **2008**, *41*, 7063.

(39) Willcock, H.; O'Reilly, R. K. *Polym. Chem.* **2010**, *1*, 149.

(45) Lowe, A. B. *Polym. Chem.* **2010**, *1*, 17.

(134) Syrett, J. A.; Haddleton, D. M.; Whittaker, M. R.; Davis, T. P.; Boyer, C. *Chem. Commun.* **2011**, *47*, 1449.

(183) Bertozzi, C. R.; Kiessling, L. L. *Science* **2001**, *291*, 2357.

(184) Gestwicki, J. E.; Cairo, C. W.; Strong, L. E.; Oetjen, K. A.; Kiessling, L. L. *J. Am. Chem. Soc.* **2002**, *124*, 14922.

(185) Geng, J.; Mantovani, G.; Tao, L.; Nicolas, J.; Chen, G.; Wallis, R.; Mitchell, D. A.; Johnson, B. R. G.; Evans, S. D.; Haddleton, D. M. *J. Am. Chem. Soc.* **2007**, *129*, 15156.

(186) Hawker, C. J.; Wooley, K. L. *Science* **2005**, *309*, 1200.

(187) Kiessling, L. L.; Gestwicki, J. E.; Strong, L. E. *Curr. Opin. Chem. Biol.* **2000**, *4*, 696.

(188) Kiessling, L. L.; Gestwicki, J. E.; Strong, L. E. *Angew. Chem., Int. Ed.* **2006**, *45*, 2348.

(189) Voit, B.; Appelhans, D. *Macromol. Chem. Phys.* **2010**, *211*, 727.

(190) Kiessling, L. L.; Strong, L. E.; Gestwicki, J. E. In *Annu. Rep. Med. Chem.*; Academic Press Inc: San Diego, 2000; Vol. 35, p 321.

(191) Haddleton, D. M.; Edmonds, R.; Heming, A. M.; Kelly, E. J.; Kukulj, D. *New J. Chem.* **1999**, *23*, 477.

(192) Okada, M. *Prog. Polym. Sci.* **2001**, *26*, 67.

(193) Ohno, K.; Tsujii, Y.; Fukuda, T. *J. Polym. Sci., Part A: Polym. Chem.* **1998**, *36*, 2473.

(194) Ting, S. R. S.; Granville, A. M.; Quémener, D.; Davis, T. P.; Stenzel, M. H.; Barner-Kowollik, C. *Aust. J. Chem.* **2007**, *60*, 405.

(195) Roy, R. *Trends Glycosci. Glycotechnol.* **1996**, *8*, 79.

(196) Ladmiral, V.; Melia, E.; Haddleton, D. M. *Eur. Polym. J.* **2004**, *40*, 431.

(197) García-Oteiza, M. C.; Sánchez-Chaves, M.; Arranz, F. *Macromol. Chem. Phys.* **1997**, *198*, 2237.

(198) Geng, J.; Mantovani, G.; Tao, L.; Nicolas, J.; Chen, G. J.; Wallis, R.; Mitchell, D. A.; Johnson, B. R. G.; Evans, S. D.; Haddleton, D. M. *J. Am. Chem. Soc.* **2007**, *129*, 15156.

(199) Geng, J.; Lindqvist, J.; Mantovani, G.; Chen, G.; Sayers, C. T.; Clarkson, G. J.; Haddleton, D. M. *QSAR Comb. Sci.* **2007**, *26*, 1220.

(200) Hetzer, M.; Chen, G.; Barner-Kowollik, C.; Stenzel, M. H. *Macromol. Biosci.* **2010**, *10*, 119.

(201) Xu, N.; Wang, R.; Du, F.-S.; Li, Z.-C. *J. Polym. Sci., Part A: Polym. Chem.* **2009**, *47*, 3583.

(202) Nurmi, L.; Lindqvist, J.; Randev, R.; Syrett, J.; Haddleton, D. M. *Chem. Commun.* **2009**, 2727.

(203) Becer, C. R.; Babiuch, K.; Pilz, D.; Hornig, S.; Heinze, T.; Gottschaldt, M.; Schubert, U. S. *Macromolecules* **2009**, *42*, 2387.

(204) Gress, A.; Volkel, A.; Schlaad, H. *Macromolecules* **2007**, *40*, 7928.

(205) Boyer, C.; Bousquet, A.; Rondolo, J.; Whittaker, M. R.; Stenzel, M. H.; Davis, T. P. *Macromolecules* **2009**, *43*, 3775.

(206) Semsarilar, M.; Ladmiral, V.; Perrier, S. b. *Macromolecules* **2010**, *43*, 1438.

(207) Hu, Z.; Fan, X.; Zhang, G. *Carbohydr. Polym.* **2010**, *79*, 119.

(208) Huisgen, R. *Angew. Chem., Int. Ed.* **1968**, *7*, 321.

(209) Tornoe, C. W.; Christensen, C.; Meldal, M. *The Journal of Organic Chemistry* **2002**, *67*, 3057.

(210) Rostovtsev, V. V.; Green, L. G.; Fokin, V. V.; Sharpless, K. B. *Angew. Chem., Int. Ed.* **2002**, *41*, 2596.

(211) Hein, J. E.; Fokin, V. V. *Chem. Soc. Rev.* **2010**, *39*, 1302.

(212) Davis, B. G.; Lloyd, R. C.; Jones, J. B. *The Journal of Organic Chemistry* **1998**, *63*, 9614.

(213) Tanaka, T.; Nagai, H.; Noguchi, M.; Kobayashi, A.; Shoda, S.-i. *Chem. Commun.* **2009**, 3378.

(214) Kato, M.; Kamigaito, M.; Sawamoto, M.; Higashimura, T. *Macromolecules* **1995**, *28*, 1721.

(215) Matyjaszewski, K.; Xia, J. H. *Chemical Reviews* **2001**, *101*, 2921.

(216) Wang, J. S.; Matyjaszewski, K. *J. Am. Chem. Soc.* **1995**, *117*, 5614.

(217) Kamigaito, M.; Ando, T.; Sawamoto, M. *Chemical Reviews* **2001**, *101*, 3689.

(218) Ouchi, M.; Terashima, T.; Sawamoto, M. *Chemical Reviews* **2009**, *109*, 4963.

(219) Rosen, B. M.; Percec, V. *Chemical Reviews* **2009**, *109*, 5069.

(220) Matyjaszewski, K.; Xia, J. *Chemical Reviews* **2001**, *101*, 2921.

(221) Besenius, P.; Slavin, S.; Vilela, F.; Sherrington, D. C. *Reactive and Functional Polymers* **2008**, *68*, 1524.

(222) Schaefgen, J. R.; Flory, P. J. *J. Am. Chem. Soc.* **1948**, *70*, 2709.

(223) Ning, X.; Rui, W.; Fu-Sheng, D.; Zi-Chen, L. *J. Polym. Sci., Part A: Polym. Chem.* **2009**, *47*, 3583.

(224) Moad, G.; Rizzardo, E.; Thang, S. H. *Acc. Chem. Res.* **2008**, *41*, 1133.

(225) Moad, G.; Rizzardo, E.; Thang, S. H. *Aust. J. Chem.* **2009**, *62*, 1402.

(226) Moad, G.; Thang, S. H. *Aust. J. Chem.* **2009**, *62*, 1379.

(227) Tao, L.; Liu, J.; Tan, B. H.; Davis, T. P. *Macromolecules* **2009**, *42*, 4960.

(228) Luzon, M.; Boyer, C.; Peinado, C.; Corrales, T.; Whittaker, M.; Tao, L.; Davis, T. P. *J. Polym. Sci., Part A: Polym. Chem.* **2010**, *48*, 2783.

(229) Liu, B.; Kazlauciunas, A.; Guthrie, J. T.; Perrier, S. *Macromolecules* **2005**, *38*, 2131.

(230) Moad, G.; Rizzardo, E.; Thang, S. H. *Polymer* **2008**, *49*, 1079.

(231) Thibault, R. J.; Takizawa, K.; Lowenheilm, P.; Helms, B.; Mynar, J. L.; Fréchet, J. M. J.; Hawker, C. J. *J. Am. Chem. Soc.* **2006**, *128*, 12084.

(232) Campos, L. M.; Killops, K. L.; Sakai, R.; Paulusse, J. M. J.; Damiron, D.; Drockenmuller, E.; Messmore, B. W.; Hawker, C. J. *Macromolecules* **2008**, *41*, 7063.

(233) Hough, L.; McCarthy, K. C.; Richardson, A. C. *Recueil des Travaux Chimiques des Pays-Bas* **1991**, *110*, 450.

(234) Chernyak, A. Y.; Sharma, G. V. M.; Kononov, L. O.; Krishna, P. R.; Levinsky, A. B.; Kochetkov, N. K.; Rama Rao, A. V. *Carbohydr. Res.* **1992**, *223*, 303.

(235) Grandjean, C.; Gras-Masse, H.; Melnyk, O. *Chemistry – A European Journal* **2001**, *7*, 230.

(236) Grandjean, C.; Rommens, C.; Gras-Masse, H.; Melnyk, O. *Tetrahedron Lett.* **1999**, *40*, 7235.

(237) Hayes, W.; Osborn, H. M. I.; Osborne, S. D.; Rastall, R. A.; Romagnoli, B. *Tetrahedron* **2003**, *59*, 7983.

(238) Bernardes, G. J. L.; Gamblin, D. P.; Davis, B. G. *Angew. Chem.* **2006**, *118*, 4111.

(239) Chen, G.; Amajjahe, S.; Stenzel, M. H. *Chem. Commun.* **2009**, 1198.

(240) Thurecht, K. J.; Blakey, I.; Peng, H.; Squires, O.; Hsu, S.; Alexander, C.; Whittaker, A. K. *J. Am. Chem. Soc.* **2010**, *132*, 5336.

(241) Soeriyadi, A. H.; Boyer, C.; Burns, J.; Becer, C. R.; Whittaker, M. R.; Haddleton, D. M.; Davis, T. P. *Chem. Commun.* **2010**, *46*, 6338.

(242) Nicolas, J.; Mantovani, G.; Haddleton, D. M. *Macromol. Rapid Commun.* **2007**, *28*, 1083.

(243) Ladmiral, V.; Monaghan, L.; Mantovani, G.; Haddleton, D. M. *Polymer* **2005**, *46*, 8536.

(244) Hansen, T. V.; Wu, P.; Sharpless, W. D.; Lindberg, J. G. *J. Chem. Educ.* **2005**, *82*, 1833.

(245) Withey, A. B. J.; Chen, G.; Nguyen, T. L. U.; Stenzel, M. H. *Biomacromolecules* **2009**, *10*, 3215.

(246) Wong, E. H. H.; Stenzel, M. H.; Junkers, T.; Barner-Kowollik, C. *Macromolecules* **2010**, *43*, 3785.

(247) Tsarevsky, N. V.; Bencherif, S. A.; Matyjaszewski, K. *Macromolecules* **2007**, *40*, 4439.

(248) Sumerlin, B. S.; Tsarevsky, N. V.; Louche, G.; Lee, R. Y.; Matyjaszewski, K. *Macromolecules* **2005**, *38*, 7540.

(249) Zhang, W.; Zhang, Z.; Zhu, J.; Zhu, X. *Macromol. Rapid Commun.* **2010**, *31*, 1354.

(250) Ranjan, R.; Brittain, W. J. *Macromol. Rapid Commun.* **2007**, *28*, 2084.

(251) Sumerlin, B. S.; Tsarevsky, N. V.; Louche, G.; Lee, R. Y.; Matyjaszewski, K. *Macromolecules* **2005**, *38*, 7540.

(252) Quemener, D.; Davis, T. P.; Barner-Kowollik, C.; Stenzel, M. H. *Chem. Commun.* **2006**, 5051.

(253) O'Reilly, R. K.; Joralemon, M. J.; Hawker, C. J.; Wooley, K. L. *J. Polym. Sci., Part A: Polym. Chem.* **2006**, *44*, 5203.

(254) Chen, G. J.; Tao, L.; Mantovani, G.; Geng, J.; Nystrom, D.; Haddleton, D. M. *Macromolecules* **2007**, *40*, 7513.

(255) Quémener, D.; Hellaye, M. L.; Bissett, C.; Davis, T. P.; Barner-Kowollik, C.; Stenzel, M. H. *J. Polym. Sci., Part A: Polym. Chem.* **2008**, *46*, 155.

(256) Nurmi, L.; Lindqvist, J.; Randev, R.; Syrett, J.; Haddleton, D. M. *Chem. Commun. (Cambridge, U. K.)* **2009**, 2727

(257) Malkoch, M.; Thibault, R. J.; Drockenmuller, E.; Messerschmidt, M.; Voit, B.; Russell, T. P.; Hawker, C. J. *J. Am. Chem. Soc.* **2005**, *127*, 14942.

(258) Tanaka, T.; Nagai, H.; Noguchi, M.; Kobayashi, A.; Shoda, S.-i. *Chem. Commun.* **2009**, 3378.

(259) Vinson, N.; Gou, Y.; Becer, C. R.; Haddleton, D. M.; Gibson, M. I. *Polym. Chem.* **2011**, *2*, 107.

(260) Xu, J.; Tao, L.; Boyer, C.; Lowe, A. B.; Davis, T. P. *Macromolecules* **2009**, *43*, 20.

(261) Roth, P. J.; Boyer, C.; Lowe, A. B.; Davis, T. P. *Macromol. Rapid Commun.* **2011**, *32*, 1123.

(262) Perrier, S.; Takolpuckdee, P.; Mars, C. A. *Macromolecules* **2005**, *38*, 2033.

(263) Qiu, X.-P.; Winnik, F. M. *Macromol. Rapid Commun.* **2006**, *27*, 1648.

(264) Chan, J. W.; Yu, B.; Hoyle, C. E.; Lowe, A. B. *Polymer* **2009**, *50*, 3158.

(265) Ferreira, J.; Syrett, J.; Whittaker, M.; Haddleton, D.; Davis, T. P.; Boyer, C. *Polym. Chem.* **2011**, *2*, 1671.

Chapter 6

Conclusions and Further Work

The aim of this work was to synthesise multi arm star polymers using an appropriate controlled radical polymerisation technique and to try and understand the factors that contribute to the final properties of the star. Other industrial focussed studies within the group had previously looked at varying the reaction parameters to yield different results in engine tests. These tests are laborious, time consuming and require large (100g) scale synthesis. Therefore, the principle was to find a way of understanding the architecture of the star polymer on a small scale, rather than to look directly at the polymers performance as a viscosity modifier in these tests.

Using a new facility at the university, a multi detector GPC suite, the structure of the polymer was investigated. Although the ultimate goal was to investigate multi-arm star polymers, it was necessary to test the method for analysing the structure of stars using well defined star polymers first. Core-first stars were made by ATRP of MMA using different well-defined multifunctional initiators. These stars were analysed using multi-detector GPC using a universal calibration and conventional GPC. Universal calibration was seen to estimate the MW more accurately than conventional GPC with respect to the values expected.

Although star-star coupling was seen to occur in some of the reactions, this was minimised by terminating the reactions at low conversions, below 50%. Interestingly, there was a visible change in the Mark-Houwink plots for these two polymer architectures, with a step up in the intrinsic viscosity. However, there is no evidence of a decrease in the gradient, α, which would be expected with coupling due to increased polymer density in solution. Comparison of the plots shows that at the same MW on the MWD of the polymers, the intrinsic viscosity is lower for a star with more arms.

Each star's functionality was determined using their intrinsic viscosity contraction factor and Zimm Stockmayer theory, and seen to agree with the functionality of the core initiator at the M_p. At the highest concentration at the peak molecular weight, M_p, the functionality is approximately 4 for the 3-arm star, 6 for the 5-arm star, 8 for the 8-arm star, and 21 for the 21-arm star. The determination of functionality using this technique uses a number of approximations and assumptions, however, the error of ± 1 at the M_p was in agreement with a previous study of PMMA core-first star polymers by Robello and co-workers.[73]

The functionality of the stars was seen to change over their MWD, which is thought to be because of initiator efficiency, termination, and star-star coupling occurring in the reaction.

Moving to multi-arm star polymers, PMMA with a star architecture was synthesised using an arms first method in RAFT chemistry. 2-Cyanoprop-2-yl dithiobenzoate and 4-cyanopentanoic acid dithiobenzoate were synthesised to control the polymerisation of MMA, and was seen to do so with good first order kinetics and linear molecular weight growth with conversion. The amount of MMA in the reaction at the point of crosslinking was seen to have little effect up to a ratio of [MMA] / [RAFT agent] of 1:10, therefore arm polymerisation was taken to high conversion for subsequent reactions. The reaction was optimised by varying the ratio of [crosslinker] / [macroRAFT agent], and by changing crosslinker. The cross-linking efficiency of the crosslinker was seen to decrease with increasing ethylene glycol spacer length between the vinyl groups in the series ethylene glycol dimethacrylate>diethylene glycol dimethacrylate>triethylene glycol dimethacrylate.

The series of broad PDI star polymers of varying size, made using the three crosslinkers, were analysed using multi-detector GPC to determine their MWD and also produce pseudo Mark-Houwink plots. The average exponent, α, of the plots were seen to be smaller for star polymers, and decreased for larger star polymers. Using the intrinsic viscosity shrink factor and Zimm and Stockmayer theory to determine the number of arms for four stars made using EGDMA as a crosslinker were shown to have functionalities varying from 10s to 100s of arms. Two models for analysing the star polymers were investigated. Using the regular arm length model derived by Zimm and Stockmayer was seen to be the most reliable model when compared to the simple method using the molecular weight of the star and arm polymers.

Using the information about star formation gathered from the PMMA star polymers, formation of oil soluble star polymers using industrially applicable monomers and RAFT agent. However, RAFT co-polymerisation of $C_{12\text{-}15}$MA and MMA, using a C_{12}-trithio-butyl acrylate RAFT agent, **RAFT agent 3**, showed hybrid RAFT-FRP behaviour. The molecular weight can be targeted using the ratio of [RAFT agent] to [monomer]; however, relatively polydisperse polymers were produced.

Further reaction of the formed macro-RAFT agents with EGDMA, DEGDMA, and TEGDMA showed chain extension and some star formation. Analysis of the stars by GPC showed that the crosslinker efficiency decreases with the series: EGDMA > DEGDMA > TEGDMA. This suggests that increasing the length of the ethylene glycol moieties separating the vinyl groups is detrimental to star formation and coincides with the data seen for PMMA stars. This may have been due to cyclisation, and possibly suggests some form of phase separation or partial solubility. TEGDMA yields no star polymer; the increase in molecular weight can be accounted for by the addition of crosslinker, but without crosslinking. Analysis by ^{1}H NMR does <u>not</u> show evidence of

unreacted pendent vinyl peaks and therefore supports the hypothesis of Sawamoto *et al*., that TEGDMA undergoes intramolecular cyclisation.[140] It would be interesting to study other crosslinkers, particularly focussing on the solubility of the crosslinker.

As **RAFT agent 3** was seen to be working like a conventional CTA in the early stages of the polymerisation, it was possible to calculate a chain transfer constant, C_s, value for **RAFT agent 3** in the polymerisation of $C_{12\text{-}15}$MA and MMA. The C_s was calculated to be <1, which implies that $k_{tr} < k_p$.

By increasing the ratio of **RAFT agent 3** to monomer at the beginning of the reaction, with the remaining monomer fed into the reactor afterwards, it was seen that the PDI of the macro-RAFT agents can be decreased from 1.5 to 1.2.

Given more time, it would be beneficial to control the concentration of monomer in the reactor more closely than was carried out so far. A study into the effect of having higher or lower [M] at various stages of the reaction on the PDI and the chain end functionality would be interesting both commercially and in understanding the mechanism of RAFT using **RAFT agent 3**.

Stars formed using the narrow PDI macro-RAFT agents were seen to produce stars of narrow PDI with high arm incorporation. Increasing reaction time or amount of crosslinker was seen to have a small increase in molecular weight of star polymer formed, but did not increase the percentage arm incorporation. Reaction of the star with further crosslinker was seen to preferentially form star-star coupling over incorporation of further arms. UV GPC analysis of the unreacted arms shows evidence of the RAFT end group's presence in the polymer. This suggests that the crosslinking reaction is still the limiting factor in increasing the arm incorporation, and it is not due to termination during the RAFT arm polymerisation. Using more crosslinker in star

formation is seen to form larger stars, but does not increase arm incorporation into the star.

The aim of the final chapter of work was to utilise the study of star polymer formation from earlier chapters to make star glycopolymers. Alkyne bearing polymers were synthesised using RAFT chemistry. A protected monomer was seen to be required, and a series of polymers were synthesised using 2-cyanoprop-2-yl dithiobenzoate, with varying M_n and narrow PDI. When targeting high molecular weight the kinetic plot showed deviation from first order kinetics and an increase in PDI was seen in the final polymer. These polymers were deprotected to yield alkyne scaffolds for post polymerisation modification. The RAFT chemistry was seen to be as effective as in the synthesis of these alkyne scaffolds as literature routes using ATRP.

Mannose and galactose azide was reacted with the P(PgMA) series of polymers to yield water soluble glycopolymers. A second route to introducing mannose and galactose groups to the polymers was attempted, using thiol-yne chemistry. Mannose was modified at the anomeric carbon to yield a thiol functional sugar; which was then reacted with an alkyne bearing polymer (**P(PgMA)6**) to yield a glycopolymer in low yield. After dialysis the polymer was partially soluble in water and ^{1}H NMR and IR data showed partial functionalisation of the alkyne polymer by thio mannose. These results show the difficulty of thiol-yne chemistry in the modification of P(PgMA) polymers. Further investigation is needed, as the resultant polymer may have interesting properties due to the high density of sugars in proximity.

A Poly(TMS-propargyl methacrylate) macroRAFT agent was crosslinked using EGDMA and a novel crosslinker, **crosslinker 10**. EGDMA was seen to produce high molecular weight star polymer in low yield, deprotection and subsequent CuAAC with mannose

azide yielded a star glycopolymer, with unreacted arms. Using **crosslinker 10,** star polymer with narrow PDI and a cleavable core was synthesised in low yield. This polymer was deprotected to yield an alkyne polymer and reacted with mannose azide in a CuAAC reaction. However the reaction was not seen to proceed to a high conversion of alkyne groups, possibly due to steric hindrance of the star. Finally, an oil soluble alkyne bearing star polymer was synthesised by copolymerisation of long chain alkyl methacrylate with TMSPgMA and crosslinking with EGDMA. The deprotection of the TMS groups in the polymer was seen to be successful yielding an oil soluble alkyne bearing polymer for further reaction.

Further work is needed towards the synthesis of multi-arm glycopolymer stars. The click reaction in the dense star polymers was seen to progress slowly, therefore an alternative route is needed; polymerisation of glycomonomers by RAFT followed by a crosslinking reaction. Alternatively, click onto the macroRAFT agent followed by crosslinking could work if the RAFT agent is not destroyed during the click process.

6.1 References

(73) Robello, D. R.; Andre, Alix; McCovick, T. A.; Mourey, T. H. *Macromolecules* 2002, *35*, 9334.

(140) Baek, K.-Y.; Kamigaito, M.; Sawamoto, M. *Macromolecules* 2001, *34*, 215.